Conceptual Model Report for the Hill Country Trinity Aquifer Groundwater Availability Model

Prepared by
Editors
Nate J. Toll
Ronald T. Green, Ph.D., P.G.,
Ronald N. McGinnis
Leanne M. Stepchinski
Rebecca R. Nunu
Gary R. Walter, Ph.D.
From Southwest Research Institute®

Jevon Harding, P.G.
Neil E. Deeds, Ph.D., P.E.
From INTERA Incorporated

Contributors
Mauricio E. Flores, G.I.T.
Kirk D.H. Gulliver
From Southwest Research Institute®

Prepared for:
Texas Water Development Board
P.O. Box 13231, Capitol Station
Austin, Texas 78711-3231

May 31, 2018

This page is intentionally blank.

Geoscientist and Engineering Seal

This report documents the work of the following Licensed Texas Geoscientists and Engineers:

Dr. Neil Deeds and Jevon Harding conducted the analysis and documentation for work associated with Sections 4.2, 4.5, and 4.6.3 of this project.

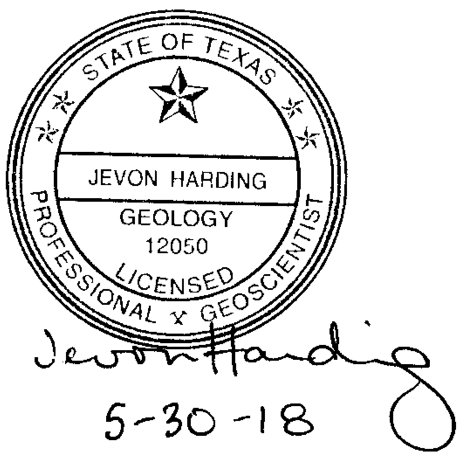

Dr. Ronald Green oversaw and conducted analysis and documentation associated with the remaining sections of this project.

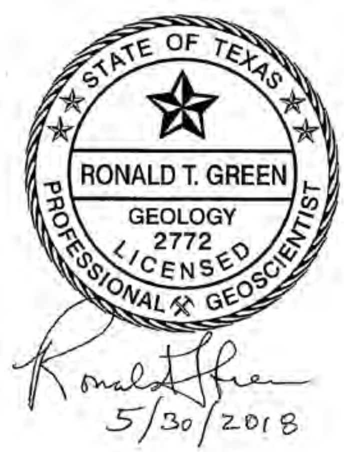

Table of Contents

Table of Figures

Table of Tables

This page is intentionally blank.

1.0 Introduction

The Trinity Aquifer is classified as one of nine major aquifers in Texas (Figure 1.0). It extends from the Texas-Oklahoma border to south-central Texas and provides water to large areas throughout the 52 counties it overlies. The Trinity Aquifer is subdivided into the Trinity (Hill Country) Aquifer and the Northern Trinity and Woodbine Aquifer. This report focuses solely on the Hill Country portion of the Trinity Aquifer and will hereby be referenced as the HCT Aquifer. Historically, the HCT Aquifer has not been a prolific source of water in comparison to other aquifers in the region, such as the Edwards (Balcones Fault Zone [BFZ]) Aquifer. However, renewed interest has been placed on the HCT Aquifer as a water resource in south-central Texas, especially in and around Austin and San Antonio, as demands continue to increase due to development and population growth. Numerous studies have explored the aquifer system, as in-depth and continuing investigations focus on refining previous groundwater availability models (Mace et al., 2000; Jones et al., 2011), interactions with the Edwards (BFZ) Aquifer (Small, 1986; Ridgeway and Petrini, 1991; LBG-Guyton Associates and NRS Consulting Engineers, 1995; Smith and Hunt, 2009; Fratesi et al., 2015), and potential brackish water production (LBG-Guyton Associates and NRS Consulting Engineers, 2003).

In 2017, the Texas Water Development Board (TWDB) contracted Southwest Research Institute® (SwRI) to update the conceptual model of the HCT Aquifer with three objectives: (1) expand the model region to include the downdip portion of the Trinity Aquifer and all of GMA 9; (2) develop an understanding of interformational flow between the Edwards (BFZ) Aquifer and HCT; and (3) extend the datasets for water elevations, water chemistry, recharge, discharge, and hydraulic parameters, both spatially and temporally. This report includes descriptions of the following components to satisfy these objectives: (1) physiography and climate, (2) geology, (3) hydrostratigraphy, (4) hydrostratigraphic framework, (5) water elevations and regional groundwater flow, (6) recharge, (7) rivers, streams, reservoirs, springs, and other surface water features, (8) hydraulic properties, (9) subsidence, (10) discharge, and (11) water quality. The refinement of the conceptual model for the HCT Aquifer will ultimately facilitate TWDB to develop a new GAM to assess future groundwater conditions of the aquifer.

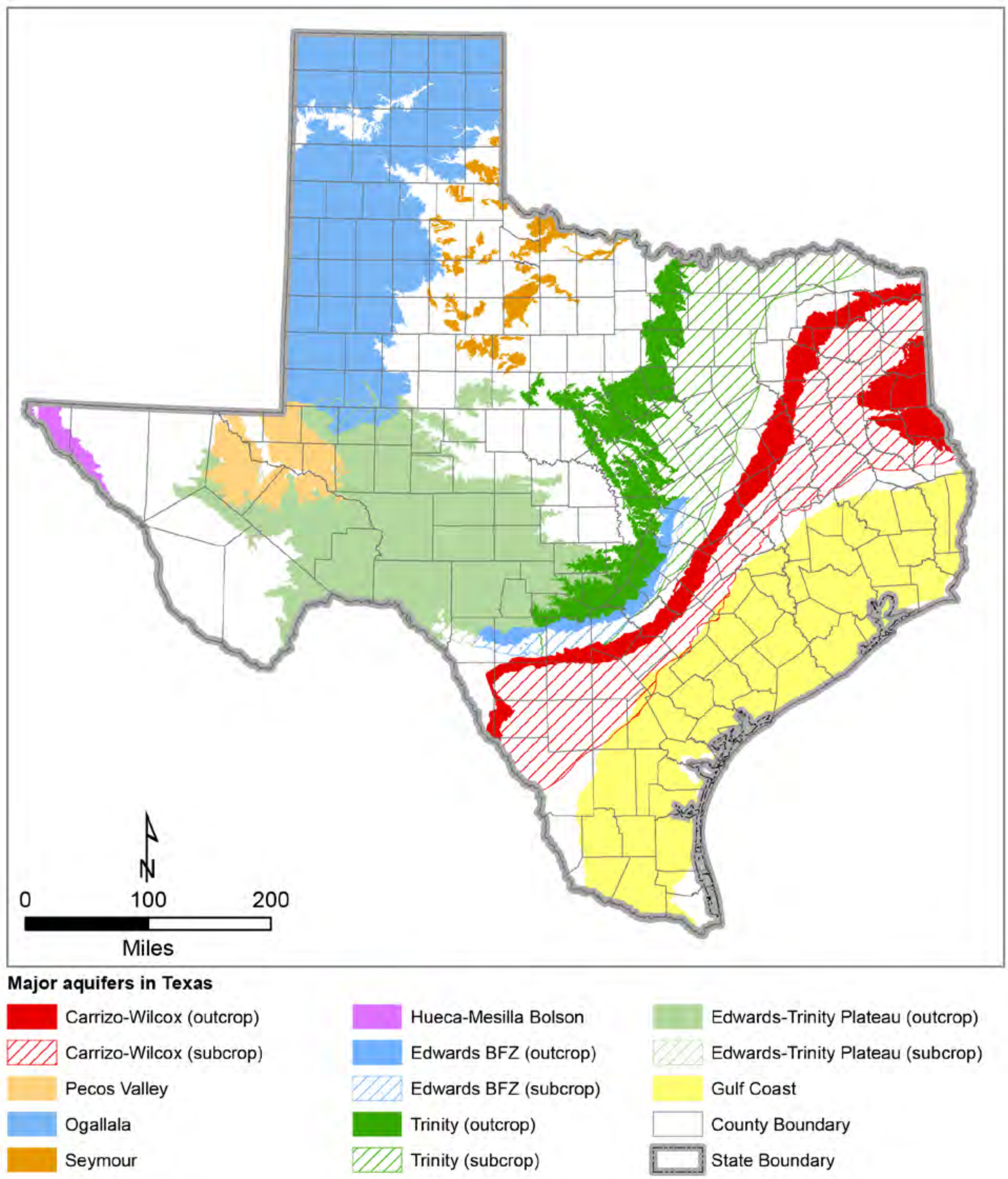

Figure 1.0.1 Major aquifers in Texas.

2.0 Study Area

The outcrop and subcrop regions of the HCT aquifer cover 19 counties in Texas. To meet the objectives for updating the conceptual framework of the aquifer, the study area and model boundary are extended to encompass 28 counties total, from Val Verde and Edwards counties in the west to Travis, Williamson, and Bastrop counties to the east (Figure 2.0.1). Moreover, the new study area includes the entirety of GMA 9 and the downdip boundary of the HCT Aquifer. It is important to note that while this study boundary is intended to facilitate the improvement of a future GAM, it is not the domain for that numerical model.

Figure 2.0.2 shows major urban areas and roadways within the study region. Major cities, particularly Austin and San Antonio, as well as major roadways, are most dense along the southeastern edge of the study area, which is coincident with the I-35 corridor.

The HCT study area encompasses numerous political and administrative boundaries tasked with protecting both surface water and groundwater resources within the region. Five regional water planning areas (RWPAs) are within the study area: Brazos G, Region F, Lower Colorado, Plateau, and South Central Texas (Figure 2.0.3). Figure 2.0.4 illustrates that GMA 7, 8, 9, 10, 12, and 13 also lie within the study area. The study area encompasses 23 Groundwater Conservation Districts (GCDs), as labeled and shown in Figure 2.0.5. Major rivers and streams within these basins are depicted in Figure 2.0.6. Examples include the Nueces River, Medina River, Guadalupe River, and Colorado River, which occur within their respectively named river basins (Figure 2.0.7). These surface water features are protected by eight different river authorities (Figure 2.0.8).

In addition to the HCT Aquifer, the Edwards-Trinity (Plateau) Aquifer, Edwards (BFZ) Aquifer, and the uppermost extent of the Carrizo-Wilcox Aquifer fall within the study area (Figure 2.0.9). Minor aquifers, specifically a significant portion of the Hickory, Marble Falls, and Ellenburger-San Saba aquifers, as well as a sliver of the Queen City Aquifer, are encompassed by the model boundary (Figure 2.0.10).

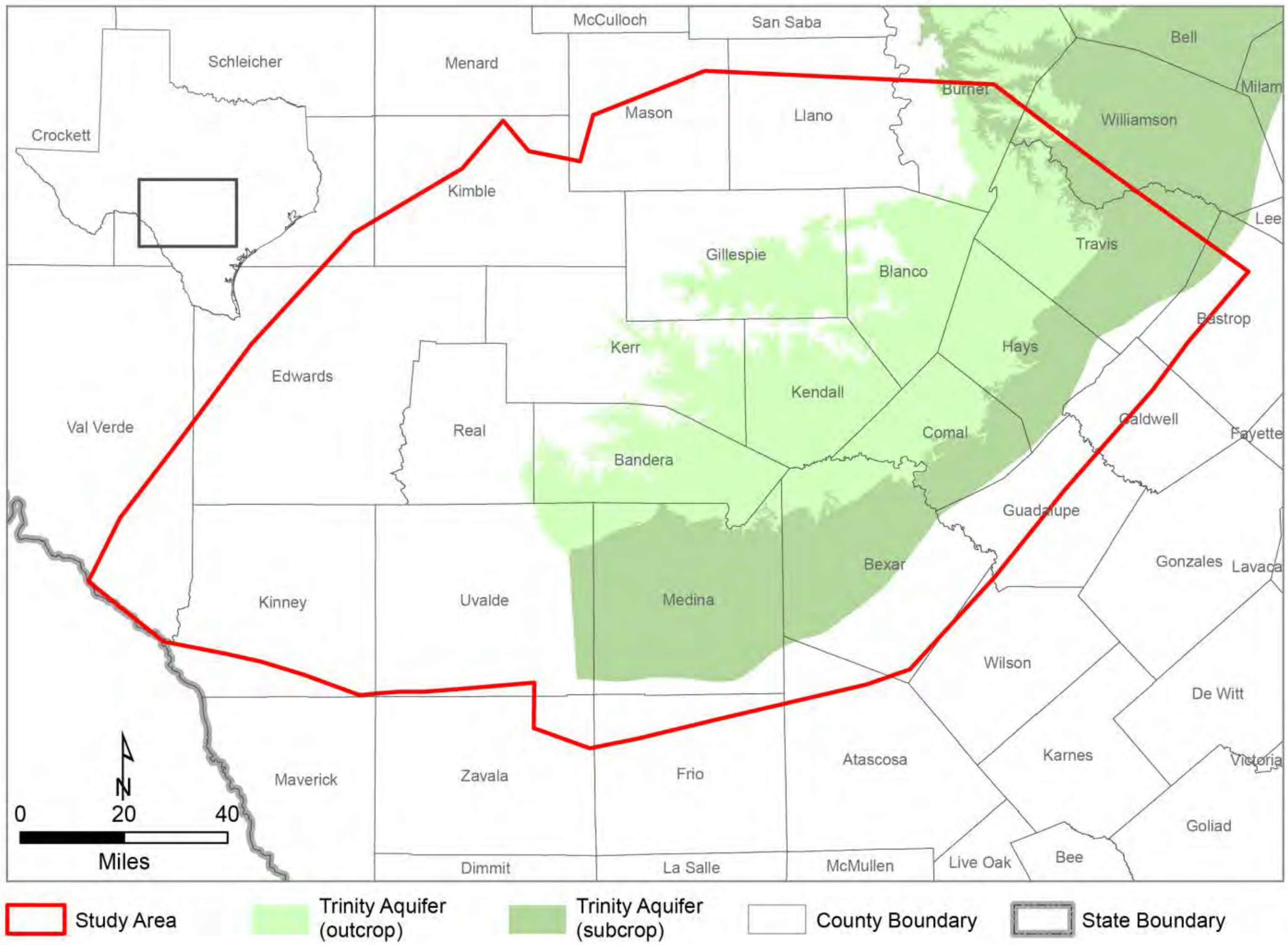

Figure 2.0.2.11 Study boundary and model domain for the updated conceptual framework of the HCT.

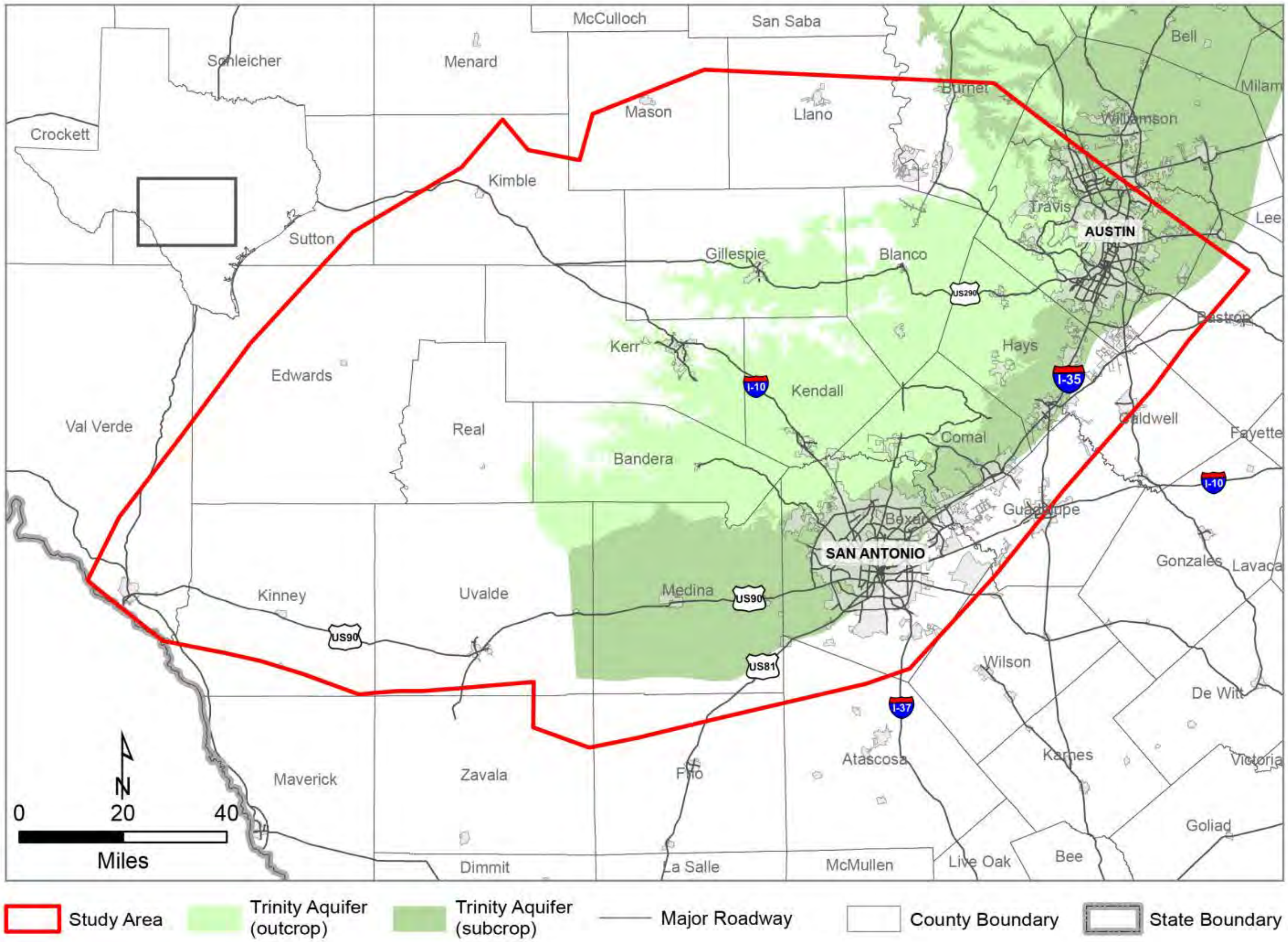

Figure 2.0.2 Major roads and urban areas within the study area.

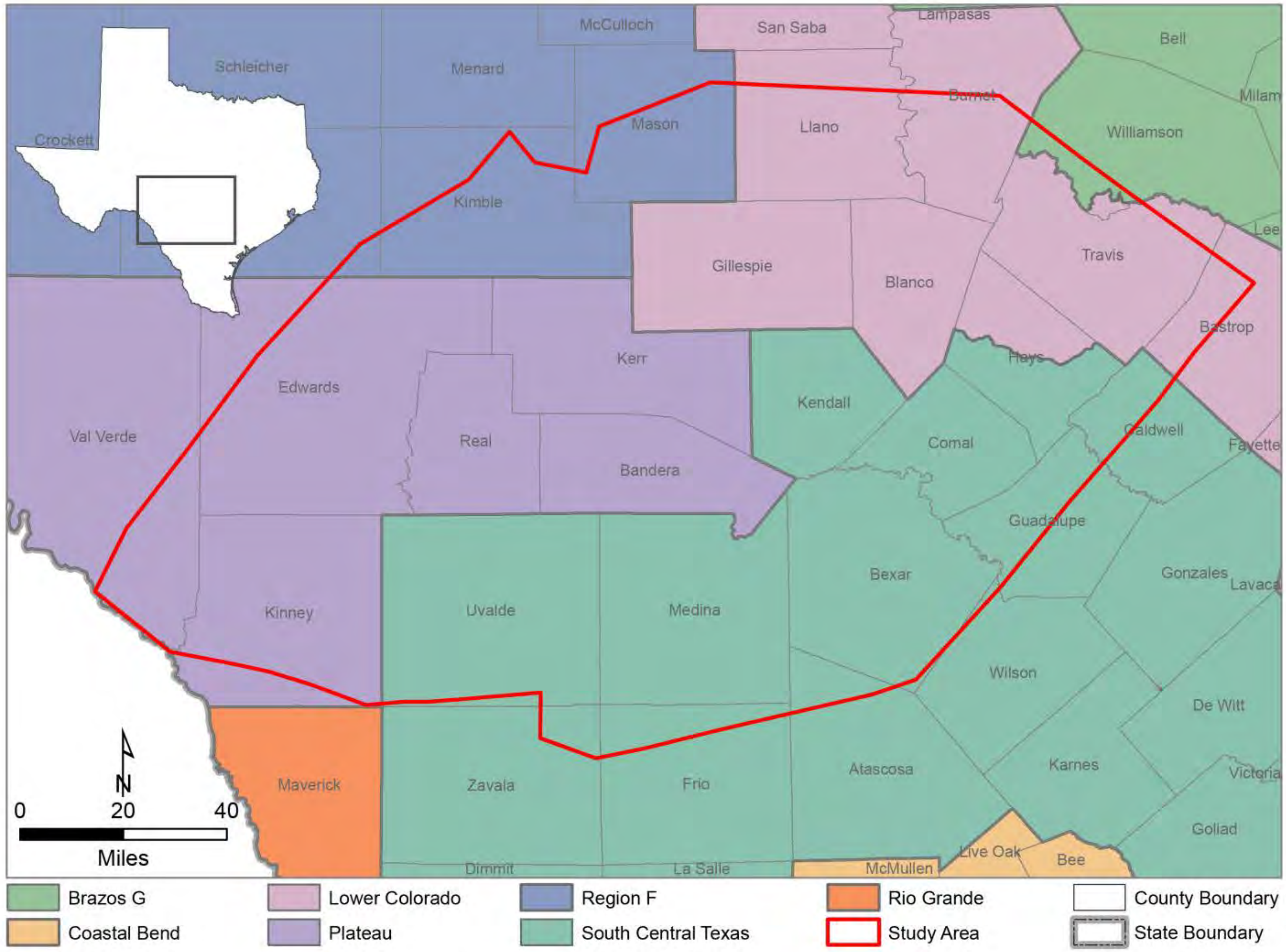

Figure 2.0.3 **RWPAs within the study area.**

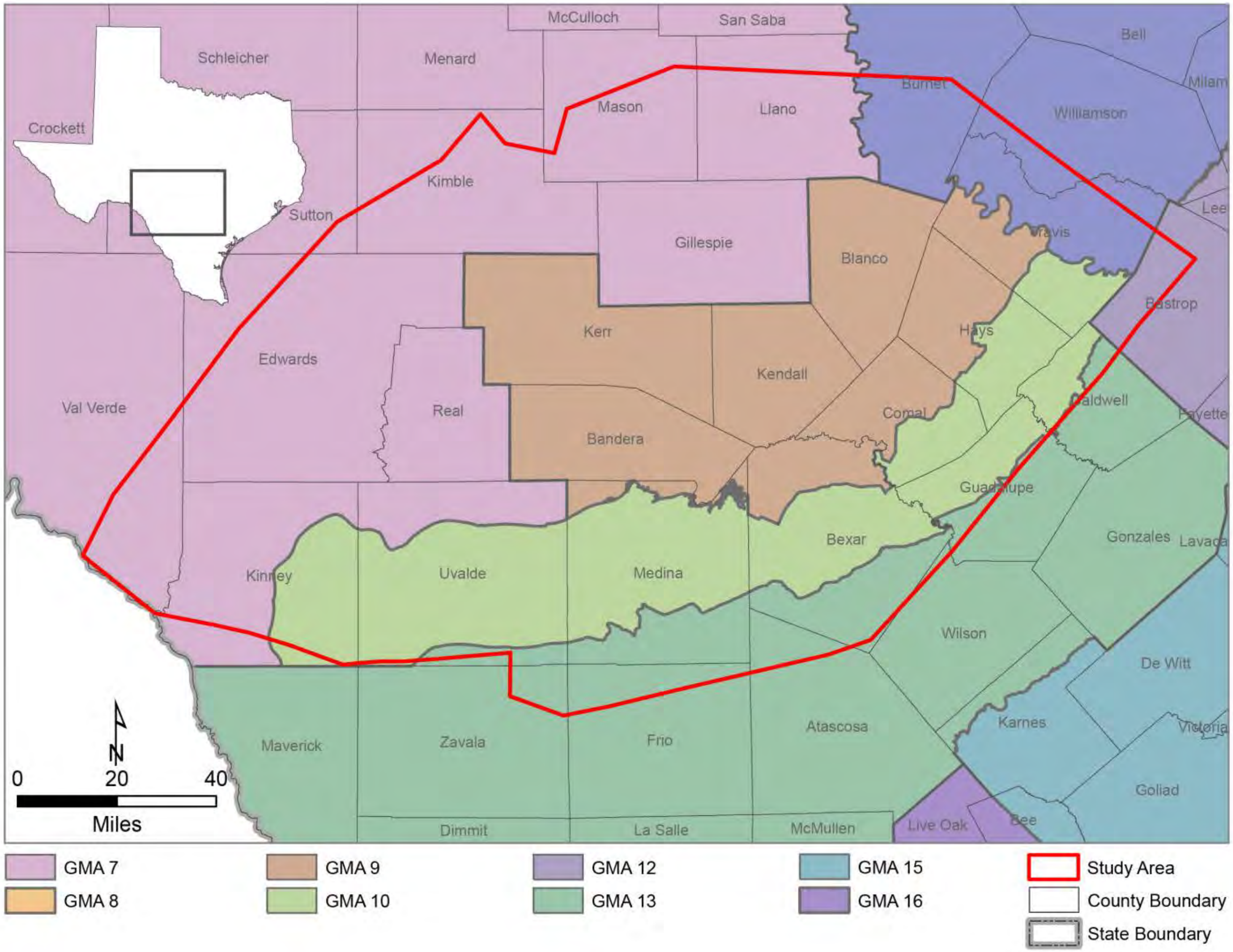

Figure 2.0.4 **GMAs within the study area.**

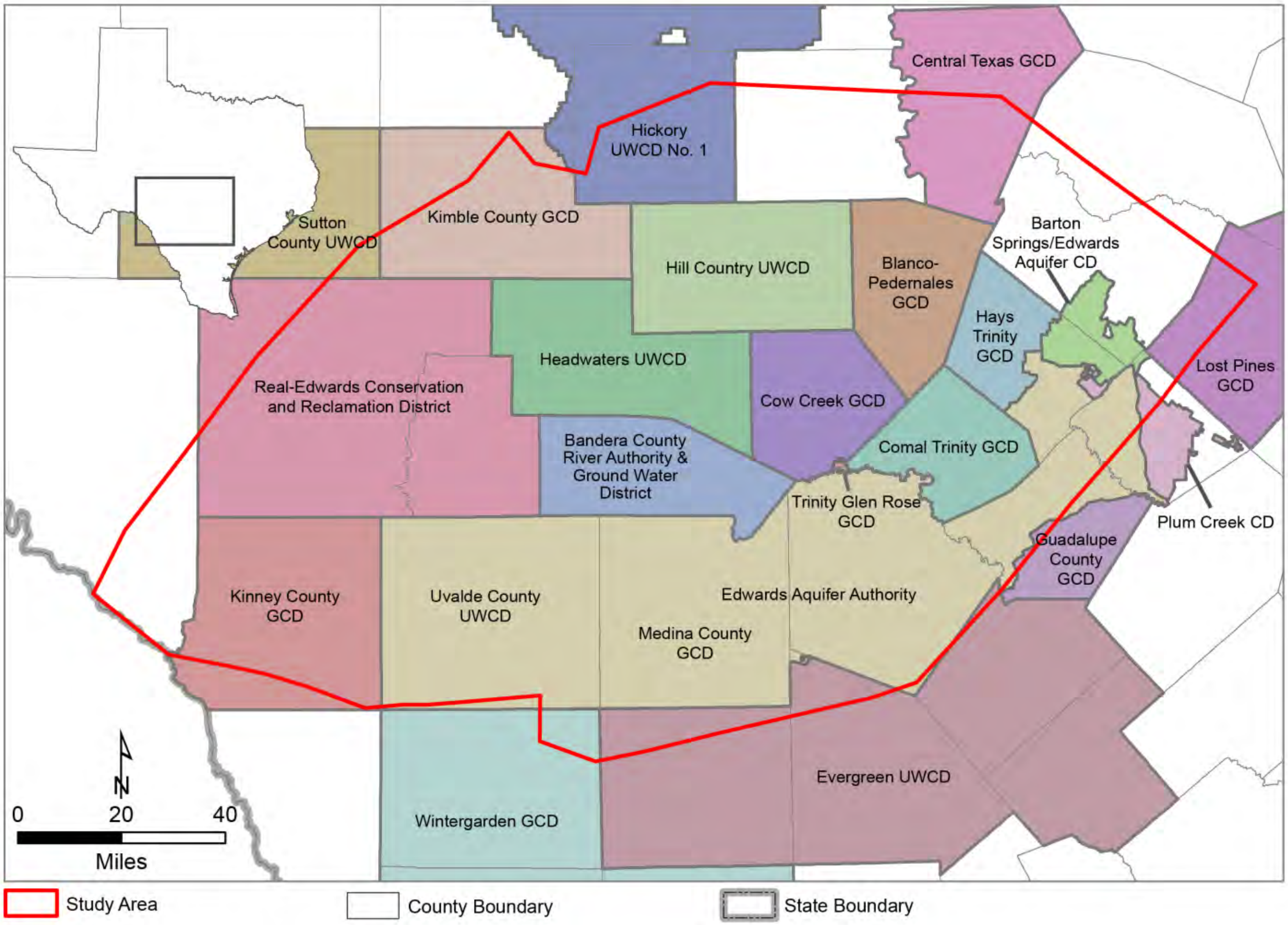

Figure 2.0.5 GCDs within the study area.

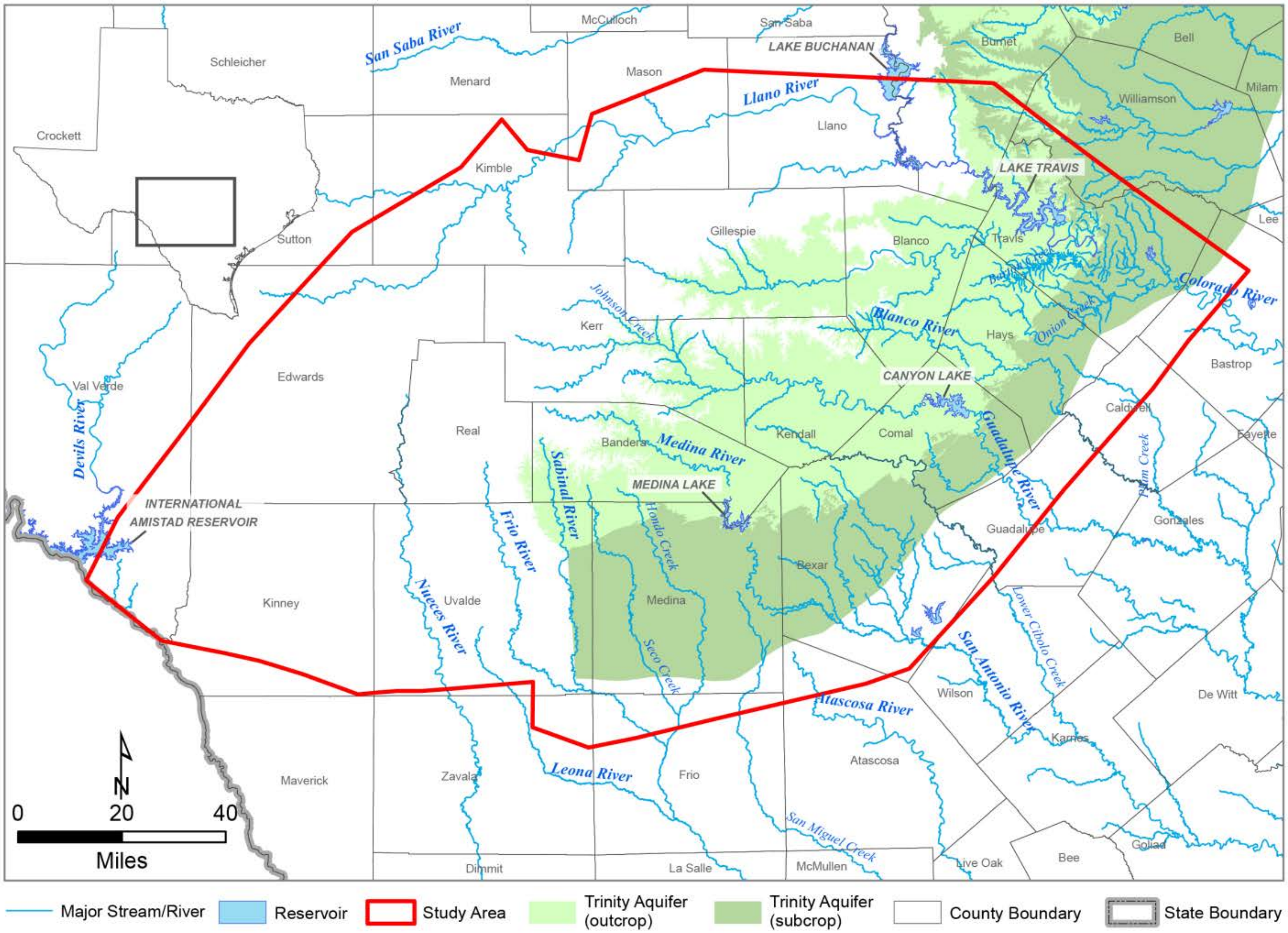

Figure 2.0.6 **Major streams and rivers within the study area.**

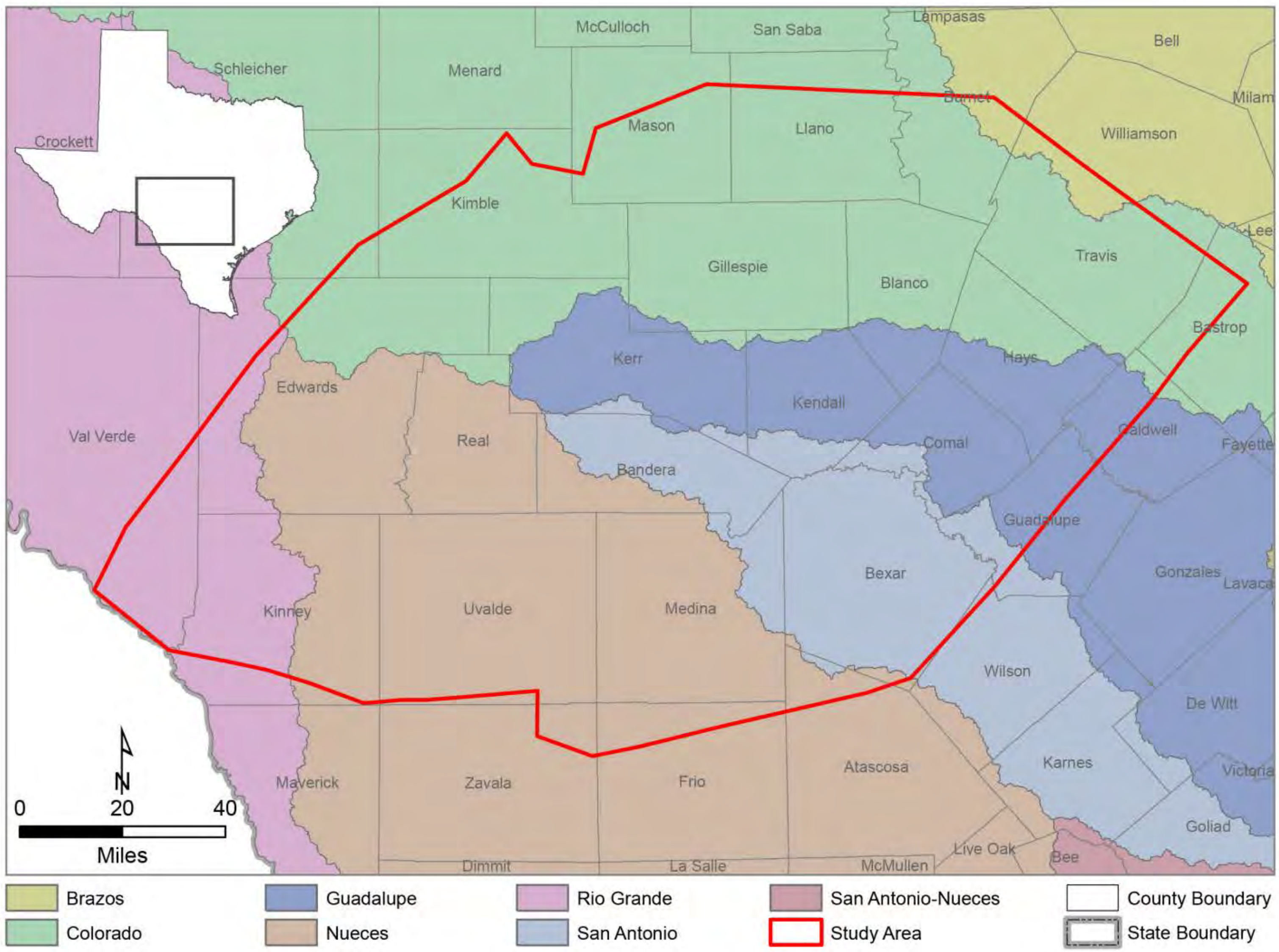

Figure 2.0.7 Major river basins within the study area.

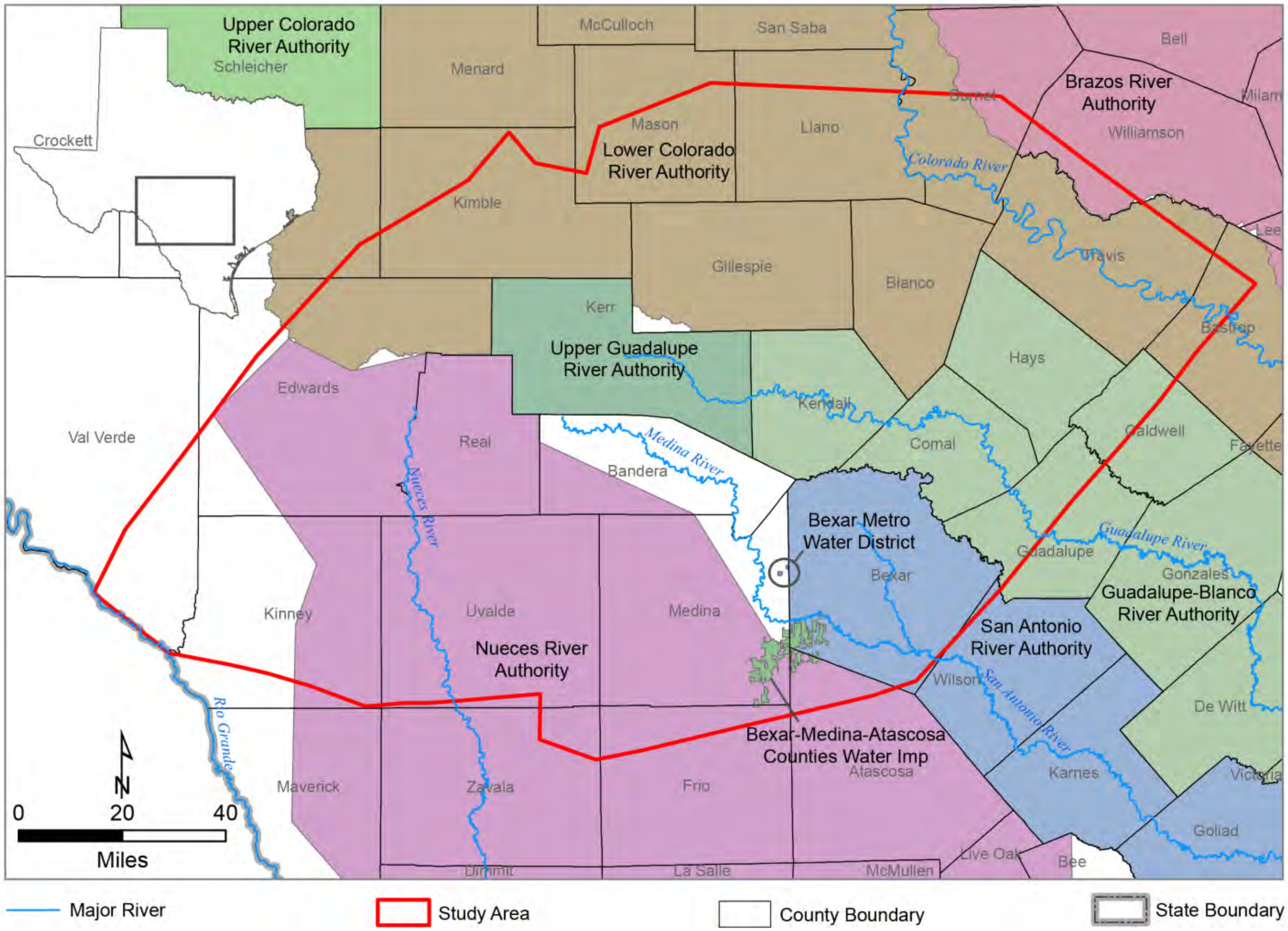

Figure 2.0.8 River authorities within the study area.

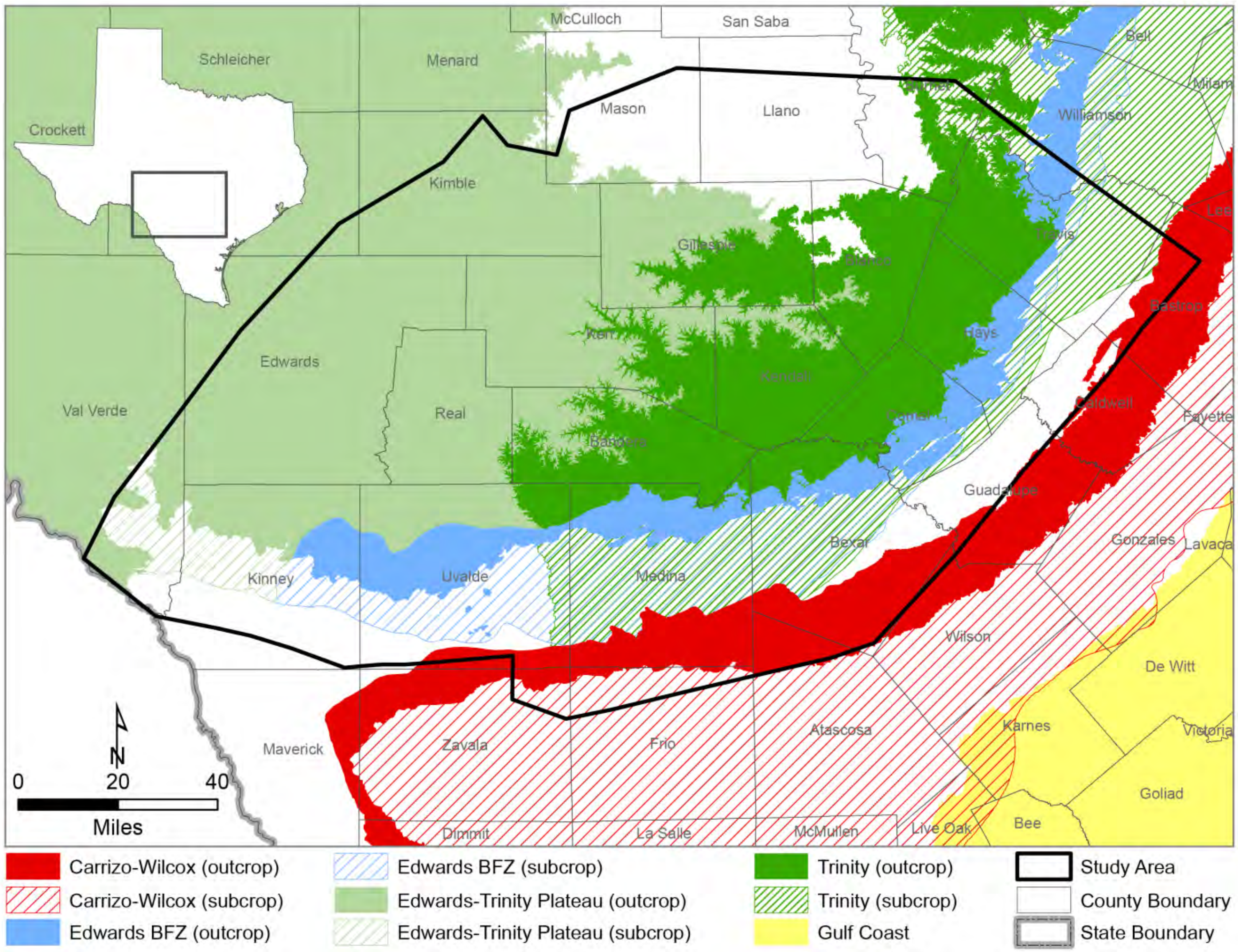

Figure 2.0.9 Major aquifers within the study area.

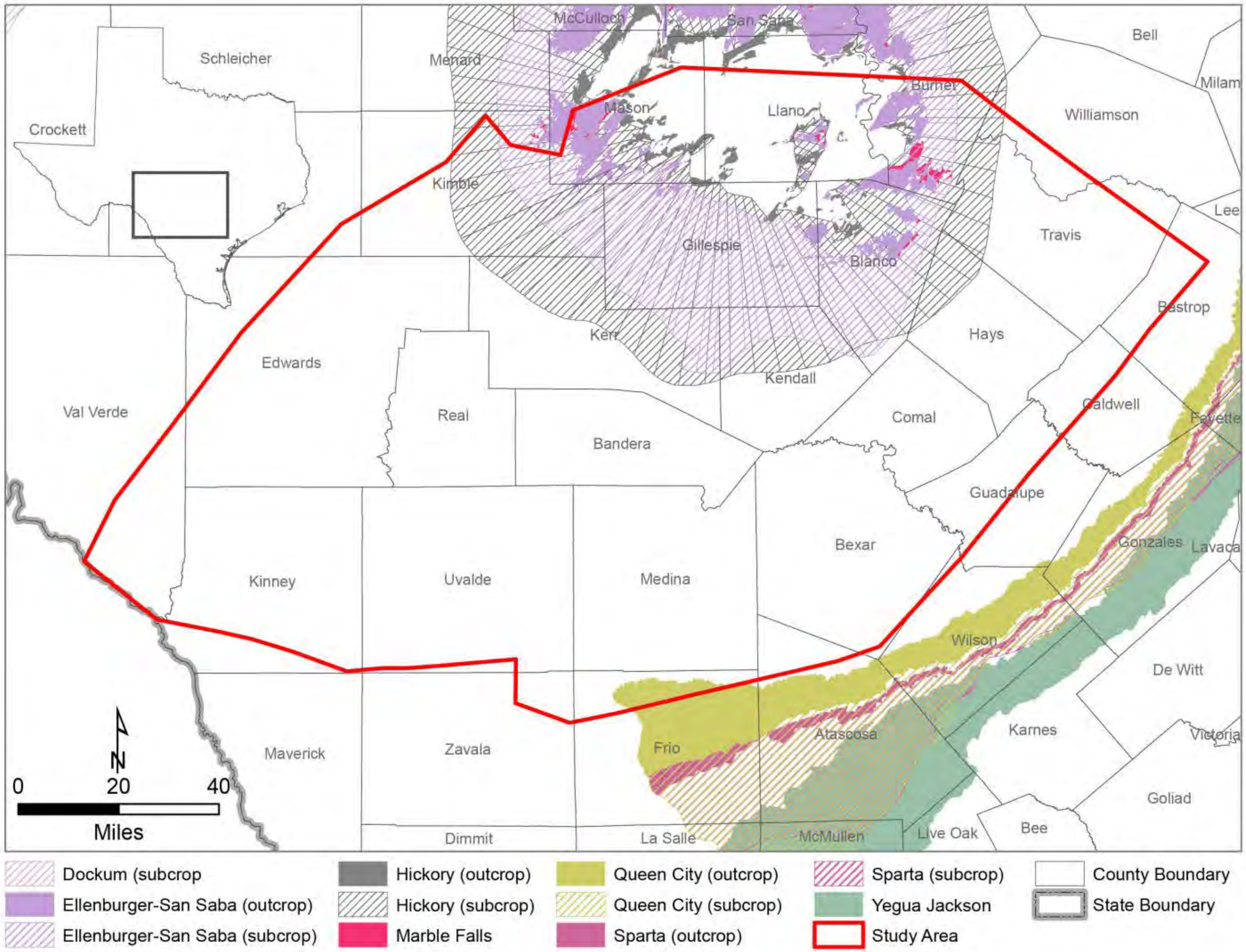

Figure 2.0.10: Minor aquifers within the study area.

2.1 Physiography and Climate

The study area is located in the Coastal Plain and the Great Plains national physiographic provinces as defined by the U.S. Geological Survey (USGS, 2002). Additionally, the study area encompasses portions of the Edwards Plateau, Central Texas Uplift, Balcones Escarpment, and Gulf Coastal Plains Texas Physiographic Provinces (Figure 2.1.1) as defined by Wermund (1996) and the Bureau of Economic Geology. Wermund (1996) describes the Edwards Plateau and Balcones Escarpment as a plateau including the Hill Country, capped with limestone and entrenched by streams; the Central Texas Uplift is described as a central, granite hill-studded basin, Balcones Escarpment, and the Gulf Coastal Plains (including the Blackland Prairies and the Interior Coastal Plains regions) as the product of deltaic sediment deposits which erodes to the southeast.

The study area contains four Level III ecological regions as designated by a 2007 Texas Commission on Environmental Quality (TCEQ) study (Figure 2.1.2) (Griffith et al., 2007). These include the Edwards Plateau, the Southern Texas Plains, the Texas Blackland Prairies, the East Central Texas Plains, and the Chihuahuan Deserts. Ecological regions, or ecoregions, are areas containing generally similar ecosystems and types, quantities, and qualities of environmental resources. Ecological frameworks are valuable tools for environmental research, as well as the assessment, management, and monitoring of ecosystems and ecosystem components.

The majority of the study area lies in the Edwards Plateau ecological region. This region is characterized by elevated plateaus, rolling hills, and broad valleys and plains. Vegetation includes mostly woodlands, shrublands, and grasslands. The Llano Uplift and the Balcones Fault Zone are major geologic features of the area. Much of this region is underlain by limestone, with karst topography. A majority of the soils are Mollisols and are shallow to moderately deep on plateaus and hills, transitioning to deeper soils on valley floors and plains. Juniper oak and mesquite oak savannah with some Ashe juniper woodland covers most of the Edwards Plateau, and the land in this region is presently utilized for livestock grazing and wildlife hunting.

The Texas Blackland Prairies, present along most of the eastern border of the study area, contain fine-textured, clayey soils. This region contains a higher percentage of cropland than surrounding regions, which is increasingly under conversion to urban, suburban, and industrial use. The Southern Texas Plains present in the southernmost portion of the study area are cut by streams and arroyos and have low-growing thorny brush vegetation. While previously covered by grassland and savannah vegetation, these areas are presently dominated by mesquite vegetation. The East Central Texas Plains ecological region, also known as the Post Oak Savannah due to its original land cover of post oak savannah type vegetation, is currently utilized as pasture land. The soils in this region are dominantly acidic sandy loam along ridges and clay loams in the lowlands. A small area of Chihuahuan Basins and Playas, sub-ecoregions of the Chihuahuan Deserts, is present in the southwestern corner of the study area. This ecoregion experiences some of the lowest rainfall in the state and is characterized by alkaline and gypsiferous soils with desert shrub vegetation.

Figure 2.1.3 illustrates the topography in the study area. The ground-surface elevation generally decreases with dip from northwest to southeast. The maximum elevations of about 2,420 ft in the northwest and the lowest elevations of about 338 ft are southeast of the Balcones Fault Zone. Faulting in this area resulted in steep drop-offs in elevation, particularly in Bexar and Medina counties. The drainage features of the major rivers are reflected in the topographic gradients in much of the study area.

Figure 2.1.4 shows the climatic classifications as defined by Larkin and Bomar (1983). Subtropical classification is subdivided based on moisture content as follows. The westernmost portion of the study area is classified as Subtropical Steppe, with semi-arid to arid climatic conditions. The central portion is classified as Subtropical Subhumid, with hot summers and dry winters. The eastern portion is classified as Subtropical Humid, characterized by warm summers. The Subtropical climate is caused by flow of air from the Gulf of Mexico onshore. This inflowing maritime air decreases in moisture content heading westward away from the coast. Seasonal intrusions of continental air also cause a decrease in air moisture content in the area.

Parameter-elevation Regressions on Independent Slopes Model (PRISM) datasets developed and presented online by Oregon State University provide distributions of average annual temperature and precipitation across the 48 conterminous United States for the 30-year period 1981 to 2010 (PRISM Climate Group, 2016). These data indicate that the average annual temperature in the study area ranges from a low of 63° F in the northern central portion of the study area to a high of 70° F in the southern and southwestern portions of the study area (Figure 2.1.5).

PRISM precipitation data are available at over 131 precipitation stations within the study area (Figure 2.1.6) from as early as 1931 through the present. Measurement of precipitation at most gages began in the 1940s or 1950s. Measurement by NEXRAD radar in the study area generally began in 2001. In general, measurements are not continuous on a month-by-month or year-by-year basis at the gages. Examples of the historical variation in annual precipitation at a few selected gages are shown in Figure 2.1.8. The long-term monthly variation in precipitation for these same selected gages is shown in Figure 2.1.9. For each selected gage, the time period for the monthly average precipitations shown in Figure 2.1.9 is the same as the time period for the annual precipitation shown in Figure 2.1.8. The monthly average data indicate that precipitation peaks in late spring to early summer, and again in early fall at a majority of the selected sites.

Average annual lake evaporation in the study area ranges from a high of 66 inches per year in the west to a low of 52 inches per year in the east (TWDB, 2009), as shown in Figure 2.1.10. The evaporation rates in the study area significantly exceed the average annual rainfall, resulting in precipitation deficits (evaporation exceeding precipitation). The study area has a precipitation deficit of 30 inches per year in the east to almost 50 inches per year in the west. Monthly variations in lake surface evaporation are shown in Figure 2.1.10 for each quadrangle in the study area. These values represent the average of the monthly lake surface evaporation data from January 1980 through December 2016. Figure 2.1.10 shows that average lake evaporation peaks in July.

Figure 2.1.11 illustrates the types of vegetation present in the study area as defined by the Texas Parks and Wildlife Department (Fyre et al., 1984). The predominant types of vegetation include

Live Oak-Mesquite Parks in the north, Mequite-Blackbrush Brush to the southwest, converted Cropland in the southwest, and Live Oak-Mesquite-Ashe Juniper Parks, Live Oak-Ashe Juniper Parks, and Live Oak-Ashe Juniper Woods to the northwest and throughout the central regions of the study area.

Soil properties may have a significant impact on the amount of precipitation that infiltrates to groundwater and the amount of moisture that is lost to evapotranspiration. Figure 2.1.12 illustrates the drainage values of the various soils across the region as defined by the USDA (Soil Survey Staff, Natural Resources Conservation Service, USDA, 2018). The study area is dominated by well drained soils, transitioning into a mix of well drained and moderately well drained soils to the southern and southeastern borders. There are isolated areas of excessively drained, somewhat excessively drained, and somewhat poorly drained soils. All Soil Survey Geographic Database (SSUGRO) Soil properties are included in the GAM geodatabase for the entire study area.

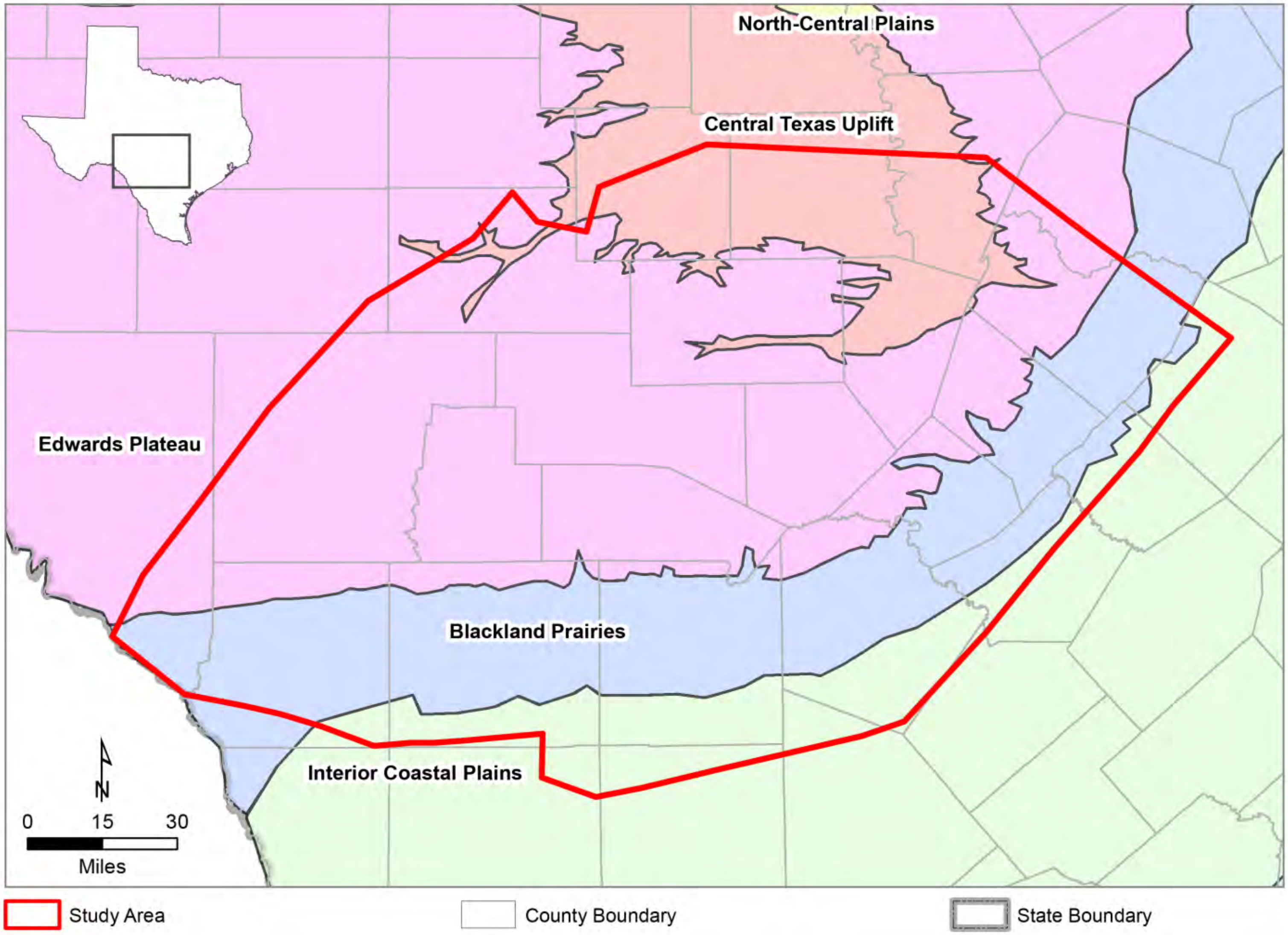

Figure 2.1.1 Physiographic provinces as defined by Wermund (1966)

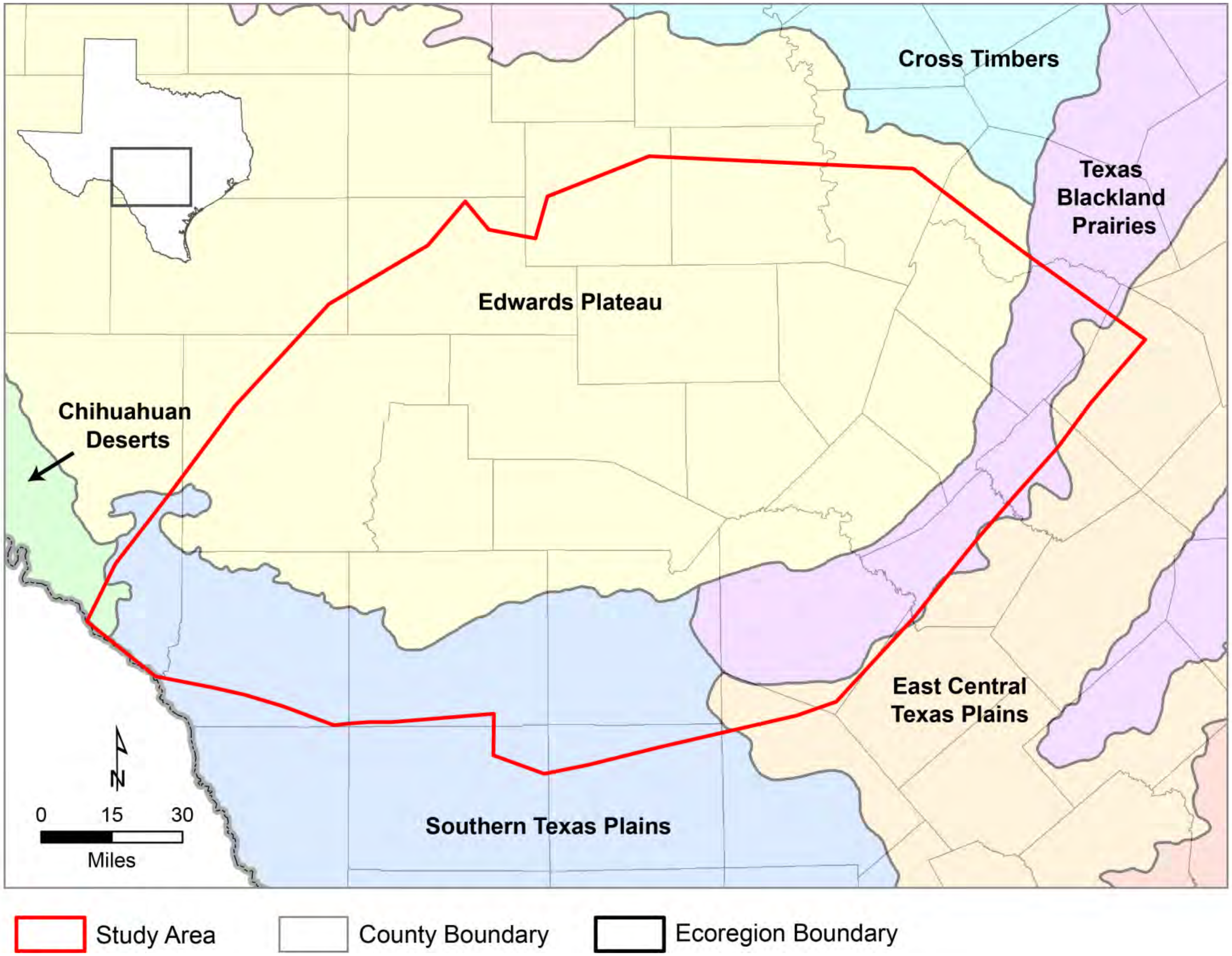

Figure 2.1.2 Level III ecological regions as defined in Griffith et al. (2007).

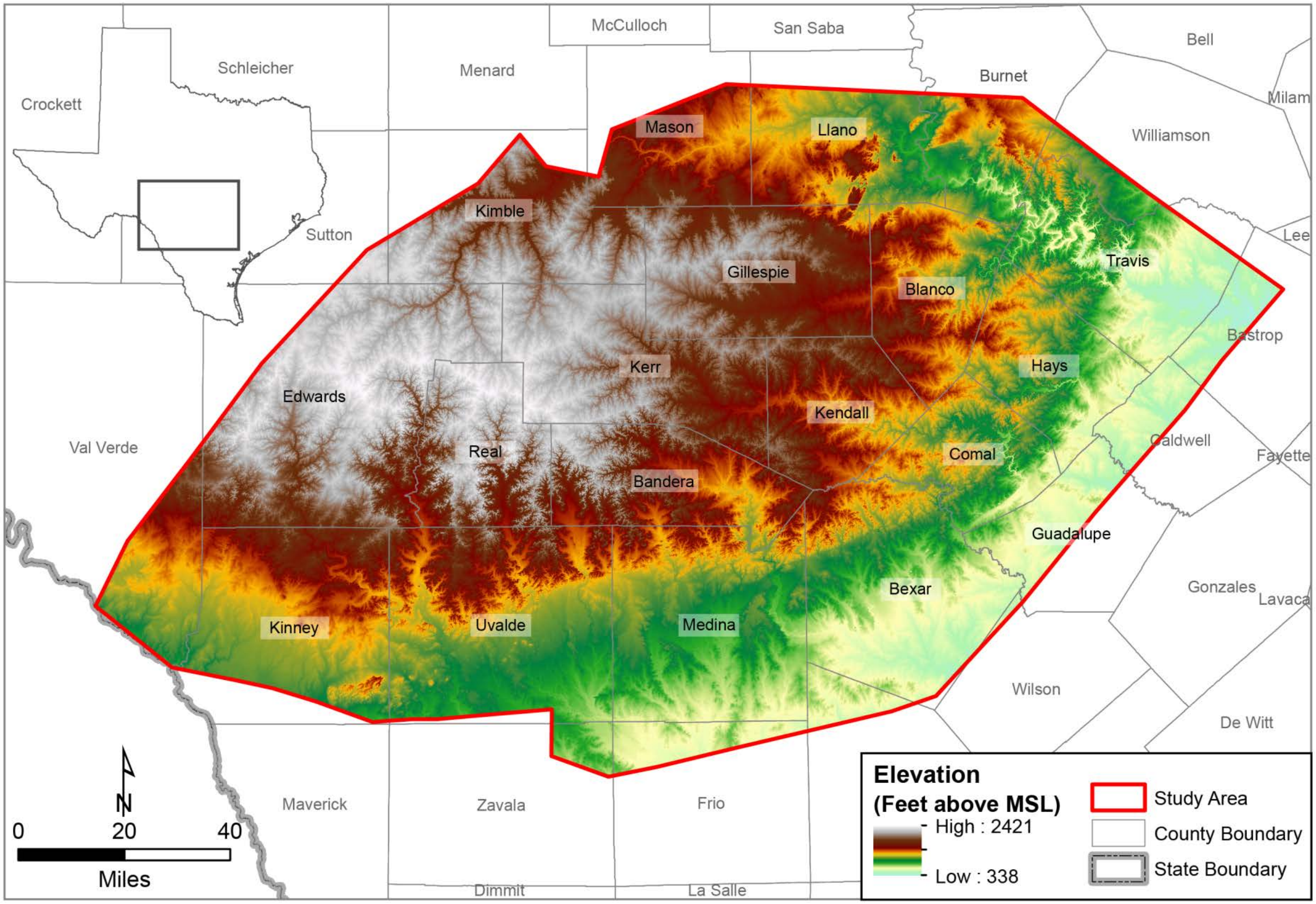

Figure 2.1.3 **Topographic elevation of the study area.**

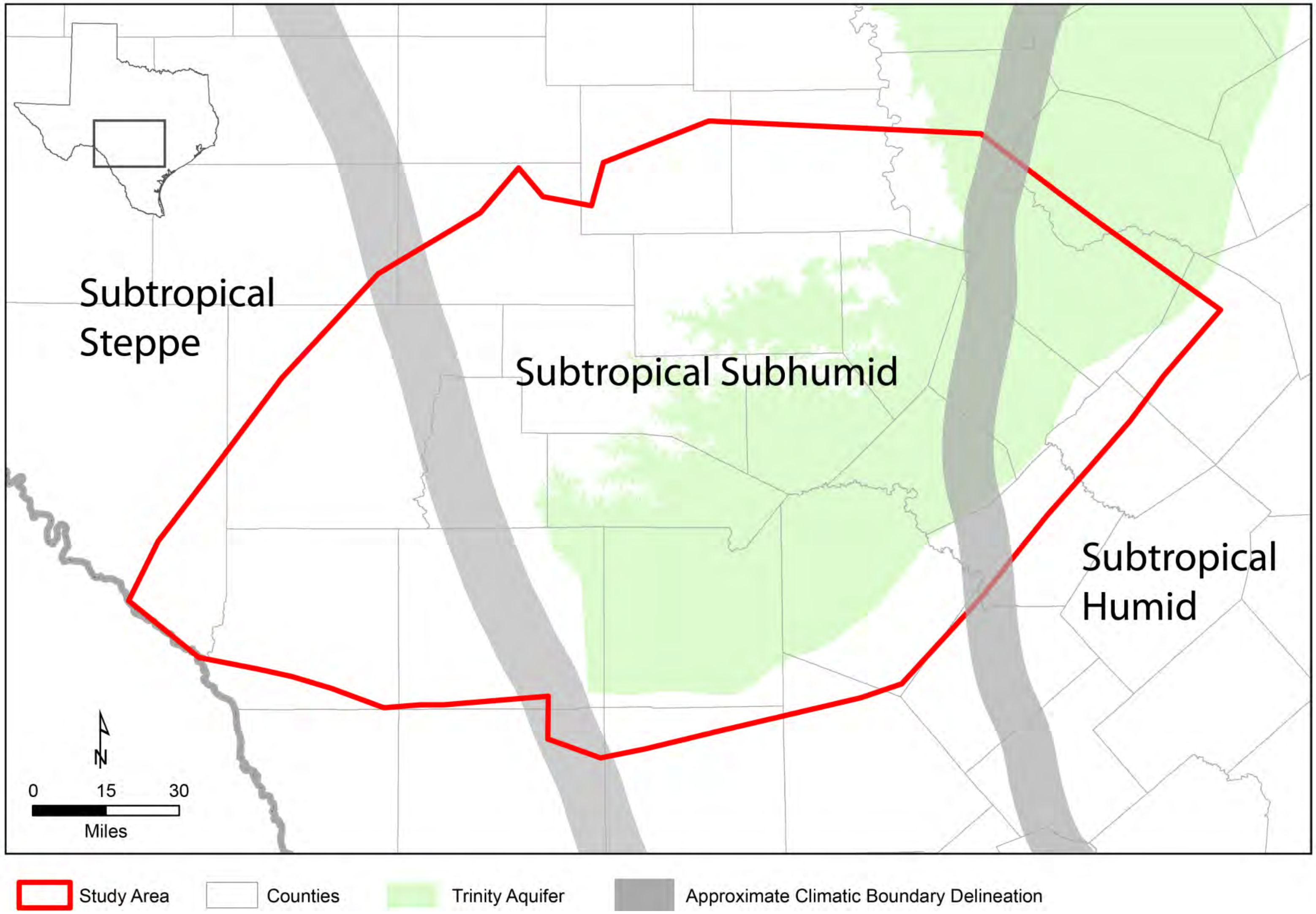

Figure 2.1.4 Climatic classifications as defined by Larkin and Bomar (1983).

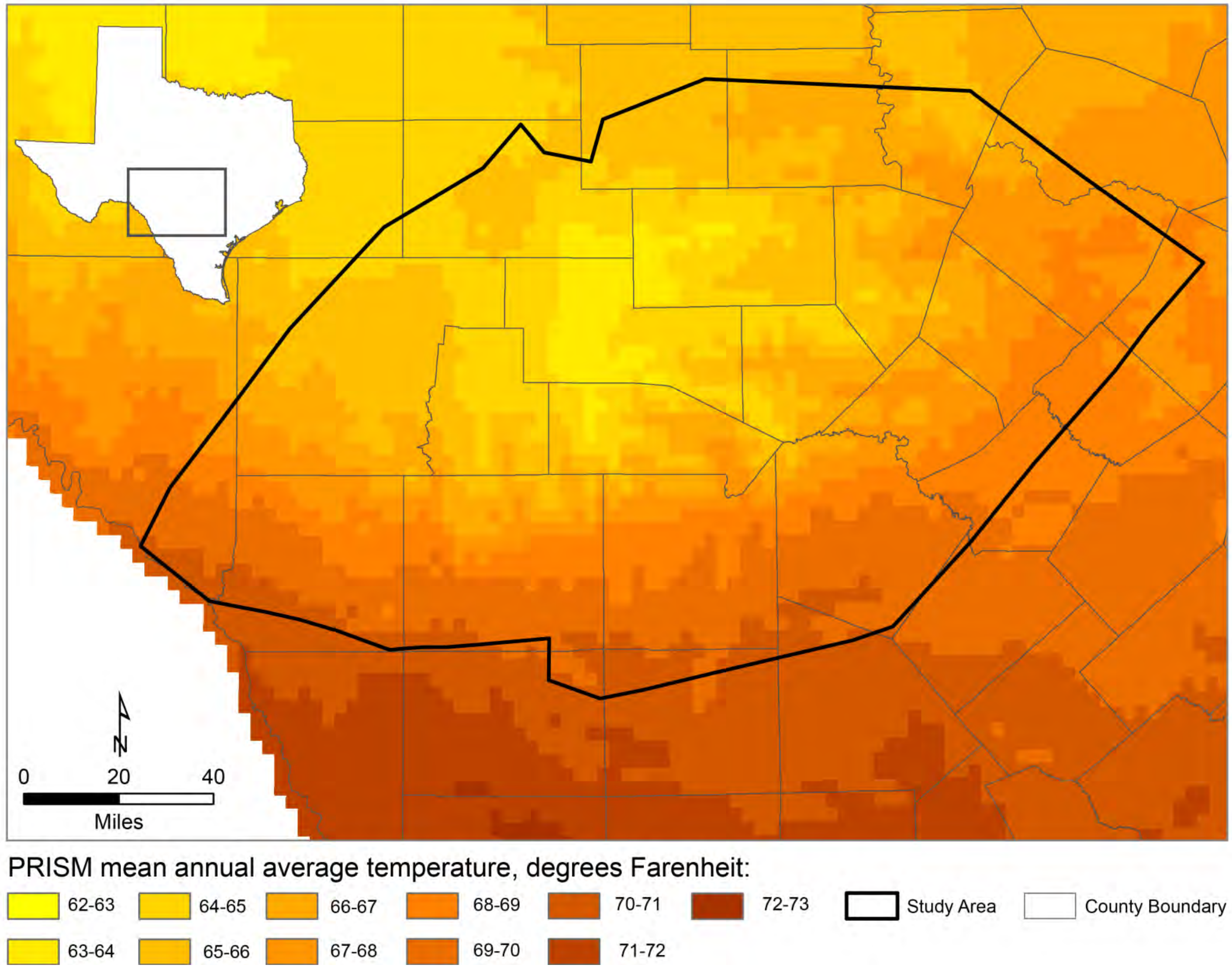

Figure 2.1.5 **Mean annual average temperature data from 1980-2010 for the study area (PRISM Climate Group, 2016).**

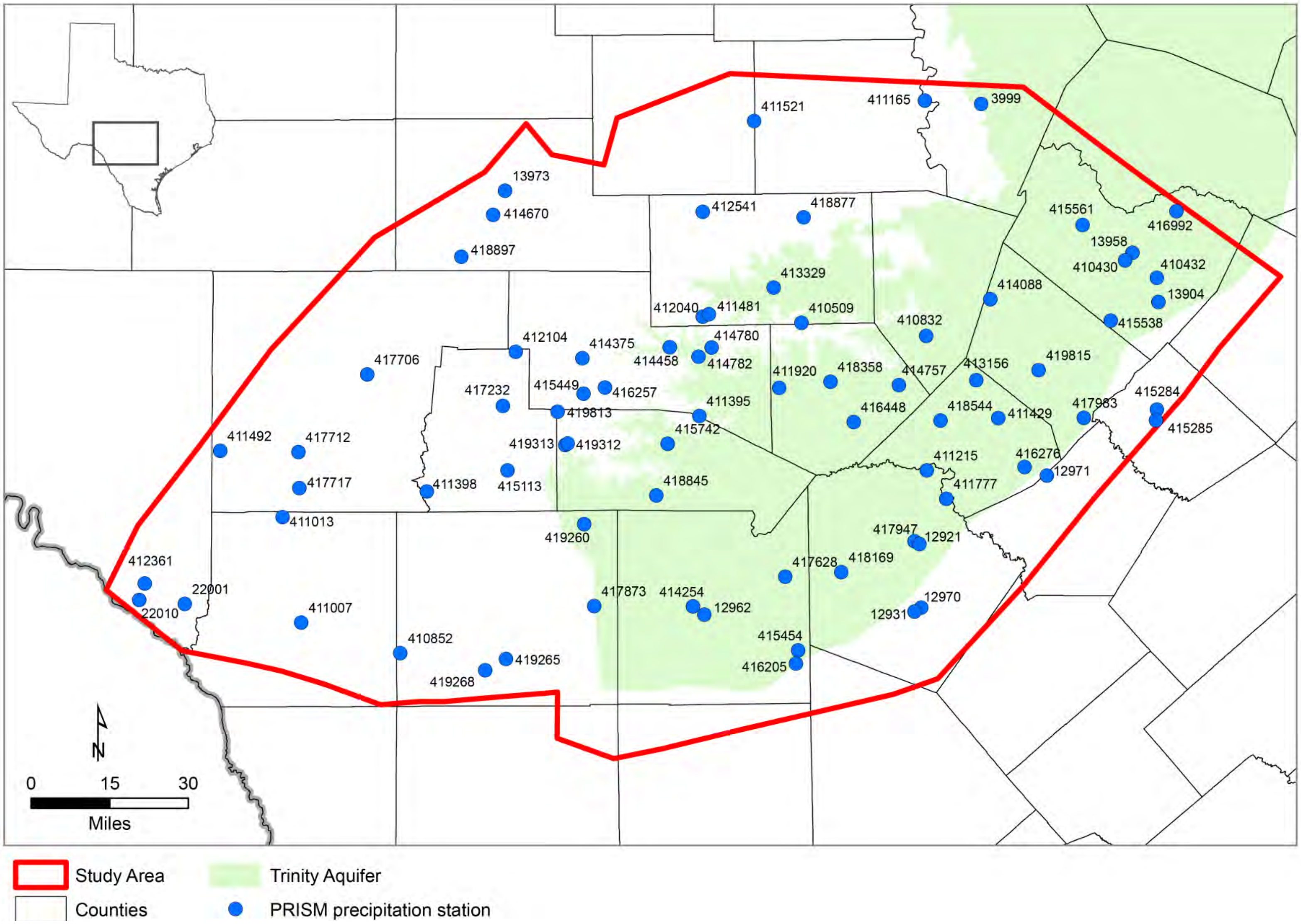

Figure 2.1.6 Locations of PRISM precipitation stations in the study area.

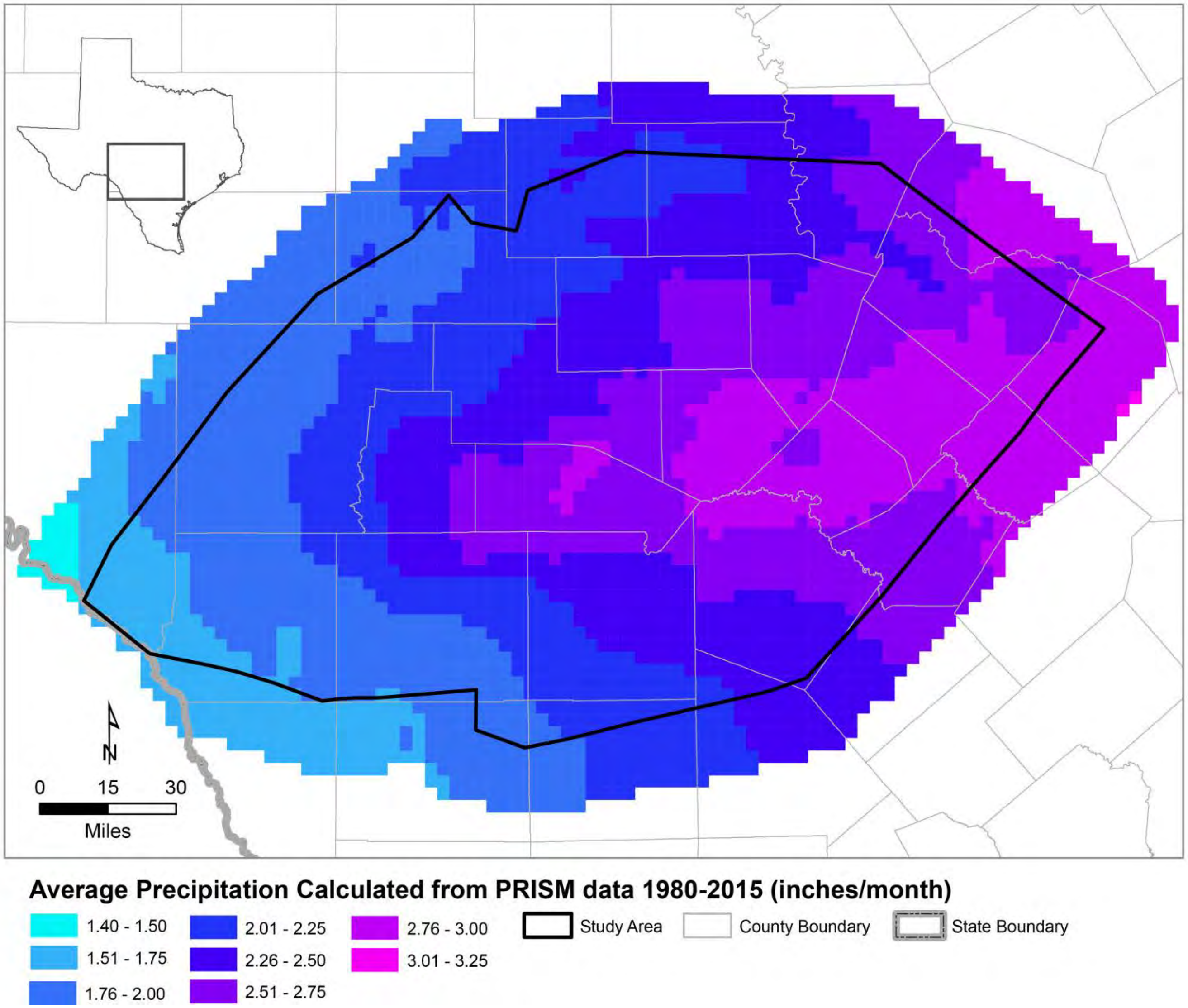

Figure 2.1.7 **Average annual precipitation in the study area from 1980-2015 (PRISM Climate Group, 2016).**

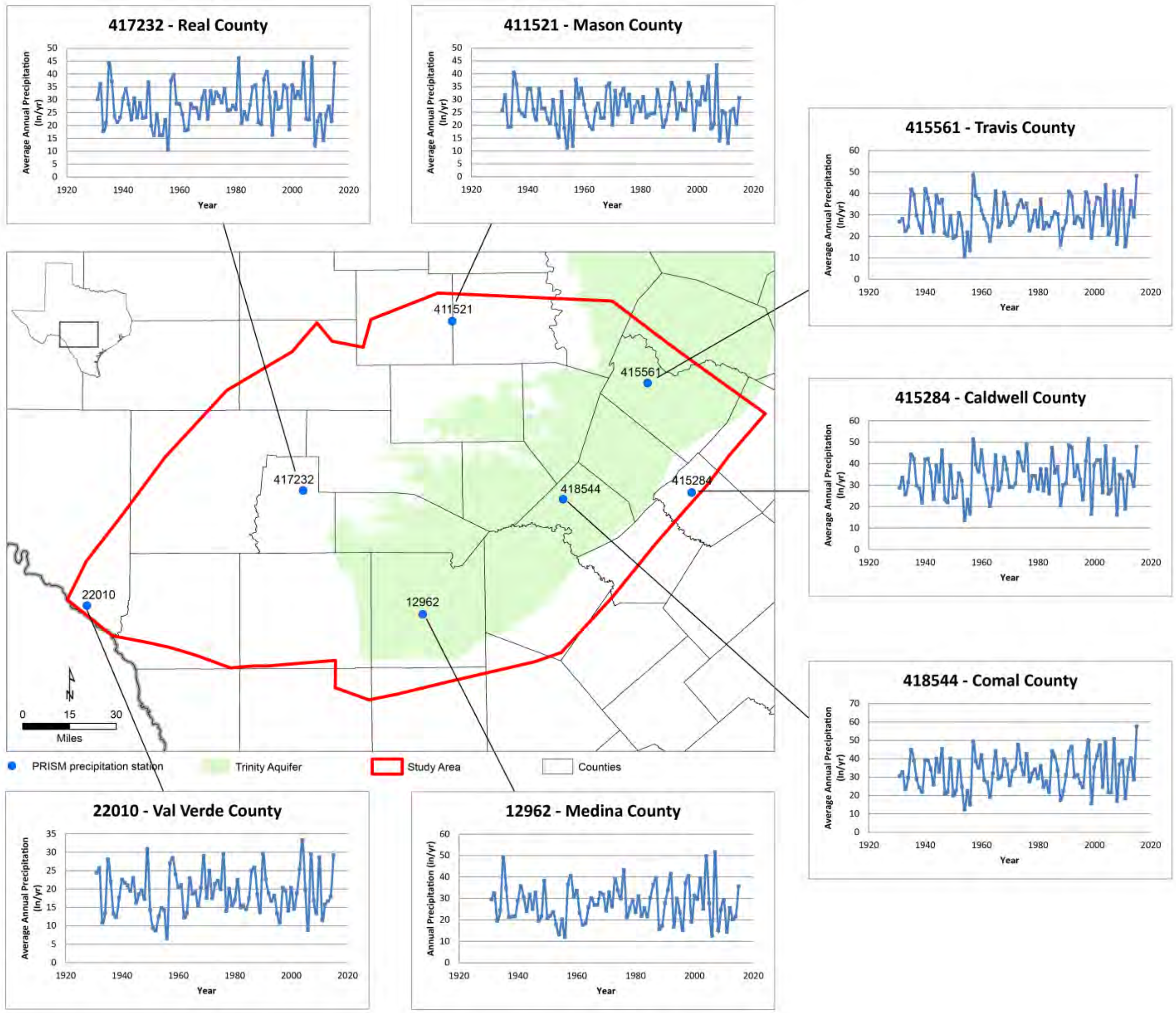

Figure 2.1.8 **Examples of the historical variation in annual precipitation at selected gages from 1920-2010, as available (PRISM Climate Group, 2016).**

Figure 2.1.9 **The long-term monthly variation in precipitation for the selected gages in Figure 2.1.8 is shown from 1920-2010, as available (PRISM Climate Group, 2016).**

Figure 2.1.10 **Average annual lake evaporation in the study area per quadrangle (map) as well as average monthly lake evaporation from January 1954 through December 2011 for each quadrangle (graphs) (TWDB, 2009).**

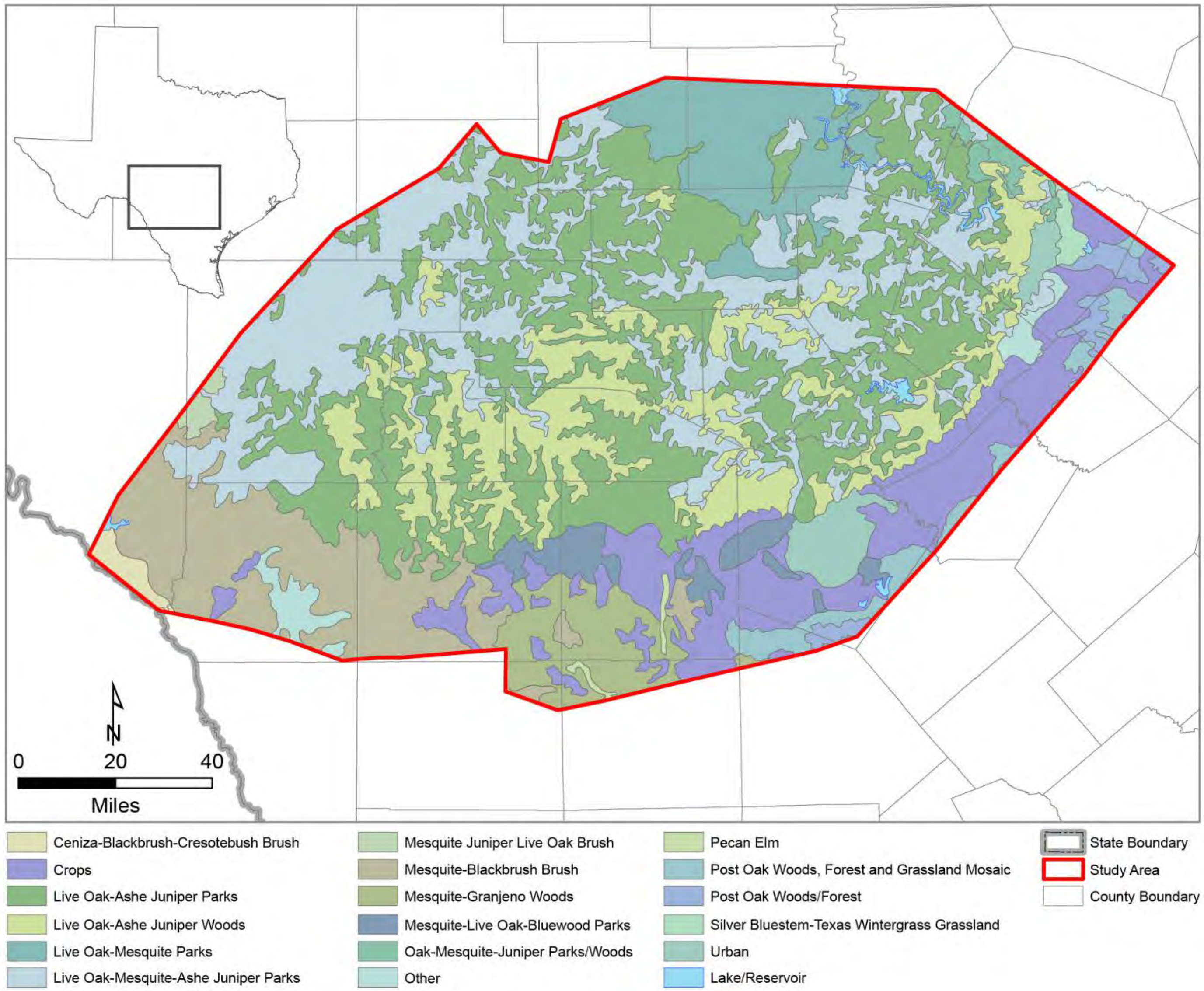

Figure 2.1.11 Map of the types of vegetation present in the study area (TPWD, 1984).

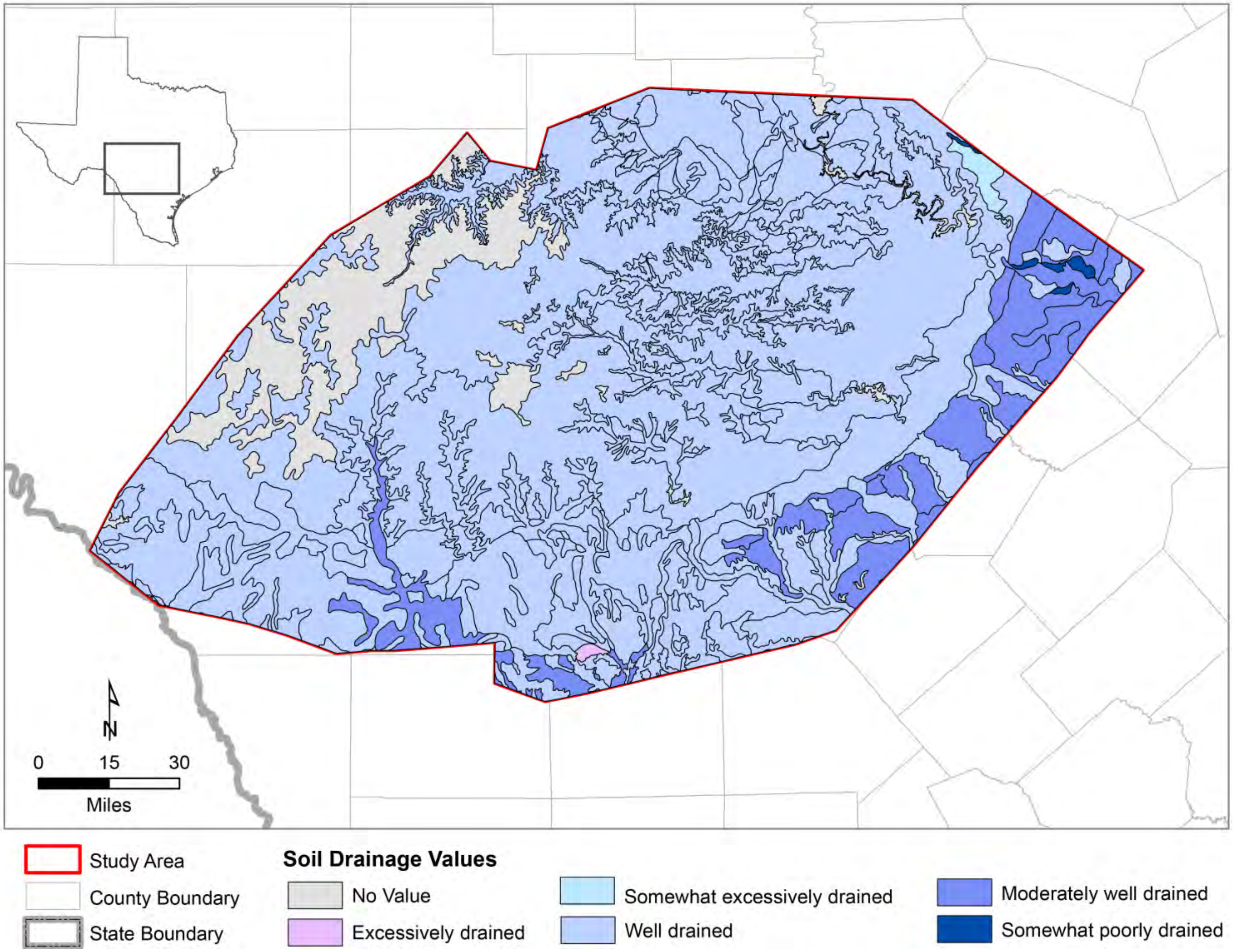

Figure 2.1.12 Map of the types of soil drainage present in the study area (Soil Survey Staff, Natural Resources Conservation Service, USDA, 2018).

2.2 Geology

This section provides a description of the geology within the HCT Aquifer study area. The discussion is divided into the geologic setting, surface geology, stratigraphy, and structural geology. In addition, generalized geologic cross-sections from literature have been modified for the study area and are included in this section.

2.2.1 Geologic Setting

The HCT Aquifer, as defined in George et al. (2011), includes several smaller aquifers within the Trinity Group. These aquifers include the Glen Rose, Hensell, Cow Creek, and Hosston (refer to section 1.0 and 2.0 for further discussion on other aquifers within the study domain). The rocks that make up the Trinity Aquifer in this area are early to middle Cretaceous in age and lay uncomfortably on top of Pre-Cretaceous-age rocks (Figure 2.2.1). Cretaceous-age lithologies consist of limestone, sand, clay, gravel, and conglomerate. The HCT Aquifer crosses numerous depositional domains as shown in Figure 2.2.1 and Figure 2.2.2. These domains include Llano Uplift, Eastern Edwards Plateau, Hill Country, Balcones, and Gulf Coastal Plain. In addition, there are facies markers and structural geologic features that impact deposition and geometry of the units within this study area (Figure 2.2.2 and Figure 2.2.3). These include, Maverick Basin, Devils River Trend, San Marcos Arch, Ouachita-Marathon fold thrust belt, Laramide fold thrust belt, Devils River Uplift, and Balcones Fault Zone (Figure 2.2.2 and Figure 2.2.4). Figure 2.2.5, Figure 2.2.6, and Figure 2.2.7 are generalized cross-sections from Barker and Ardis (1996) and Rose (2016) that have been modified for this study area.

We relied heavily on literature to provide geologic and tectonic information for such a large and diverse domain. For a detailed description on the geology of the HCT domain we suggest reviewing the resources listed in Table 2.2.1.

2.2.2 Surface Geology

Over a large part of the southern end of the study area, are Post-Cretaceous rocks that include Quaternary-age alluvial and fluvial sediments, and Tertiary rocks consisting of Uvalde Gravels and Claiborne and Wilcox Groups. Upper Cretaceous rocks include the Navarro and Taylor Groups, as well as Austin and Eagle Ford Formations. Also included in the Upper Cretaceous outcrop but grouped separately in the surface geology are the Buda, and Del Rio Clay. Outcrop of the Edwards and Trinity rocks occurs over the majority of the study area. Pre-Cretaceous rocks crop out only in the northern portion of the study area in the vicinity of the Llano Uplift.

2.2.3 Stratigraphy/Lithology

The stratigraphy of the Trinity Groups in the Hill Country Aquifer is revealed through creek bed exposures, hillsides, roadcuts, and quarries, as well as scattered water well cuttings and cores. Few large-scale contiguous, non-weathered exposures exist, which makes it difficult to trace out the stratal geometries (Ward and Ward, 2007). Therefore, much of what is known about these formations has been pieced together by correlating marker beds across large areas of the Edwards Plateau (Stricklin et al., 1971) in outcrop and in core.

In the HCT Aquifer region, the Pre-Cretaceous rocks that underlie the Trinity Group include Precambrian metamorphic and igneous rocks and Paleozoic sedimentary rocks. The Llano Uplift was a topographic high during the deposition of the Trinity Group. The Llano Uplift shed debris into the Trinity depositional basin. The topographic high and the variable erosion of the Llano Uplift contributed to uneven terrain at the time of Trinity Group deposition. The lateral and vertical distributions of the Trinity Group were greatly influenced by the Llano Uplift (Stricklin et al., 1971). In the vicinity of the Llano Uplift (updip) the Trinity Group thins to less than 150 ft. Beneath the Balcones Fault Zone (downdip) it thickens to greater than 1,000 ft thick and further downdip it thickens to more than 2,000-ft thick (Barker and Ardis, 1996 and this report).

The base of the HCT Aquifer is the Hosston Formation, which overlies the Pre-Cretaceous rocks. The Hosston is a silisiclastic siltstone and sandstone in the updip region and dolomitic mudstone and grainstone in the downdip region (Barker and Ardis, 1996). This unit varies greatly in thickness from less than 200 ft updip to greater than 1,000 ft downdip. Further updip along the southern flanks of the Llano Uplift, the Hosston grades into the Sycamore Sand (Amsbury, 1974). The Sligo Formation overlies the Hosston and is composed of evaporates, limestone and dolostone. Downdip, the Sligo is shallow-marine carbonate that is up to 500-ft thick and updip it thins to less than 250 ft where it grades into terrigenous clastics.

Above the Sligo is the Hammett Formation, which is also referred to as the Pine Island Shale Member (Murray, 1961). This unit is a mixture of clay, silt, mud, dolomite, and carbonate (Amsbury, 1974). The unit thins to near zero updip and thickens to greater than 100 ft downdip. The Hammett Formation has a transitional boundary with the overlying Cow Creek Formation. The Hammett-Cow Creek contact is arbitrarily determined to be the first well-developed limestone as you transition from shale (Lozo and Stricklin, 1956). The Cow Creek Formation is a fine- to coarse-grained calcarenitic limestone at the bottom that transitions into silty carbonate grains throughout the middle and consists of cross-bedded beach coquina at the top (Barker and Ardis, 1996). The Cow Creek Formation thins to near zero updip and thickens to greater than 300-ft downdip (Imlay, 1945). Overlying the Cow Creek Formation is the Hensell Formation. For much of the HCT Aquifer region the Hensell Formation is comprised of weakly cemented clay, quartz, and calcareous sand (Inden, 1974). In some parts of the HCT Aquifer region, especially the furthest downdip portions and southern Bexar County, the Hensell Formation (referred to Bexar Shale in these locations) is comprised of a mixture of dark mudstone, clay, and shale (Barker and Ardis, 1996). According to Loucks (1977), the shales in the Hensell Formation are the fine-grained, marine equivalent of the near-shore (updip), terrigenous sands. The Hensell Formation varies in thickness from less than 50 ft in the updip to greater than 200 ft thick in the downdip (Imlay, 1945).

Above the Hensell Formation lies the Glen Rose Formation. This consists of the formal subdivisions the Lower Glen Rose Formation and the Upper Glen Rose Formation. The Upper Glen Rose Formation represents the top of the Trinity Group for much of the Trinity Aquifer domain. Lozo and Stricklin (1956) and Stricklin et al. (1971) established these informal lithostratigraphic subdivisions of the Glen Rose Formation that Scott and Filkorn (2007) formalized. These subdivisions are now used throughout the updip and downdip regions of the HCT Aquifer region. The boundary between the two members was put at the top of a widespread, meter-thick unit rich in the small bivalve "Corbula" (Eoursivivas harveyi). Both the Lower and Upper Glen Rose formations are comprised of cyclic depositional units on several scales. Lithologic units include shallow-water wackestone, packstone, and grainstone, as well as finely crystalline dolostone beds and a terrigenous claystone (Ferrill et al., 2011). Where the Glen Rose Formation crops out in the Hill Country, the Lower Glen Rose Formation is about 260 ft thick (Abbott, 1966), and the upper Glen Rose Formation is about 480 ft thick (estimated from Abbott, 1966; Stricklin et al., 1971; and Farlow et al., 2006). The Glen Rose Formation in the subsurface and downdip is much thicker, in excess of 1,500 ft (Welder and Reeves, 1964).

For most of the Hill Country, the top of the Trinity Group is overlain by the Walnut Formation, which, in turn, is overlain by the Kainer Formation of the Edwards Group. The Edwards Group consists of massive, porous, highly fractured lower Cretaceous limestone with thicknesses that range from less than 500 ft thick in the updip and greater than 1,000 ft in the downdip (Rose, 1972). Above the Edwards Group is the Georgetown Formation. The Georgetown Formation is comprised of discontinuous beds of alternating thin, fine-grained limestone or marly limestone. It ranges in thickness from less than 60 ft in the updip and greater than 100 ft to absent in other parts of the Hill Country region (Rose, 1972).

2.2.4 Structural Geology

Rocks of both the Edwards and Trinity aquifers crop out in the Edwards Plateau region of Texas, and their southern outcrop boundary are within the Balcones Fault Zone (Figure 2.2.4). The tectonic history and structural development of the Balcones Fault Zone have been documented extensively (Cope, 1880; Hill, 1889, 1890; Foley, 1926; Weeks, 1945; George, 1952; Sandidge, 1959; Murray, 1961; Young, 1972; Rose, 1986; Collins, 2000; Ferrill et al., 2004, 2008, 2009, 2011, 2012; Ferrill and Morris, 2008; Morris et al., 2009a, b, 2014; Zahm et al., 2010). The rocks in this study domain have experienced a relatively simple stress and deformation history dominated by southeast-directed extension toward the Gulf of Mexico basin. The San Marcos and Sabine arches are nearby northwest-trending structures that suggest an additional component of regional Laramide shortening (Halbouty, 1966; Laubach and Jackson, 1990 and references therein). The Balcones Fault Zone formed in the Oligocene, accommodating subsidence of the northwest margin of the Gulf of Mexico basin (Foley, 1926; Murray, 1961; Young, 1972). The system marks the boundary between flat-lying, stable strata of central Texas and the gentle, coastward-dipping sedimentary rocks that are subsiding toward the Gulf of Mexico. The Balcones Fault Zone changes trend from nearly east-west between Del Rio and San Antonio to nearly north-south between Austin and Dallas. In the Hill Country region, the Balcones Fault Zone changes trend by 30° from 080° west of San Antonio to 050° northeast of San Antonio. This fault zone is a 15- to 18-mile-wide en echelon system of mostly south-dipping normal faults that formed during the middle to late Tertiary (Foley, 1926; Murray, 1961; Young, 1972). The zone has a maximum total displacement across its extent of about 1500 ft (Weeks, 1945). The larger normal faults in the Balcones Fault Zone have displacements of 100–1,000 ft) or more (Hill, 1889, 1890; Hovorka et al., 1998; Collins, 2000). Although the overall geometry of the Balcones Fault Zone parallels the strike of the Mesozoic–Paleozoic unconformity (top of Ouachita orogen rocks) and is indirectly controlled by the relict Ouachita structure, faults in the systems have orientations that accommodated Tertiary regional extension. Individual fault and fracture strikes are relatively consistent throughout the region, with an average strike of between 055° and 065° (Ferrill and Morris, 2008; Ferrill et al., 2011; Morris et al., 2014; McGinnis et al., 2015). Faults are generally considered to be steep (60-70°) to nearly vertical based on local measurements and nearly linear fault traces in areas of significant topographic relief (Hill, 1889; McGinnis et al., 2015). Offset of Cretaceous platform carbonate strata (Rose, 1972) across the Balcones Fault Zone, including the Edwards and Trinity aquifers, resulted in a broad, weathered escarpment of vegetated limestone hills rising from the predominantly clastic coastal plains to the uplands of the Texas Craton. Within the fault system, the dip of bedding varies from gentle coastward to nearly horizontal, with occasional localized dip of hanging wall beds northward into some faults. Faulting has been interpreted as being rooted in the deeply buried foreland-basin sediments of the Ouachita orogeny (Murray, 1956).

Faults of the Balcones Fault Zone exert important first-order controls on fluid flow within the Trinity and the overlying Edwards aquifers and their hydrologic properties are a source of uncertainty in describing groundwater flow in this region. The faults that make up the Balcones Fault Zone juxtapose both permeable and relatively impermeable hydrogeologic units, they cause substantial structural thinning of the lower Cretaceous strata, and they provide potential pathways for infiltration of surface water into the groundwater systems and for lateral and vertical movement of groundwater (Ferrill and Morris, 2008; Ferrill et al., 2008, 2011; McGinnis et al., 2015). Extensional deformation in the Balcones Fault Zone has produced a network of faults likely to influence intra-aquifer permeability due to fault zone processes producing permeability anisotropy with maximum transmissivity parallel to fault strike (Ferrill et al., 2009). Displacement on these faults has thinned the aquifer along each fault, further restricting aquifer connectivity perpendicular to fault strike. Displacement on the large faults can thin the Trinity units by 50–100 percent of their total stratal thickness, and juxtapose Pre-Cretaceous rocks against Trinity strata or Trinity strata against Edwards strata. The impact of this scale of offset is that potential water-bearing units can be absent in places or there is the opportunity for interaquifer communication. Understanding the fault network in the Balcones Fault Zone is a daunting task, however, it is a necessary effort in order to reduce uncertainty in hydrologic models for this area.

Table 2.2.1 Literature used for geologic and hydrogeologic context.

Structural/Tectonic	**Stratigraphic/Lithologic**
Barnes (1977) Del Rio Sheet	Abbott (1966)
Barnes (1979) Seguin Sheet	Amsbury (1974)
Barnes (1980) Sonora Sheet	Amsbury (1988)
Barnes (1981a) Llano Sheet	Amsbury (1996)
Barnes (1981b) Austin Sheet	Amsbury and Jones (1996)
Barnes (1983) San Antonio Sheet	Barker and Ardis (1996)
Collins (2000)	Barnes (1977) Del Rio Sheet
Collins and Hovorka (1997)	Barnes (1979) Seguin Sheet
Cope (1880)	Barnes (1980) Sonora Sheet
Ewing (1991)	Barnes (1981a) Llano Sheet
Ferrill et al. (2009)	Barnes (1981b) Austin Sheet
Ferrill et al. (2008)	Barnes (1983) San Antonio Sheet
Ferrill et al. (2011)	Bebout and Loucks (1974)
Ferrill and Morris (2008)	Bebout (1977)
Ferrill et al. (2004)	Bebout et al. (1981)
Ferrill et al. (2012)	Farlow et al. (2006)
Flawn et al. (1961)	Flawn et al. (1961)
Foley (1926)	Hill (1891)
Fratesi et al. (2015)	Imlay (1945)
George (1952)	Inden and Moore (1983)
Halbouty (1966)	Loucks (1977)
Hill (1889)	Lozo and Smith (1964)
Hill (1890)	Phelps et al. (2014)
Hovorka et al. (1998)	Phelps (2011)
Laubach and Jackson (1990)	Rose (1986b)
McGinnis et al. (2015)	Rose (1972)
Morris et al. (2009a)	Rose (2016a)
Morris et al. (2009b)	Rose (2016b)
Murray (1961)	Scott (2007)
Rose (1986a)	Scott and Filkorn (2007)
Rose (1972)	Smith et al. (2000)
Sandidge (1959)	Stricklin and Amsbury (1974)
Weeks (1945)	Stricklin and Smith (1973)
Young (1972)	Stricklin et al. (1971)
Zahm et al. (2010)	Tucker (1962)
Hydrostratigraphic/Hydrogeologic	Ward and Ward (2007)
Barker and Ardis (1996)	Welder and Reeves (1964)
Clark et al. (2016)	Wierman et al. (2010)
Fratesi et al. (2015)	Winter (1961)
Hovorka et al. (1998)	
Johnson et al. (2010)	
Wierman et al. (2010)	

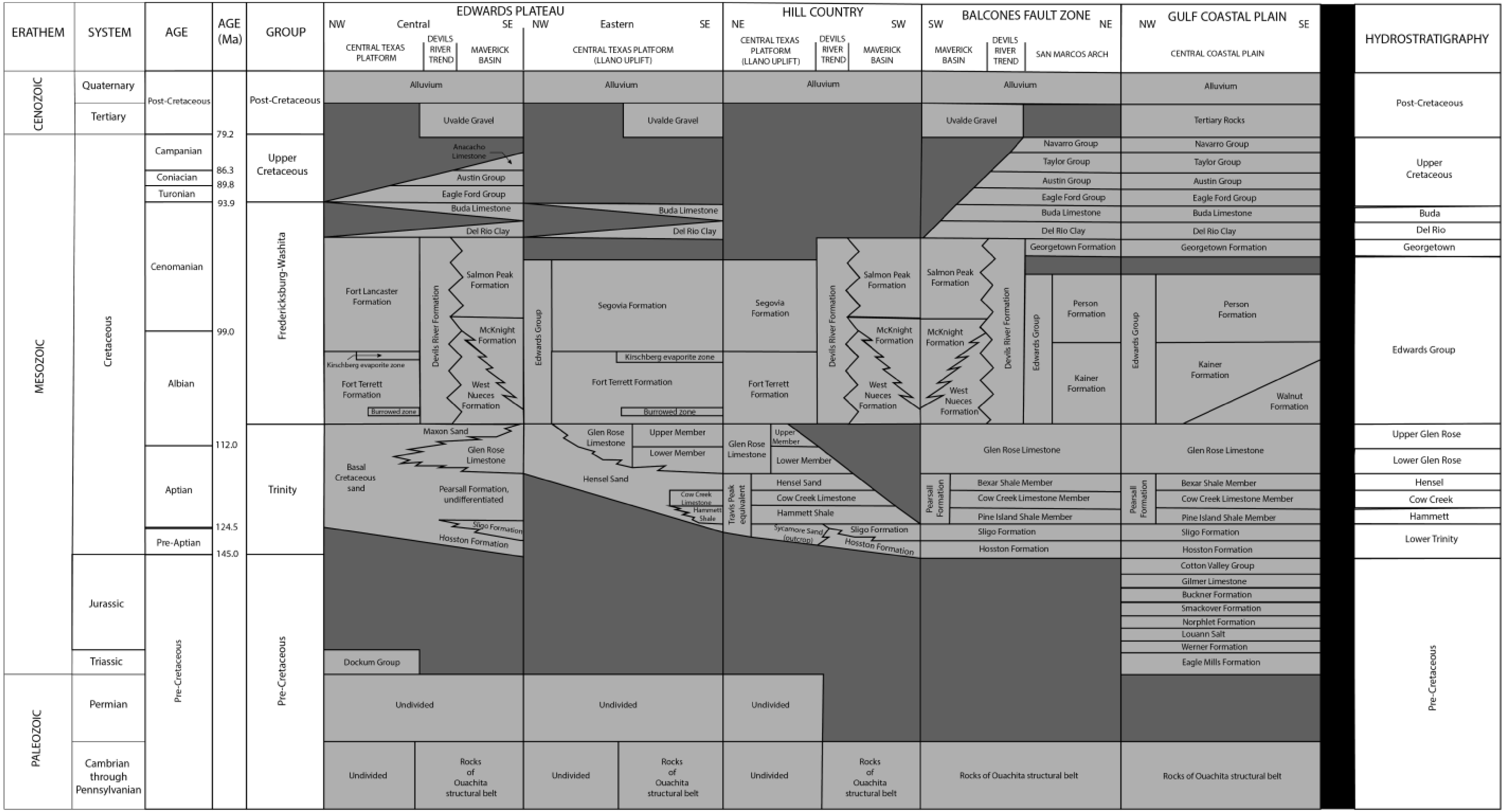

Figure 2.2.1 **Stratigraphic and hydrostratigraphic column of the Hill Country. Stratigraphic units are grouped into depositional domains. (Modified from Barker and Ardis, 1996 and Rose, 2016).**

This page is intentionally blank.

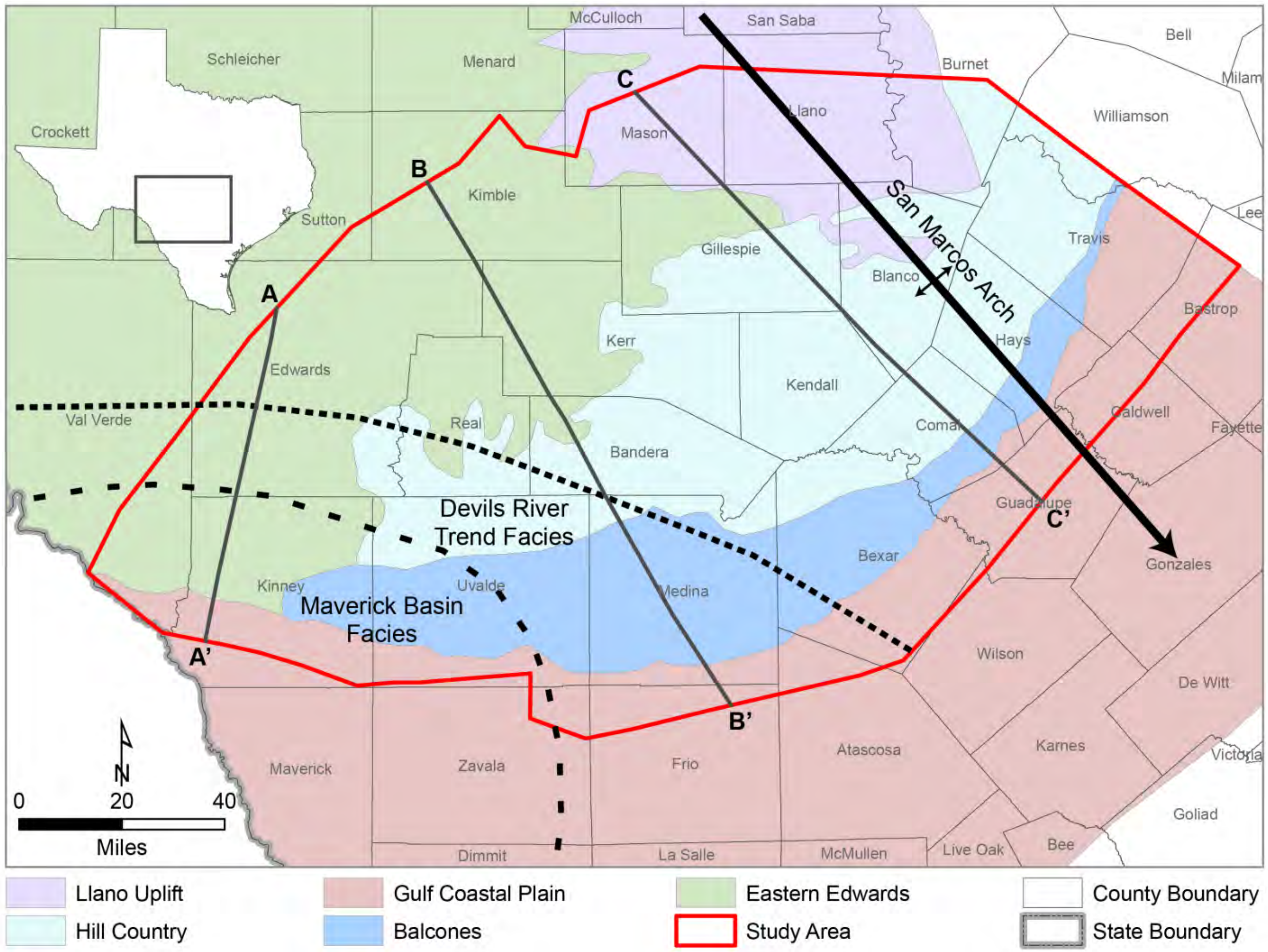

Figure 2.2.2 **Map showing depositional domains as defined by Barker and Ardis, 1996 and Rose, 2016. Facies markers (Maverick Basin and Devils River Trend) are also shown as well as San Marcos Arch. Figure 2.2.1 references these domains and facies for the stratigraphic nomenclature of the study area.**

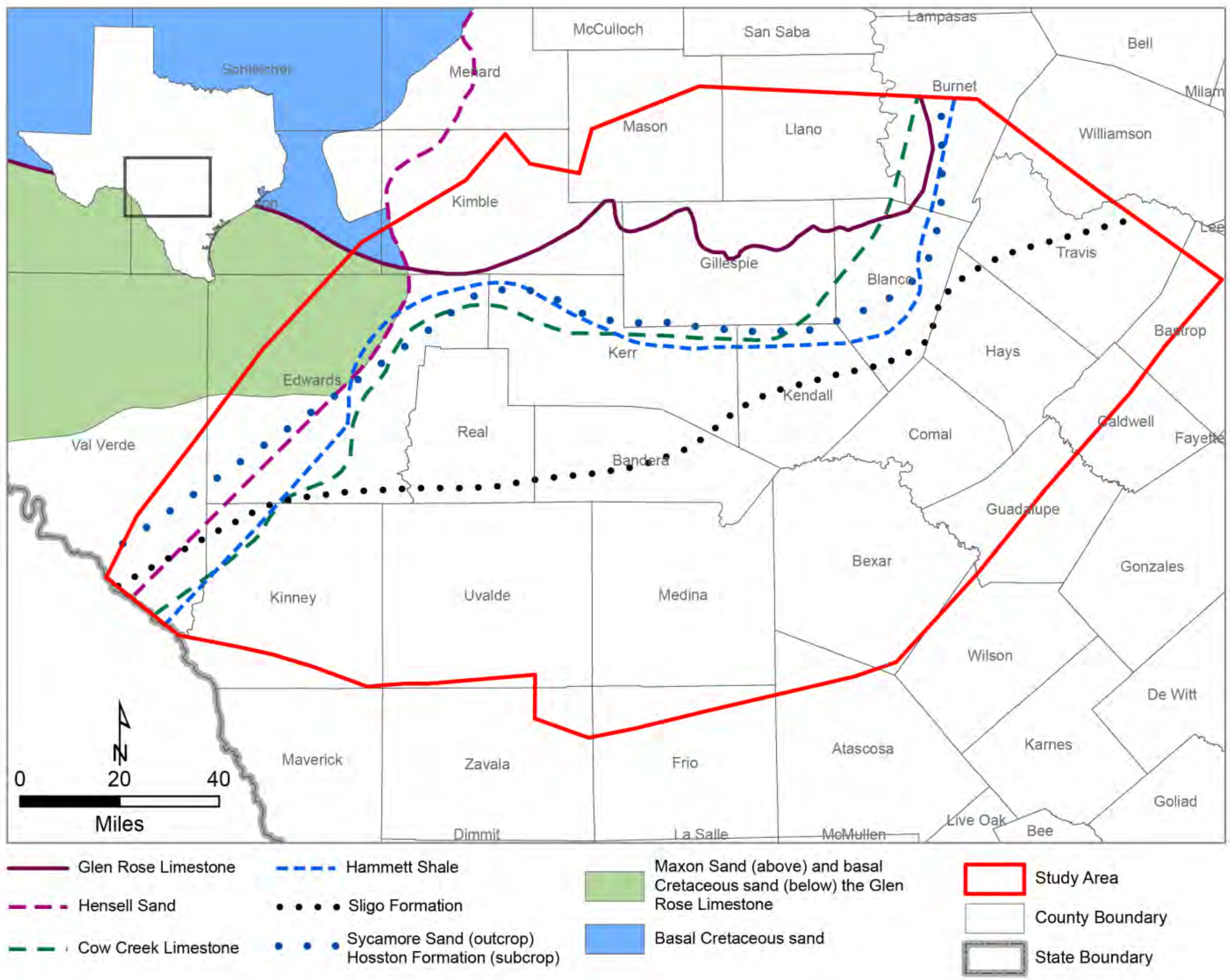

Figure 2.2.3 **Updip limits and lateral distribution of Trinity units across study area. Modified from Figure 8 in Barker and Ardis (1996).**

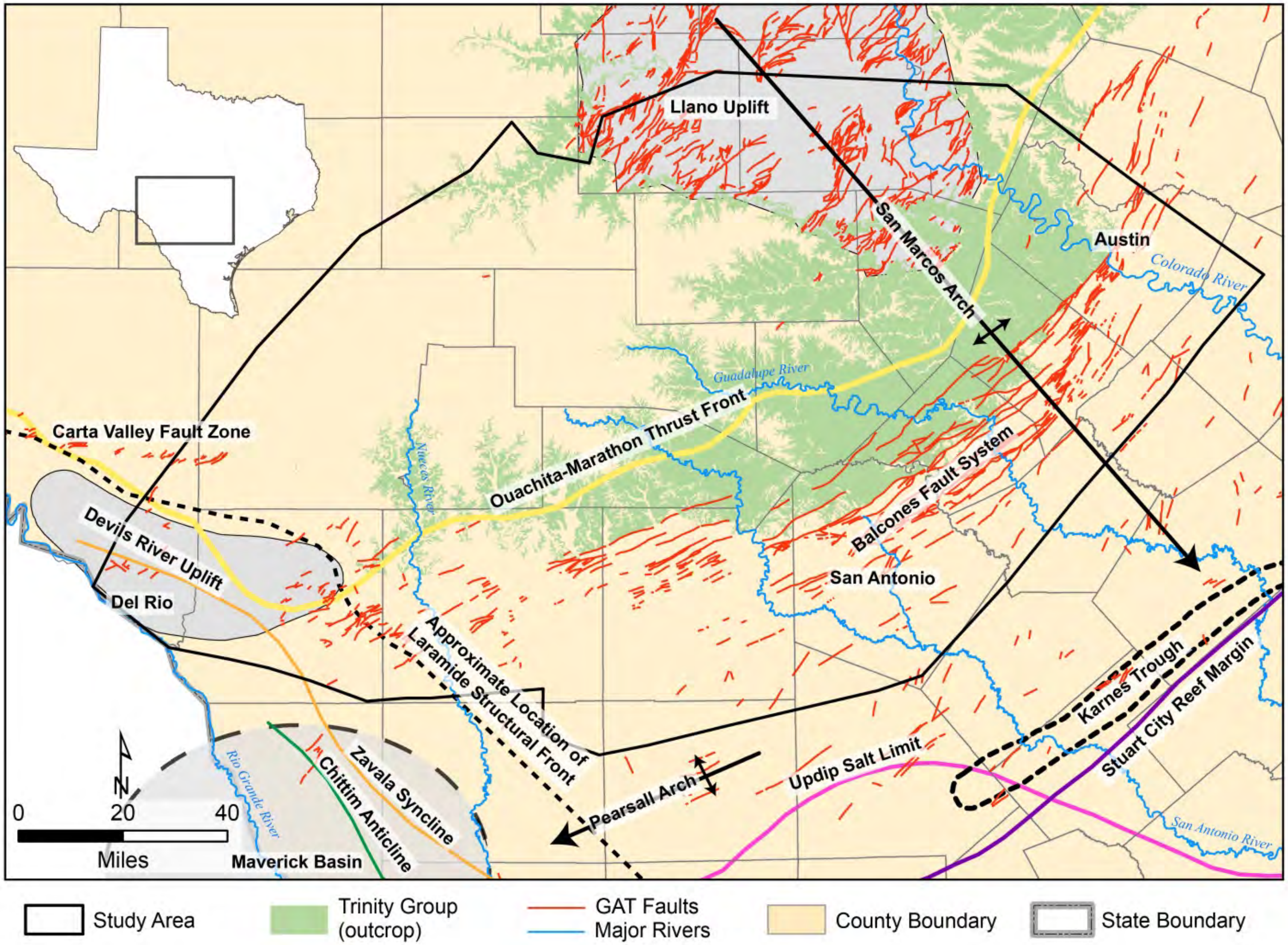

Figure 2.2.4 **Geologic and tectonic synthesis map showing Trinity Group outcrop. Modified from figure 1 in Ferrill et al., 2014, 2017a and b.**

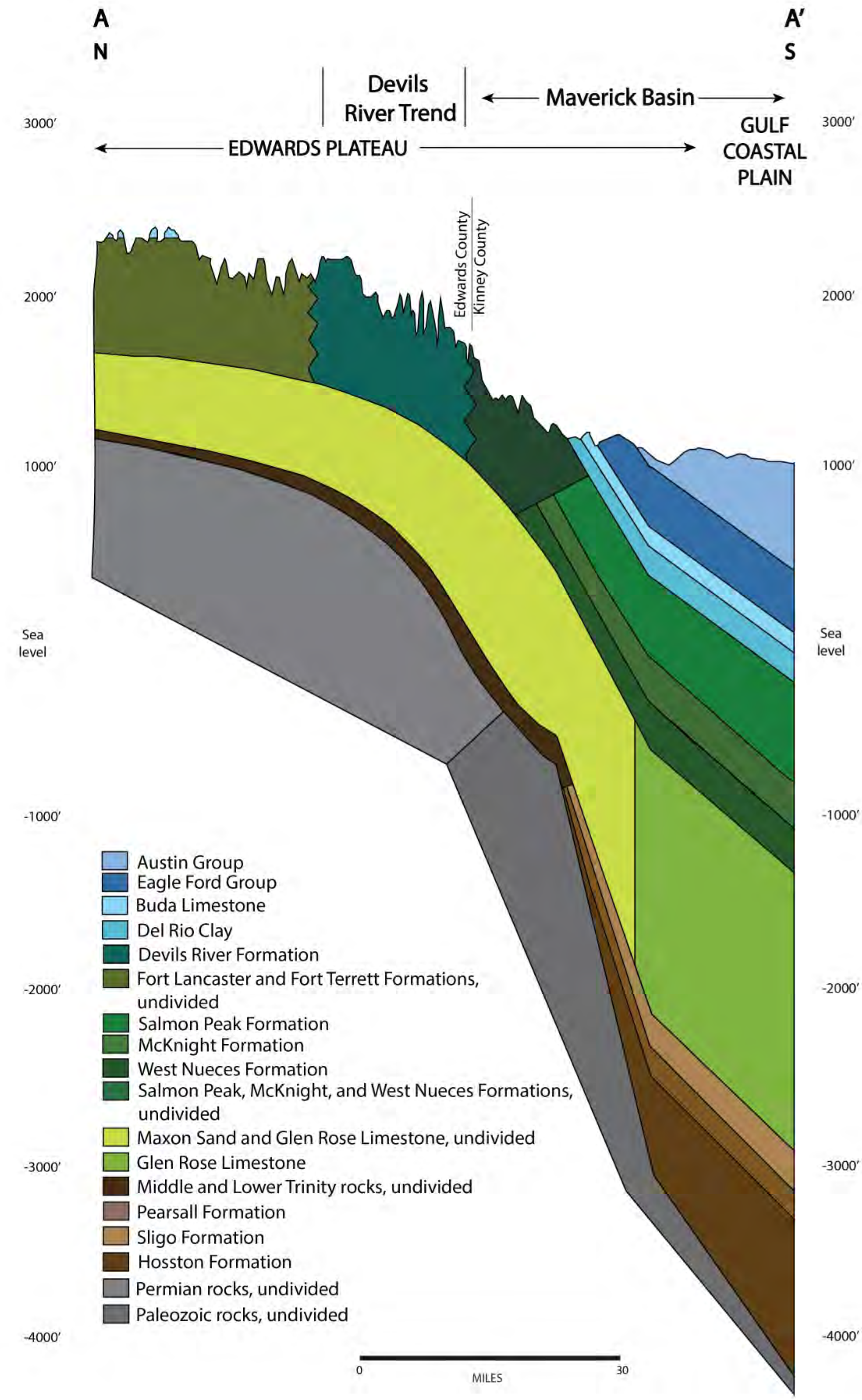

Figure 2.2.5 Generalized geologic cross-section A-A' modified from Barker and Ardis (1996). Location of section on Figure 2.2.1.

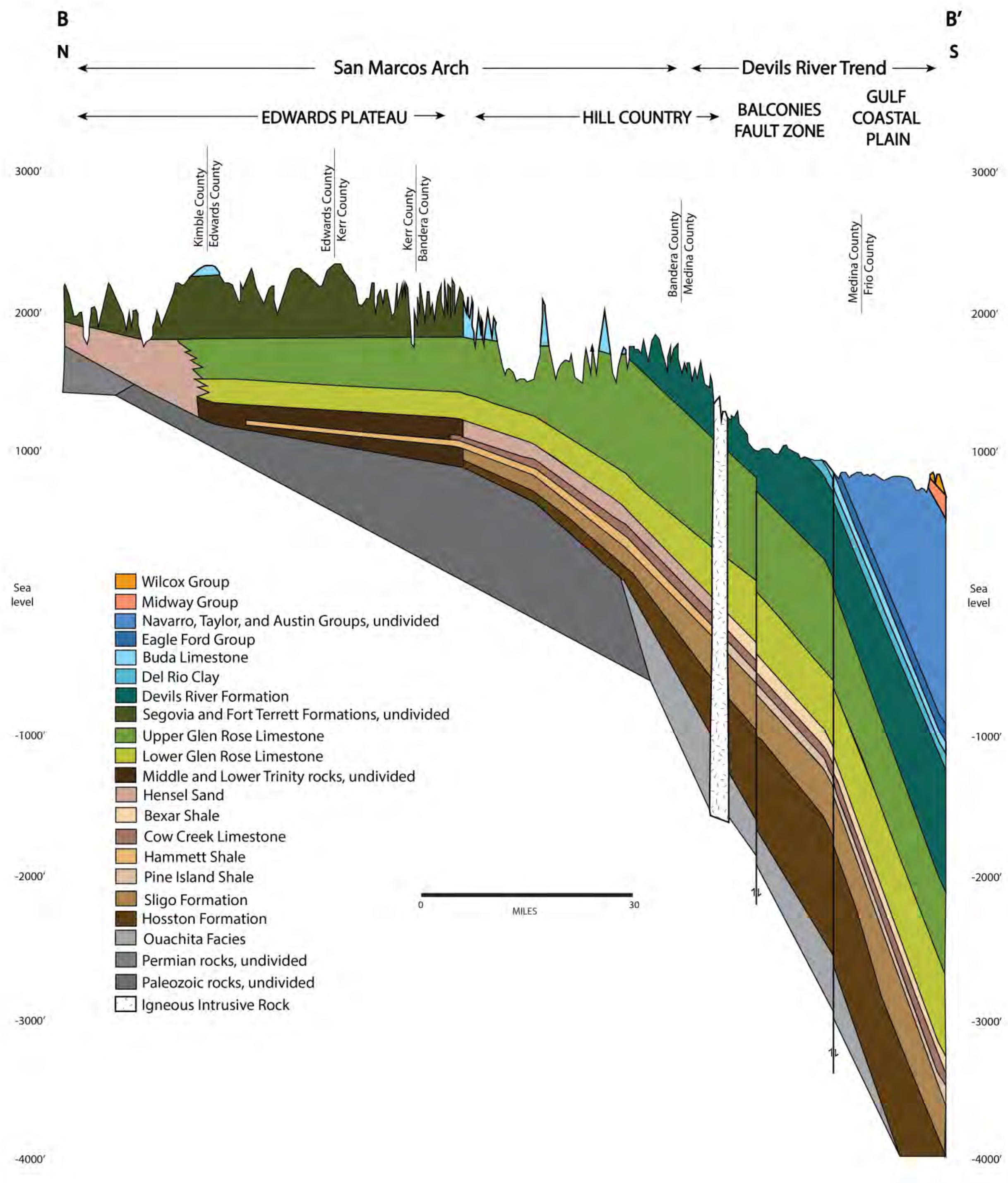

Figure 2.2.6 Generalized geologic cross-section B-B' modified from Barker and Ardis (1996). Location of section on Figure 2.2.1.

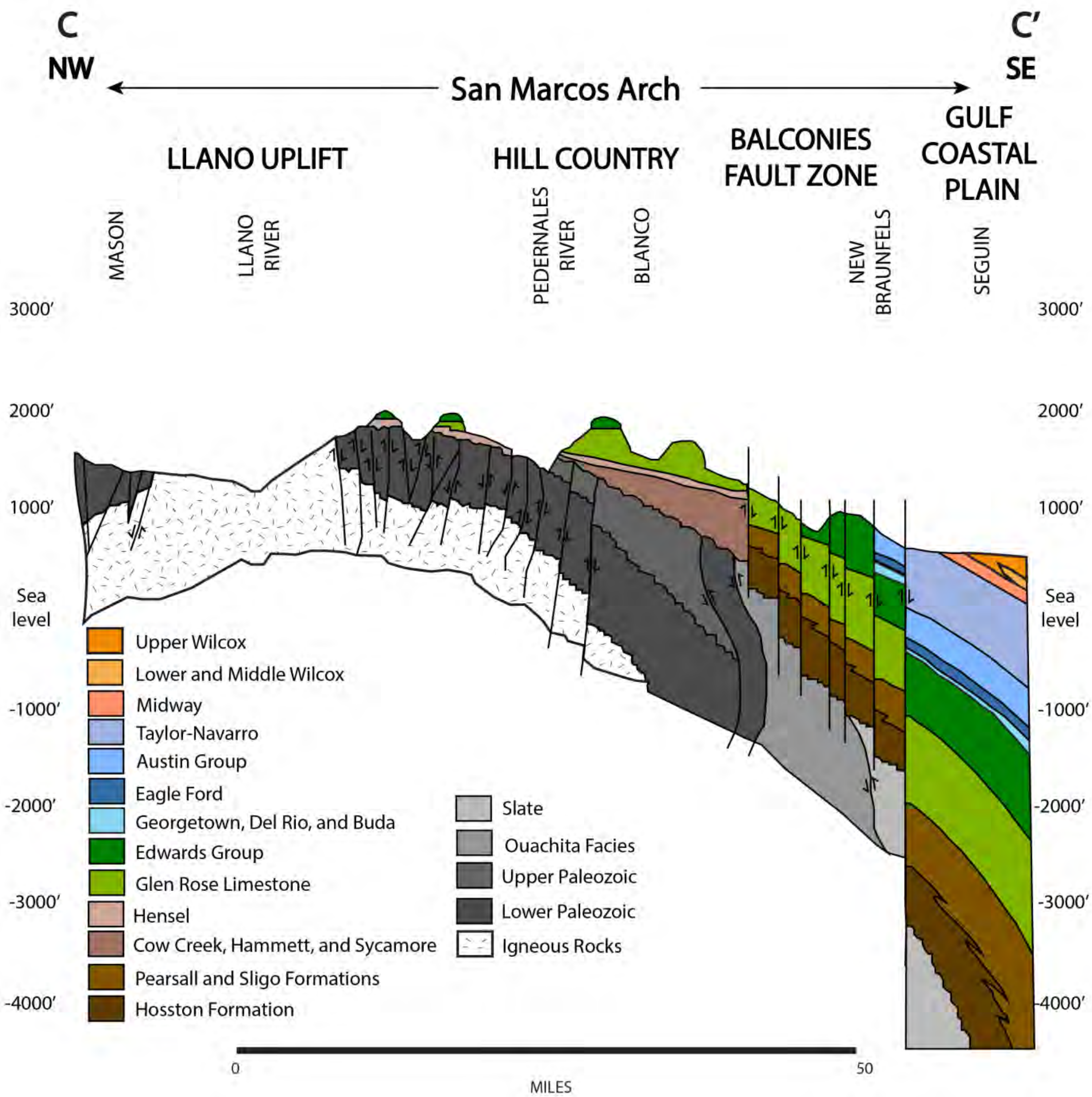

Figure 2.2.7 Generalized geologic cross-section C-C' modified from Rose (2016). Location of section on Figure 2.2.1.

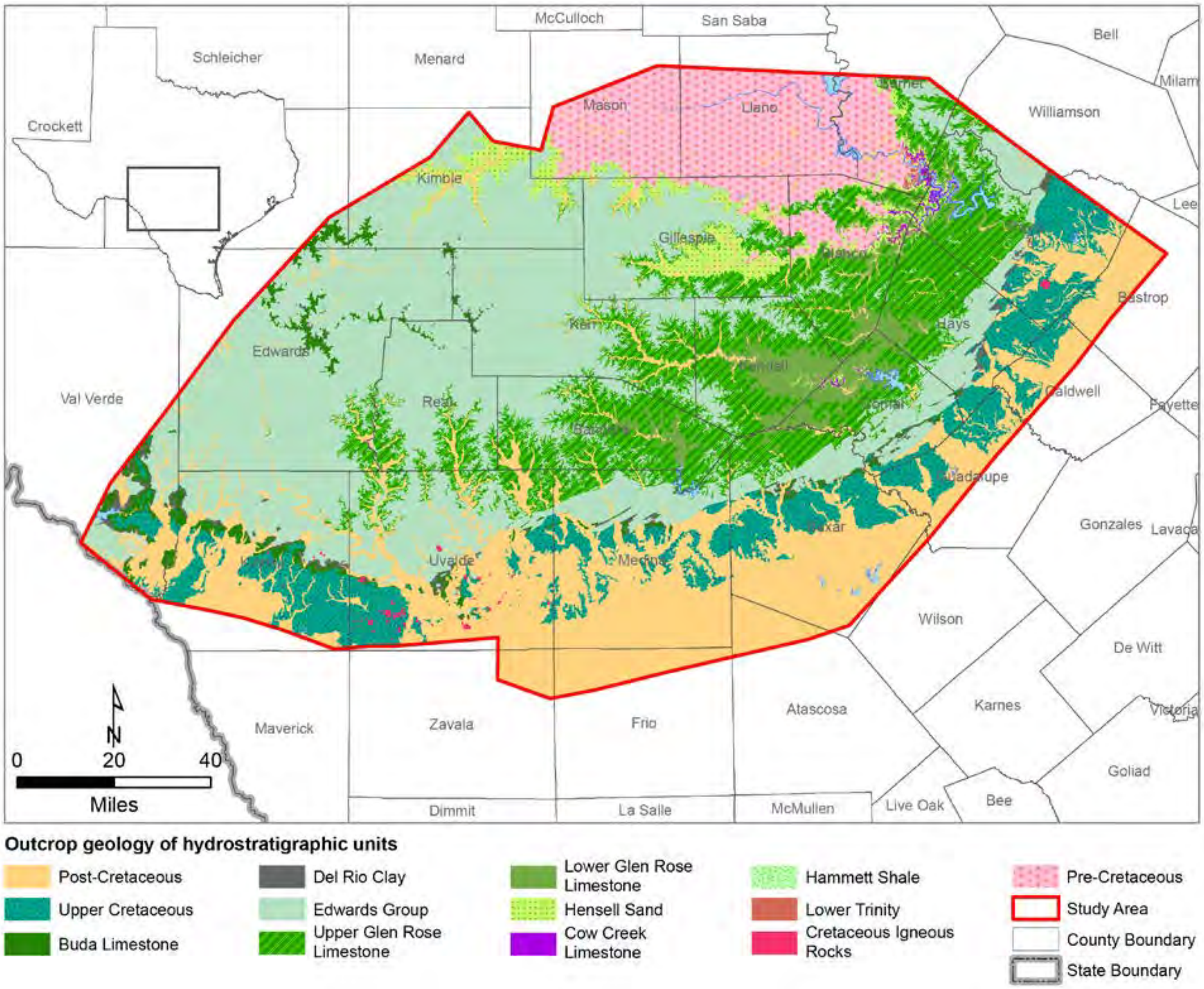

Figure 2.2.8 Generalized surface geology within the study area.

3.0 Previous Investigations

Previous investigations related to groundwater flow/availability models, hydrogeology, and the stratigraphy and geologic framework of the Hill Country region are an integral part of updating the HCT Aquifer conceptual model. The developments from this report will be incorporated into an updated groundwater availability model (GAM) developed by the TWDB. Two GAMs have already been developed (Mace et al., 2000a,b; Jones et al., 2011), with similarities in spatial extent but differences in model layers, calibration periods, and additional parameter data incorporated in the most recent GAM.

The original GAM was completed by Mace et al. (2000a,b) to simulate groundwater elevations and availability through 2050, encompassing most of the Hill Country area. Parts of Bandera and Uvalde counties are excluded from this domain. This model was calibrated for 1975, 1996, and 1997 and is comprised of three layers: the Edwards Group, and the Upper and Middle Trinity aquifers. In 2011, Jones et al. updated and expanded upon this GAM by using the same study area and model boundary but including the Lower Trinity Aquifer as a fourth layer. Additionally, the model was calibrated for 1980-1997 using annual stress periods; Mace et al. (2000a,b) calibrated the model using a summation of monthly stress periods for 1975 steady-state conditions and 1996 and 1997 transient conditions. The most recent GAM generally performed better than the original (Chowdhury et al., 2009) due to the extended calibration period and additional recharge data, which included gain-loss, precipitation and infiltration distribution data, and recharge through structural controls from the Balcones Fault Zone. However, it does not cover the portion of the Trinity Aquifer beyond the estimated 1,000 mg/L TDS line, nor does the domain of the GAM extend sufficiently west to include areas of the Edwards-Trinity Plateau region. As such, the updated conceptual framework in this report incorporates an extended area east-west from Val Verde County to Williamson County to include all of GMA 9. Additionally, it includes the downdip/confined portions of the Trinity Aquifer to assess interformational flow with the Edwards (BFZ) Aquifer and the effects of potential brackish groundwater production.

Although the HCT Aquifer is the focus of this report, this evaluation cannot be fully engaged without recognizing the hydraulic relationship with the Edwards (BFZ) Aquifer (Small, 1986; Ridgeway and Petrini, 1991; LBG-Guyton and Associates and NRS Consulting Engineers, 1995; Smith and Hunt, 2009; Fratesi et al., 2015). Hydraulic testing using nested wells conducted by the Barton Springs Edwards Aquifer Conservation District provides insight on the hydraulic properties and the hydraulic relationship among the sub-units of the Edwards and Trinity aquifers (Hunt et al., 2010, 2015; 2016).

Several studies investigating the hydrogeology of the HCT Aquifer (expressed in terms of formation and geographical location) include: aquifers of Texas (Guyton and Rose, 1945; George et al., 2011); Trinity Aquifer (Lang, 1953; Wierman et al., 2010); Cretaceous aquifers (Nordstrom, 1982); Glen Rose Formation (Hammond, 1984); Antlers and Travis Peak formations (Nordstrom, 1987); central Texas (Klemt et al., 1975; Baker et al., 1990a); north-central Texas (Baker et al.,1990b; Langley, 1999); Bandera and Kerr counties (Ashworth et al., 2001); Bell, Burnet, and Travis County (Brune and Duffin, 1983; Duffin and Musick, 1991); Blanco County (Follett, 1973); Caldwell County (Follett, 1966); Comal County (George et al., 1952); Edwards County (Long, 1962, 1963); Hays County (DeCook, 1963; Muller and McCoy, 1987; Broun et al., 2007); Hill County (Ashworth, 1983; Bluntzer, 1992); Kendall County

(Reeves, 1967); Kerr County (Reeves, 1969); Real County (Long, 1958); Travis County (George et al., 1941); Cypress Creek/Jacob's Well (Broun et al., 2008a,b); Dripping Springs (Muller, 1990); Seco Creek (Brown, 1999). The western boundary of the study domain was the focus of a U.S. Geological Survey Regional Aquifer-System Analysis (RASA) (Kuniansky, 1989; Kuniansky and Hooligan, 1994; Barker et al., 1994; Barker and Ardis, 1996). Although the focus of this RASA was the Edwards-Trinity Aquifer, information gained during these studies was useful in developing the hydrogeological framework of the western boundary of the study domain.

The basis of developing the hydrostratigraphic framework model partly extends from the work of Fratesi et al. (2015). The authors of that study created the first three-dimensional stratigraphic framework model that incorporated offset (faulted) layers in the Hill Country area. The framework model was constructed to support a refined conceptual and numerical model of the San Antonio segment of the Edwards (BFZ) Aquifer. The domain of the model is the first to incorporate all three zones of the Edwards (BFZ) Aquifer, which inherently encompasses the extent of HCT Aquifer. In doing so, the Glen Rose Limestone of the HCT Aquifer was constructed as a part of this finite element model to account for the hydraulic communication between the Edwards and Trinity aquifers, and thus established the spatial extent and top surface elevation of the Glen Rose within the model domain. Moreover, Table 2.2.1-1 lists the numerous studies that were additionally used on this project to provide geologic and hydrogeologic context for construction of a hydrostratigraphic framework model.

4.0 Hydrologic Setting

The Hydrologic Setting Section describes the features and properties of the study area that influence groundwater flow. These features and properties include the hydrostratigraphy, hydrostratigraphic framework, water elevations and regional groundwater flow, recharge, surface water bodies, hydraulic properties, discharge, and water quality.

4.1 Hydrostratigraphy and Hydrostratigraphic Framework

The Edwards and Trinity aquifers are the primary water source that supplies water for agriculture, industry, municipal, and recreation throughout central and south Texas (Sharp and Banner, 1997; Hovorka et al., 1998; Johnson et al., 2002). Both aquifers are complex karst-, limestone-, and sand-aquifer systems that have permeability architectures that include a combination of host-rock permeability, fractures and fault zones, and dissolution features. Although the strata that make up the Edwards Aquifer are younger and stratigraphically overlie the strata that comprise the Trinity Aquifer, displacement along faults of the Balcones Fault Zone has placed the Edwards Aquifer laterally against (juxtaposed) the Trinity Aquifer. The location and amount of fault juxtaposition vary by location, geometry, and displacement on faults. Along faults that define the structural interface between the Edwards and Trinity aquifers, caves and some fault zones provide conduits for groundwater flow and potential pathways for interaquifer communication. The occurrence of and degree to which interaquifer communication occurs is subject to debate, and various hydrologic and geochemical studies have attempted to constrain the amount of water that the Trinity Aquifer contributes to the Edwards Aquifer (Schultz, 1992; Johnson et al., 2010; Fratesi et al., 2015).

The Edwards Aquifer is a karst aquifer (Maclay and Small, 1983; Johnson et al., 2002) consisting of porous, highly-fractured lower Cretaceous limestone. Stratigraphically, the aquifer is in the Kainer and Person Formations of the Edwards Group and the overlying Georgetown Formation (Maclay and Small, 1983). The aquifer is constrained between an upper confining unit consisting of the Del Rio Clay, Buda Limestone, and Eagle Ford Formation and the underlying Upper Glen Rose Formation of the Trinity Group (Clark, 2000). The Edwards Aquifer extends along the Balcones Escarpment from Bell County in the north and east, curving southwestward through Williamson, Travis, Hays, Comal, and Bexar, then westward through Medina, Uvalde, and Kinney Counties (TNRIS, 1997; Zahm et al., 1998; Hayes, 2000).

The Trinity Aquifer consists of three parts: (i) the upper part consists of the Upper Member of the Glen Rose Formation, (ii) the middle part consists of the Lower Member of the Glen Rose Formation and the Cow Creek Limestone, which are separated by the Hensell Sand or Bexar Shale, and (iii) the lower part consists of the Hosston Formation and overlying Sligo Formation and is separated from the Cow Creek Limestone by the intervening Hammett Shale (Mace et al., 2000). The Trinity Aquifer extends across a large portion of the Texas Hill Country to the north and west of the main faults of the Balcones Fault Zone (Mace et al., 2000).

The northwest part of the study domain contains the Edwards-Trinity (Plateau) Aquifer (Figure 2.0.9). The aquifer units are composed predominantly of limestone and dolomite of the Edwards

Group and sands of the Trinity Group (Mace 2011). The division between the Edwards, Trinity, and Edwards-Trinity Aquifers are based on regional contrast in hydraulic conductivity that determines the relative capacity within the different units across large areas of this region (Barker and Ardis, 1996). For discussion on revision to the aquifer boundaries, refer ro section 5.0 of this report.

4.1.1 Hydrostratigraphic characterization

The two main lithologies that characterize the water-bearing units within the HCT Aquifer domain are Cretaceous-age limestone and sand/sandstone. The non-water-bearing units (confining units) are dominated by clay and shale. The main challenge in characterizing the hydrostratigraphy in this region is to accurately characterize the lithologic variations across such a challenging depositional, structural geologic, and erosional environment, specifically where the (i) lithology transitions from sand (aquifer) or limestone (aquifer) to silt or shale (confining unit), or from sand (aquifer) to limestone (aquifer), (ii) where faults offset and juxtapose different hydrologic units against each other (e.g., when sand and limestone are juxtaposed, when sand/limestone and clay/silt are juxtaposed), and (iii) when units are eroded or truncated across the study area . For this study, we collected 3,960 stratigraphic formation picks for twelve hydrostratigraphic units. We correlated these units across the domain using geophysical logs (spontaneous potential [SP], natural gamma, and resistivity) and stratigraphic picks and unit thickness information from literature for 877 wells (Figure 4.1.1). We collected (from literature) or interpreted (from logs) stratigraphic tops for the Buda Limestone, Del Rio Clay, Georgetown Formation, Edwards Group, Hensell Formation, Cow Creek Formation, Hammett Formation, Sligo Formation, Hosston Formation, and Pre-Cretaceous undifferentiated units (top only). In addition, we interpreted lithology (sand, limestone, and shale thicknesses) throughout the Trinity Aquifer units from 11 representative wells (Figure 4.1.1) using natural gamma, SP, and resistivity log data (See LAS data files in the database delivery).

4.1.2 Fault Model

Hovorka et al. (1998) produced a fault map that was used to model flow in the Edwards and Trinity aquifers. We utilized that fault map for this project. The Balcones Fault Zone model for this project contains 36 faults that strike between N40° – 70°E with an average dip of 70° to the southeast and a few to the northwest (Figure 4.1.2). This fault distribution represents a small subset of the total number of faults that exist within the study area. However, the faults represented here have the largest displacements and form the largest fault blocks in the study area. According to Hovorka et al. (1998), fault throws (vertical component of displacement) on these faults range from 100 to 850 ft. In the Fratesi et al. (2015) study a more complex fault model was used (Figure 4.1.3). The objective of that model was to include faults that had a throw of 65 ft or greater. For that study 130 faults met the criteria and were incorporated in the model. Figure 4.1.4 is a fault map showing an even greater distribution of faults within the study domain.

Fault distribution has primary control on the permeability architecture of stratified rocks in that it creates a difference in permeability between rock layers. If a stratigraphic sequence is not faulted, vertical inhomogeneity and anisotropy produced by layering will dominate bulk permeability. If a stratigraphic sequence is faulted, the faults exert additional controls on aquifer permeability and flow. These are (i) fault offsets alter the overall geometry of and communication between fault blocks (Allan, 1989; Maclay, 1989; Ferrill and Morris, 2001); (ii) fault zones commonly form relatively impermeable barriers to across-fault flow, form permeable pathways for along-fault flow, or form both barriers and pathways (Arnow, 1963; Caine et al., 1996; Knipe, 1997; Yielding et al., 1997; Ferrill and Morris, 2003). Fault conductivity may be influenced by the current stress field and fault activity (Finkbeiner et al., 1997; Ferrill et al., 1999b); and fault-block deformation by formation of small faults and fractures leads to permeability anisotropy (Antonellini and Aydin, 1994; Mayer and Sharp, 1998; Ferrill et al., 2000).

In rock layers like those that make up the Trinity and Edwards aquifers, groundwater flow and dissolution can enhance the permeability effects of fault systems. In addition, major faults produce tilting of fault blocks and locally thin the aquifer to some fraction of its original thickness. Aquifer communication is decreased in directions perpendicular to the fault strike because of thinning and generally have increased permeability parallel to the fault zone. Smaller faults and extension fractures within fault blocks produce permeability anisotropy within fault blocks. The role of fault-block deformation in the Trinity and Edwards aquifers is variable and has a major influence on fluid flow. When performing groundwater simulations it is important to consider how to implement the permeability anisotropy that is a result of this deformation.

4.1.3 Hydrostratigraphic Framework Model

The stratigraphic framework model was developed to set the boundaries, define distribution of layer thicknesses, and to provide a sufficient-resolution, data- and observation-constrained stratigraphic framework to support the development of the conceptual model and a future groundwater availability model for the HCT Aquifer domain. In addition, the model was constructed with goals of producing a three-dimensional representation of the faulted aquifers and confining strata that can be used to determine and illustrate potential stratigraphic and structural controls upon recharge, groundwater flow, and transmissivity within or between the hydrostratigraphic units. The stratigraphic framework model substantially expands the previous HCT Aquifer domain. To reduce uncertainties in future groundwater availability models (i.e., with fewer inaccuracies and less uncertainty), it is important to have a data-constrained stratigraphic framework model.

The hydrostratigraphic model was created using currently available data, including published geologic and topographic maps, stratigraphic-horizon picks from literature and wells, and stratigraphic interpretations. We followed the approach for model construction that is summarized in Figure 4.1.5, Figure 4.1.6, and Figure 4.1.7.

The hydrostratigraphic model was structured into eleven stratigraphic layers, these include the Edwards (structured surface, Figure 4.1.8; isopach, Figure 4.1.9), the Upper Glen Rose (structured surface, Figure 4.1.10; isopach, Figure 4.1.11), Lower Glen Rose (structured surface, Figure 4.1.12; isopach, Figure 4.1.13), Hensell (structured surface, Figure 4.1.14; isopach, Figure 4.1.15), Cow Creek (structured surface, Figure 4.1.16; isopach, Figure 4.1.17), Hammett (structured surface, Figure 4.1.18; isopach, Figure 4.1.19), the Sligo (structured surface, Figure 4.1.20; isopach, Figure 4.1.21), Hosston (structured surface, Figure 4.1.22; isopach, Figure 4.1.23), and the Pre-Cretaceous formations (structured surface, Figure 4.1.24). Lateral changes in aquifer geometry and fault juxtaposition are illustrated in three vertical geologic cross sections extracted from the hydrostratigraphic framework model (Figure 4.1.25, Figure 4.1.26, and Figure 4.1.27). By developing a detailed hydrostratigraphic model, additional layers can be incorporated into the numerical model without having to develop a new model. As new data become available, this model can be efficiently modified in an iterative fashion to keep the hydrostratigraphic framework up-to-date for use as the basis for increasingly refined groundwater flow and availability modeling.

4.1.4 Stratigraphic Framework Model Software

Three primary software programs were used to develop the stratigraphic framework model: (i) Microsoft Excel 2010, (ii) ESRI ArcGIS 10.4, and (iii) Schlumberger Petrel 2015.1. These programs were used to organize tabulated data, assemble and analyze geographically distributed data and interpretations, and conduct three-dimensional stratigraphic framework modeling, respectively.

Microsoft Excel 2010 was used to compile well data including locations, well-head elevation (datum), stratigraphic picks, and thickness information. A spreadsheet of formation thicknesses across the model domain and a quality controlled database of well picks was compiled using this information.

ESRI ArcGIS 10.4 was used to assemble topography, geologic maps, structural data, and other geographically distributed data. These data were used as the basis for defining the model domain and constructing the stratigraphic framework model. Digital data used to create the model were georeferenced. Well picks were evaluated using published maps and point shapefiles.

Petrel is a Windows PC software package that is used primarily by the oil and gas industry and was used to construct stratigraphic framework models. This software package allows surface and subsurface data to be assimilated from multiple sources. Stratigraphic and structural geologic interpretation can then be performed using the database. This integrated software package was selected for this application because of its flexibility in handling data, interpretation, and model development and manipulation, which eliminates the need for multiple highly specialized tools, which would otherwise be required. Petrel has a wide range of export options that facilitate preparing data for input into models and into other software packages.

The stratigraphic framework model was developed in the custom GAM coordinate system. This system uses an Albers projection and the North American 1983 geographic coordinate system and vertical datum. Vertical positions are in ft with respect to mean sea level.

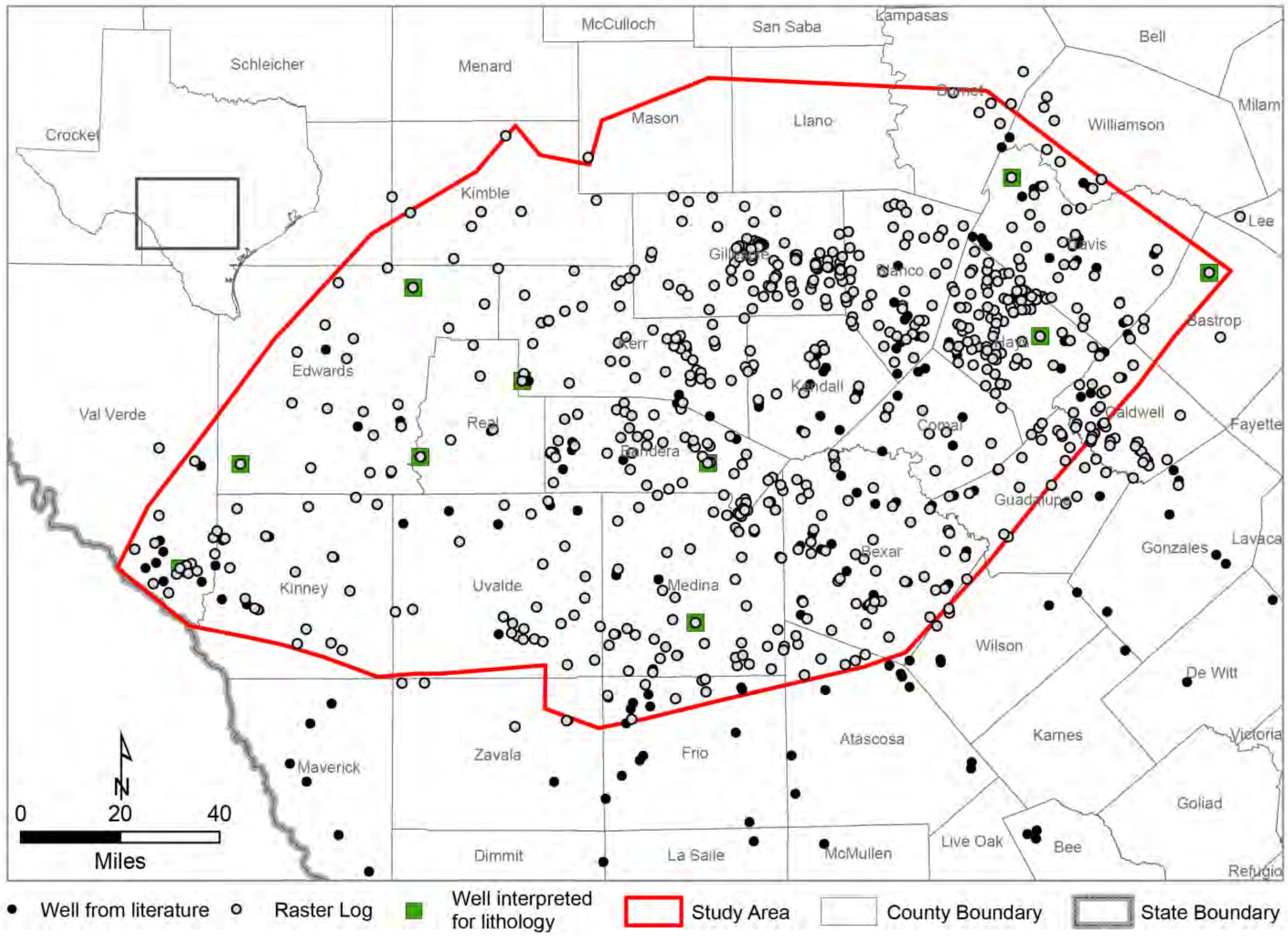

Figure 4.1.1 Wells used for hydrostratigraphic characterization.

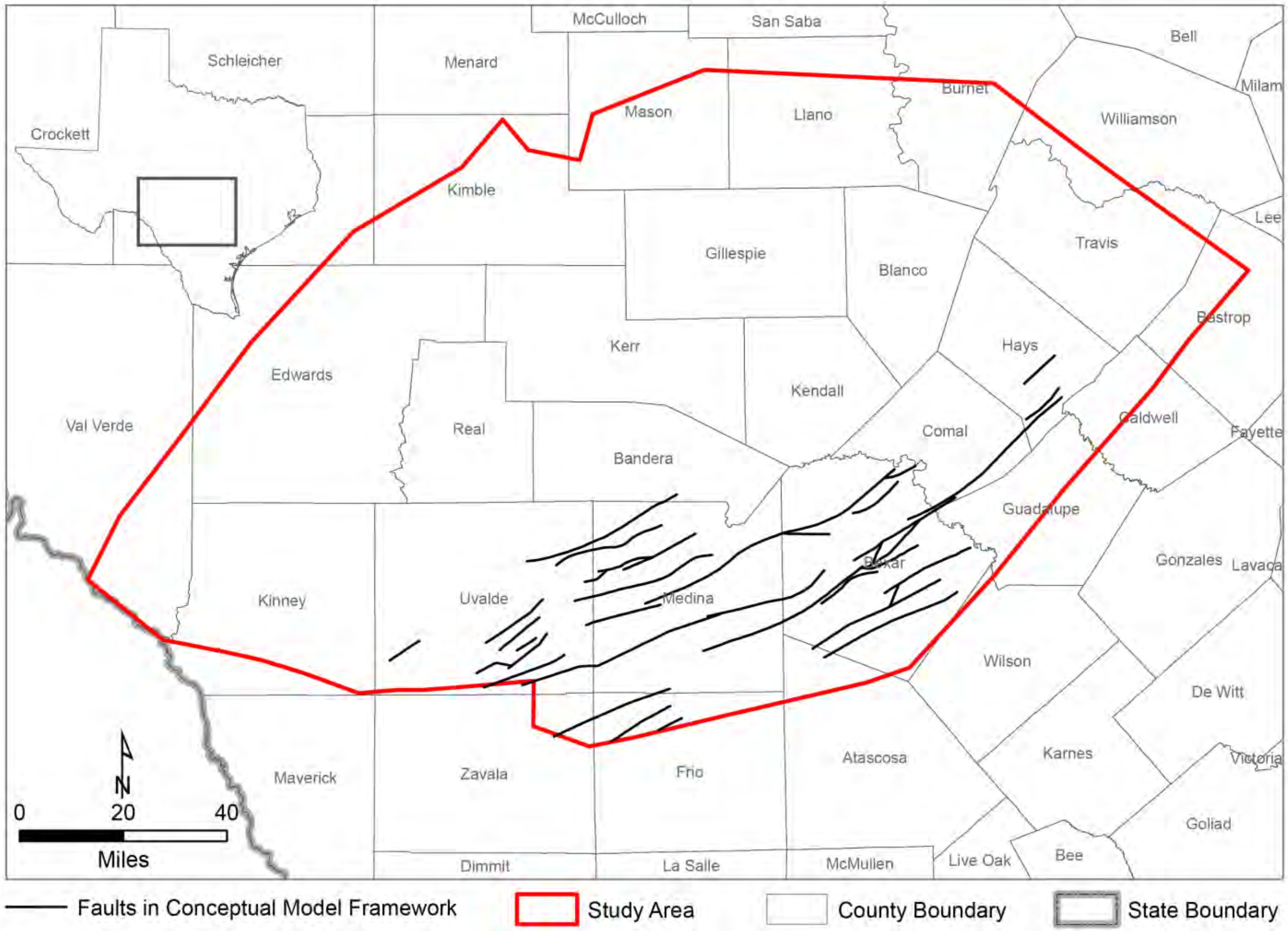

Figure 4.1.2 Fault map of faults that were modeled in this study.

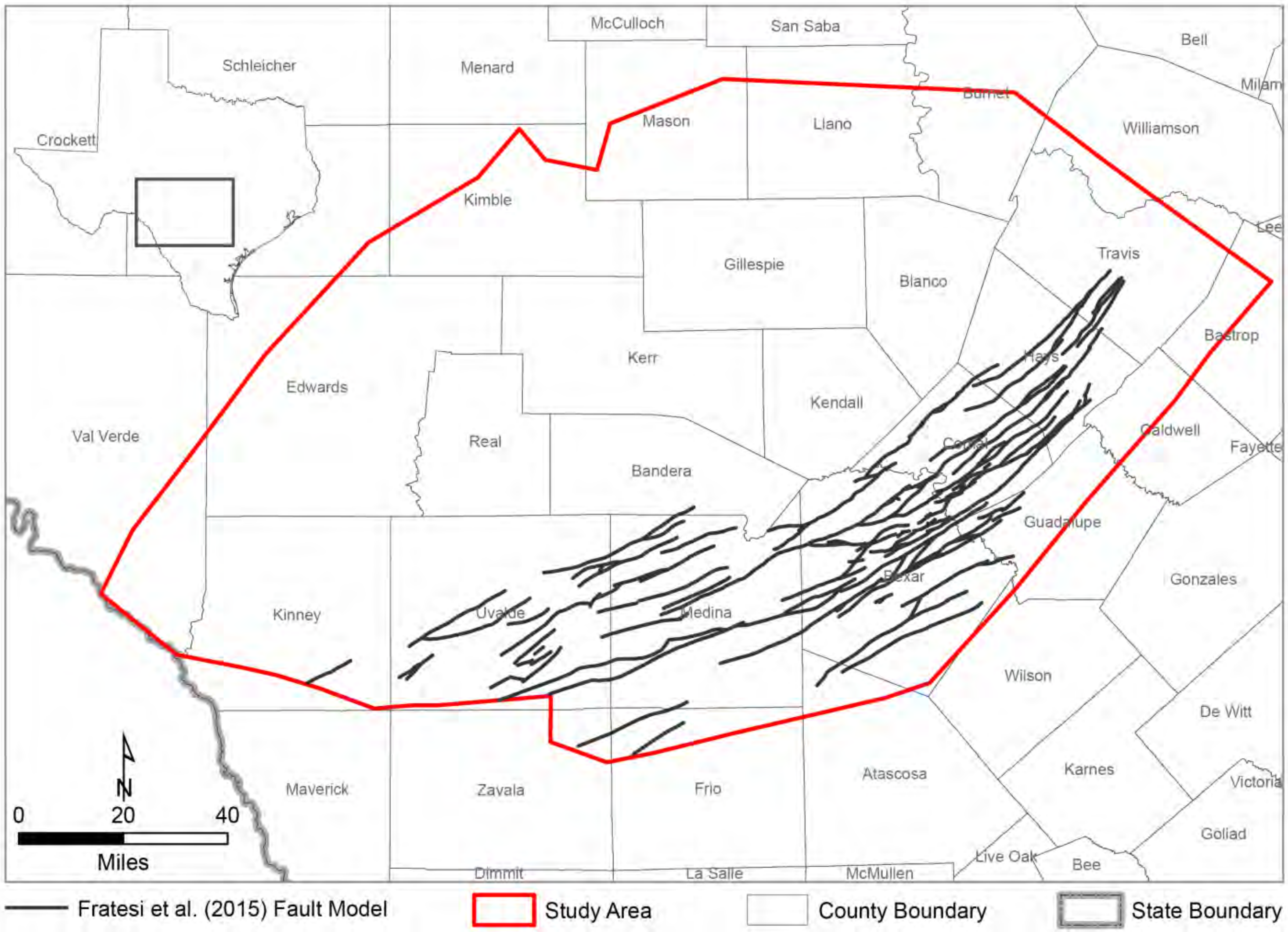

Figure 4.1.3 Fratesi et al. (2015) fault model.

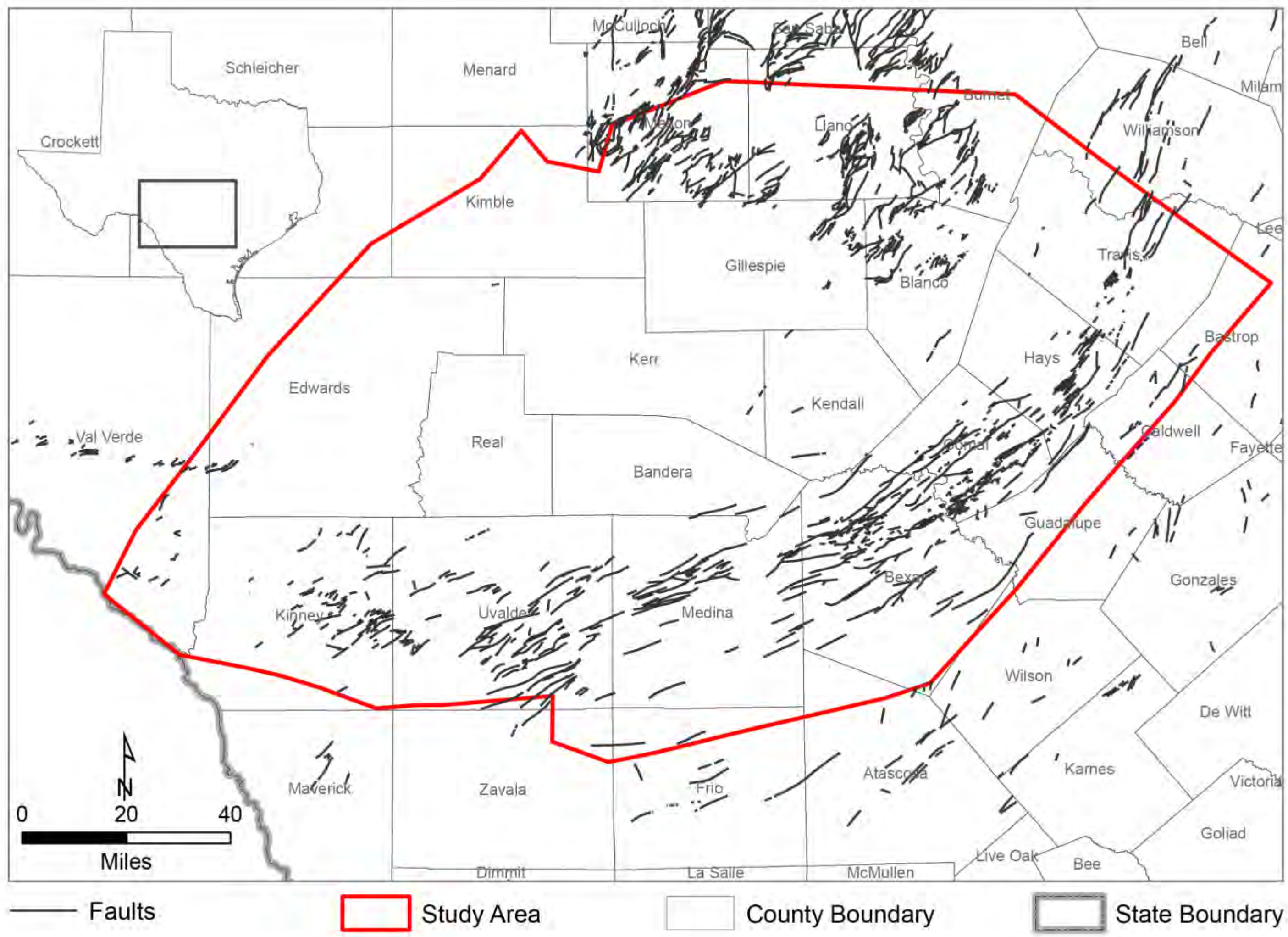

Figure 4.1.4 **High resolution fault map representing faults from numerous sources (Collins and Hovorka, 1997; Barnes, 1977, 1983; Fisher, 1983; Ferrill and Morris, 2008; Ferrill et al., 2003, 2004, 2005, 2008, 2011; Fratesi et al., 2013).**

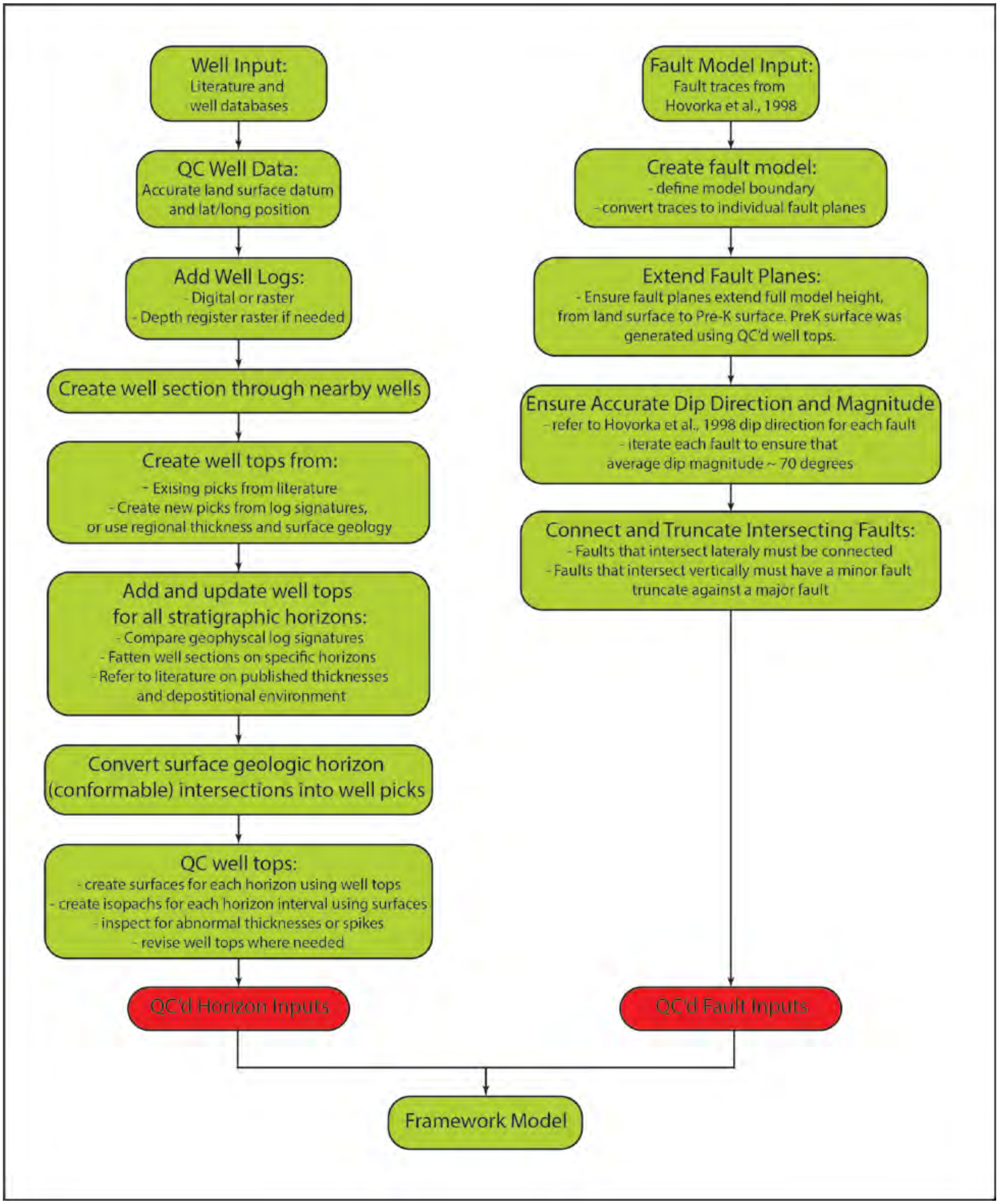

Figure 4.1.5 **Flow chart for developing horizon and fault input for implementation into the hydrostratigraphic framework model.**

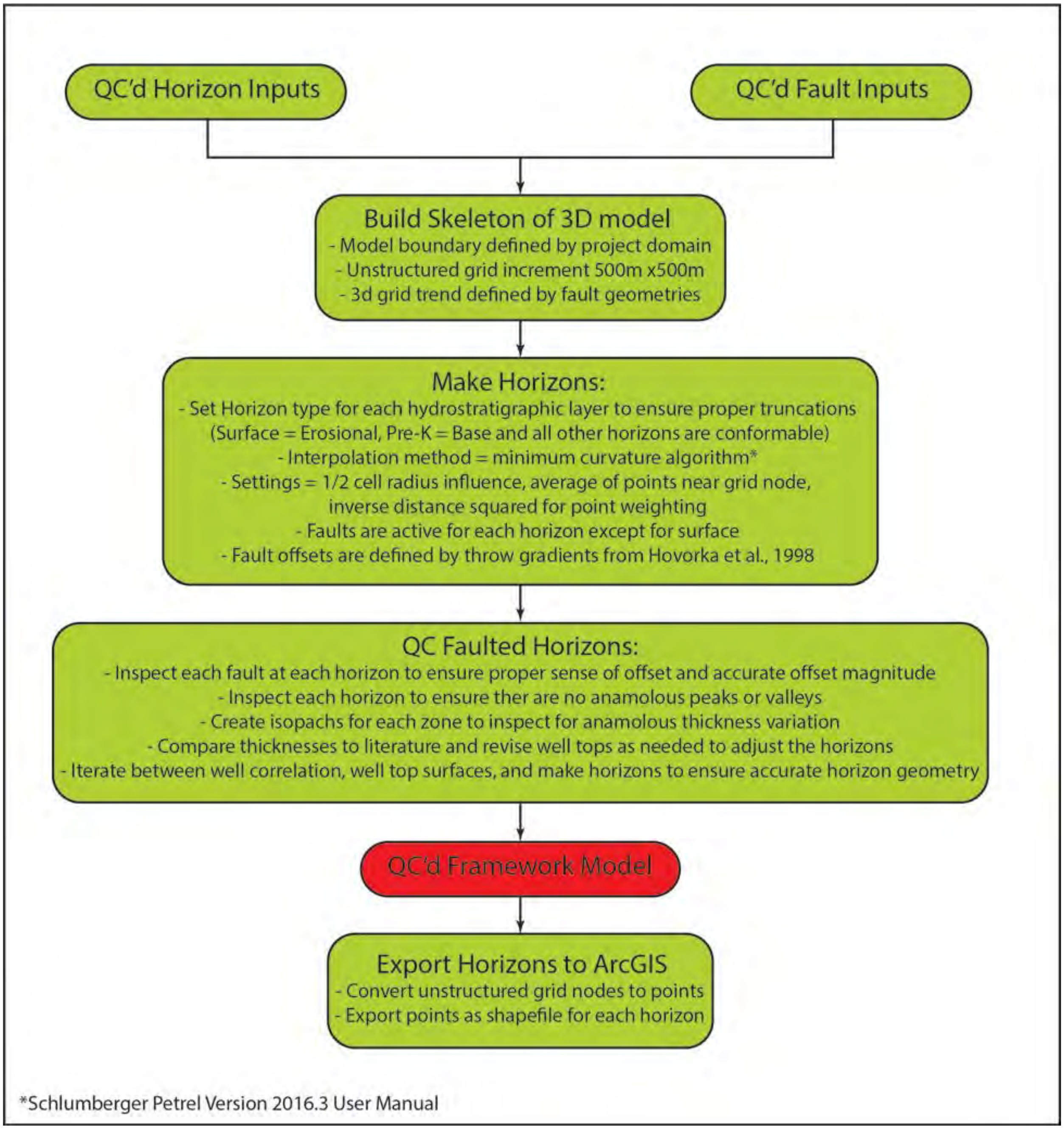

Figure 4.1.6 Flow chart for developing the hydrostratigraphic framework model.

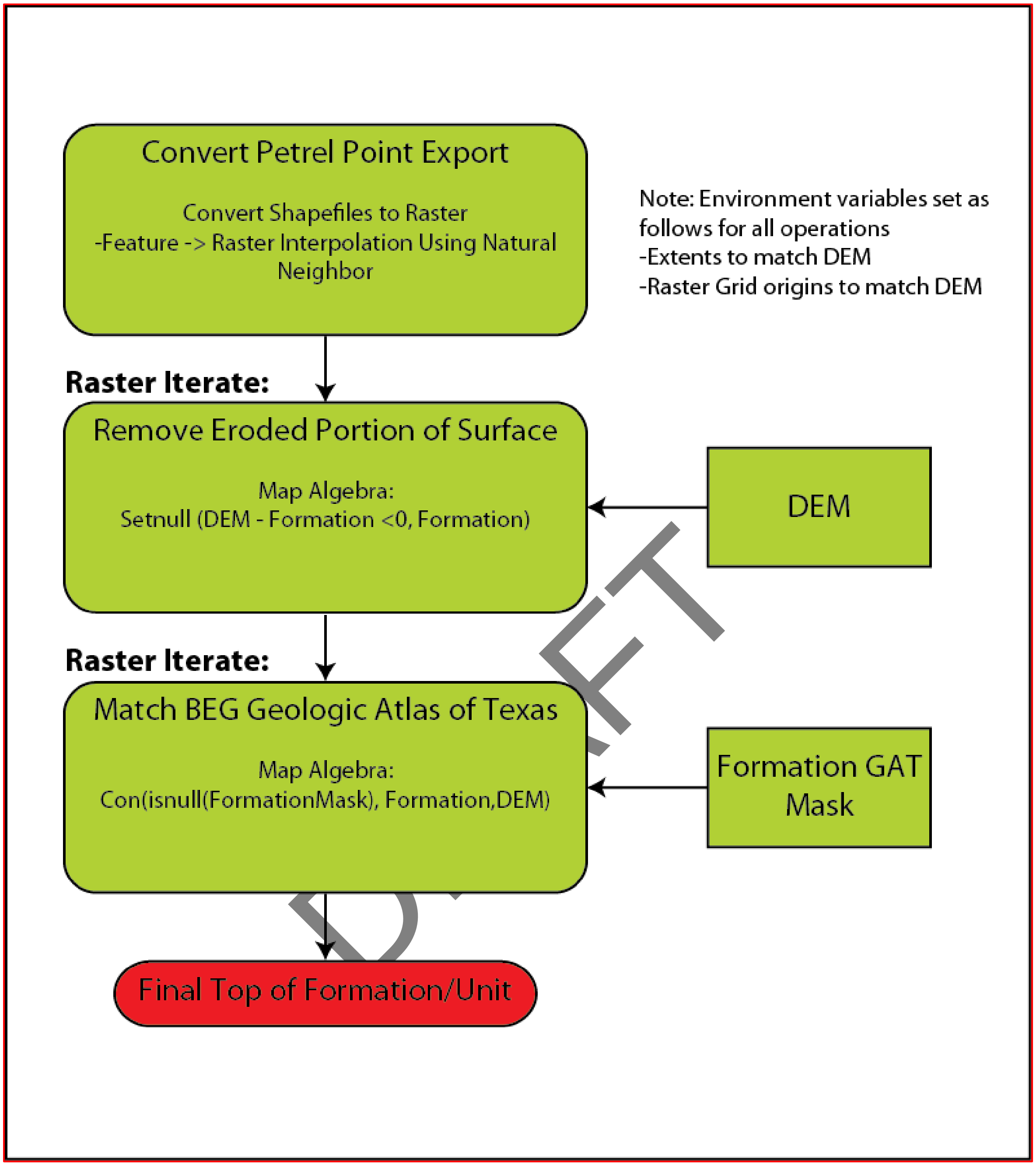

Figure 4.1.7 Flow chart for developing the finalized raster surfaces using ESRI ArcGIS modelbuilder.

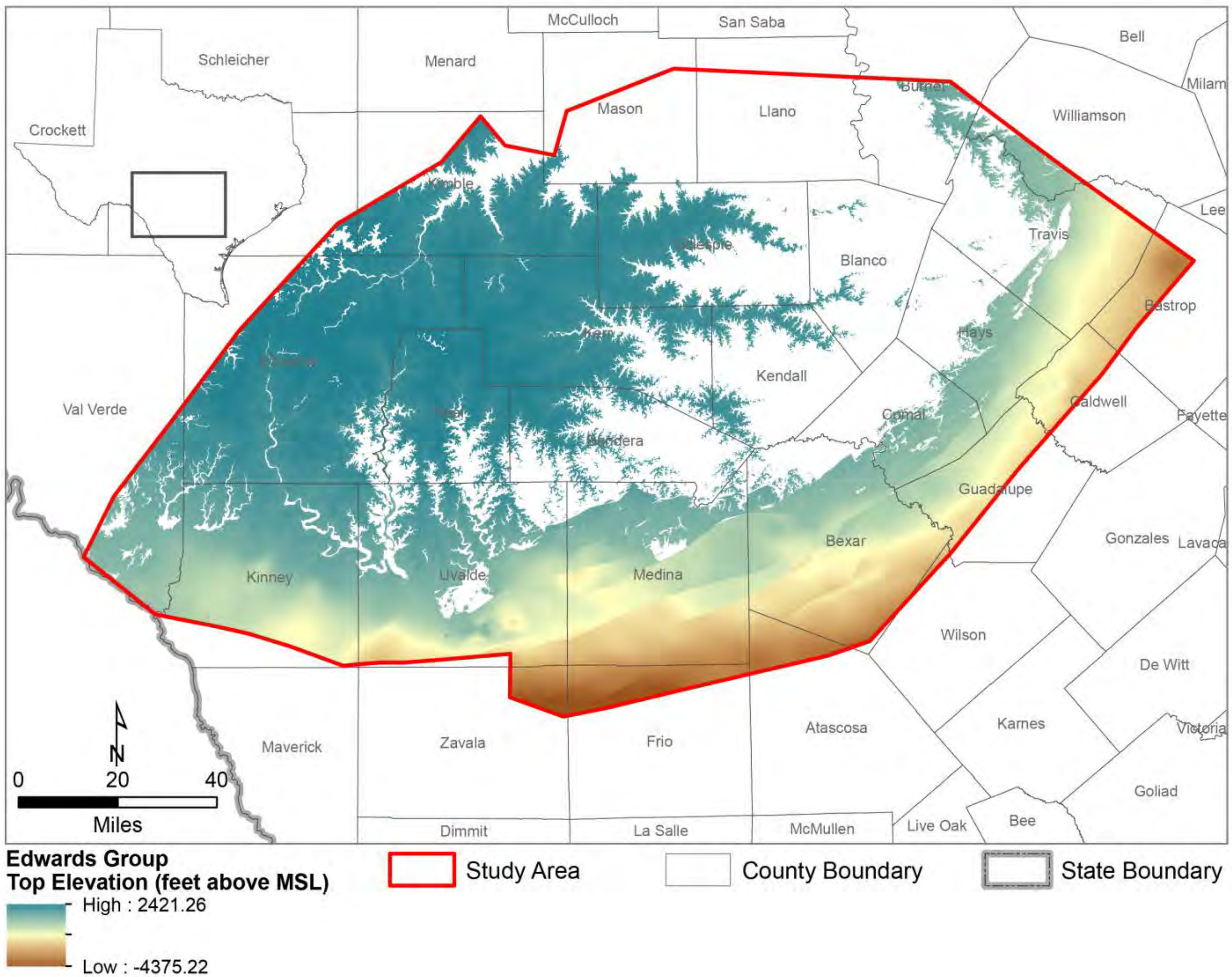

Figure 4.1.8 The elevation (in ft above mean sea level (MSL)) of the top of the Edwards Group.

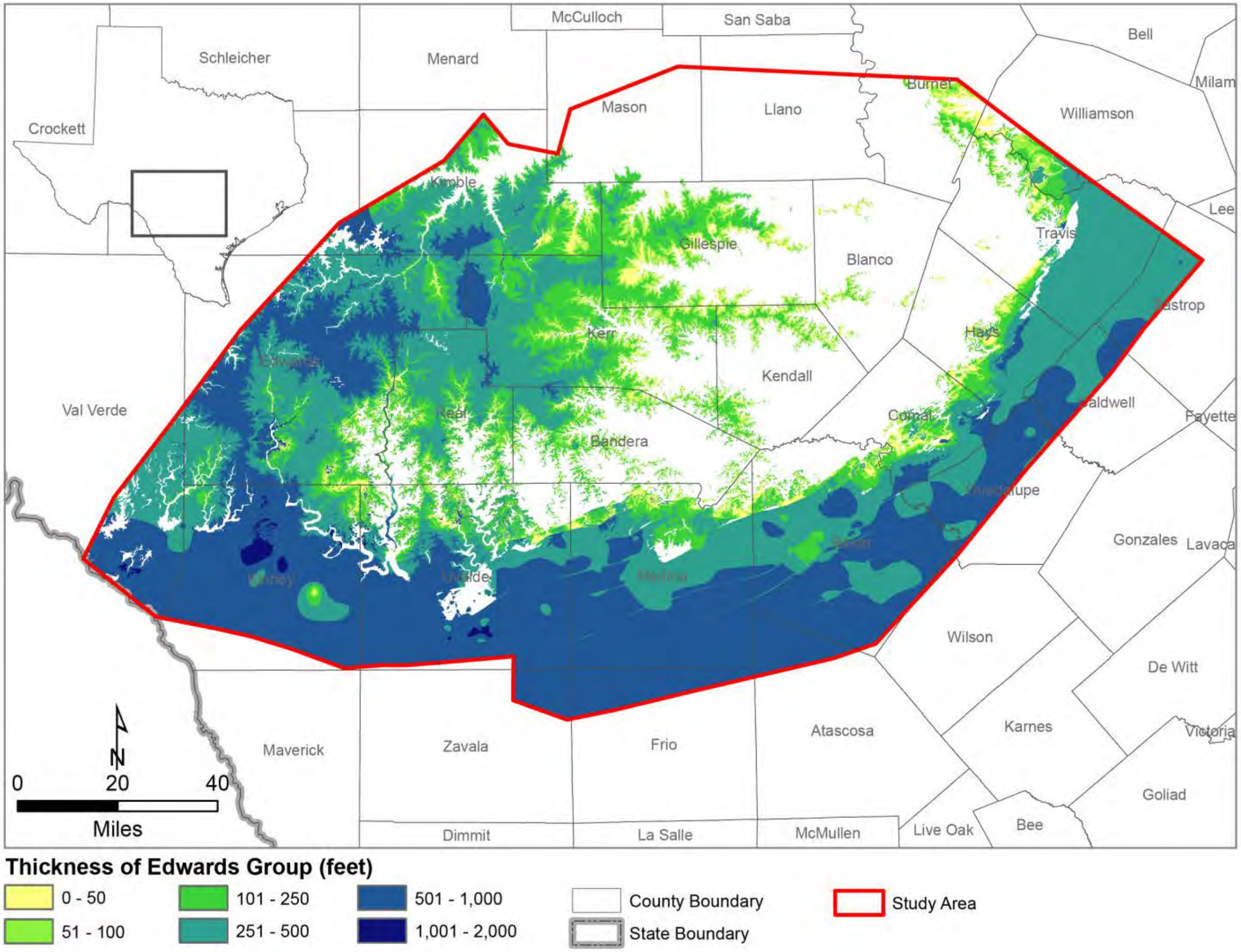

Figure 4.1.9 Thickness (in ft) of the Edwards Group.

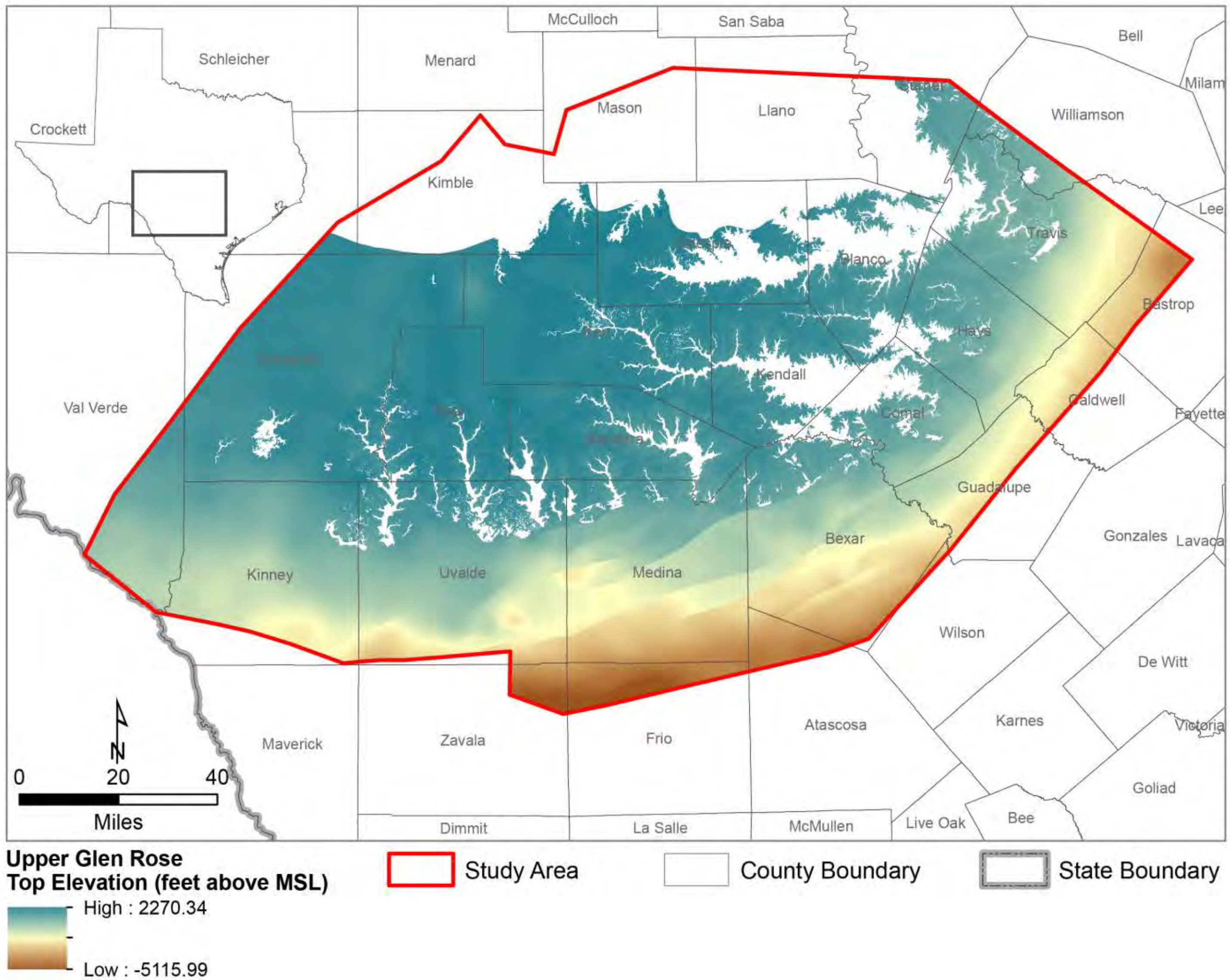

Figure 4.1.10 The elevation (in ft above mean sea level (MSL)) of the top of the Upper Glen Rose.

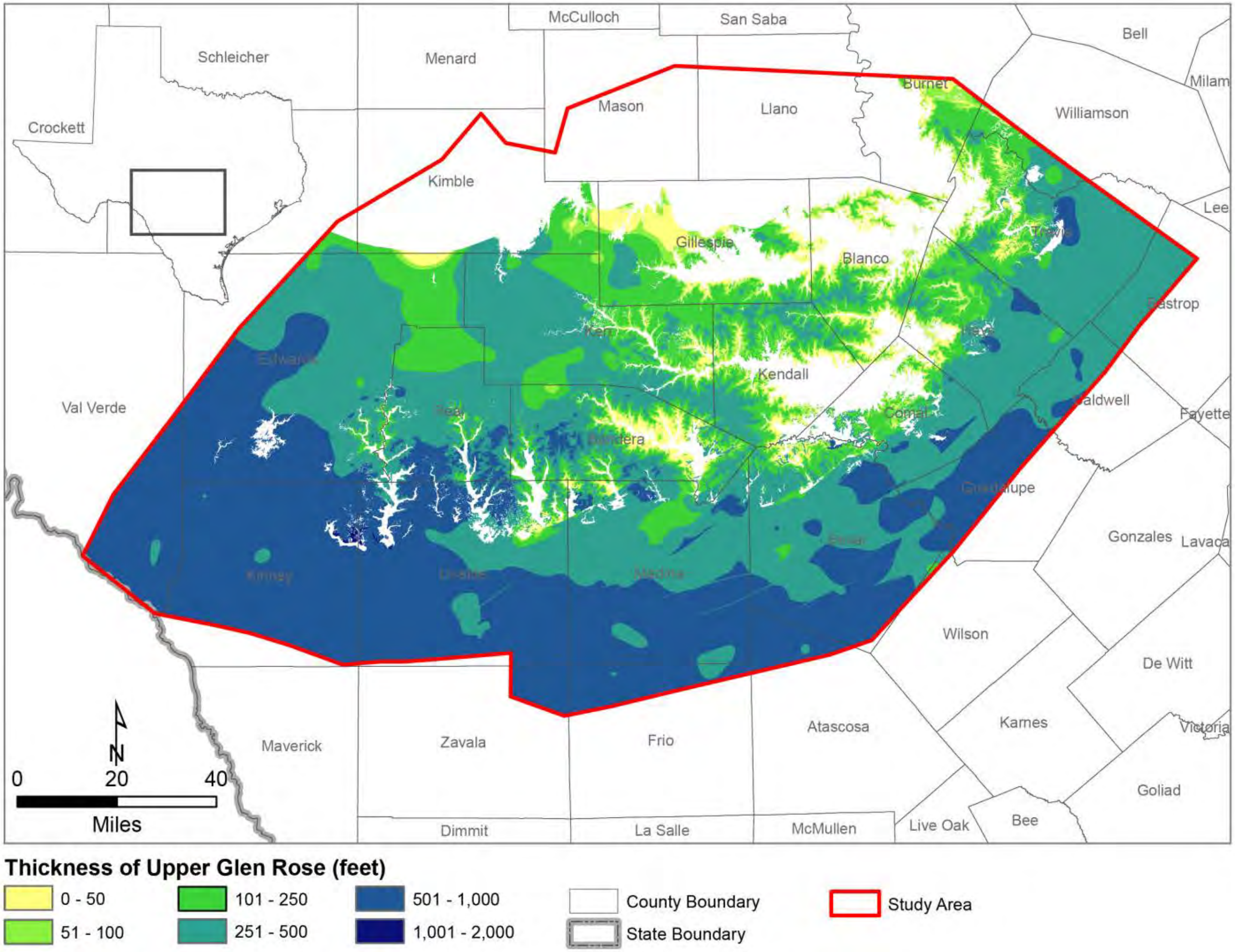

Figure 4.1.11 Thickness (in ft) of the Upper Glen Rose.

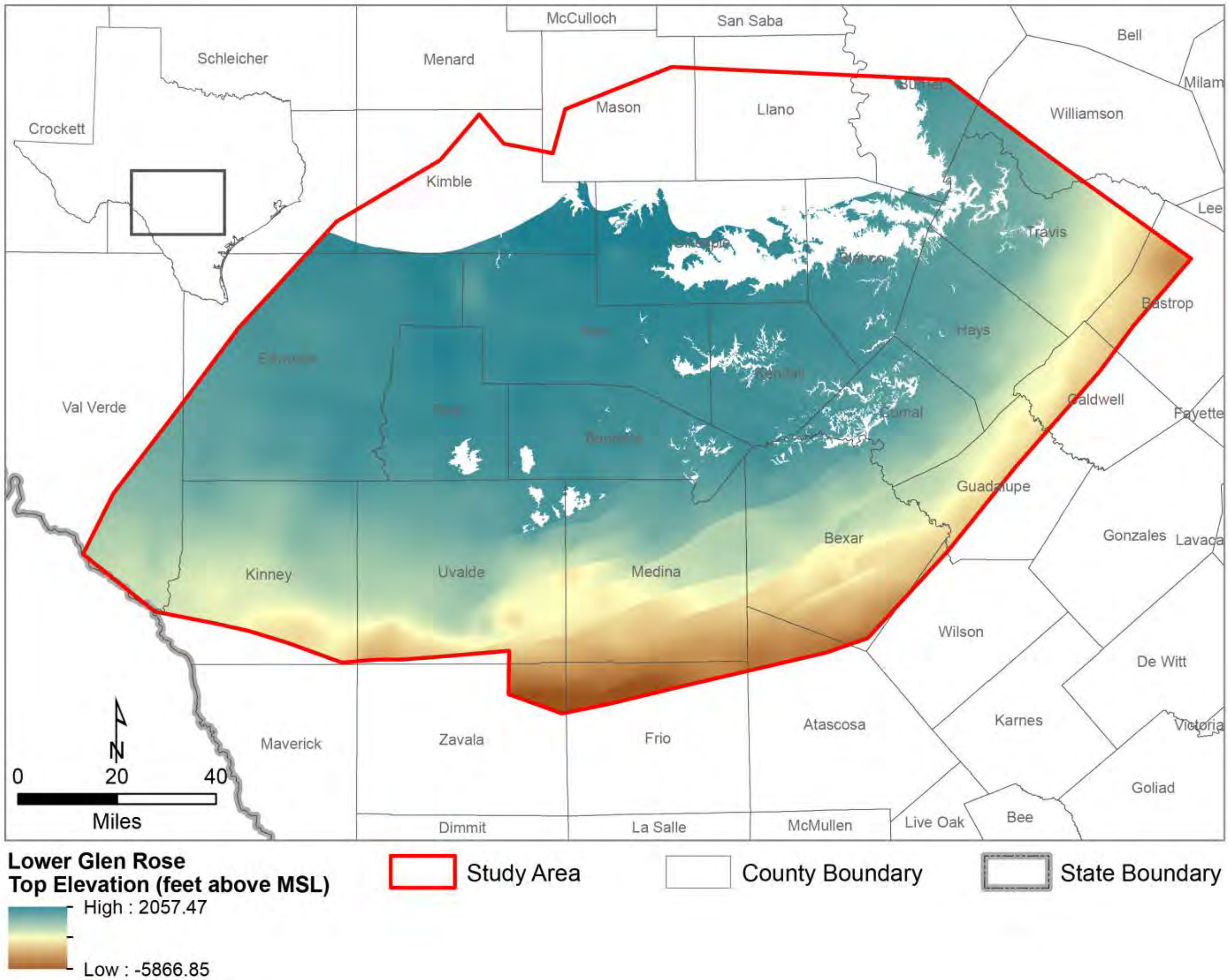

Figure 4.1.12 The elevation (in ft above mean sea level (MSL)) of the top of the Lower Glen Rose.

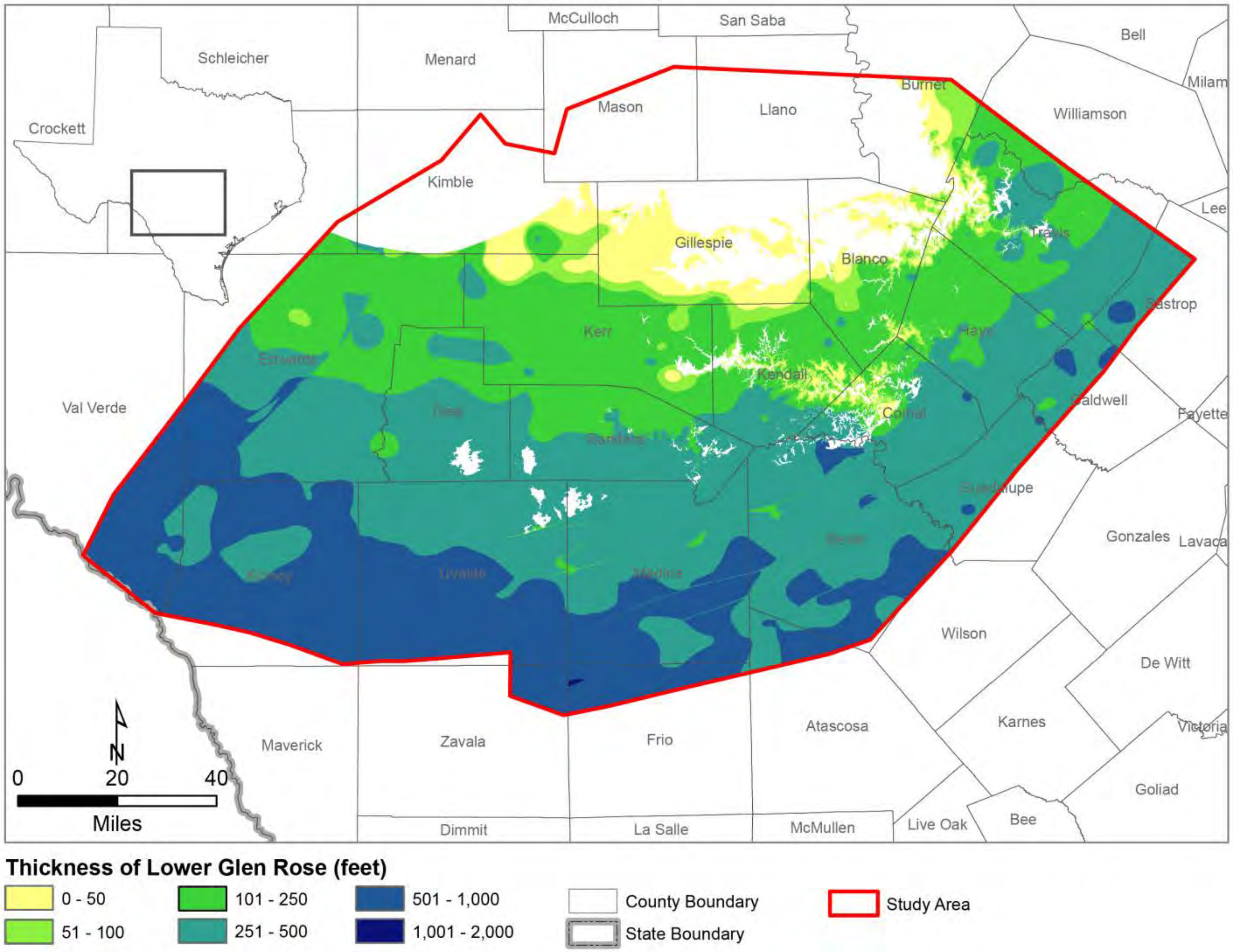

Figure 4.1.13 Thickness (in ft) of the Lower Glen Rose.

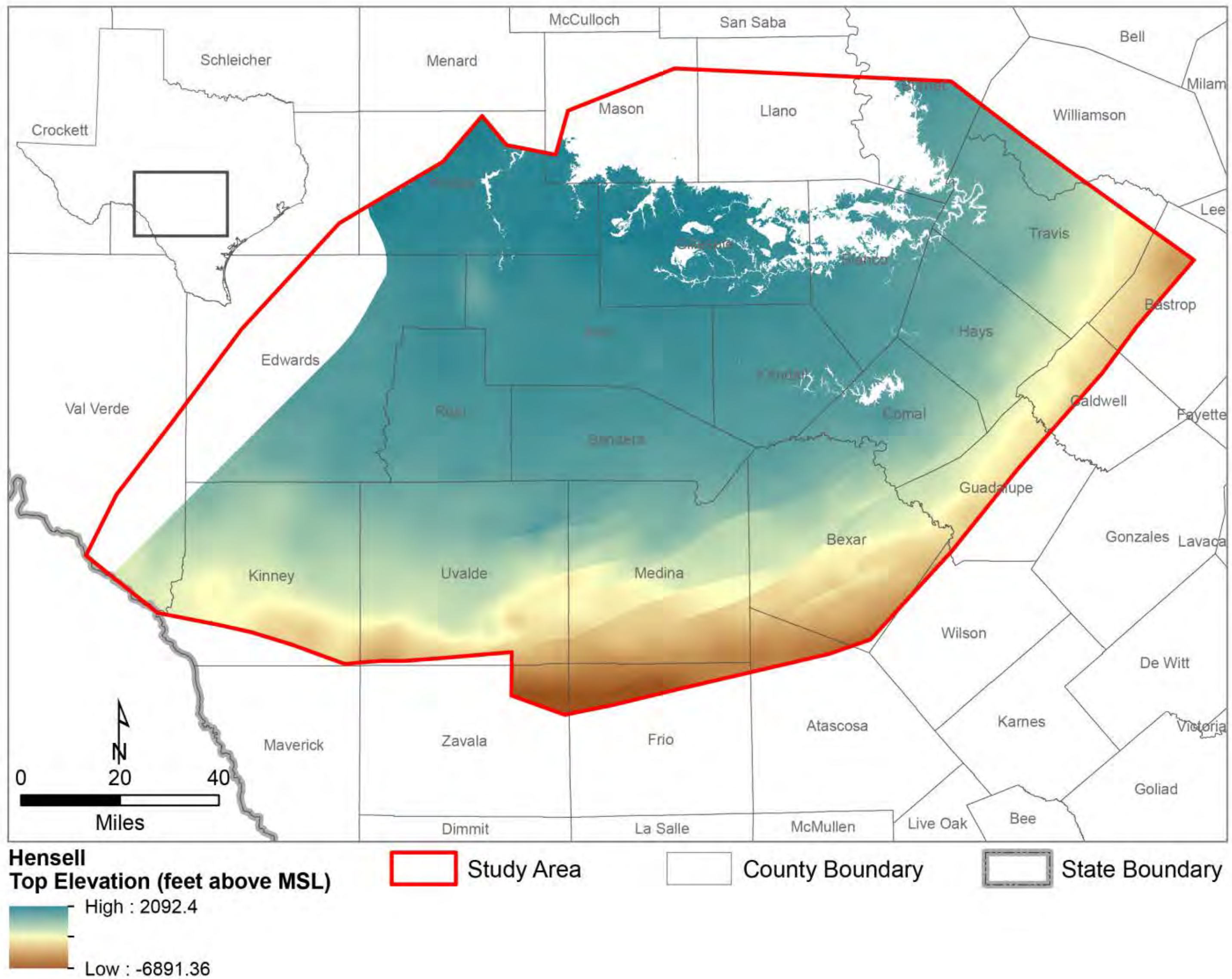

Figure 4.1.14 The elevation (in ft above mean sea level (MSL)) of the top of the Hensell.

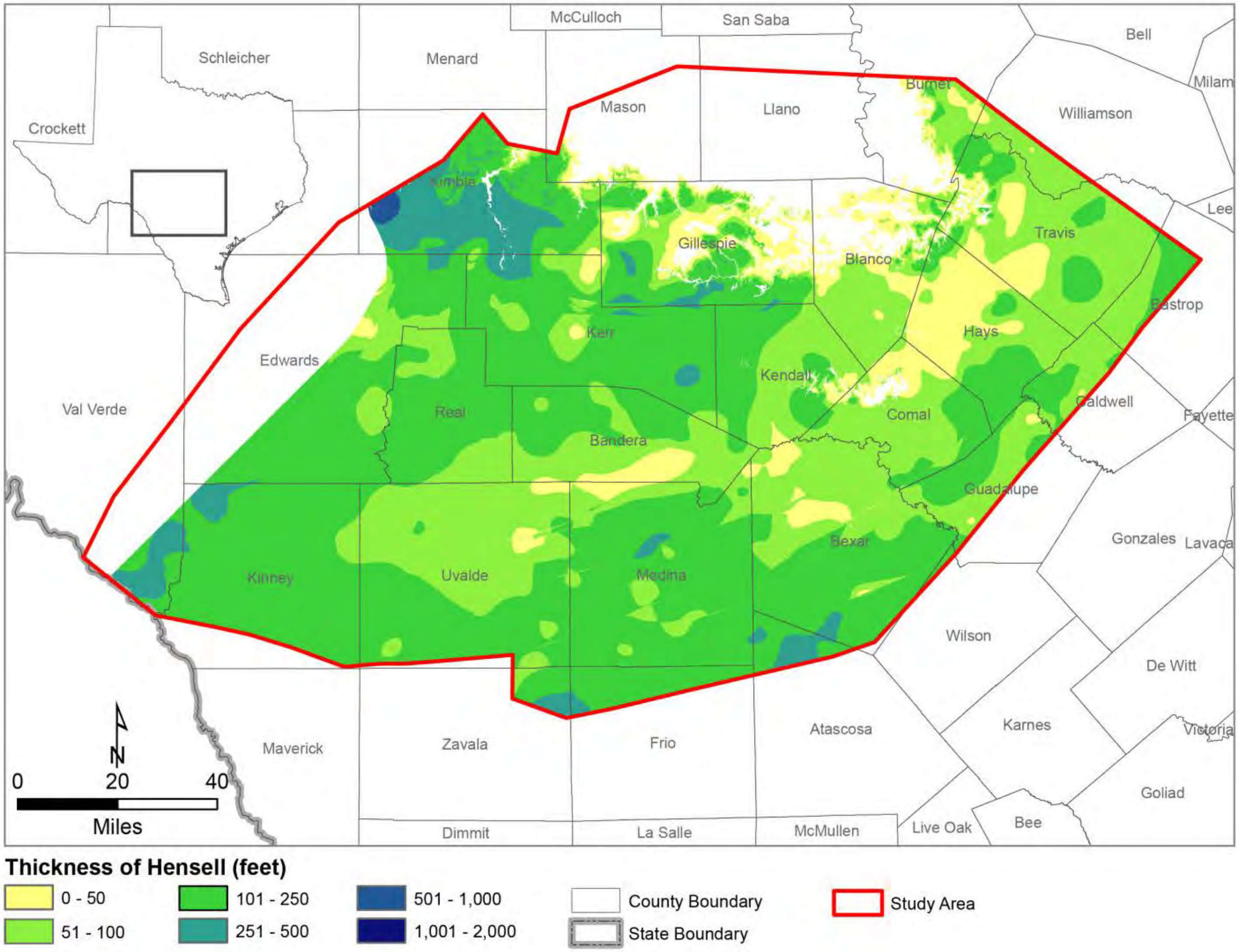

Figure 4.1.15 **Thickness (in ft) of the Hensell.**

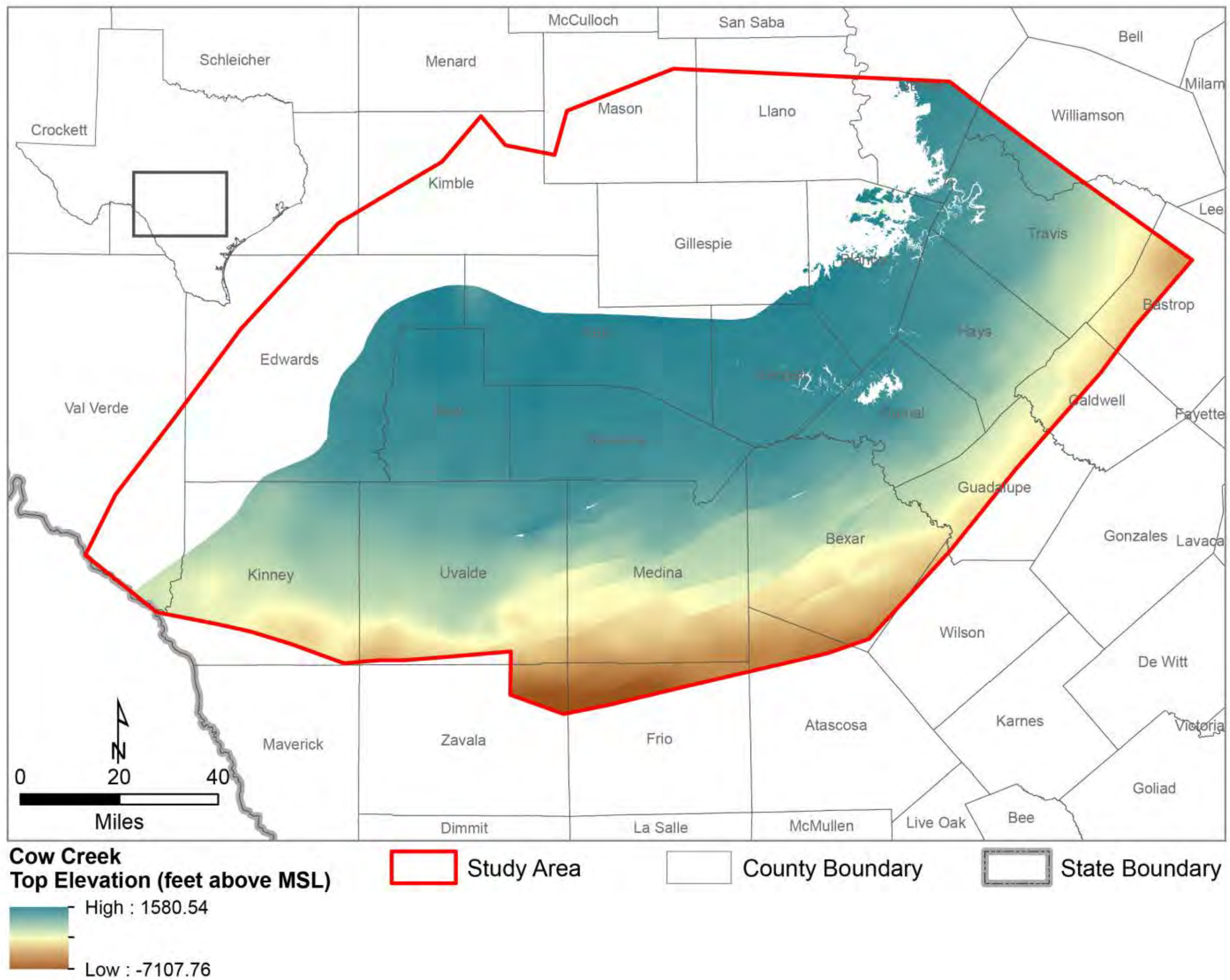

Figure 4.1.16 The elevation (in ft above mean sea level (MSL)) of the top of the Cow Creek.

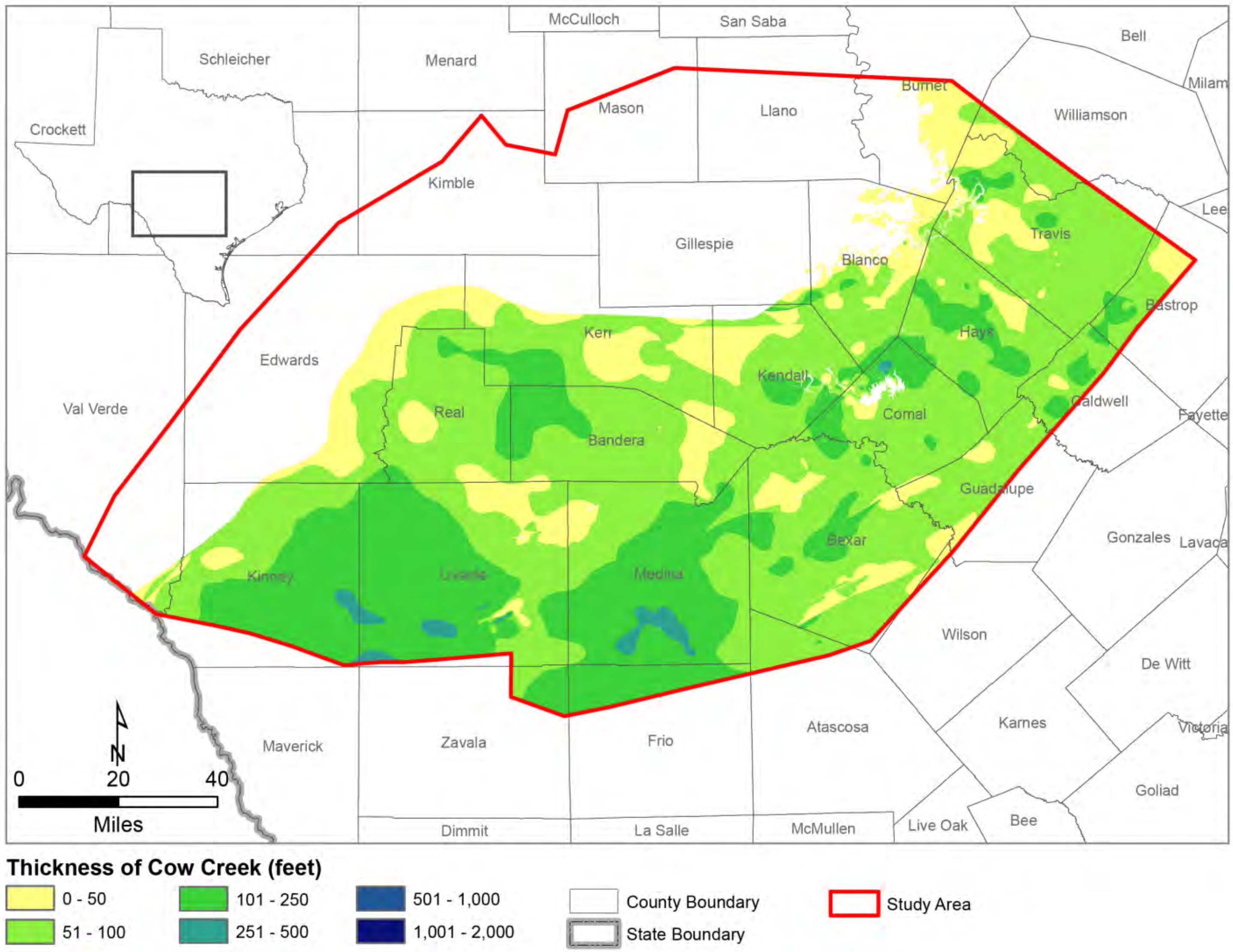

Figure 4.1.17 Thickness (in ft) of the Cow Creek.

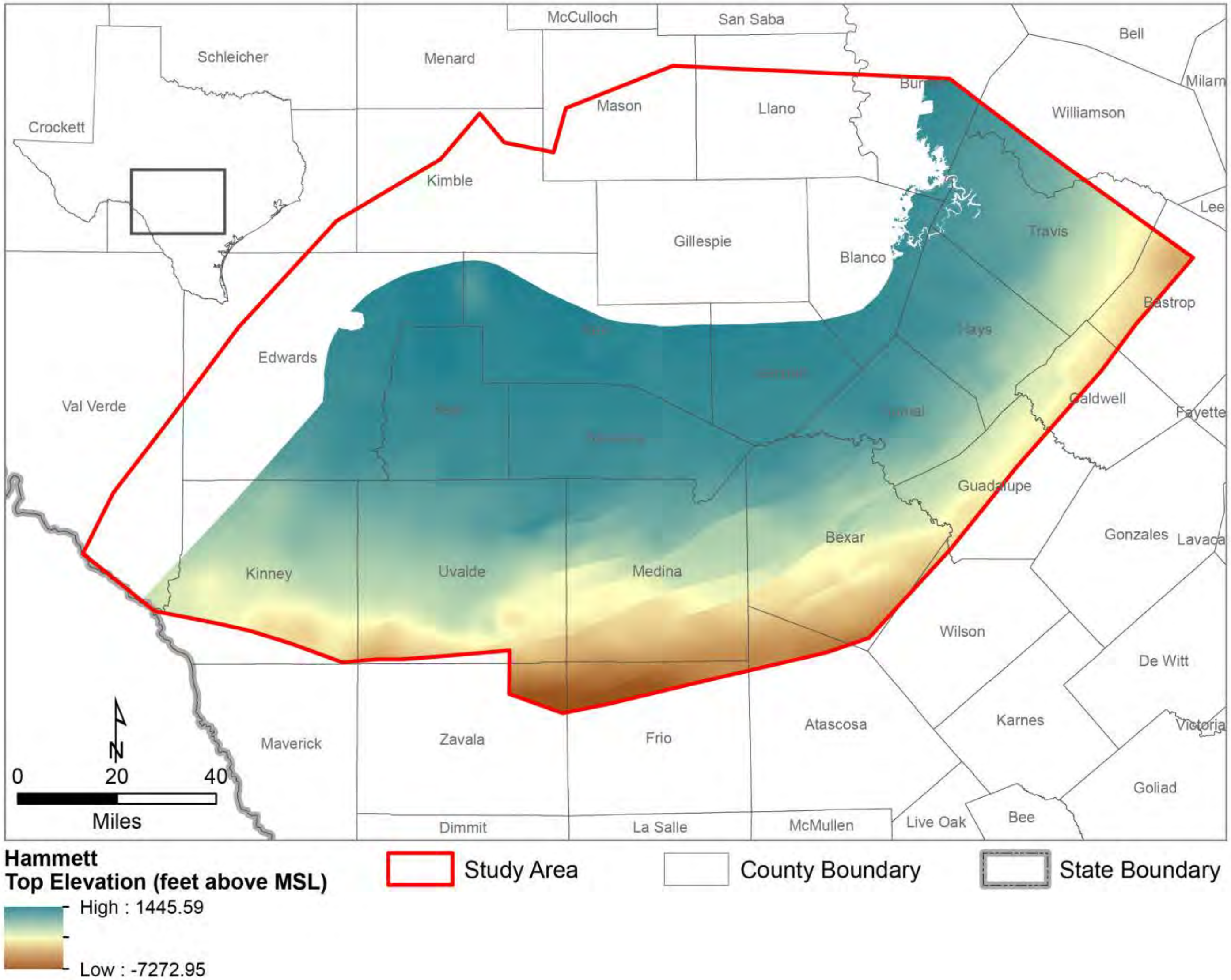

Figure 4.1.18 The elevation (in ft above mean sea level (MSL)) of the top of the Hammett.

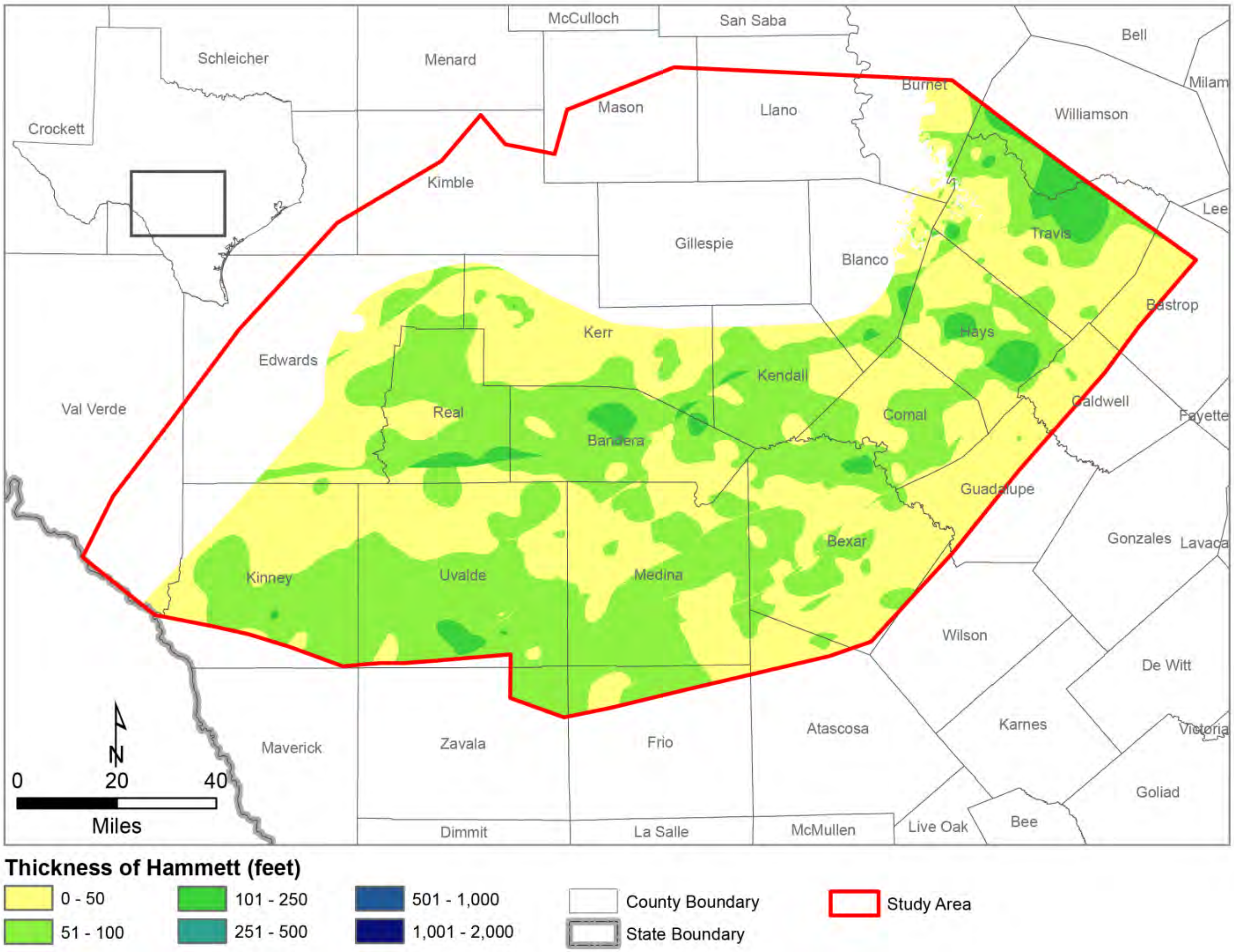

Figure 4.1.19 Thickness (in ft) of the Hammett.

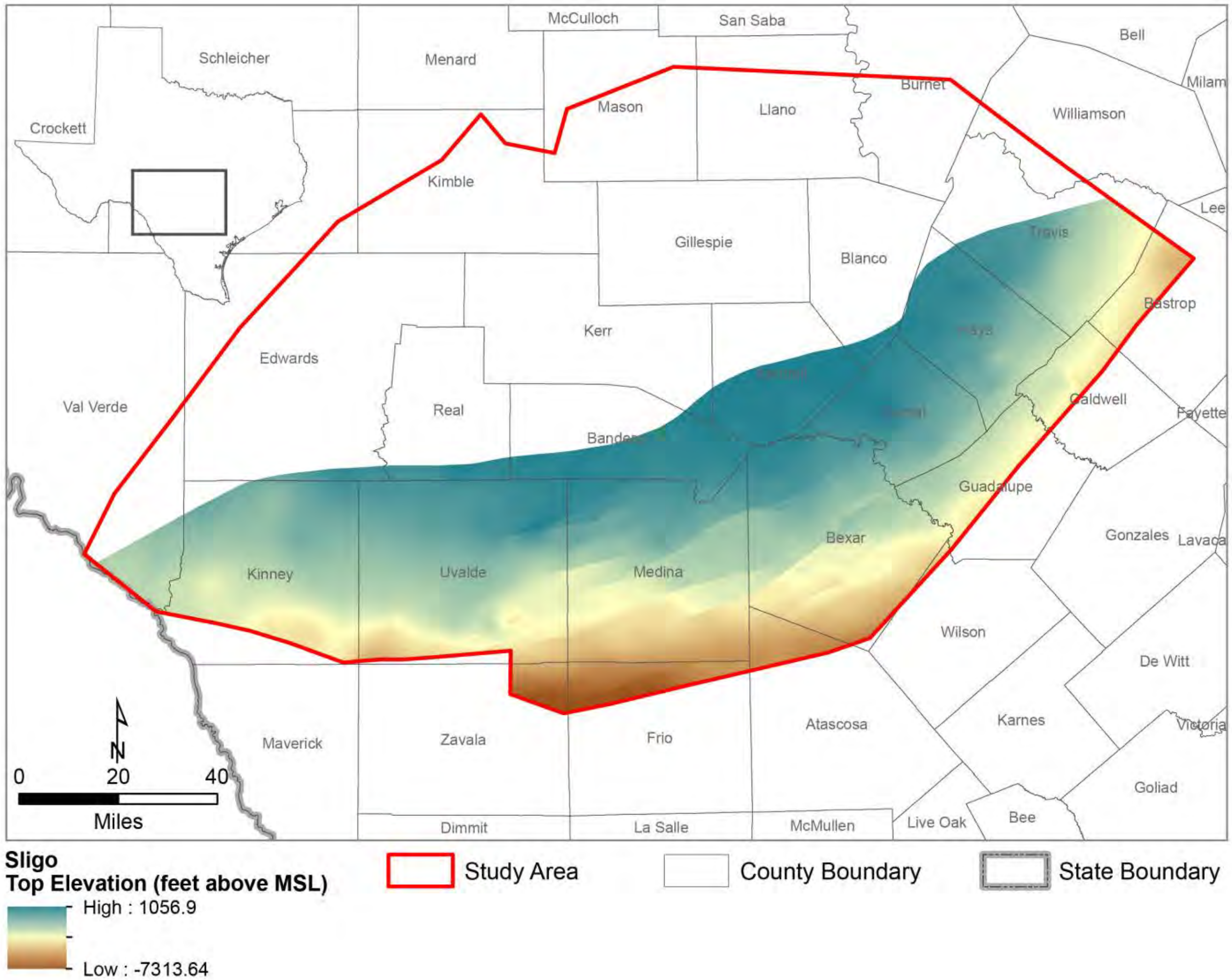

Figure 4.1.20 **The elevation (in ft above mean sea level (MSL)) of the top of the Sligo.**

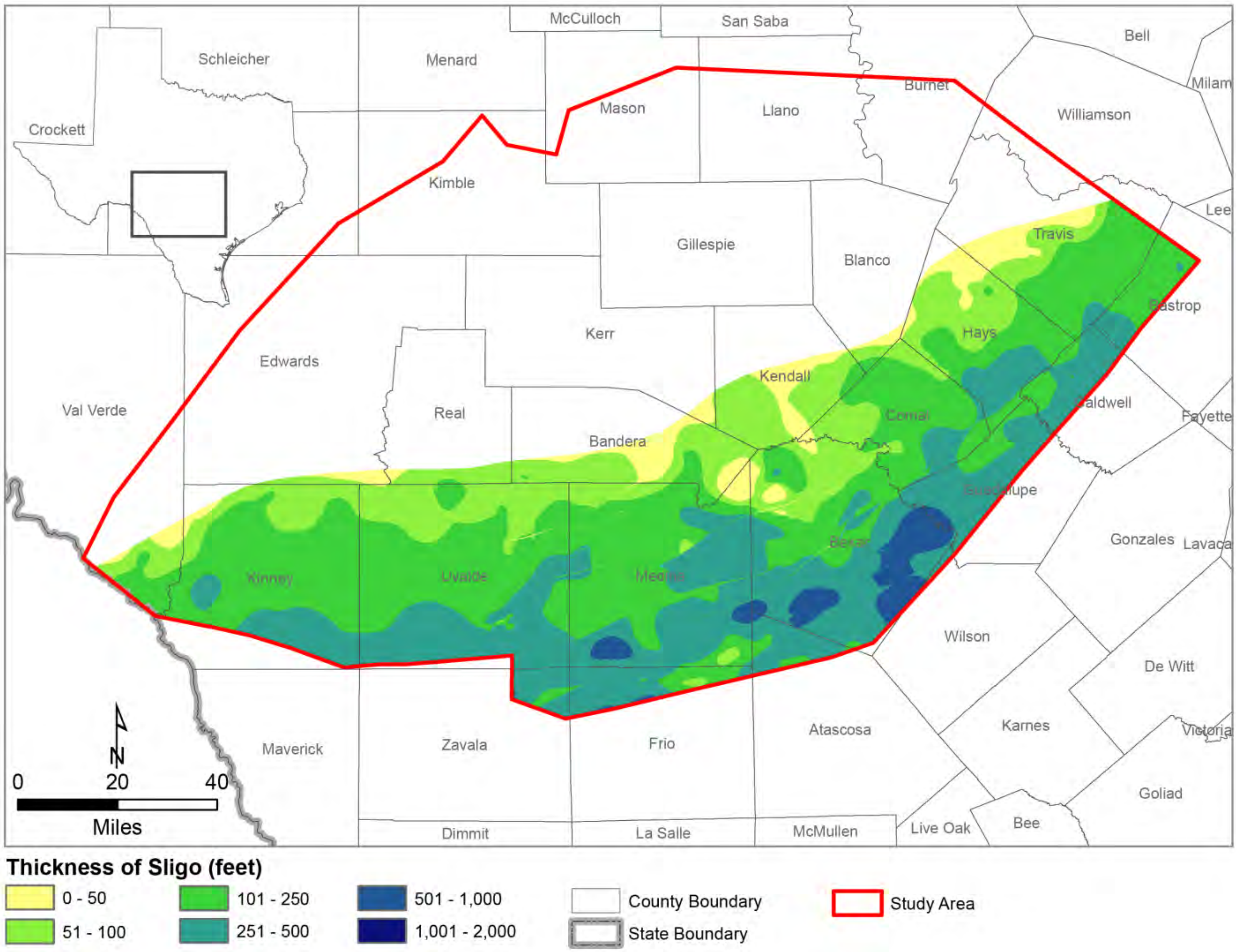

Figure 4.1.21 Thickness (in ft) of the Sligo.

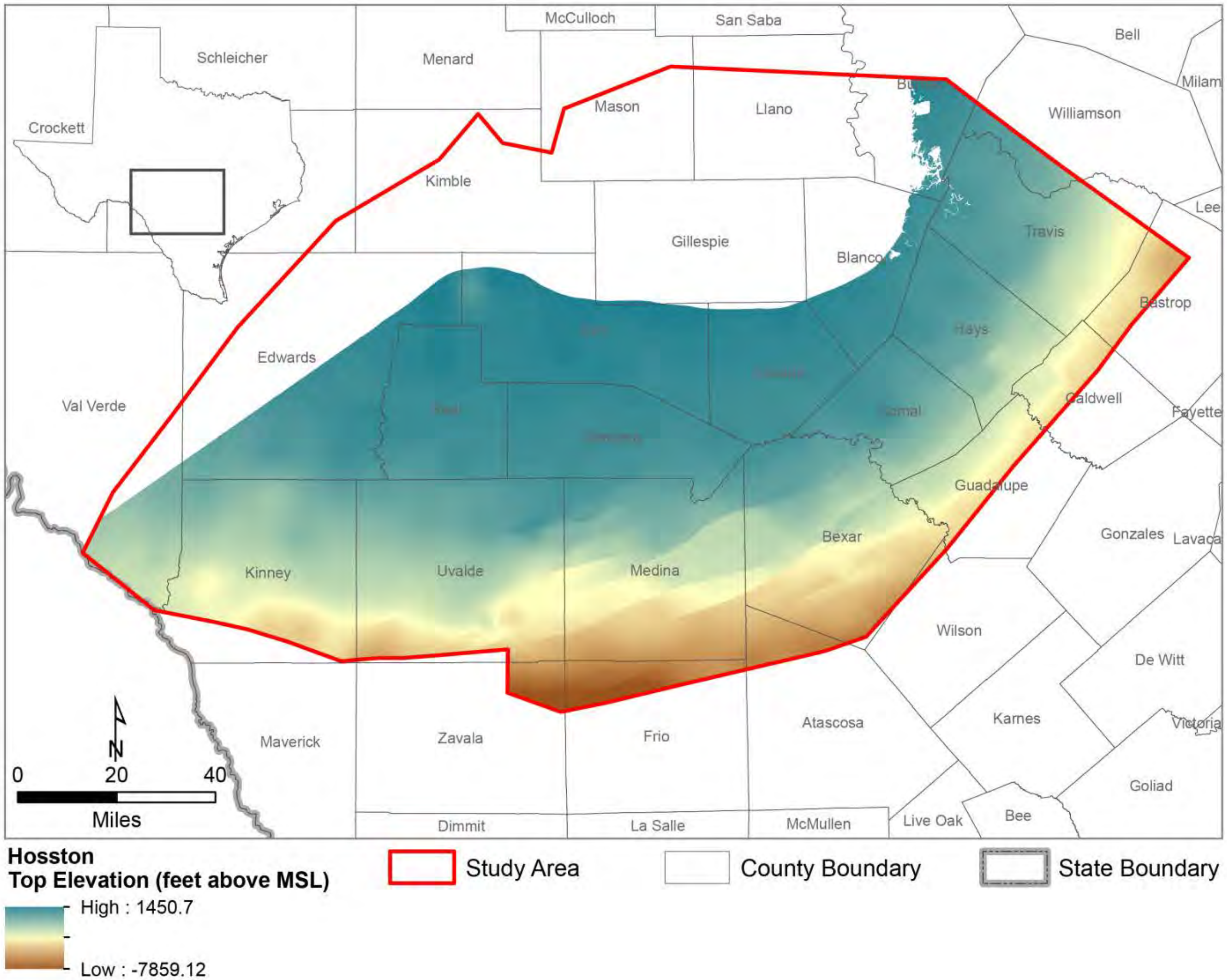

Figure 4.1.22 The elevation (in ft above mean sea level (MSL)) of the top of the Hosston.

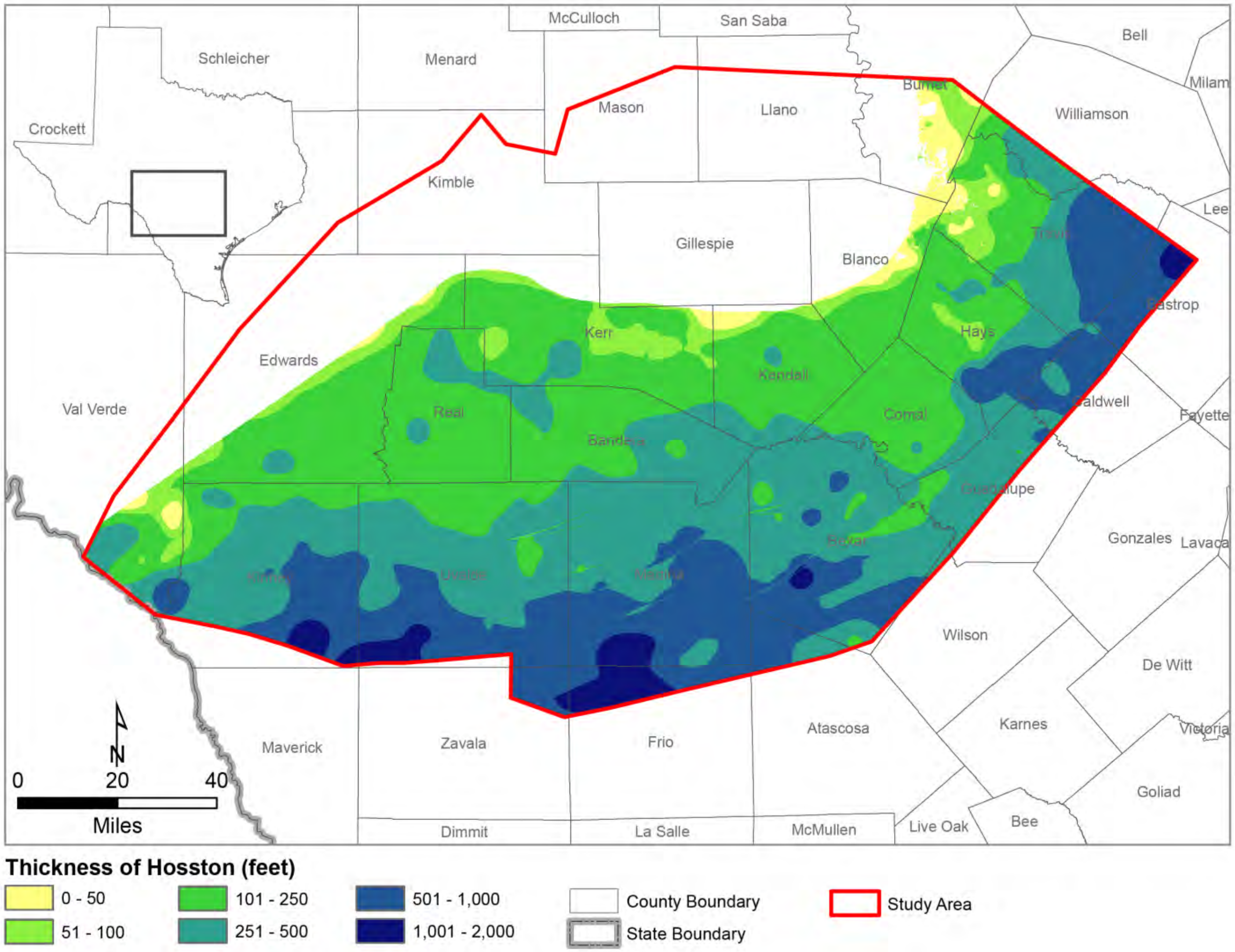

Figure 4.1.23 Thickness (in ft) of the Hosston.

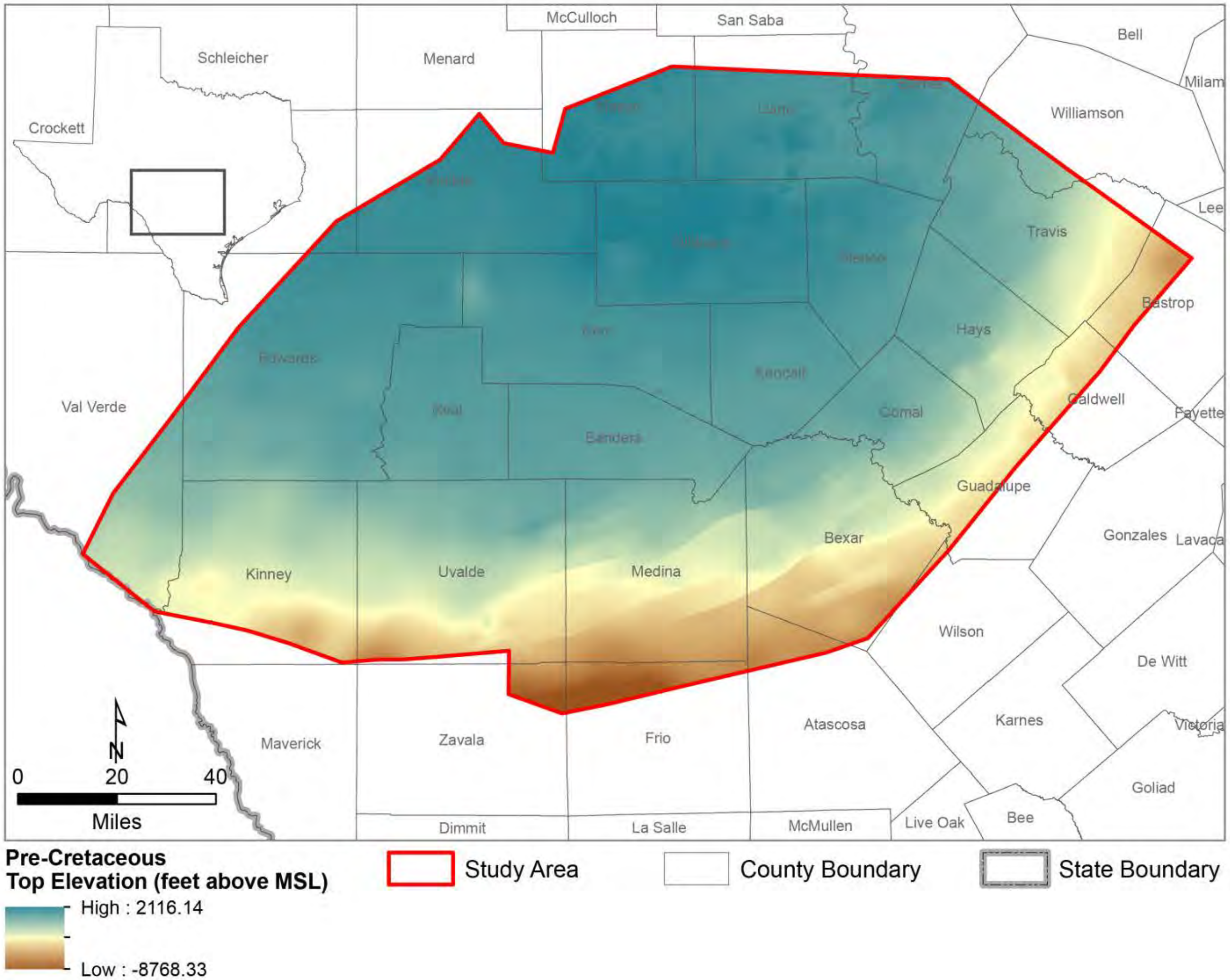

Figure 4.1.24 The elevation (in ft above mean sea level (MSL)) of the top of the Pre-Cretaceous.

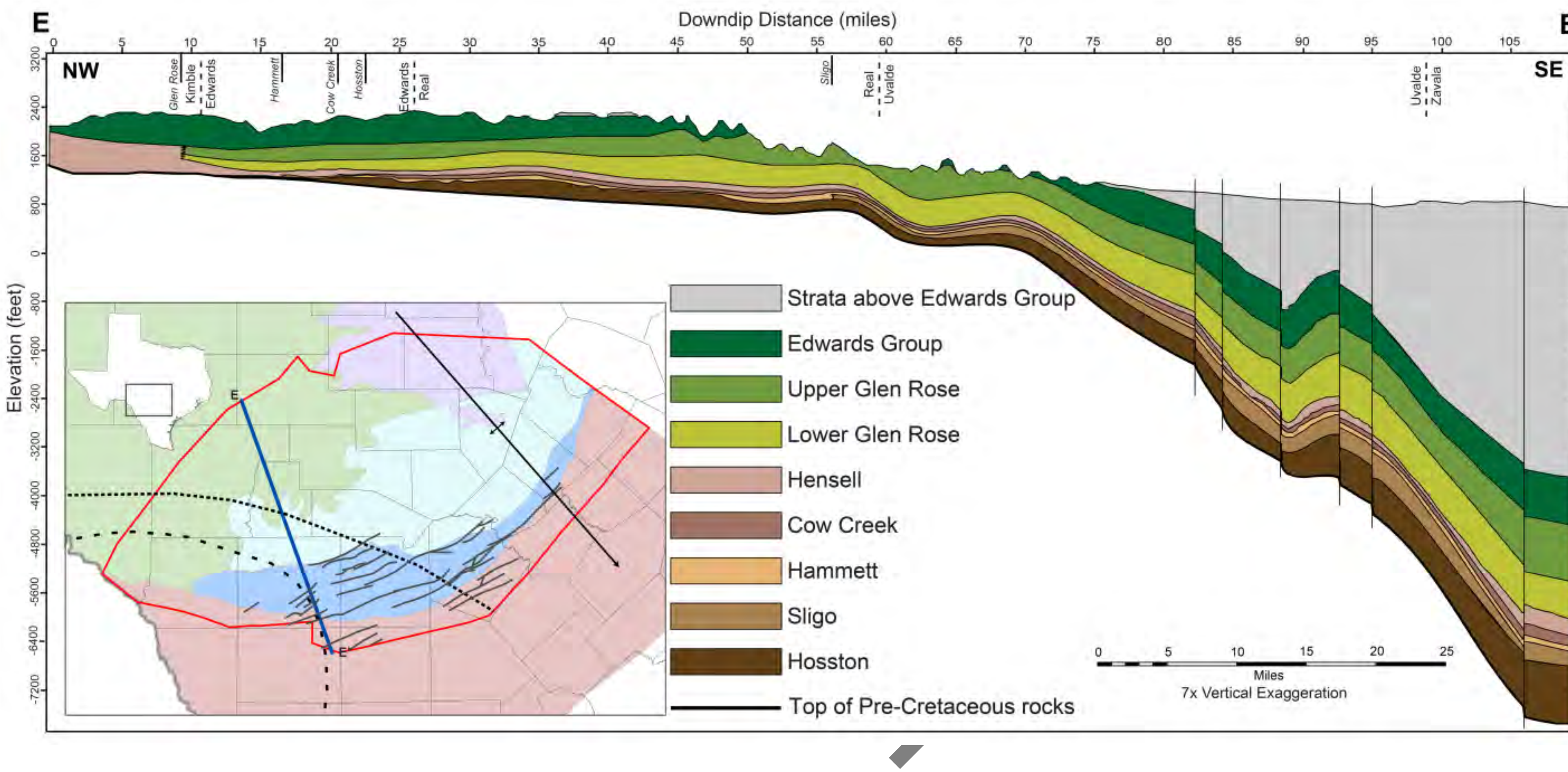

Figure 4.1.25 E-E' cross-section through the HCT hydrostratigraphic framework model.

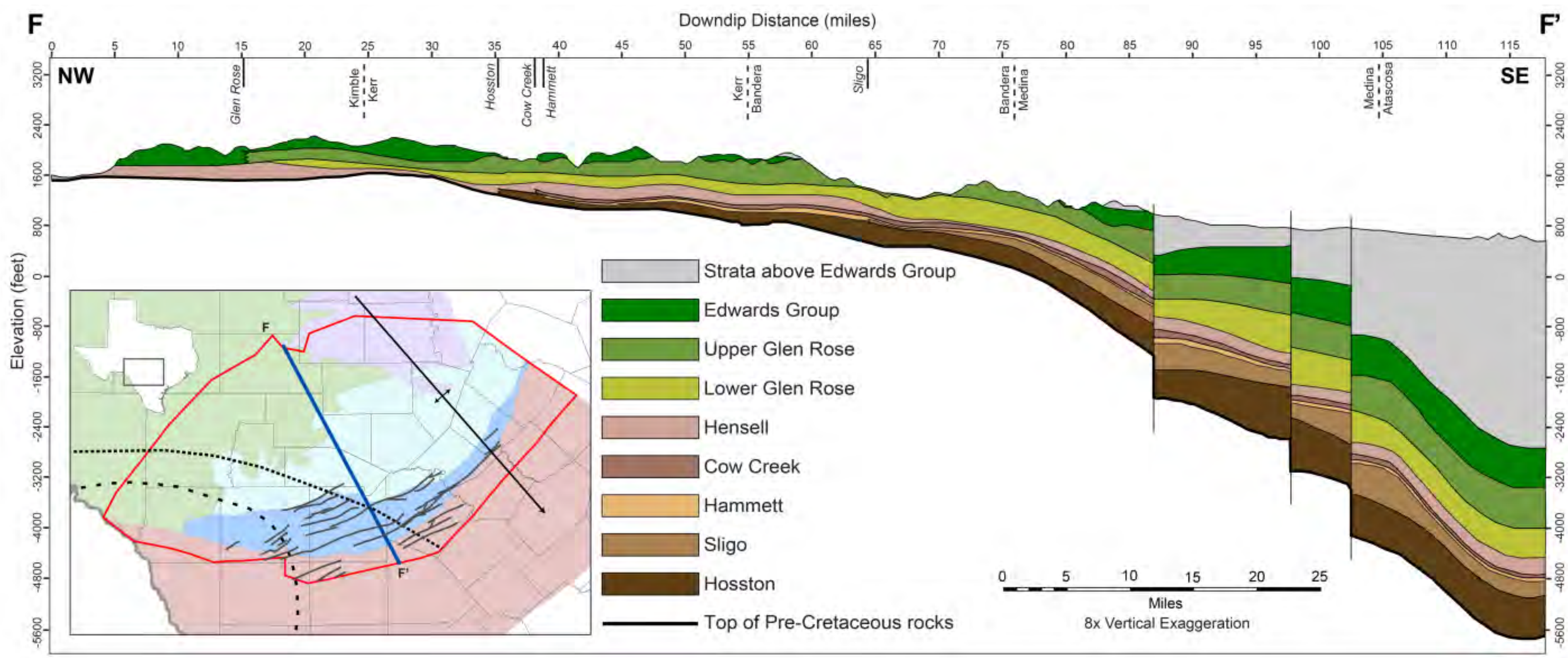

Figure 4.1.26 F-F' cross-section through the HCT hydrostratigraphic framework model.

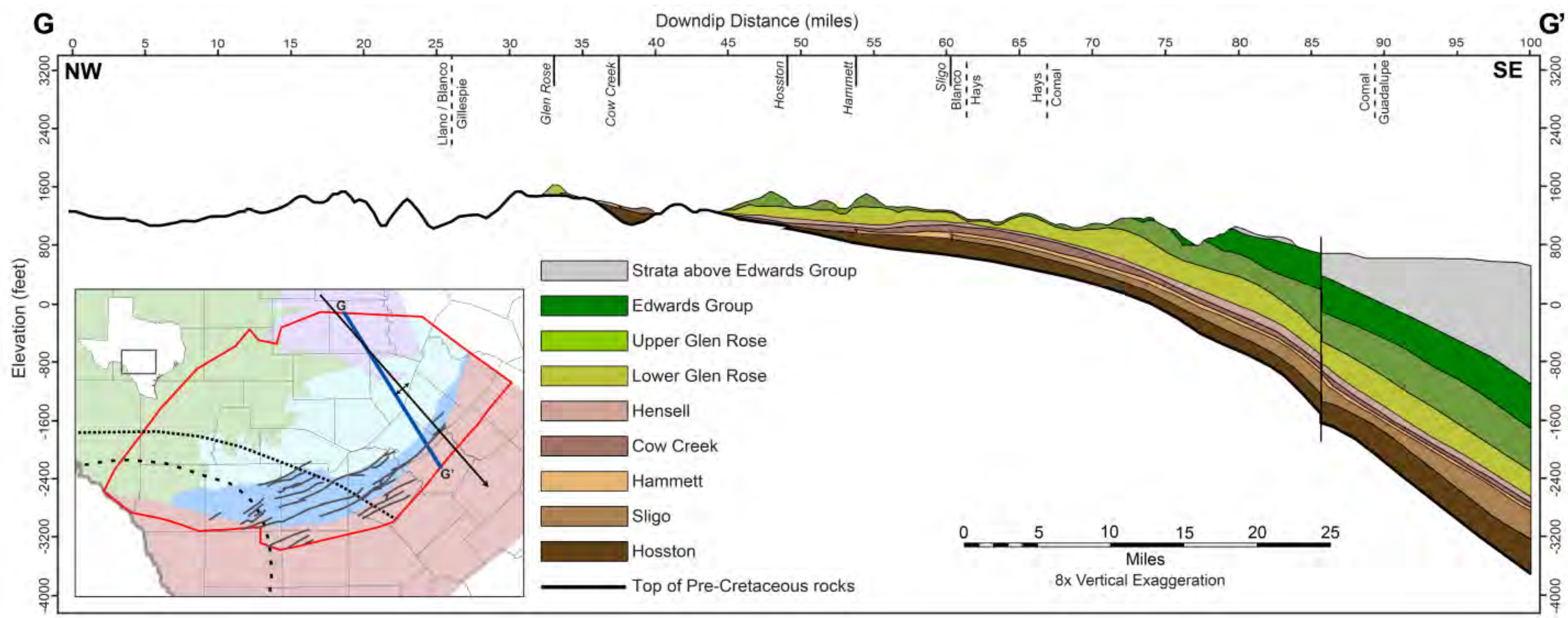

Figure 4.1.27 G-G' cross-section through the HCT hydrostratigraphic framework model.

4.2 Water elevations and Groundwater Flow

This section discusses water elevations and groundwater flow in the Trinity hydrostratigraphic units of the current study area. The water elevations in the overlying Edwards hydrostratigraphic unit in the extent of the Edwards-Trinity Plateau Aquifer are also discussed. The Edwards-Trinity Plateau Aquifer is hydraulically connected to the Hill Country portion of the Trinity Aquifer, so this information is necessary for any future groundwater model based on the current study area to accurately represent regional groundwater flow. This section also includes some discussion of the Edwards hydrostratigraphic unit in the extent of the Edwards Balcones Fault Zone Aquifer because there is potentially significant lateral flow between Trinity hydrostratigraphic units and the Edwards hydrostratigraphic unit in that region. The following subsections provide the sources used to collect water-level data, discuss and present an estimate of the pre-development water elevation, discuss available transient water-level data and present an analysis of select transient data, present estimated historical water elevation contours, and discuss water elevation calibration targets.

Due to the size and complexity of the study area, the region was divided into three zones for discussion purposes. These zones are shown Figure 4.2.1. The “HCT” region refers to the central portion of the study area, coincident with the TWDB extent of the Hill Country portion of the Trinity Aquifer within the study area. The “Edwards-Trinity Plateau” region refers to the western portion of the study area, coincident with the TWDB extent of the Edwards-Trinity Plateau Aquifer within the study area. The “Edwards Balcones Fault Zone” region refers to the southern portion of the study area, coincident with the TWDB extent of the Edwards Balcones Fault Zone Aquifer within the study area. Note that, for the purposes of this discussion, both the Edwards-Trinity Plateau region and the Edwards Balcones Fault Zone region extend beyond the current official aquifer extents to the southern boundary of the study area.

4.2.1 Assigning wells to hydrostratigraphic units

The stratigraphic surfaces developed for this report (see Section 4.1) represent a major update to the understanding of geological structure in the HCT region. Therefore, in the current analysis, wells were assigned to aquifers based on these newly-developed stratigraphic surfaces rather than relying on aquifer assignments in the source datasets. This process was also necessary to standardize the assigned hydrostratigraphic unit names for all wells, as most data sources use different naming conventions for the same formations and aquifers. For this reason, water elevations could only be considered for the current analysis if wells had depth or open interval information available. When open-interval information was available, the water-elevation well was assigned to a stratigraphic layer if the entire screen fell within that layer. When only total depth information was available, a water-elevation well was assigned to a stratigraphic layer if the total depth fell within the aquifer. However, if the distance between the total depth and the bottom of the overlying layer was less than the average open-interval length for the assigned stratigraphic layer, that well data were not considered representative of the stratigraphic layer.

An exception to this methodology was implemented for the Edwards Balcones Fault Zone Aquifer extent. For the purposes of the current analysis, if a well fell in the Edwards Balcones Fault Zone Aquifer extent and had an Edwards Balcones Fault Zone Aquifer designation in its source dataset, that well was not used for any analysis of the Trinity hydrostratigraphic units. This was implemented because the well assignment process used in the current analysis did assign some of these wells to Trinity hydrostratigraphic units, and they were anomalous in water elevation and hydraulic properties compared to neighboring Trinity wells. As the Edwards Balcones Fault Zone Aquifer is easily distinguishable from Trinity hydrostratigraphic units in this region, an Edwards Aquifer designation in a source dataset was considered to be reasonably reliable. It was assumed that these erroneous well assignments from the current methodology were due to uncertainty caused by severe offsets in the stratigraphic surfaces representing the faulted Edwards Balcones Fault Zone region, coupled with uncertainty in well location, which affects the estimated depth from ground surface of the well open-interval or well bottom. The current well assignment methodology is assumed to be reliable in the rest of the study area outside the Edwards Balcones Fault Zone region, as the stratigraphic surfaces are smoother, and correspondingly fewer anomalies were noted.

The following discussion is organized by hydrostratigraphic unit according to Figure 2.2.1. Wells in the Edwards hydrostratigraphic unit are completed in the Edwards Limestone in either the Edwards Balcones Fault Zone region or the Edwards-Trinity Plateau region. Wells in the Upper Trinity hydrostratigraphic unit are completed in the Upper Glen Rose Formation. Wells in the Middle Trinity hydrostratigraphic unit are completed in Lower Glen Rose Formation, Hensell Sand, Cow Creek Limestone, or some combination of the three. Wells in the Lower Trinity hydrostratigraphic unit are completed in the Hammett Shale, the Sligo Formation, the Hosston Sand, or some combination of the three. Well data were only considered representative of a hydrostratigraphic unit if the well was entirely screened in that hydrostratigraphic unit, with the following exceptions. If a well intersected Hammett Shale but was otherwise completely screened in the Middle Trinity formations, it was considered representative of the Middle Trinity hydrostratigraphic unit if the majority of the screen was not in the Hammett Shale. This assumes that the Hammett Shale, which acts as a confining layer, contributes very little to productivity at that well location. If a very small portion of a well open-interval (less than 10 percent) intersected either the Pre-Cretaceous basement layer or the layer above the Edwards hydrostratigraphic unit but was otherwise completely open in one of the Trinity hydrostratigraphic units, the well was considered representative of that hydrostratigraphic unit. This was considered a reasonable assumption because, in the context of this report, the Pre-Cretaceous basement layer and the layer above the Edwards hydrostratigraphic unit generally serve as upper and lower boundaries for the Edwards and Trinity hydrostratigraphic units rather than as hydrologically active layers themselves. However, the cutoff for this assumption was purposefully small to avoid erroneously including wells that are actually completed in shallow alluvium or in deeper permeable units, like the Ellenburger-San Saba Aquifer in the northern portion of the study area.

4.2.2 Data Sources

Multiple sources were queried for water elevation measurements in the current study area, including:

- TWDB groundwater database (TWDB, 2017b)
- TWDB submitted drillers reports database (TWDB, 2017d)
- TWDB Brackish Resources Aquifer Characterization System (BRACS) well database (TWDB, 2017a)
- U.S. Geologic Survey National Water Information System database (USGS, 2017)

- Texas Commission on Environmental Quality Public Water Supply well database (TCEQ, 2015)
- Water-elevation data received from GCDs in the study area, including individual records and a compilation of Middle Trinity 2009 water elevations from Barton Springs Edwards Aquifer Conservation District (Hunt et al., 2010)
- Water-elevation data collected for a groundwater model in North Medina County (Young et al., 2005).

The TWDB maintains multiple databases of groundwater wells in the state. The TWDB groundwater database (TWDB, 2017b) is the most useful for long-term, water-elevation analysis, as it includes historical time series of water elevation measurements collected by the TWDB and various state and local entities, including GCDs. Water-elevation measurements are also available from the TWDB submitted drillers reports database (TWDB, 2017d), which includes water-elevation information for water wells drilled within the state. However, this database generally only contains one water elevation per well, recorded at the time of drilling. Water elevation measurements are also available from the TWDB Brackish Resources Aquifer Characterization System (BRACS) database (TWDB, 2017a). However, like the submitted drillers database, there are few transient water-elevation measurements available. Because there is some overlap between these three databases, care was taken to remove duplicate wells and water-elevation measurements.

The U.S. Geologic Survey maintains the National Water Information System database (USGS, 2017), which provides historical time series of water-elevation measurements from their national well monitoring network. This database overlaps with the TWDB groundwater database (TWDB, 2017b), so some duplicate wells and water-elevation measurements had to be removed.

The Texas Commission on Environmental Quality maintains a Public Water Supply well database (TCEQ, 2015), which provides water-elevation measurements for public water supply wells in the state. This database does overlap with the TWDB groundwater database (TWDB, 2017b), so some duplicate wells and water-elevation measurements had to be removed.

The study area intersects twenty-three GCDs (Figure 2.0.5). During stakeholder meetings and other outreach efforts for the current project, all districts were invited to submit relevant water-level data. However, as most districts already coordinate with the TWDB's groundwater monitoring program, many received district water-elevations records were duplicates of records in the TWDB groundwater database (TWDB, 2017b). In addition, received water-elevation records could only be considered if the wells had enough completion information to assign to the current hydrostratigraphic units. Some usable non-duplicate water elevations were obtained from a water-elevation monitoring dataset received from Hays-Trinity GCD and a water-elevation database compiled as part of Hunt and Smith (2010) received from Barton Springs Edwards Aquifer Conservation District. In general, because most GCDs only recently began monitoring activities, or in some cases, only recently were formed, GCD data pertains to recent groundwater elevations collected in the past five to ten years, rather than historical water elevations.

The number of wells with water-level data and the number of water-level measurements for those wells by hydrostratigraphic unit and region are summarized in Table 4.2.1. The spatial distribution of wells with water-level data for the Edwards, Upper Trinity, Middle Trinity and Lower Trinity hydrostratigraphic units are shown in Figure 4.2.2, Figure 4.2.3, Figure 4.2.4, and Figure 4.2.5, respectively. Wells and water-level measurements in the Edwards hydrostratigraphic unit are densely distributed in both the Edwards Balcones Fault Zone region and the Edwards-Trinity Plateau region. However, the Edwards-Trinity Plateau region has far fewer long-term (greater than 10 years) water-elevation records available than the Edwards Balcones Fault Zone region. Wells and water-level measurements in the Upper Trinity hydrostratigraphic unit are distributed in dense clusters along the Edwards Balcones Fault Zone region in Travis, Hays, Comal and Medina counties and in the Edwards-Trinity Plateau region in Gillespie, Kimble, Kerr, Real, Edwards and Val Verde counties. However, there are very few long-term water-elevation records for the Upper Trinity hydrostratigraphic unit available anywhere in the study area except a cluster in Val Verde County. Wells and water-level measurements in the Middle Trinity hydrostratigraphic unit are densely distributed across all of the HCT region and along the northern edge of the Edwards Balcones Fault Zone region. There are few measurements in the Edwards-Trinity Plateau region except for dense clusters in Real County and along outcrop areas in Kimble County. Wells and water-level measurements in the Lower Trinity hydrostratigraphic unit are densely distributed along the southern portion of the HCT region in Travis, Hays, Comal, northwestern Bexar, and Bandera counties. There are some measurements along the northern edge of the Edwards Balcones Fault Zone region, but almost none available in the Edwards-Trinity Plateau region. There are few long-term, water-elevation records for the Lower Trinity hydrostratigraphic unit available outside small clusters in Travis, Hays, Kendall, Bandera and Kerr counties.

The temporal distribution of the number of wells with water-level measurements by decade and the number of water-level measurements in each hydrostratigraphic unit by decade are tabulated in Table 4.2.2 and Table 4.2.3, respectively. These values are also shown in Figure 4.2.6 a and Figure 4.2.6b, Figure 4.2.7a, and Figure 4.2.7b for the Edwards, Upper Trinity, Middle Trinity and Lower Trinity hydrostratigraphic units, respectively. While water elevations in the Edwards hydrostratigraphic unit have been measured regularly since the 1930s/1940s, the majority of water elevations for the Trinity hydrostratigraphic units weren't measured until recently. Regular measurement of water elevations in the Middle Trinity hydrostratigraphic unit began in the 1990s, while measurements for the Upper and Lower Trinity hydrostratigraphic units did not begin in earnest until the 2000s. There are still very few measurements for the Upper Trinity hydrostratigraphic unit, even in the 2010s.

4.2.3 Creation of Water-Level Contours

Using the water-elevation measurements compiled for the current project as control points, water-elevation surfaces were created using the TopoToRaster and contoured using the Contour tool in ESRI ArcMap 10.3. Water elevation contours were created for each hydrostratigraphic unit for selected years (see Section 4.2.4 and Section 4.2.5). However, contours were not created unless at least 10 water-elevation control points were available for a selected hydrostratigraphic unit and time period. The Trinity hydrostratigraphic units underlying the Edwards hydrostratigraphic unit in the Edwards-Trinity Plateau Aquifer region are assumed to be contiguous with and hydraulically connected to the Trinity hydrostratigraphic units in the HCT region. Therefore, one continuous water-elevation surface was contoured across these two regions for each hydrostratigraphic unit. This is consistent with previous water-elevation contours created in the study area, including Mace et al. (2000), Kuniansky and Ardis (2004), and Jones et al. (2011).

Unlike previous regional studies, the current study area also includes the Edwards Balcones Fault Zone region. Water elevation measurements for the Trinity hydrostratigraphic units in this region were contoured separately from the HCT region. Severe fault offsets in the Edwards Balcones Fault Zone region can strongly influence flow within Trinity hydrostratigraphic units across the transition from the HCT region to the Edwards Balcones Fault Zone region, but the exact mechanisms are unclear. Significant lateral flow is assumed from the Trinity hydrostratigraphic units into the Edwards hydrostratigraphic unit where they are juxtaposed due to faulting (Mace et al., 2000; Kuniansky et al., 2004; Jones et al., 2011). In this scenario, water elevations in Trinity hydrostratigraphic units would be more continuous with the water elevations in the Edwards hydrostratigraphic unit than with the offset Trinity units below the Edwards hydrostratigraphic unit. The contouring methodology used in the current study creates topographically smooth water elevations and will not address all the complexities inherent in interpreting structure-induced groundwater flow or discontinuities in this region. For this reason, the water-elevation control points north and south of the Edwards Balcones Fault Zone region were contoured separately for the Trinity hydrostratigraphic units. The control points for the Edwards hydrogeologic unit were not analyzed separately but contoured together across the transition from the Edwards-Trinity Plateau Aquifer to the Edwards Balcones Fault Zone Aquifer in Kinney County. The division between these two aquifers is based on groundwater topography rather than structure, so it is appropriate to contour one continuous water-elevation surface across these two regions.

4.2.4 Pre-development Water-Level Contours

Pre-development conditions are defined as those existing in the aquifer before the natural flow of groundwater was disturbed by artificial discharge via pumping. Typically, pre-development conditions represent steady-state conditions in the aquifer, where aquifer recharge is balanced by natural aquifer discharge.

In some portions of the study area, pumping in the Trinity hydrostratigraphic units of the HCT region and the Edwards-Trinity Plateau region began as early as the 1930s/1940s (Section 4.6.2). However, water-elevations measured prior to the actual start of pumping and representative of pre-development conditions in the study area are scarce and insufficient to construct pre-development water-elevation contours for the aquifer. For this reason, earlier studies and modelling efforts in the study area used approximations for “near-predevelopment” conditions. Bush et al. (1993) and Barker and Ardis (1996) use water-elevations measured between 1915-1969. They do note that these water elevations may be affected by groundwater development in Bexar County. Mace et al. (2000) used water elevations measured in a 20-year window around 1975 (1965-1985) to approximate steady-state groundwater conditions. Jones et al. (2011) used an 8-year window around 1980 (1977-1985) to approximate steady-state groundwater conditions.

For the purposes of this analysis, water elevations prior to 1975 were considered for developing the estimated pre-development water-level contours. If multiple measurements prior to 1975 were available for a well, the maximum of those measurements was used. Individual water elevations measured prior to 1975 were not used if they were taken during a drought year. Drought years were defined using Lowry (1959), which describes Texas droughts that occurred in the late 18th and 19th centuries. The current study area falls in the affected zone for most of the droughts described in that bulletin, including major droughts in the 1930s and 1950s.

The locations of springs and streams were also considered, as Barker and Ardis (1996) note that these are important controls on water elevations in the Edwards-Trinity Aquifer system. Spring locations that fell within an aquifer outcrop were used to constrain the pre-development head for that aquifer. The surface elevations, based on the 10-m DEM, for each spring location were used as additional control points for the pre-development head. Perennial stream segments, as defined in the NHDPlus hydrography dataset (USEPA and USGS, 2012), provided additional constraints for the pre-development water elevations. Perennial stream segments that intersected an aquifer outcrop were sampled at 25-foot intervals and a surface elevation was assigned to each point, based on the current project's digital elevation model (DEM) surface. These elevations were used as additional control points for the pre-development head.

Edwards hydrostratigraphic unit

For this analysis, the Edwards hydrostratigraphic unit refers to the Edwards Limestone occurring in both the Edwards-Trinity Plateau Aquifer and the Edwards Balcones Fault Zone Aquifer. The estimated pre-development water-elevation contours and the locations of the control points used to create the contours for the Edwards hydrostratigraphic unit are shown in Figure 4.2.8. The estimated pre-development Water elevations in the Edwards-Trinity Plateau region range from a high of about 2,000 ft above mean sea level at the northwestern end of the study area in Kimble County to a low of around 1,000 ft above mean sea level in the southwestern portion of the study area in Kinney County. In the Edwards Balcones Fault Zone region, water elevations range from a high of about 1,000 ft above mean sea level in the outcrop and to a low of around 500 ft above mean sea level in the eastern subcrop in Caldwell and Bastrop counties. In general, the contour lines in the Edwards-Trinity Plateau Aquifer region show groundwater flowing south and southwest. The contour lines in the Edwards Balcones Fault Zone region show groundwater flowing downdip towards the south and southeast.

Upper Trinity hydrostratigraphic unit

The estimated pre-development water-elevation contours and the locations of the control points used to create the contours for the Upper Trinity hydrostratigraphic unit are shown inFigure 4.2.9. In the Edwards-Trinity Plateau region, the estimated pre-development Water elevations range from a high of about 1,900 ft above mean sea level at the north central end of the hydrostratigraphic unit in Gillespie and Kerr counties to a low of around 1,000 ft in the south-western portion in Kinney and Val Verde counties. In general, the contour lines in the Edwards-Trinity Plateau Aquifer region show groundwater flowing south and southwest, except where it intersects erosional drainages and flow instead towards the Nueces and Frio rivers. In the HCT region, the estimated pre-development Water elevations range from a high of around 1,700 ft along the boundary with the Edwards-Trinity Plateau region to a low of around 600 ft at the eastern end of the study area near the Colorado River in Travis County. In general, the contour lines in the HCT region show groundwater flowing east and southeast, generally following topography. There were insufficient data in the Edwards Balcones Fault Zone region to interpret pre-development groundwater flow.

Middle Trinity Hydrostratigraphic Unit

The estimated pre-development water-elevation contours and the locations of the control points used to create the contours for the Middle Trinity hydrostratigraphic unit are shown in Figure 4.2.10. In the Edwards-Trinity Plateau region, the estimated pre-development water-elevations range from a high of about 1,800 to 1,900 ft above mean sea level at the northern edge of the hydrostratigraphic unit along the outcrop in Gillespie and Kimble counties to a low of around

1,100 ft in the western portion in Val Verde County. In general, the contour lines in the Edwards-Trinity Plateau Aquifer region show groundwater flowing south and southwest, although this trend is largely driven by a single data point in Val Verde County and so may not reflect true conditions. There is also an area of northward flow towards the Llano River in the northern outcrop in Kimble County. In the Hill County Trinity Aquifer region, the estimated pre-development water elevations range from 1,500 ft above mean sea level along the boundary with the Edwards-Trinity Plateau region to about 700 ft above mean sea level at the eastern end of the study area near the Colorado River in Travis County. In general, the contour lines in the Hill County Trinity Aquifer region show groundwater flowing east and southeast, following topography towards the Edwards Balcones Fault Zone region. The exception is an area in Travis County that appears to drain towards the Colorado River. There was insufficient data in the Edwards Balcones Fault Zone region to interpret pre-development groundwater flow.

<u>Lower Trinity Hydrostratigraphic Unit</u>
The estimated pre-development water elevation contours and the locations of the control points used to create the contours for the Lower Trinity Hydrogeologic Unit are shown in Figure 4.2.11. Based on available information, these contours were only created in the HCT region. The estimated pre-development water elevations range from a high of about 1,500 ft above mean sea level at the northern end of the aquifer in Kerr and Kendall counties to a low of about 600 ft at the eastern end of the study area near the Colorado River in Travis County. In general, the contour lines show groundwater flowing east and southeast, following topography towards the Edwards Balcones Fault Zone region.

4.2.5 Historical Water Elevation Contours

Historical water-elevation contours for the HCT Aquifer were estimated for the years 1990, 2000, and 2010. Water elevation data are not available at regular time intervals in every well. Therefore, the coverage of water-elevation data for a particular month or even a year within an aquifer is sparse. Because the amount of available water-elevation data for a particular year of interest is typically not sufficient to interpolate a water-elevation surface, the historical water-elevation contours were developed based on data from a five-year window around the year of interest. The range of years used was 1988 through 1992 for the 1990 water elevations, 1998 through 2002 for the 2000 water elevation, and 2008 through 2012 for the 2010 water elevations. If a well had multiple water-elevation measurements during the range of years, the average of those measurements was used.

<u>Edwards Hydrostratigraphic Unit</u>

The estimated historical water-elevation contours and the locations of the control points used to create the 1990, 2000, and 2010 contours for the Edwards hydrostratigraphic unit are shown in Figure 4.2.12, Figure 4.2.13, and Figure 4.2.14, respectively. In the Edwards-Trinity Plateau region, water elevations estimated for the Edwards hydrostratigraphic unit in 1990 range from a high of around 2,000 ft above mean sea level in the northwestern portion of the hydrostratigraphic unit in southern Kimble, northern Real, northern Edwards and western Kerr counties to around 1,000 ft in the southwestern portion in Val Verde and Kinney counties. In general, the contour lines in the Edwards-Trinity Plateau Aquifer region show groundwater flowing south and southwest, along this hydraulic gradient, or east and southeast along topography towards the boundary with the HCT region. Water elevations estimated for the Edwards hydrostratigraphic unit in 2000 follow the same general trends in the Edwards-Trinity

Plateau region, although there is some evidence of drawdown in northern Edwards County and central Kerr County along the boundary with the HCT region. Water elevations estimated for the Edwards hydrostratigraphic unit in 2010 also follow the same general trends as previous years, but these are more difficult to interpret as there are many more high-density localized drawdown and recovery variations that may not be representative of the regional groundwater flow. There is some evidence of drawdown in central Kerr County along the boundary with the HCT region, as well as several areas of aquifer recovery, including Gillespie County and southern and western Edwards County. The slight groundwater divide along the boundary between the Edwards-Trinity Plateau Aquifer subcrop and the Edwards Balcones Fault Zone Aquifer subcrop in Kinney County is evident in all time periods.

In the Edwards Balcones Fault Zone region, water elevations estimated for the Edwards hydrostratigraphic unit in 1990 range from a high of around 1,200 ft along the northern edge of the outcrop in Medina County to lows of around 500 to 600 ft in the subcrop in Bexar, Comal, Hays and Travis counties. In general, the contour lines show groundwater flowing south and southeast, down from the outcrop into the subcrop. Water elevations estimated for the Edwards hydrostratigraphic unit in 2000 follow the same general trends in the Edwards Balcones Fault Zone region, although there is some evidence of drawdown in the subcrop in western Medina County and water elevations are lower in the outcrop in Medina County.

<u>Upper Trinity Hydrostratigraphic Unit</u>

The locations of the water-elevation control points for the Upper Trinity hydrostratigraphic unit in for 1990, 2000, and 2010 are shown in Figure 4.2.15, Figure 4.2.16, and Figure 4.2.17, respectively. There were insufficient data to create 1990 water-elevation contours, so these water elevations are presented as point data. The estimated historical water elevations are shown as contours for 2000 and 2010.

Across the Edwards-Trinity Plateau and HCT regions, water elevations at control points for the Upper Trinity hydrostratigraphic unit in 1990 range from a high of about 1,950 ft above mean sea level in eastern Kerr County to a low of 1,130 ft in Val Verde County. Water elevations estimated for the Upper Trinity hydrostratigraphic unit in 2000 indicate somewhat lower water elevations along the boundary with the HCT region as compared to the 1990 control points. Water elevation elevations range from a high around 2,000 ft above mean sea level in northern Edwards County to a low around 800 ft along the boundary with the Edwards Balcones Fault Zone region in Travis County. In general, the 2000 contour lines show flow from the northern Edwards-Trinity Plateau region towards the south and southwest towards Uvalde and Val Verde counties or towards the east across the Upper Trinity outcrop in the Hill Country region towards the boundary with the Edwards Balcones Fault Zone region. Water elevations estimated for the Upper Trinity hydrostratigraphic unit in 2010 follow the same general trends as previous years, although there is some evidence of drawdown in southwestern Edwards County and potential recovery in central Kerr County along the boundary with the HCT region. There are also significantly lower water elevations in Bandera County, but it is unclear if this is pattern is due to different control points or a true decrease in water elevations.

In the Edwards Balcones Fault Zone region, water elevations of control points for the Upper Trinity hydrostratigraphic unit in 1990 range from about 880 to 820 ft above mean sea level along the northern edge Edwards hydrostratigraphic unit outcrop. Water elevations estimated for the Upper Trinity hydrostratigraphic unit in 2000 do indicate slightly higher water elevations along the northern edge in Medina County as compared to the 1990 control points. In general, the contour lines are similar to those in the Edwards stratigraphic unit in this region, with groundwater flowing south and southeast. Water elevations estimated for the Upper Trinity hydrostratigraphic unit in 2010 follow the same general trends in the Edwards Balcones Fault Zone region, although there is some evidence of drawdown in east-central Bexar County.

Middle Trinity Hydrostratigraphic Unit

The estimated historical water-elevation contours and the locations of the control points used to create the 1990, 2000, and 2010 contours for the Middle Trinity hydrostratigraphic unit are shown in Figure 4.1.18, Figure 4.1.19, and Figure 4.1.20, respectively.

In the Edwards-Trinity Plateau region, there are insufficient data to contour the western portion of this region, so the analysis focuses on the eastern portion of the region. Across the Edwards-Trinity Plateau and HCT regions, the Water elevations estimated for the Middle Trinity hydrostratigraphic unit in 1990 range from a high of around 1,700 ft above mean sea level in Gillespie County to a low around 700 ft near the Colorado River in Travis County. In general, contour lines show groundwater flowing south and southeast from the Edwards-Trinity Plateau region towards the boundary with the Edwards Balcones Fault Zone region or east across the HCT region towards the boundary with the Edwards Balcones Fault Zone region. Water elevations estimated for the Middle Trinity hydrostratigraphic unit in 2000 follow the same general trends as in 1990, although there is some evidence of drawdown in eastern Kerr County and in Travis County, and recovery in Kimble County. Water elevations estimated for the Middle Trinity hydrostratigraphic unit in 2010 also follow the same general trends as previous years, but these are more difficult to interpret as there are many more high-density localized drawdown and recovery variations that may not be representative of the regional groundwater flow.

In the Edwards Balcones Fault Zone region, there were insufficient data to interpret Water elevations for the Middle Trinity hydrostratigraphic unit in 1990. In both 2000 and 2010, the Water elevations estimated for the Middle Trinity hydrostratigraphic unit range from a high of around 1,100 at the northern edge of the Edwards Balcones Fault Zone Aquifer outcrop in Uvalde County to a low around 400 to 500 ft in central Travis and Comal counties. In general, the contour lines show groundwater flowing south and southeast.

Lower Trinity Hydrostratigraphic Unit

The estimated historical water-elevation contours and the locations of the control points used to create the 1990, 2000, and 2010 contours for the Lower Trinity hydrostratigraphic unit are shown in Figure 4.2.21, Figure 4.2.22, and Figure 4.2.23, respectively. There are insufficient data to contour Water elevations for the Lower Trinity hydrostratigraphic unit in the Edwards-Trinity Plateau region until 2010, so the analysis mostly focuses on the HCT region. Water elevations estimated for the Lower Trinity hydrostratigraphic unit in 1990 range from 1,400 ft above mean sea level in eastern Kerr County to a low of around 600 ft in Travis County. In general, contour lines show groundwater flowing south and southeast, from the northwest towards the boundary with the Edwards Balcones Fault Zone region. Water elevations estimated for the Lower Trinity hydrostratigraphic unit in 2000 follow the same general trends as in 1990 although with higher water elevations in Kendall and Blanco counties and a steeper gradient towards the northeast in Travis County. Water elevations estimated for the Lower Trinity hydrostratigraphic unit in 2010 add additional information to characterize portions of the Edwards-Trinity Plateau region show groundwater flowing to the south and southwest in Real County in that region. Otherwise, flow in the rest of the Hill Country region is similar to trends in previous years, although with some evidence of drawdown in the area near the Comal/Kendall county boundary.

In the Edwards Balcones Fault Zone region, there were insufficient data to interpret Water elevations for the Lower Trinity hydrostratigraphic unit in 1990 and 2000. Water elevations estimated for the Lower Trinity hydrostratigraphic unit in 2010 range from about 1,000 ft above mean sea level in northern Medina County to a low of about 500 ft in Comal and Travis counties. In general, the contour lines show groundwater flowing southeast.

4.2.6 Transient Water Elevation Data in Individual Wells

An evaluation of the transient behavior of water elevations in the study area was conducted using transient water-level data in wells. Transient data were considered to consist of ten or more water-level measurements in a given well over a period of ten or more years. The locations of wells with transient water-level data in the Edwards, Upper Trinity, Middle Trinity and Lower Trinity were shown previously in Figure 4.2.2, Figure 4.2.3, Figure 4.2.4, and Figure 4.2.5. All hydrographs for these wells could not be presented and discussed in the main body of the report. Instead, hydrographs for these wells, showing the transient Water elevations and land-surface elevation, are provided in Appendix A.

The hydrographs discussed here were selected based on several criteria. First, a review of all hydrographs was conducted in order to select those with a long-term (greater than 10 years) record. Second, hydrographs were selected based on spatial location to cover as much of each hydrostratigraphic unit as possible. Third, an effort was made to select hydrographs with sufficient data to define a water-level trend and with data that appear to be free of measurements potentially impacted by drilling and/or pumping activities.

In addition to the water-level data (blue line and symbol), each hydrograph shown in Figure 4.2.24 through Figure 4.2.28 includes the elevation of the land surface (green line). The land-surface elevation is based on the value of the DEM surface at that well location. Including the ground surface allows evaluation of the depth to groundwater in the well. For all hydrographs, the time scale of the x-axis is 1950 to 2020. The scale of the water elevation on the y-axis varies from hydrograph to hydrograph depending on the range of the observed data; however, the division of the y-axis is consistent at 10 ft.

<u>Edwards Hydrostratigraphic Unit</u>

Select hydrographs for wells completed in the Edwards hydrostratigraphic unit are shown in Figure 4.2.24. Only wells falling in the Edwards-Trinity Plateau region are included in this discussion of the Edwards hydrostratigraphic unit. Hydrographs from the Edwards Balcones Fault Zone region are not discussed but are included in Appendix A. In general, the Edwards hydrostratigraphic unit data in the Edwards-Trinity Plateau region show relatively flat groundwater elevations, with typical fluctuations in water elevations of less than 10 ft over the period of record. These data show no long-term decline in water elevations, indicating that pumping has not had a long-term negative effect on water elevations on the Edwards hydrostratigraphic unit in the Edwards-Trinity Plateau region. Two wells (wells 7033604 and 5734702) show increases in water elevations over time. The increase in well 7033604 occurred over the period from 1965 to 1975 in Val Verde County and the increase in well 5734702 occurred over the period from 1990 to 2005 in Gillespie County.

<u>Upper Trinity Hydrostratigraphic Unit</u>

Select hydrographs for wells completed in the Upper Trinity hydrostratigraphic unit are shown in Figure 4.2.25. As long-term hydrographs in the Upper Trinity hydrostratigraphic unit are scarce, this figure includes all records with at least 10 measurements over at least l0 years. As a result, some of the hydrographs are of poor quality with spikes that potentially indicate the influence of pumping on the measurement. In particular, long-term groundwater behavior could not be reliably interpreted from well 743302 in Kinney County and well 6901702 in Real County. Hydrographs in Val Verde County (wells 7025502, 7025603, 7026102, and 7026401) all show dramatic increases (50 to 150 ft) in groundwater elevations in the Upper Trinity hydrostratigraphic unit around 1970. These increases generally occurred sometime during the period from 1965 to 1975. Well 7026102 does not include interim data between about 1970 and 2005, but it seems reasonable to assume the recovery happened over the same timeline as the other Val Verde County wells. These wells are all located near the Amistad Reservoir which was impounded in 1969, so these increases likely reflect the influence of the reservoir on the groundwater system in the area. In Hays County, well 5857401 showed a recovery of about 30 ft during the period from 1955 to 1960 but then a decline of about 10 to 15 ft from 1960 to the late 1980s. Well 5742306 in Gillespie County shows about 15-foot decline during the period from 1985 to 1995 but relatively flat groundwater elevations before and after that period.

Middle Trinity Hydrostratigraphic Unit

Select hydrographs for wells completed in the western and west-central portion of the Middle Trinity hydrostratigraphic unit are shown in Figure 4.2.26. Wells in the west and west-central portions of the Middle Trinity hydrostratigraphic unit (wells 5625906, 5656805, 5751802, and 6918303) show relatively flat groundwater elevations for most of the period of record, although two wells have shown recent declines in water elevations. Well 5751802 in Gillespie County showed a decline and recovery of about 20 ft in the 1990s and a more recent decline of about 10 ft from 2005 to 2015. Well 69118303 in Real County showed a slow 10-foot decline from 1985 to 2010, followed by a sharp 40-foot decline to the present. Wells in the central part of the study area (wells 6916201, 6801505, 5757703, and 5749701) have been steadily declining over the period of record. Wells in Kerr County have the highest drawdowns, with almost 150 ft of decline over 40 years at well 6916201, about 100 ft decline over 30 years at well 5757703, and about 50 ft of decline over 30 years at well 6801505.

Select hydrographs for wells completed in the east and east-central portions of the Middle Trinity hydrostratigraphic unit are shown in Figure 4.2.27. Wells near outcrops of the Middle Trinity hydrostratigraphic unit (wells 6811103, 6811715, 5761803, and 5764702) show relatively stable water elevations over time, with typical fluctuations under 10 ft. The other wells (wells 6912501, 5758706, 5758402, 5755401) show steady declines of 60 to 80 ft over a period of about 30 years. This indicates that wells near the outcrop of the Middle Trinity hydrostratigraphic unit are more resilient to negative effects from pumping than wells located farther in the subcrop, potentially due to the higher storage potential in the outcrop, as well as closer proximity to focused recharge from surface water features.

Lower Trinity Hydrostratigraphic Unit

Select hydrographs for wells completed in the Lower Trinity hydrostratigraphic unit are shown in Figure 4.2.28. Two wells (wells 6819208 and 5763702) show historical declines followed by recent periods of stable water elevations. Wells in Bandera County (wells 6916702 and 6924102) and Travis County (wells 5850120 and 5842802) show steady declines over time, with the largest decline of about 300 ft in well 6924102 in Bandera County over a period of 30 years. Two wells in Kendall County (wells 6804909 and 6804916) show water elevations at two different time periods in the same area of the Lower Trinity hydrostratigraphic unit. Water elevations rose about 30 ft in well 6804909 from 1975 to 1995, but then water elevations declined sharply about 100 ft in the nearby well 6804916 from 2005 to 2015.

4.2.7 Transient Water-Level Calibration Targets

Recommended water-level calibration targets for use in numerical modeling are the wells with at least 10 water-elevation measurements over at least 10 years of record. The locations of these wells were shown previously in Figure 4.2.2, Figure 4.2.3, Figure 4.2.4, and Figure 4.2.5 and the hydrographs for these wells are included in Appendix A. If these are not sufficient, the compilation of water-elevation measurements for the current project can provide water-level records with shorter timeframes. However, the longer water-elevation records are recommended as they represent the long-term groundwater behavior in the study area better than point measurements. The number of long-term calibration targets available for the transient model by hydrostratigraphic table is provided in Table 4.2.3. Calibration targets in the Upper Trinity hydrostratigraphic unit are limited to the Edwards-Trinity Plateau region, whereas targets for the Middle Trinity and Lower Trinity hydrostratigraphic units are mostly limited to the HCT region.

4.2.8 Cross Formational Flow

The following subsection discusses the potential for flow between the Upper, Middle and Lower Trinity hydrostratigraphic units was investigated as well as cross-formational flow between the Trinity hydrostratigraphic units and underlying or overlying aquifers. Each of these is discussed in the following subsections.

4.2.8.1 Vertical Flow within the Trinity hydrostratigraphic units

Very low cross-formational flow is expected between the Upper, Middle and Lower Trinity hydrostratigraphic units in the study area. As discussed in Barker and Ardis (1996), the tight low-permeability interbeds in the Upper and Middle Trinity hydrostratigraphic units can severely restrict vertical flow so that groundwater moves laterally along impermeable bedding (often discharging from seeps and springs) rather than percolating into the underlying Trinity hydrostratigraphic units. One study in north Bexar County estimated that the vertical hydraulic conductivity of these confining units of the Trinity Aquifer, including the Hammett Shale, Bexar Shale, and the clays and marls of upper member of the Glen Rose Limestone, was only around 0.0001 to 0.003 ft/day (W.E. Simpson Company and William F. Guyton Associates, 1993). Thus, the low-permeability clays and marls of the Upper Trinity hydrostratigraphic unit are thought to restrict flow into underlying units and the Hammett Shale restricts flow between the Middle and Lower Trinity hydrostratigraphic units. Anaya and Jones (2009) also considered the effect of this stratification on groundwater flow in the HCT region compared to other portions of the Edwards-Trinity Plateau Aquifer. They note that the shale, sand, and limestone transgressive-regressive sequence represented by the Upper, Middle and Lower Trinity sediments introduces significant vertical anisotropy compared to the thinner, but more homogenous Trinity Sands in the northwest portion of the Edwards-Trinity Plateau Aquifer (Anaya and Jones, 2009).

To evaluate the potential for vertical flow between the Trinity hydrostratigraphic units, Water elevations from the current project's water-elevation compilation were compared for closely spaced wells completed in different hydrostratigraphic units. These comparisons are shown in Figure 4.2.29. In western Kerr County, a Middle Trinity well has water elevations at least 100 ft below water elevations in two Upper Trinity wells, showing a clear separation between those units in the Edwards-Trinity Plateau region. In northwest Bandera County, a Middle Trinity well has water elevations greater than 200 ft below the water elevation in an Upper Trinity well. The division between Trinity hydrostratigraphic units is not as clear in the HCT region. In a Middle Trinity well in Hays County, the water elevations are almost 300 ft above water elevations in a nearby Lower Trinity well. However, in another two Middle Trinity wells in Hays County, nearby Lower Trinity water elevations overlap the water elevations in the Middle Trinity hydrostratigraphic unit. Similar behavior occurs in east-central Bandera County, where two Middle Trinity wells are mostly above but sometimes overlap with water elevations in the nearby Lower Trinity wells. It is unclear if this behavior indicates natural flow between the Middle and Lower Trinity hydrostratigraphic units or if these wells may actually be screened over both units. The limited spatial coverage of appropriate well pairs with long-term measurements make it difficult to reach significant conclusions regarding vertical flow between Trinity hydrostratigraphic units. However, at least a few examples agree with the literature in that they show high resistance to cross-formational flow, as evidenced by large differences in water elevations between units.

4.2.82 Cross-Formational Flow between the Trinity hydrostratigraphic units and Underlying or Overlying Aquifers

Given the low-permeability units of the Upper Trinity hydrostratigraphic unit, little vertical flow is expected from the overlying Edwards hydrostratigraphic unit to the Trinity hydrostratigraphic units. In the Edwards Balcones Fault Zone region, Trinity pumping tests under the Edwards unit have shown no drawdown in nearby Edwards wells (Hunt et al., 2010), indicating little connection between the Trinity and Edwards hydrostratigraphic units. Recent multiport measurements in the Edwards Balcones Fault Zone region also indicated no vertical flow between the units (Wong et al., 2014). To evaluate the potential for vertical flow from the Edwards hydrostratigraphic unit in the Edwards-Trinity Plateau region, Water elevations from the current project's water-elevation compilation in Edwards wells were compared to nearby wells completed in Trinity hydrostratigraphic units. These comparisons are also shown in Figure 4.2.29. In all cases, the Edwards wells have much higher water elevations than wells in any of the Trinity hydrostratigraphic units, indicating little communication between these units. The one exception is an Upper Trinity water elevation measurement in western Bandera County that is similar to nearby Edwards water elevations. However, it is unclear if this behavior indicates natural flow between the Edwards and Upper Trinity hydrostratigraphic units or if this well may actually be screened over both units.

Any cross-formational flow between the Trinity and Edwards hydrostratigraphic units is expected to be primarily lateral rather than vertical, as permeable blocks of these units can be juxtaposed at the boundary of the Edwards Balcones Fault Zone region. Recent research has found similar water elevations, physical characteristics and geochemical properties between the juxtaposed Upper Trinity and Edwards hydrostratigraphic units, indicating lateral connections between these units (Wong et al., 2014). Dye tracing tests have also indicated lateral connections between the Upper Trinity and Edwards hydrostratigraphic units (Johnson et al., 2010). Previous groundwater models of the Trinity hydrostratigraphic units acknowledge this connection by implementing a discharge component from the Trinity hydrostratigraphic units in the HCT region into the Edwards hydrostratigraphic unit in the Edwards Balcones Fault Zone region. Kuniansky and Ardis (2004) simulated a flow of between 1,900 to 2,300 acre-ft per year per mile into the Edwards hydrostratigraphic zone along the fault zone, which they conceptualized as "equivalent to a low permeability seepage face with a slow drip of water per square foot of area."

Previous TWDB groundwater availability models in the study area (Mace et al., 2000; Jones et al., 2011) also included lateral flow into the Edwards hydrostratigraphic unit as a significant discharge component from the Trinity hydrostratigraphic units.

The water-elevation comparisons shown in Figure 4.2.29 include one comparison between a Middle Trinity well in northern Medina County north of the Edwards Balcones Fault Zone region and a nearby Edwards well within the Edwards Balcones Fault Zone region. The water elevations in the Edwards well are higher than the water elevations in the Middle Trinity well, indicating a lack of direct connection between these units. However, this is not necessarily inconsistent with the literature. Wong et al. (2014) found evidence for connections between the Upper Trinity and Edwards hydrostratigraphic units but noted that there was no probable connection between the Middle Trinity and Edwards hydrostratigraphic unit. The limited spatial coverage of appropriate well pairs with long-term measurements make it difficult to reach significant conclusions regarding lateral flow between the Edwards and Trinity hydrostratigraphic units along the northern boundary of the Edwards Balcones Fault Zone region.

Table 4.2.1 Number of wells with water-level data and number of water-level measurements by hydrostratigraphic unit by groundwater region (as defined in Figure 4.2.1).

Formation	Groundwater Region	Number of Wells with Water-Level Data	Number of Water-Level Measurements
Edwards	HCT	18	139
	Edwards-Trinity Plateau	1,992	8,887
	Edwards-BFZ	2,165	93,057
	TOTAL	4,175	102,083
Upper Trinity	HCT	28	31
	Edwards-Trinity Plateau	503	1,475
	Edwards-BFZ	613	661
	TOTAL	1,144	2,167
Middle Trinity	HCT	6,466	41,945
	Edwards-Trinity Plateau	887	3,198
	Edwards-BFZ	933	2,610
	TOTAL	8,286	47,753
Lower Trinity	HCT	2,422	7,654
	Edwards-Trinity Plateau	32	517
	Edwards-BFZ	207	497
	TOTAL	**2,661**	8,668

Table 4.2.2 Number of wells with water-elevation measurements in each hydrostratigraphic unit by decade.

Hydrostratigraphic unit	Number of wells by decade									
	Pre-1930	1930s	1940s	1950s	1960s	1970s	1980s	1990s	2000s	2010s
Edwards	15	184	138	673	451	357	272	247	1,723	1,147
Upper Trinity	0	4	1	53	61	24	19	30	642	361
Middle Trinity	1	64	103	96	426	343	345	451	4,517	2,639
Lower Trinity	1	6	3	25	46	82	48	70	1,430	1,085

Table 4.2.3 Number of water-level measurements in each hydrostratigraphic unit by decade.

Hydrostratigraphic unit	Number of water-elevation measurements by decade									
	Pre-1930	1930s	1940s	1950s	1960s	1970s	1980s	1990s	2000s	2010s
Edwards	17	2,144	3,867	11,489	14,026	13,979	12,455	11,318	18,696	14,092
Upper Trinity	0	5	2	67	205	253	80	77	729	749
Middle Trinity	1	64	106	137	535	657	1,290	7,081	20,952	16,930
Lower Trinity	1	18	30	28	91	169	144	357	3,889	3,941

Table 4.2.4 Number of water-level targets for the transient model in each hydrostratigraphic unit by groundwater region (as defined in Figure 4.2.1) and by decade.

Hydrostratigraphic Unit	Region		Well with at least 10 water elevations over at least 10 years
Edwards	HCT		0
	Edwards-Trinity Plateau		36
	Edwards-BFZ		195
		TOTAL	231
Upper Trinity	HCT		0
	Edwards-Trinity Plateau		7
	Edwards-BFZ		1
		TOTAL	8
Middle Trinity	HCT		151
	Edwards-Trinity Plateau		14
	Edwards-BFZ		3
		TOTAL	168
Lower Trinity	HCT		29
	Edwards-Trinity Plateau		0
	Edwards-BFZ		2
		TOTAL	31

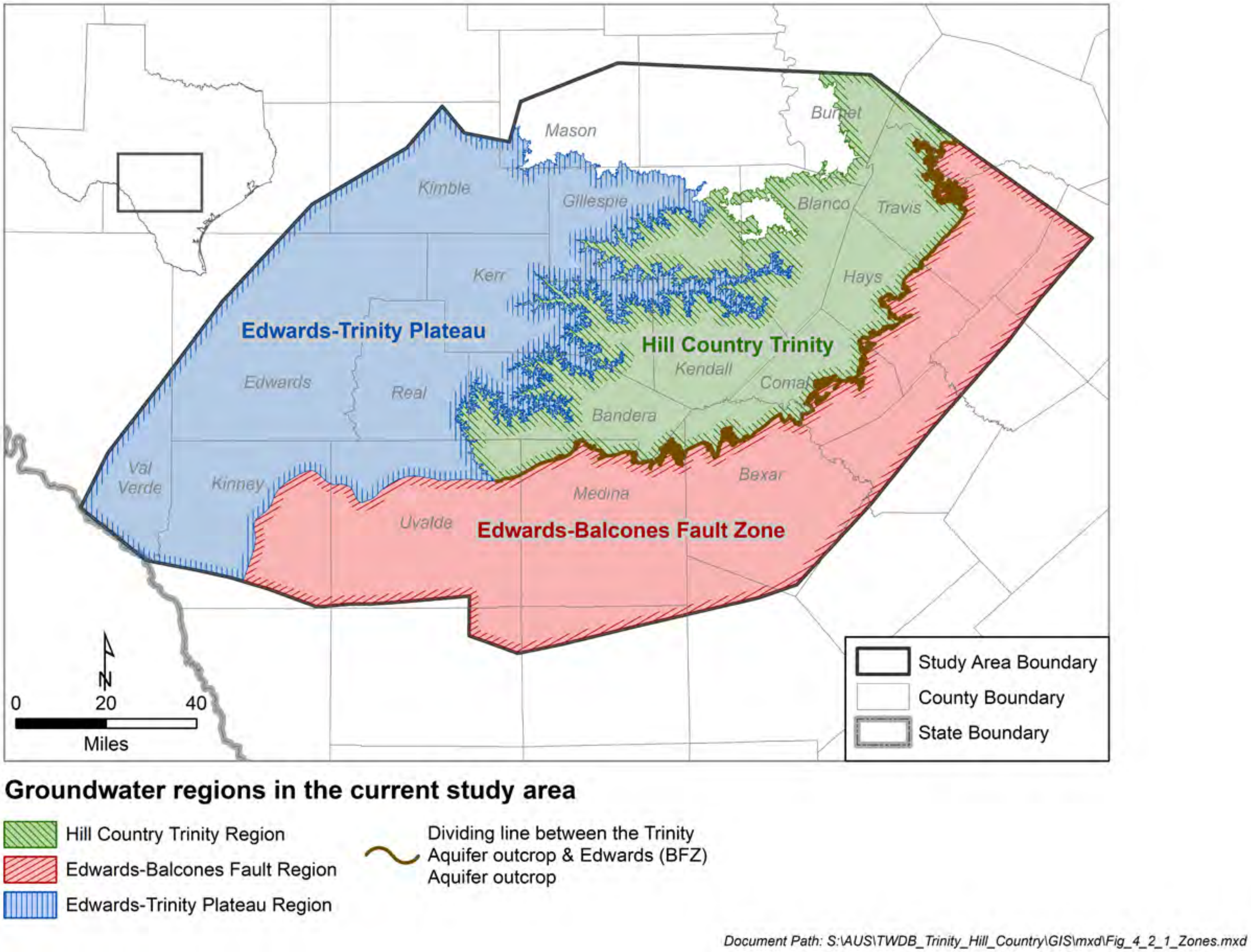

Figure 4.2.1 Groundwater regions in the current study area.

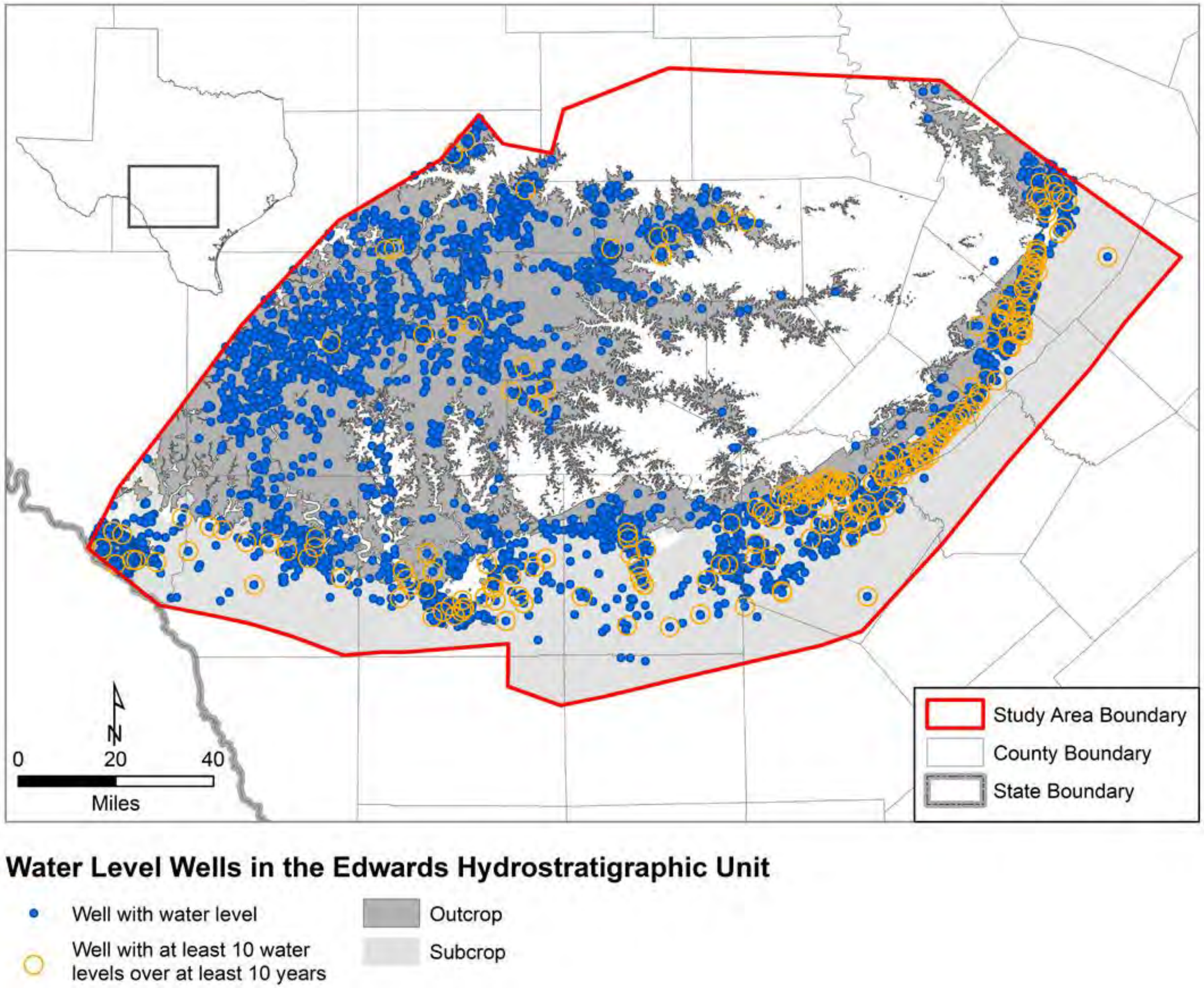

Figure 4.2.2 **Spatial distribution of wells with water-elevation measurements in the Edwards hydrostratigraphic unit.**

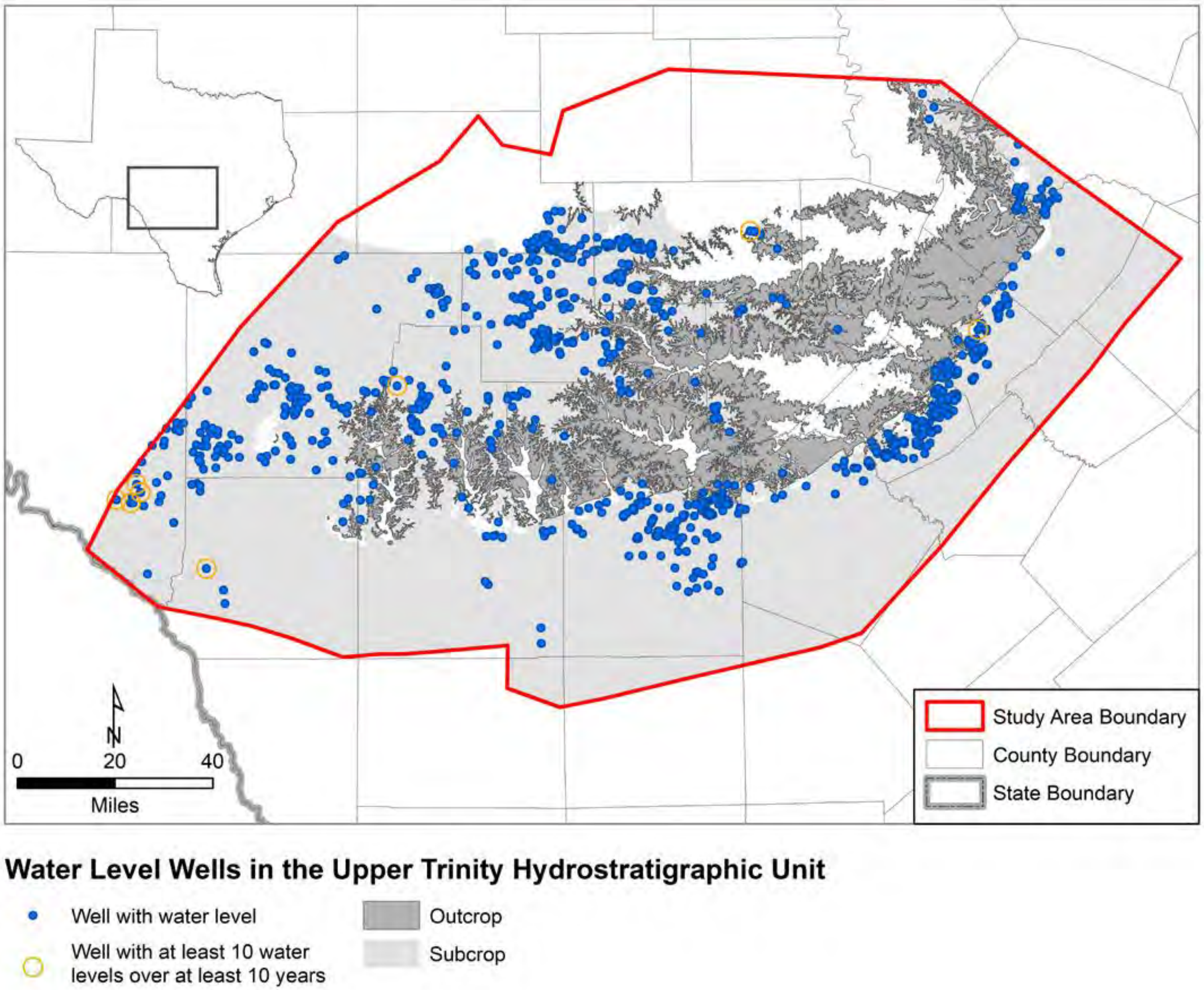

Figure 4.2.3 Spatial distribution of wells with water-elevation measurements in the Upper Trinity hydrostratigraphic unit.

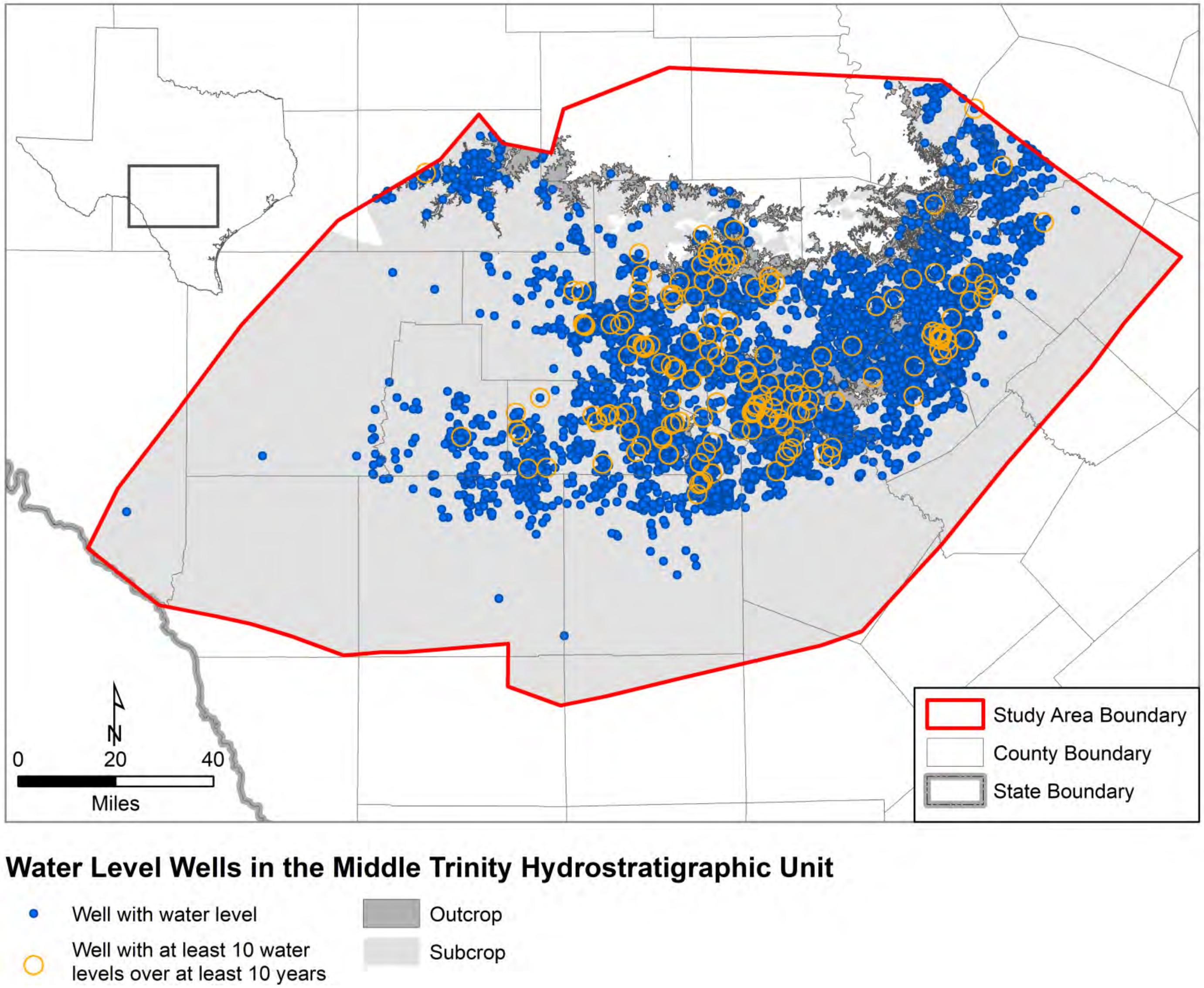

Figure 4.2.4 Spatial distribution of wells with water-elevation measurements in the Middle Trinity hydrostratigraphic unit.

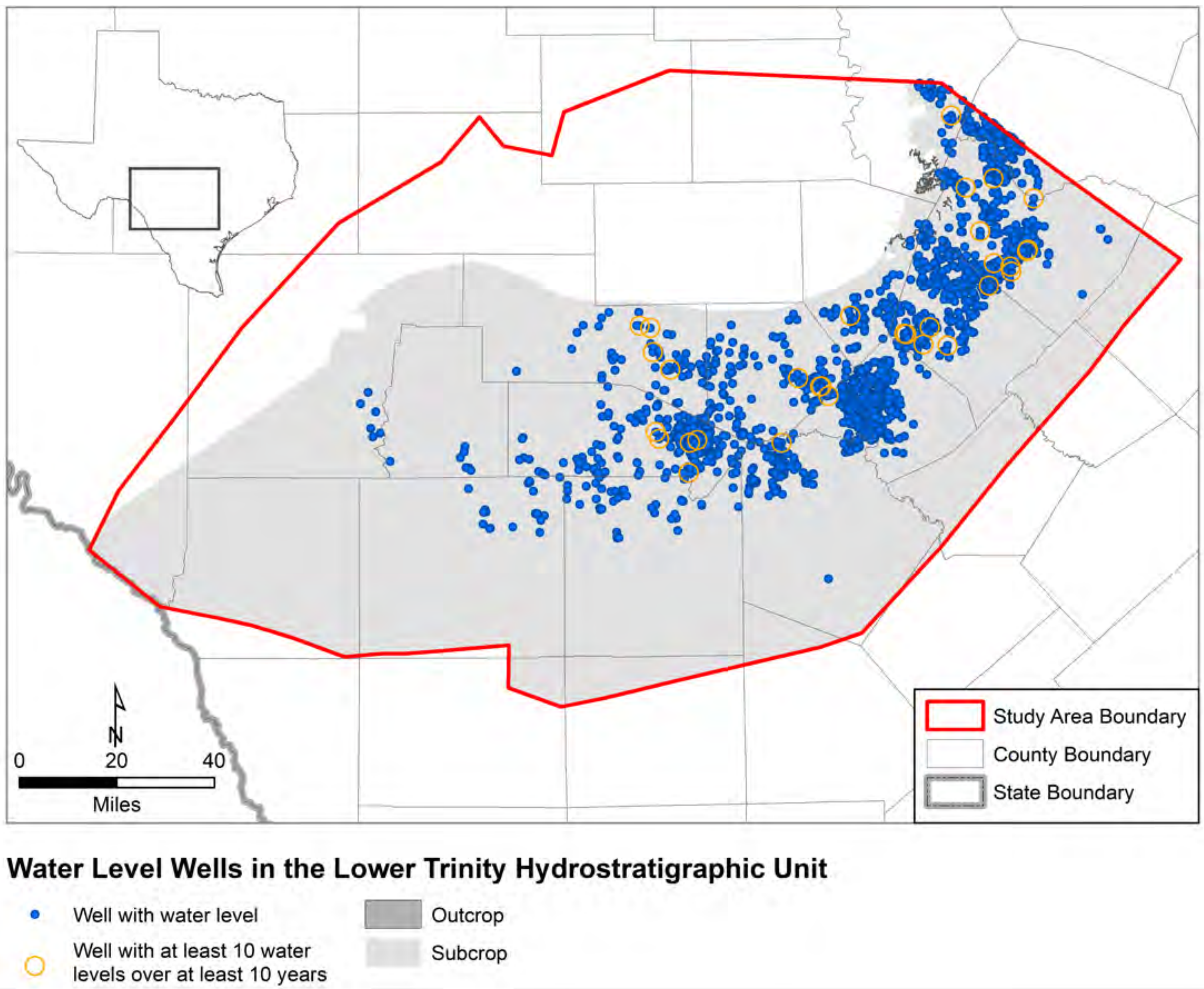

Figure 4.2.5 Spatial distribution of wells with water-elevation measurements in the Lower Trinity hydrostratigraphic unit.

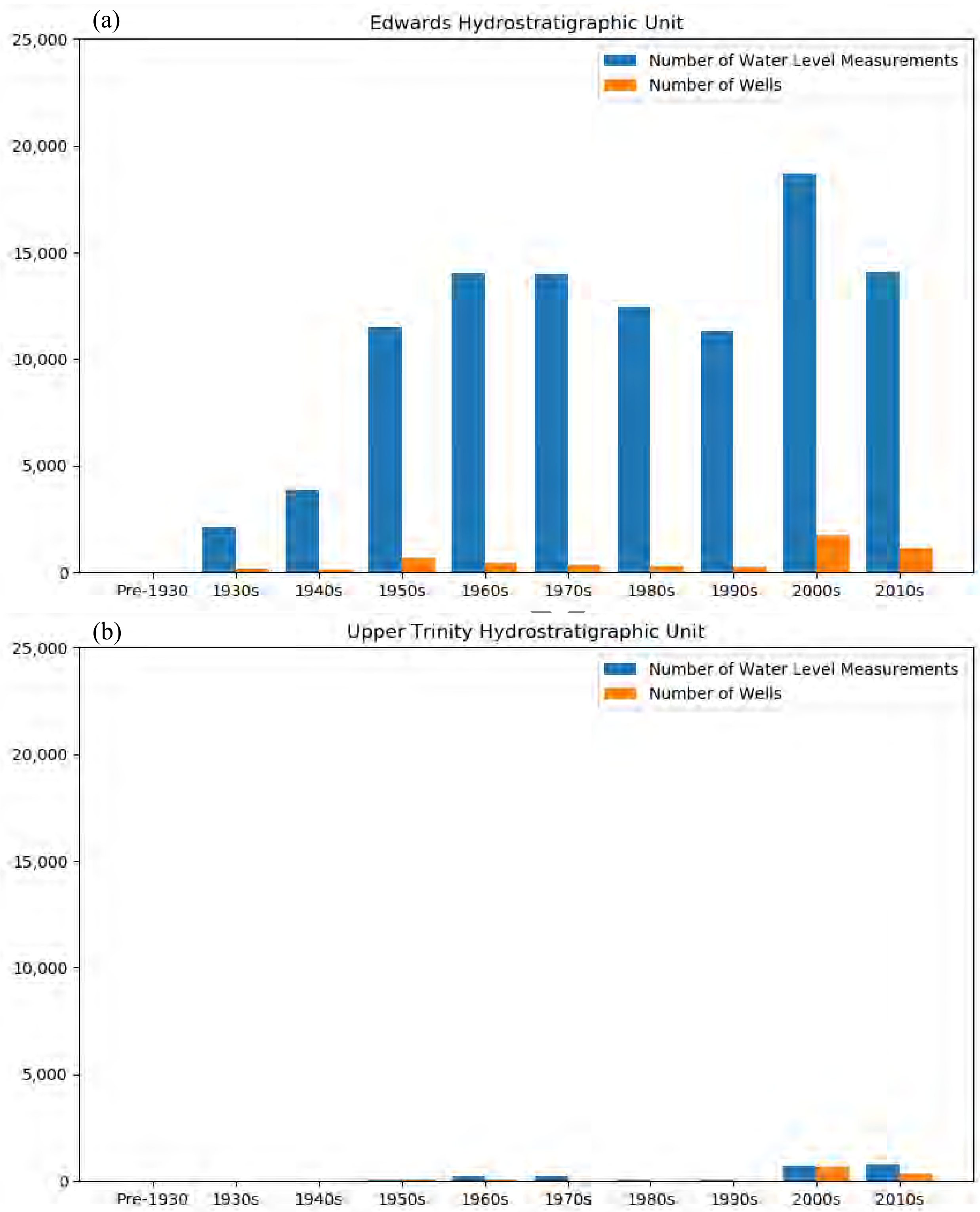

Figure 4.2.6 Temporal distribution of water-level measurements in the a) Edwards hydrostratigraphic unit and b) Upper Trinity hydrostratigraphic unit.

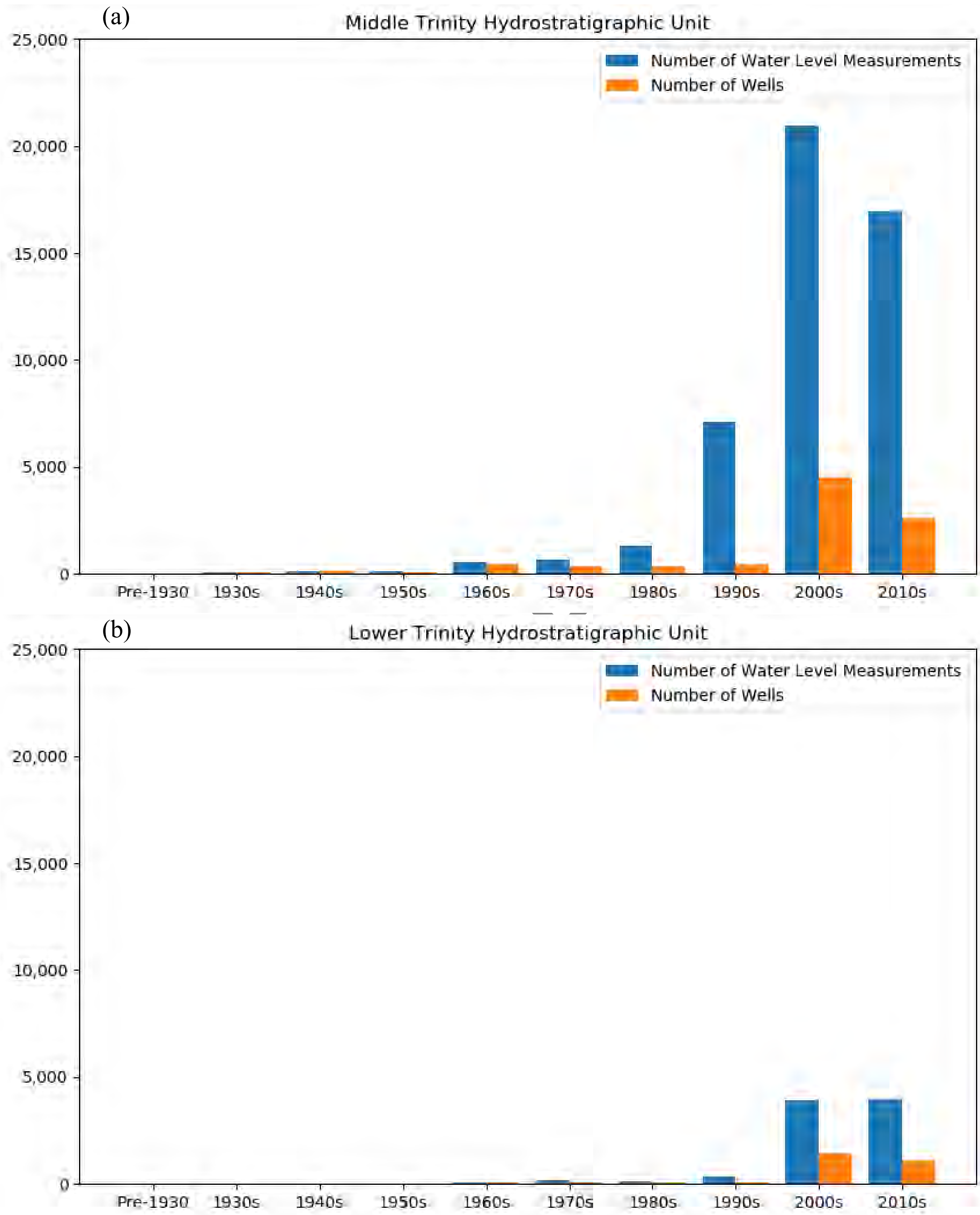

Figure 4.2.7 Temporal distribution of water-level measurements in the a) Middle Trinity hydrostratigraphic unit and b) Lower Trinity hydrostratigraphic unit.

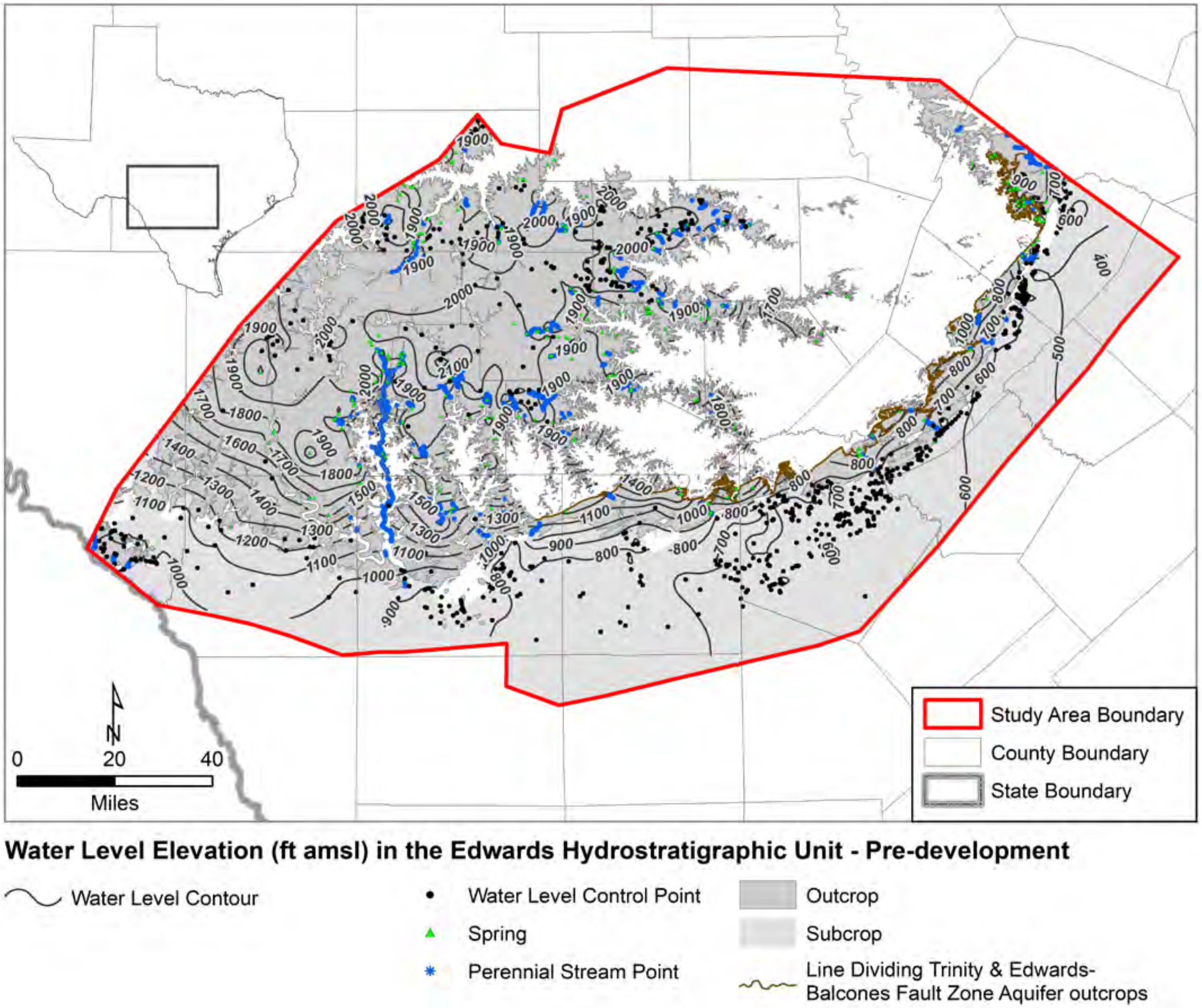

Figure 4.2.8 **Estimated pre-development water-elevation contours in ft above mean sea level for the Edwards hydrostratigraphic unit.**

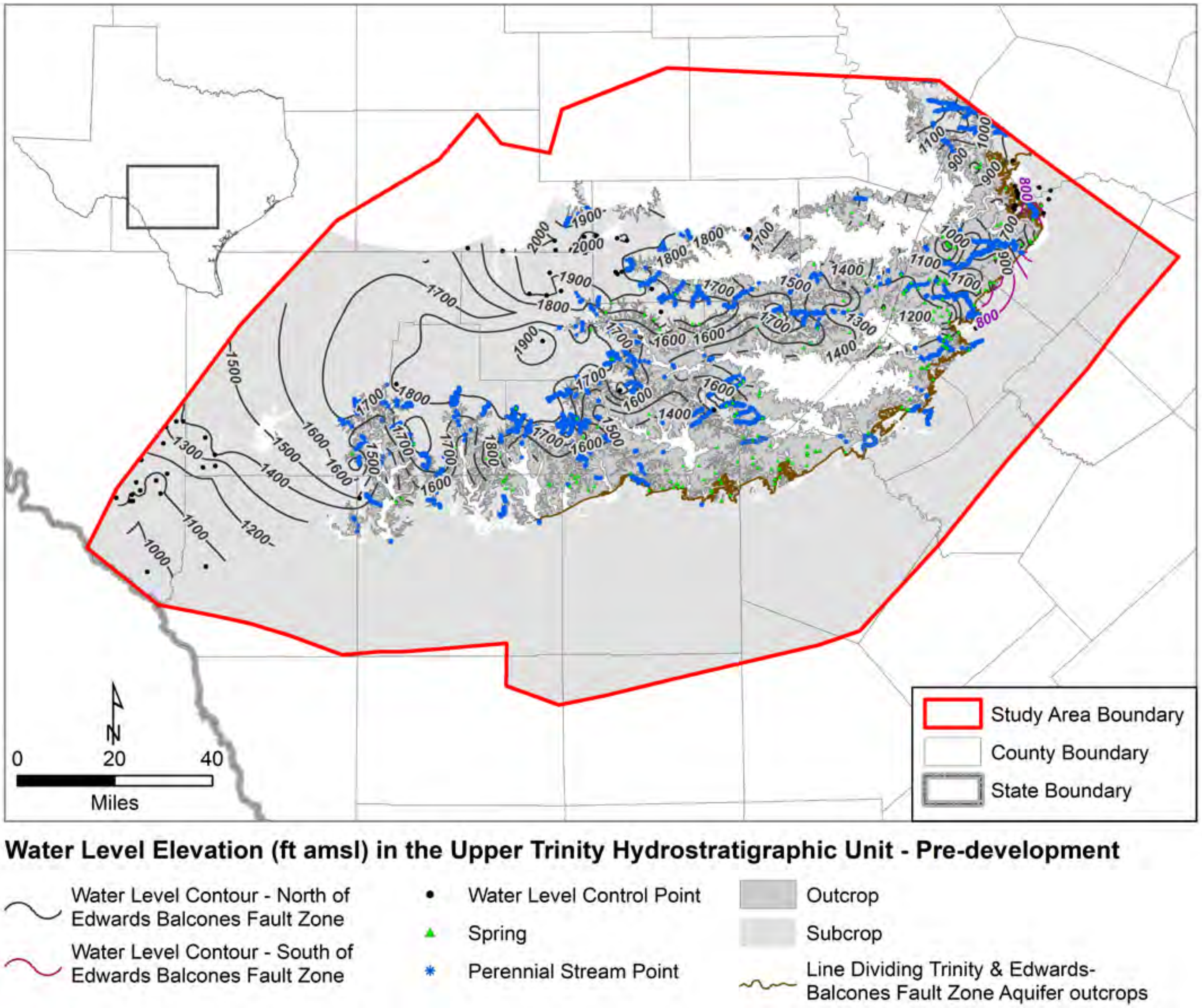

Figure 4.2.9 **Estimated pre-development water-elevation contours in ft above mean sea level for the Upper Trinity hydrostratigraphic unit.**

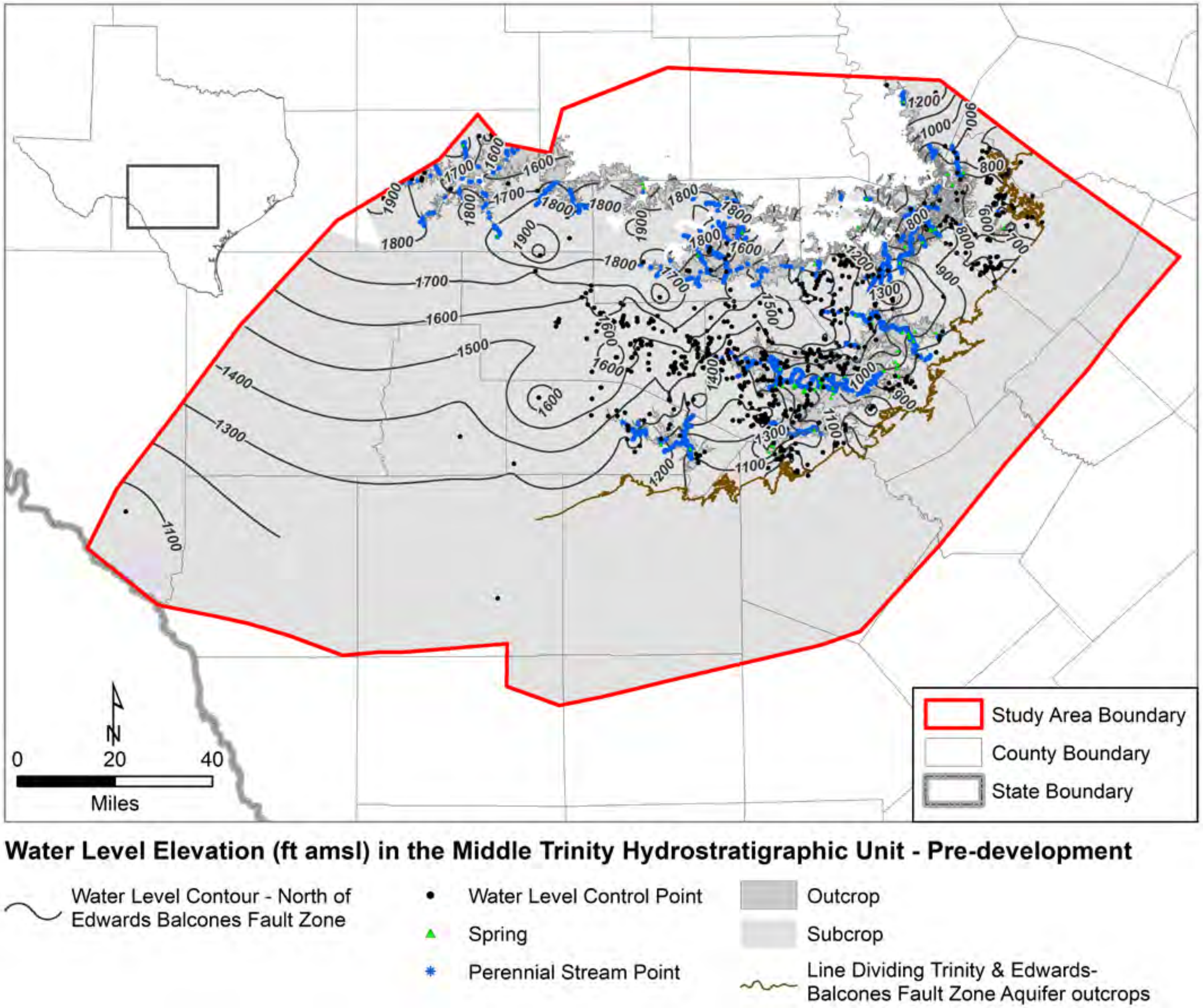

Figure 4.2.10 **Estimated pre-development water-elevation contours in ft above mean sea level for the Middle Trinity hydrostratigraphic unit.**

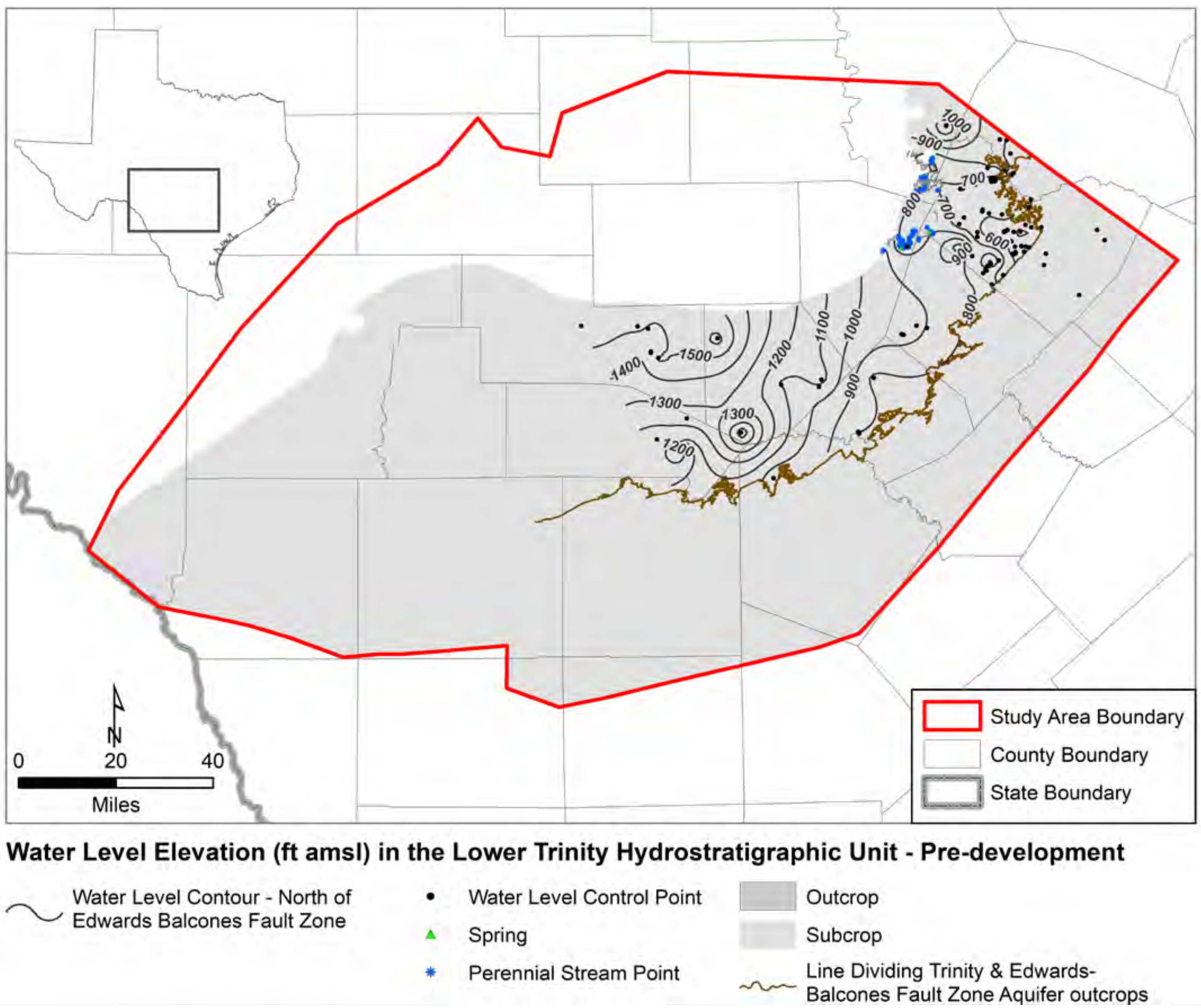

Figure 4.2.11 Estimated pre-development water-elevation contours in ft above mean sea level for the Lower Trinity hydrostratigraphic unit.

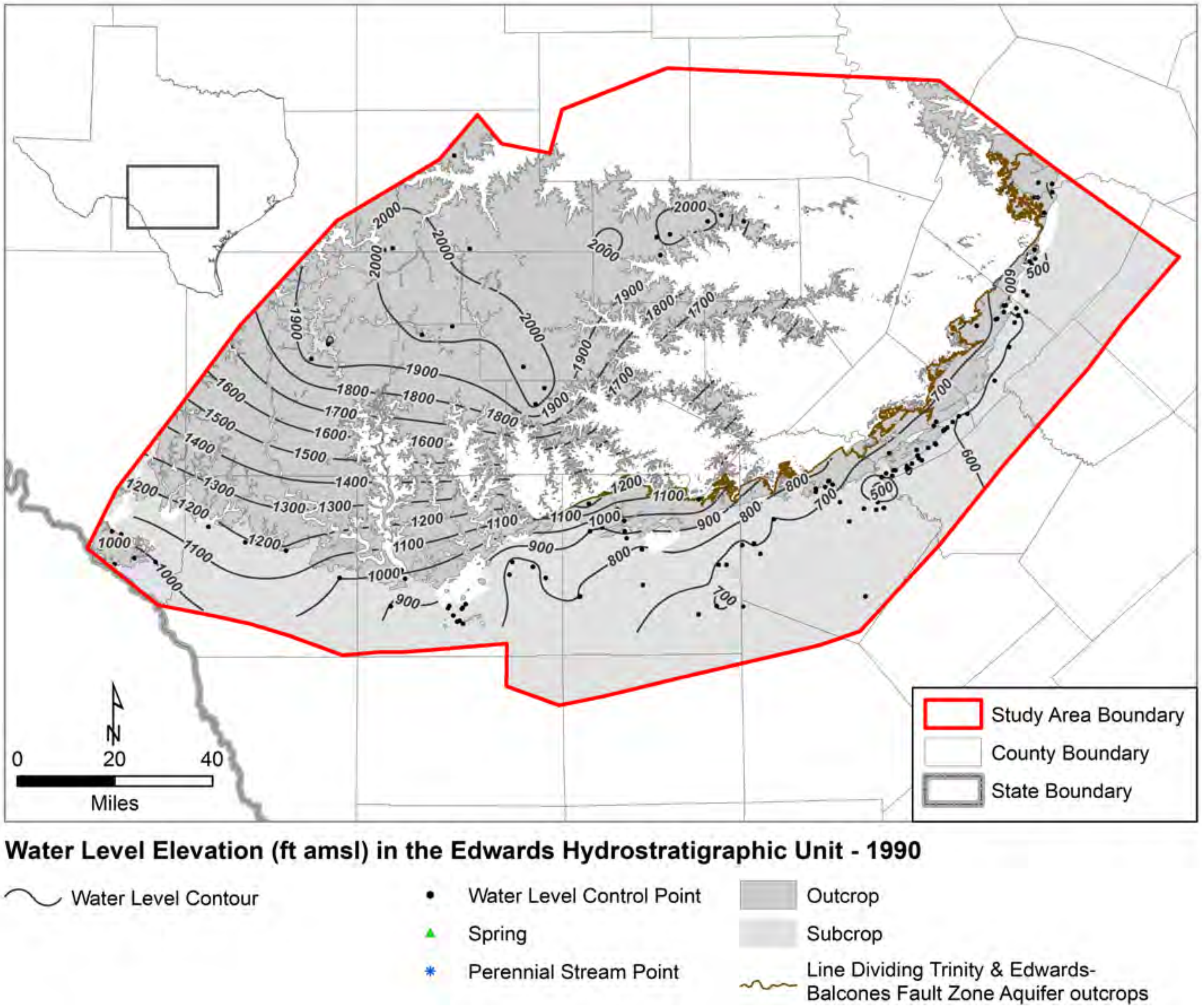

Figure 4.2.12 Estimated water-elevation contours in ft above mean sea level in the Edwards hydrostratigraphic unit in 1990.

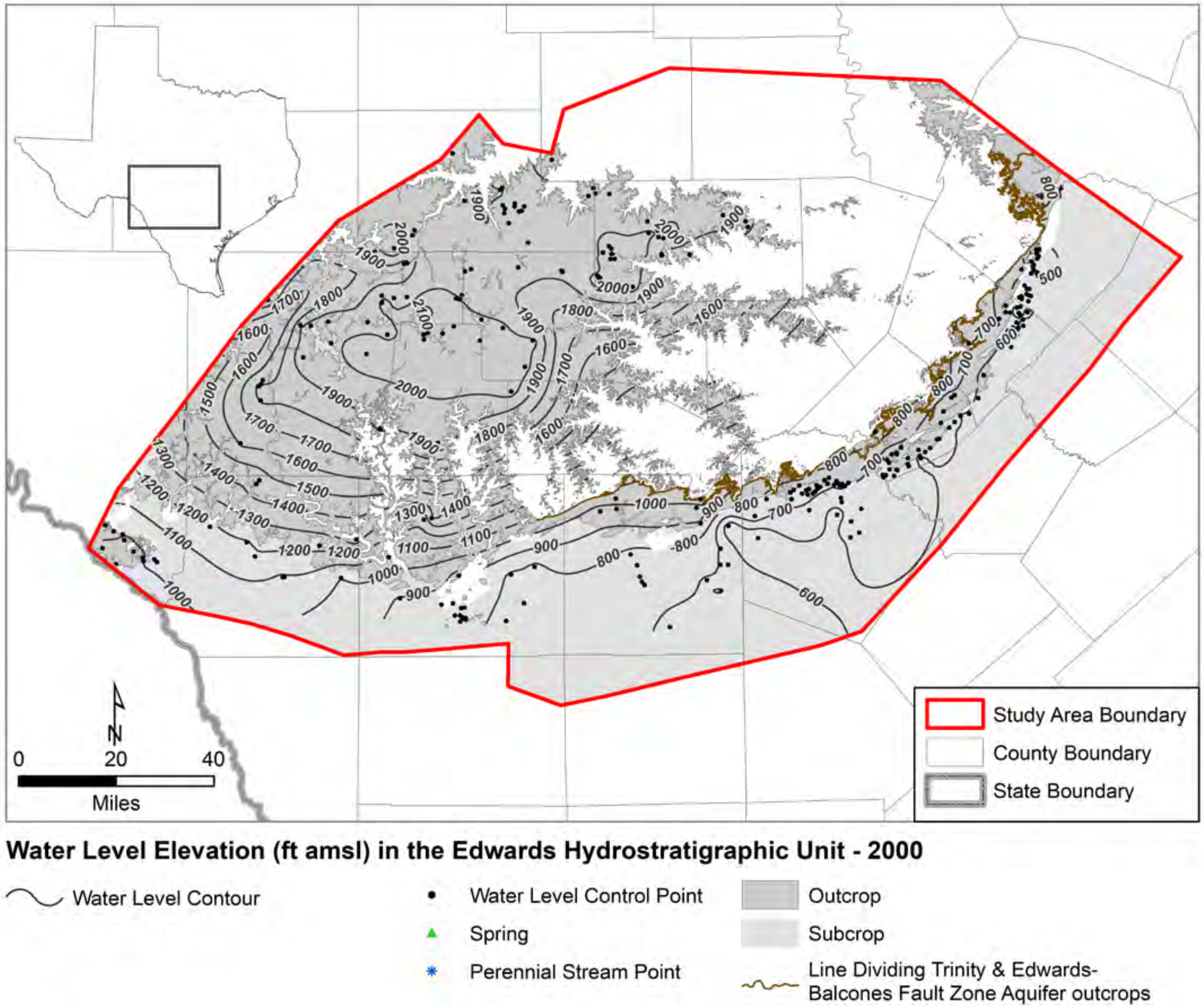

Figure 4.2.13 Estimated water-elevation contours in ft above mean sea level in the Edwards hydrostratigraphic unit in 2000.

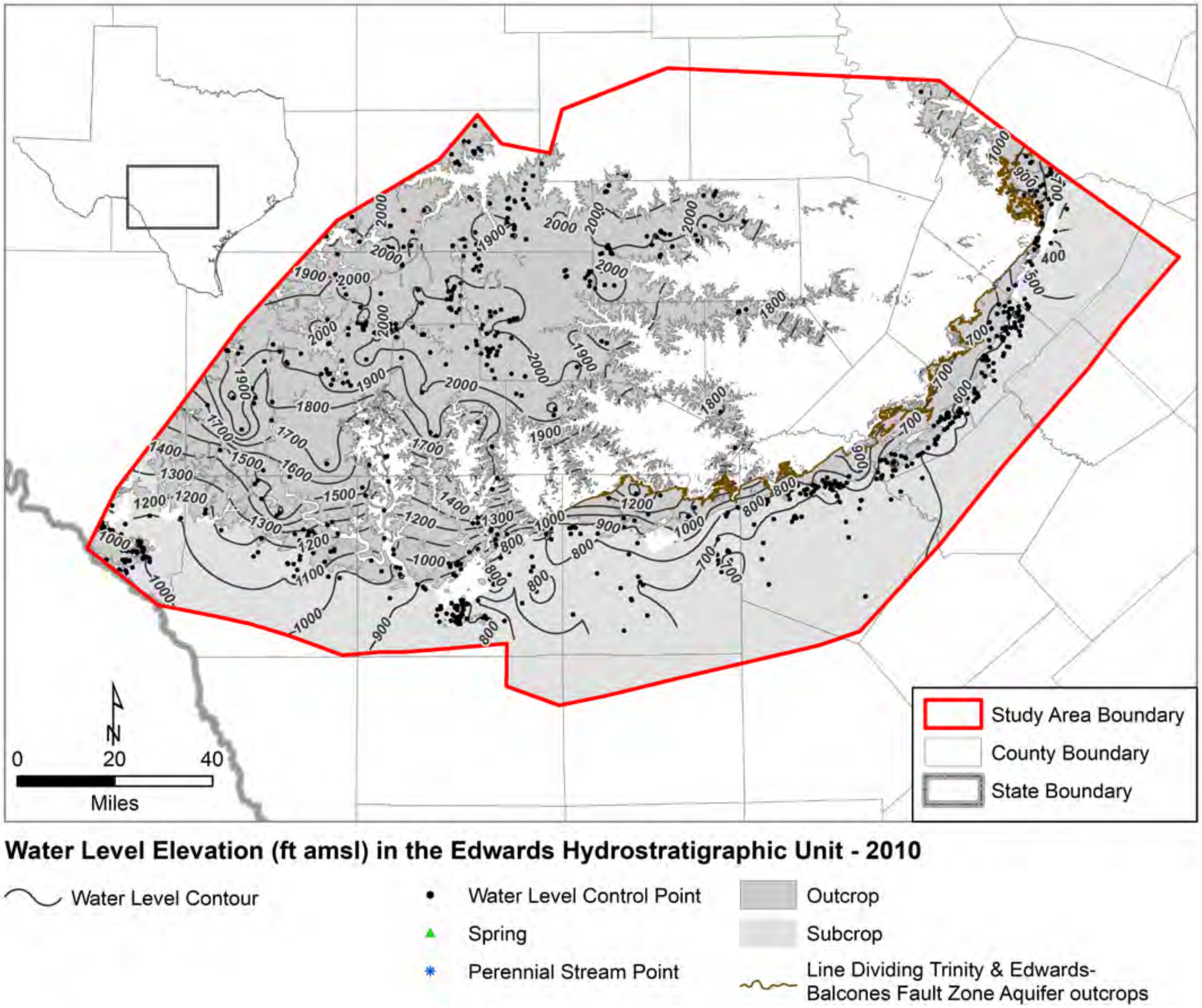

Figure 4.2.14 Estimated water-elevation contours in ft above mean sea level in the Edwards hydrostratigraphic unit in 2010.

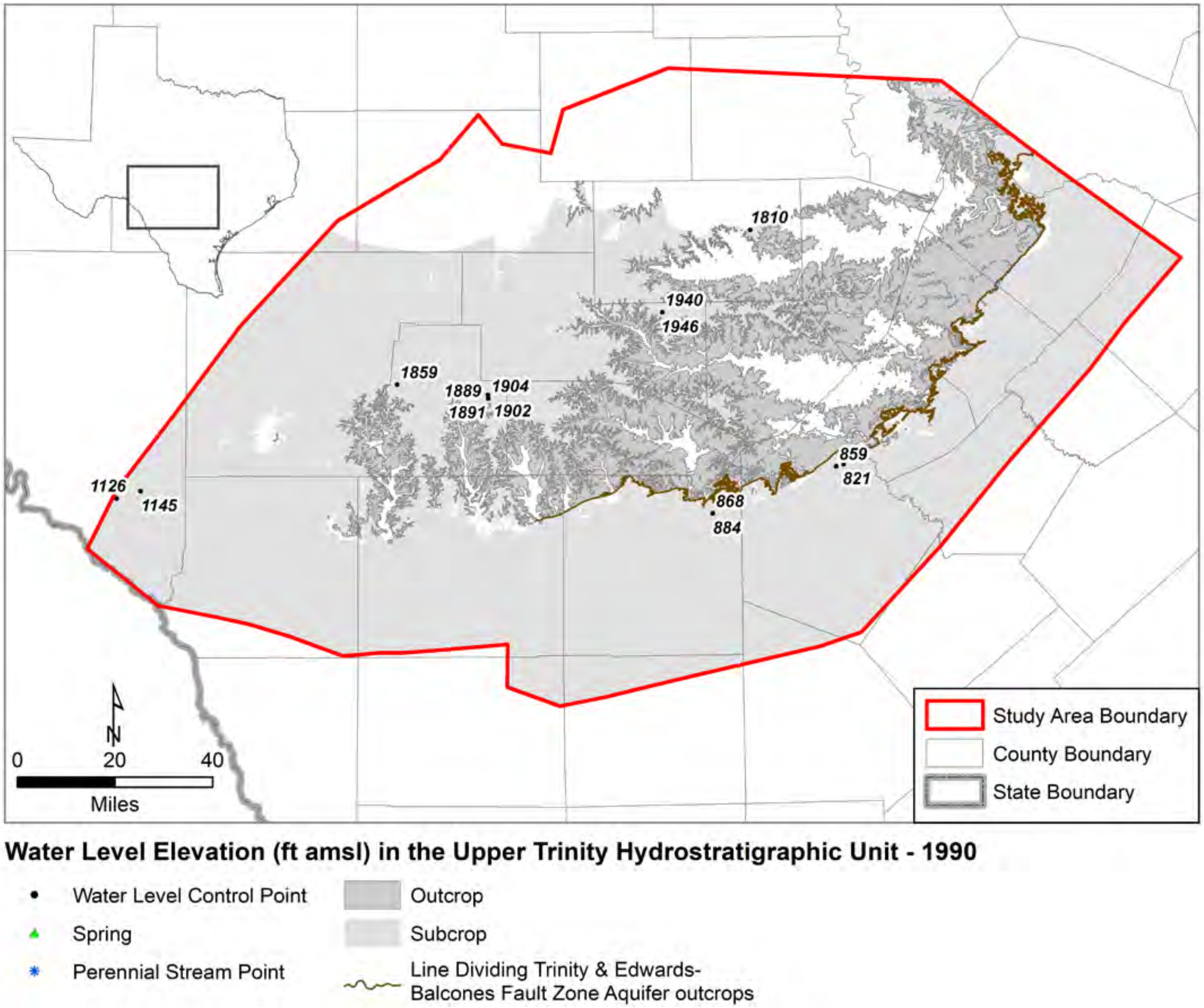

Figure 4.2.15 Estimated water-elevation contours in ft above mean sea level in the Upper Trinity hydrostratigraphic unit in 1990.

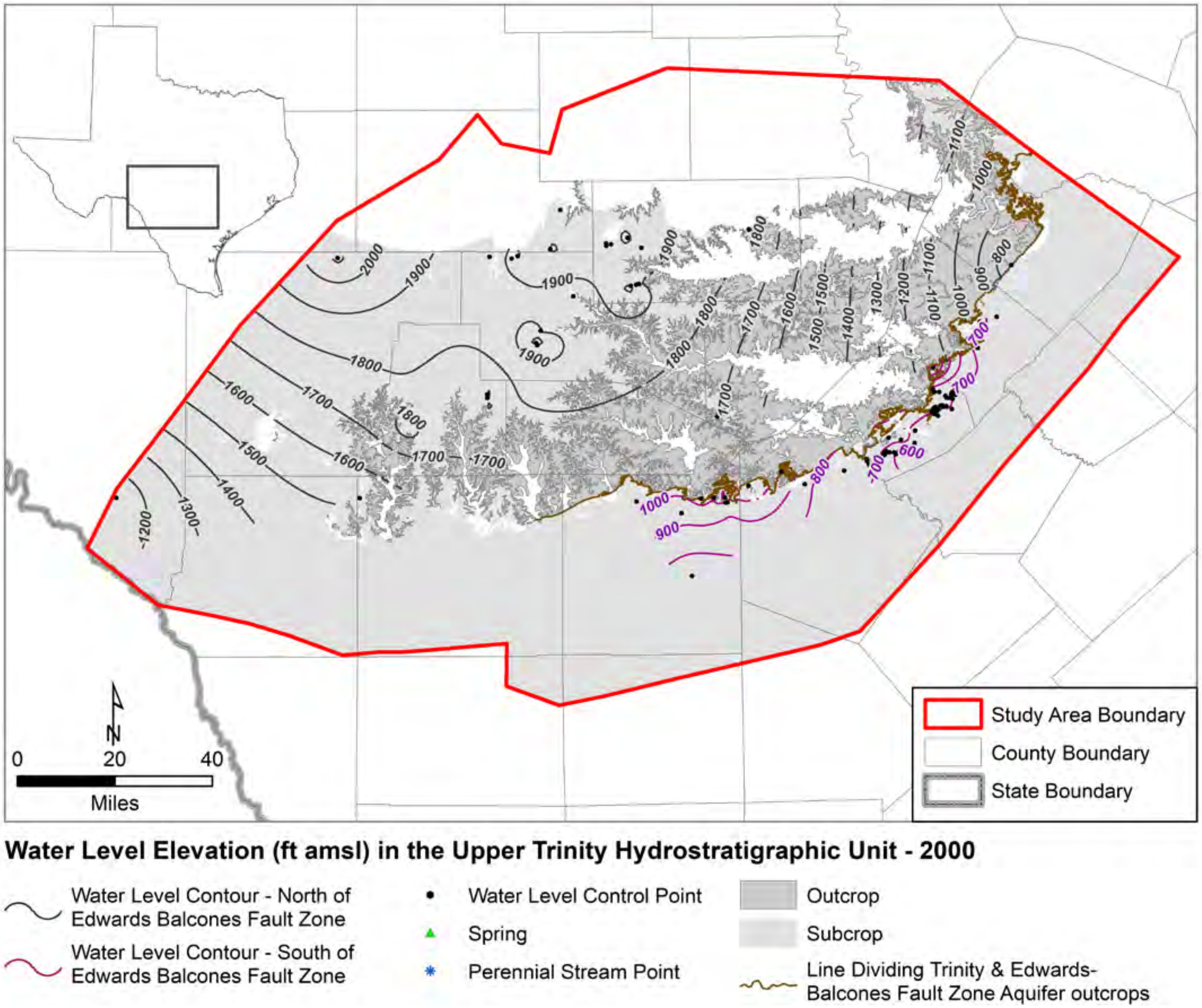

Figure 4.2.16 Estimated water-elevation contours in ft above mean sea level in the Upper Trinity hydrostratigraphic unit in 2000.

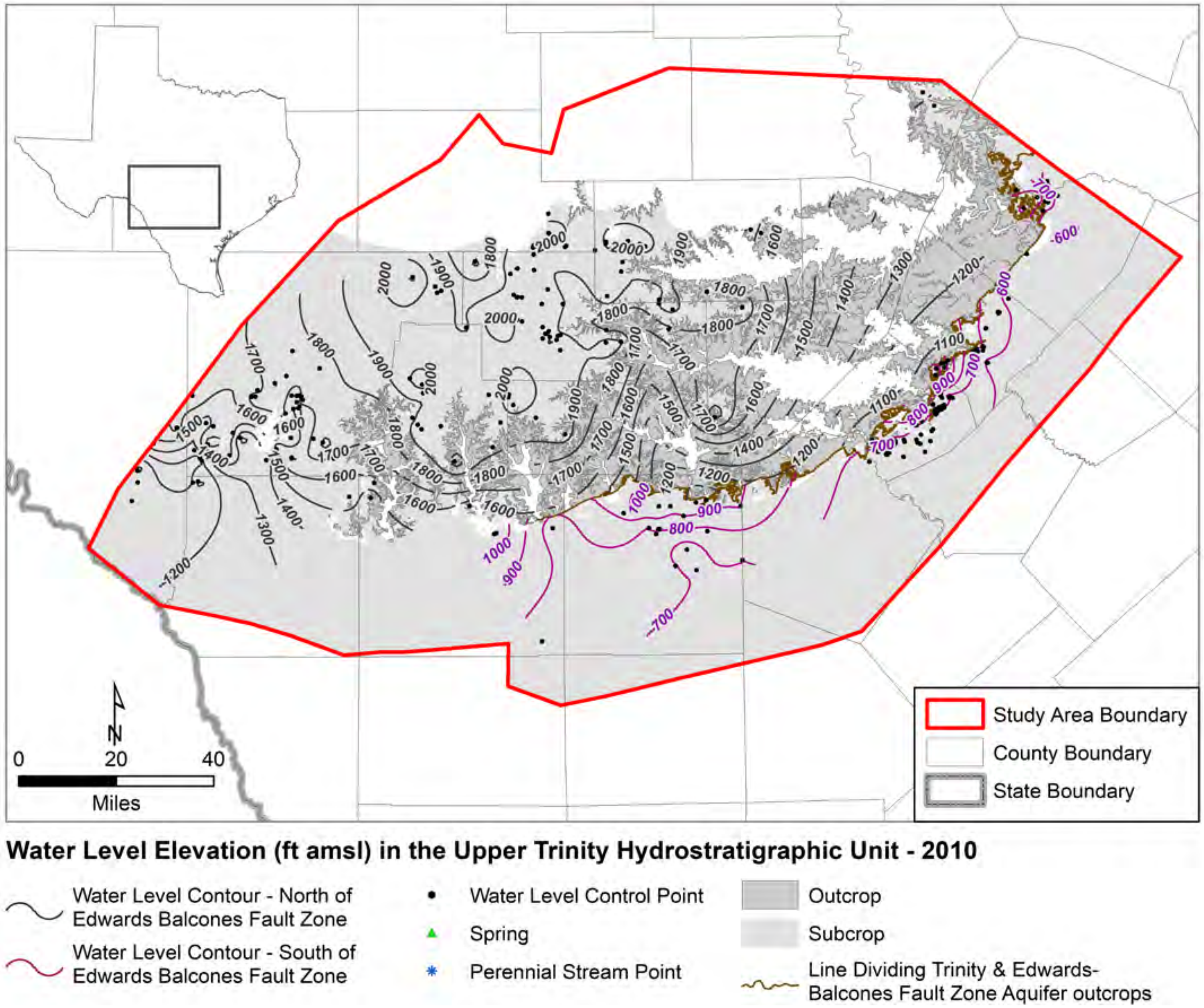

Figure 4.2.17 Estimated water-elevation contours in ft above mean sea level in the Upper Trinity hydrostratigraphic unit in 2010.

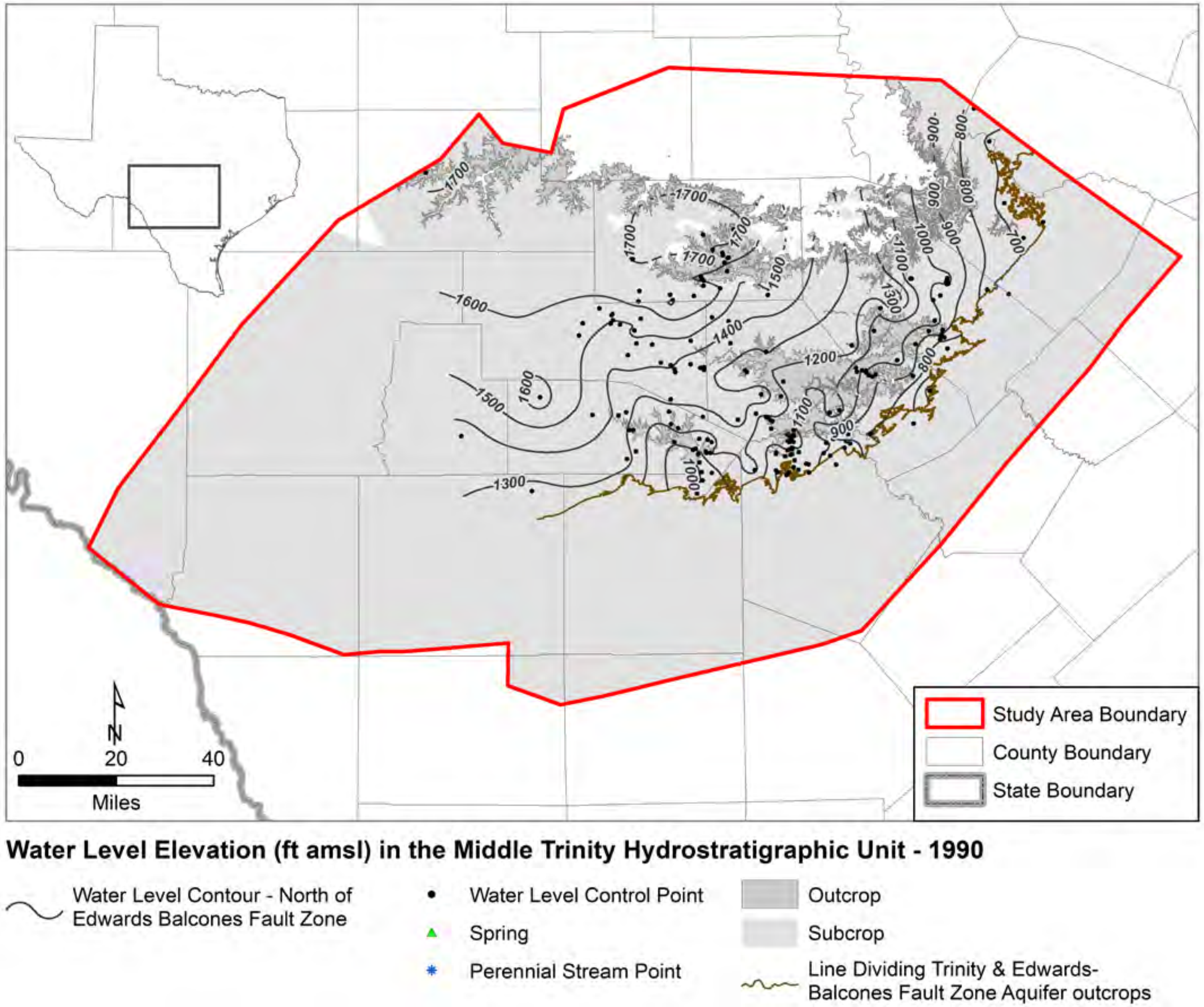

Figure 4.2.18 Estimated water-elevation contours in ft above mean sea level in the Middle Trinity hydrostratigraphic unit in 1990.

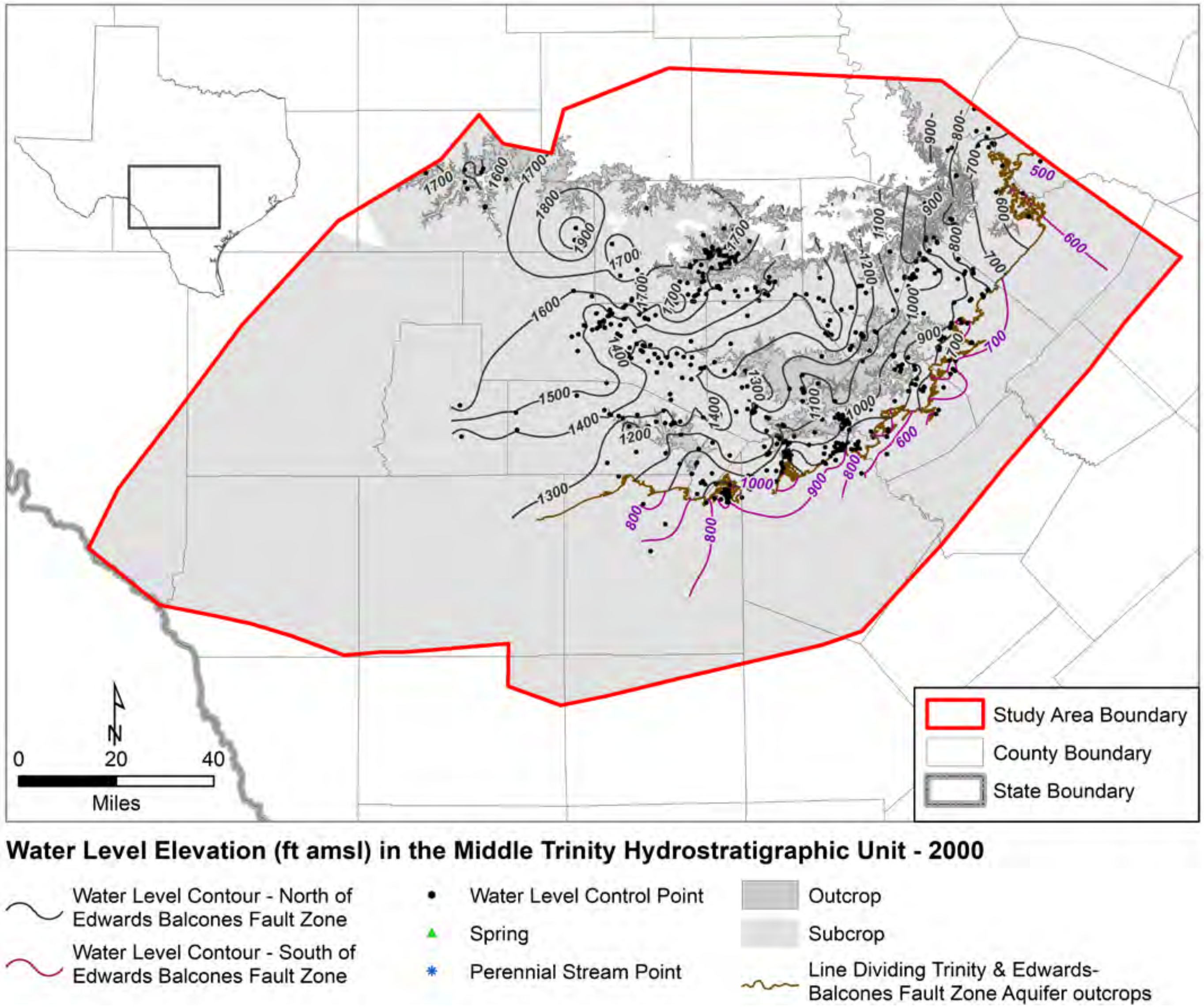

Figure 4.2.19 Estimated water-elevation contours in ft above mean sea level in the Middle Trinity hydrostratigraphic unit in 2000.

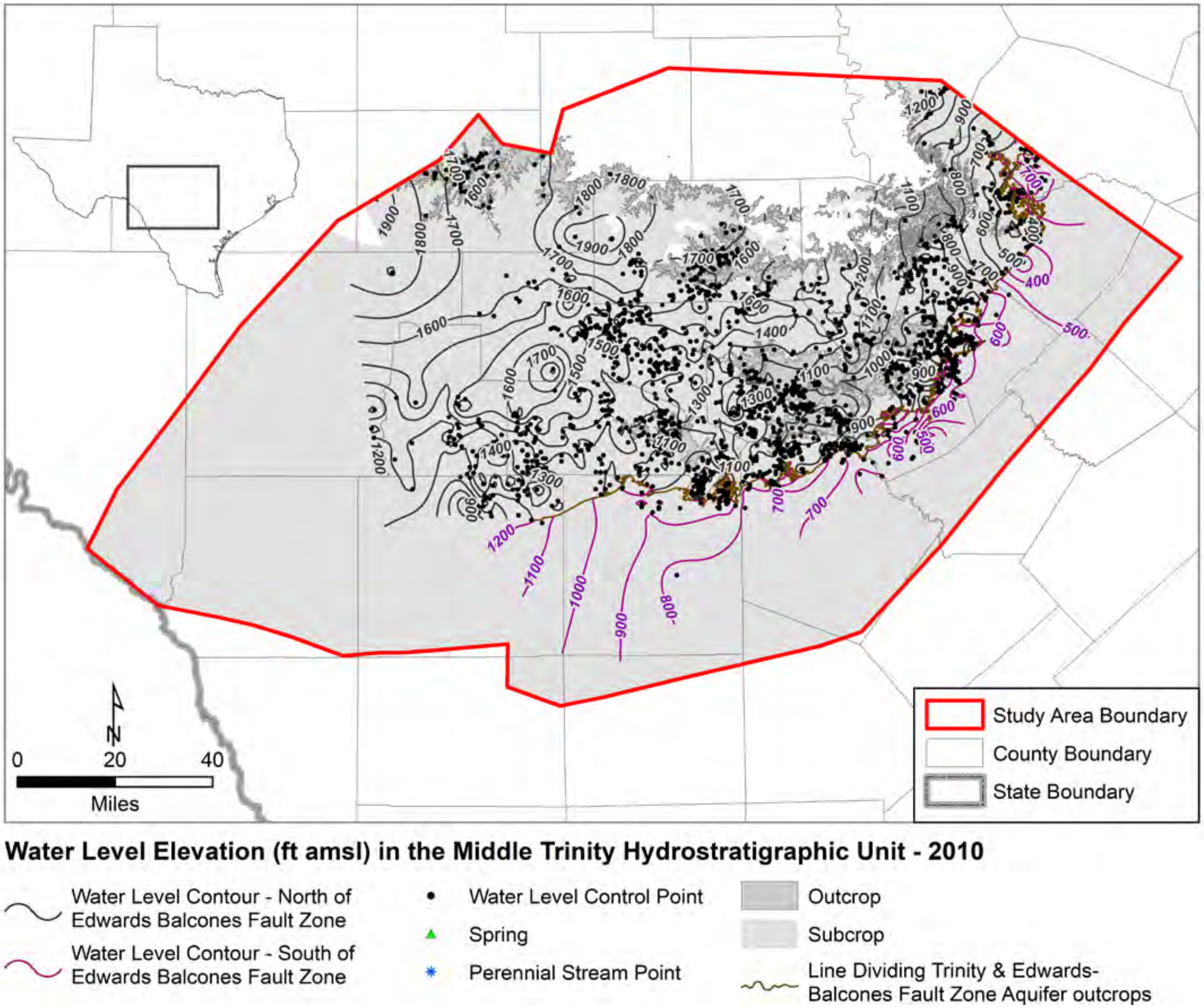

Figure 4.2.20 Estimated water-elevation contours in ft above mean sea level in the Middle Trinity hydrostratigraphic unit in 2010.

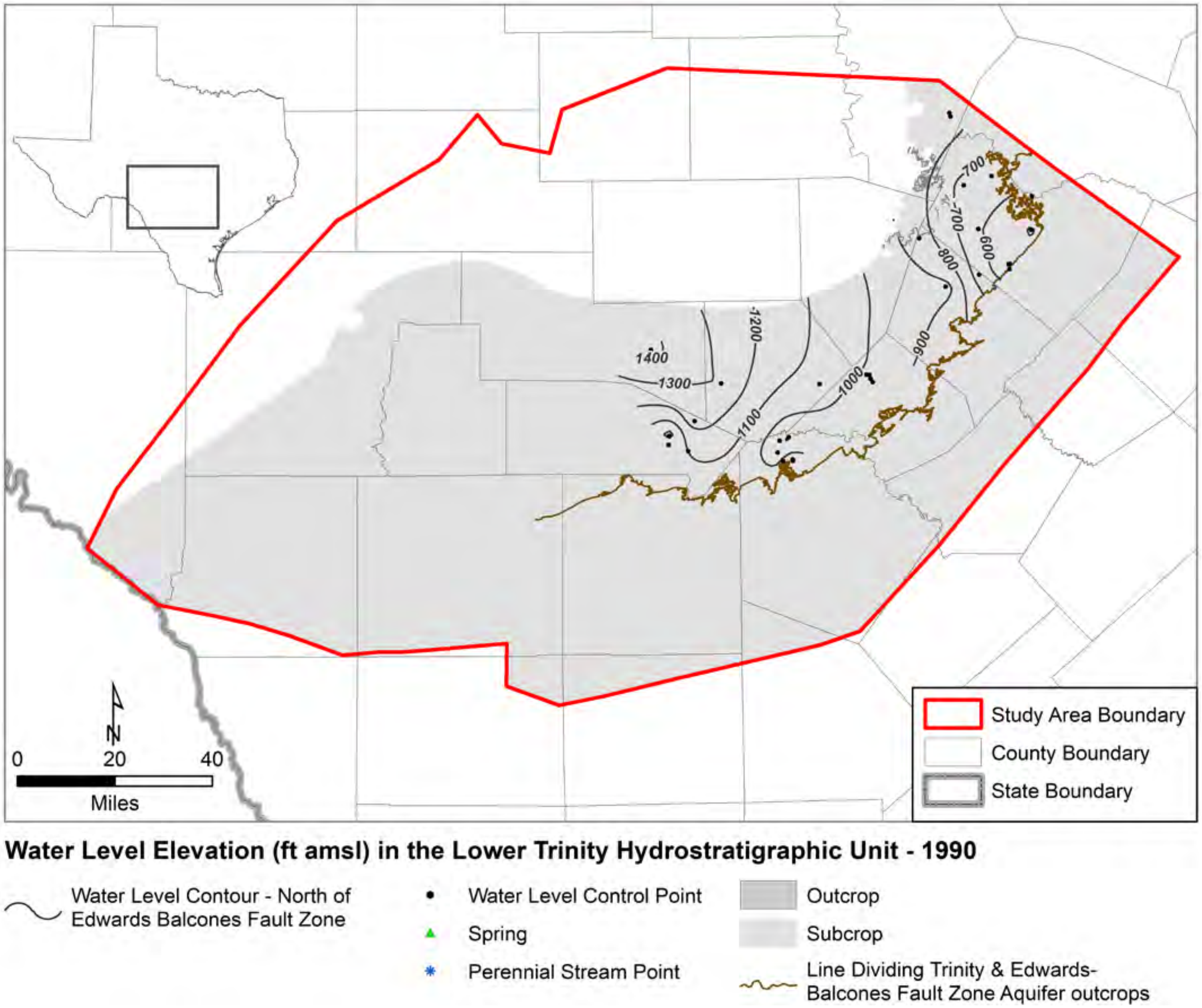

Figure 4.2.21 Estimated water-elevation contours in ft above mean sea level in the Lower Trinity hydrostratigraphic unit in 1990.

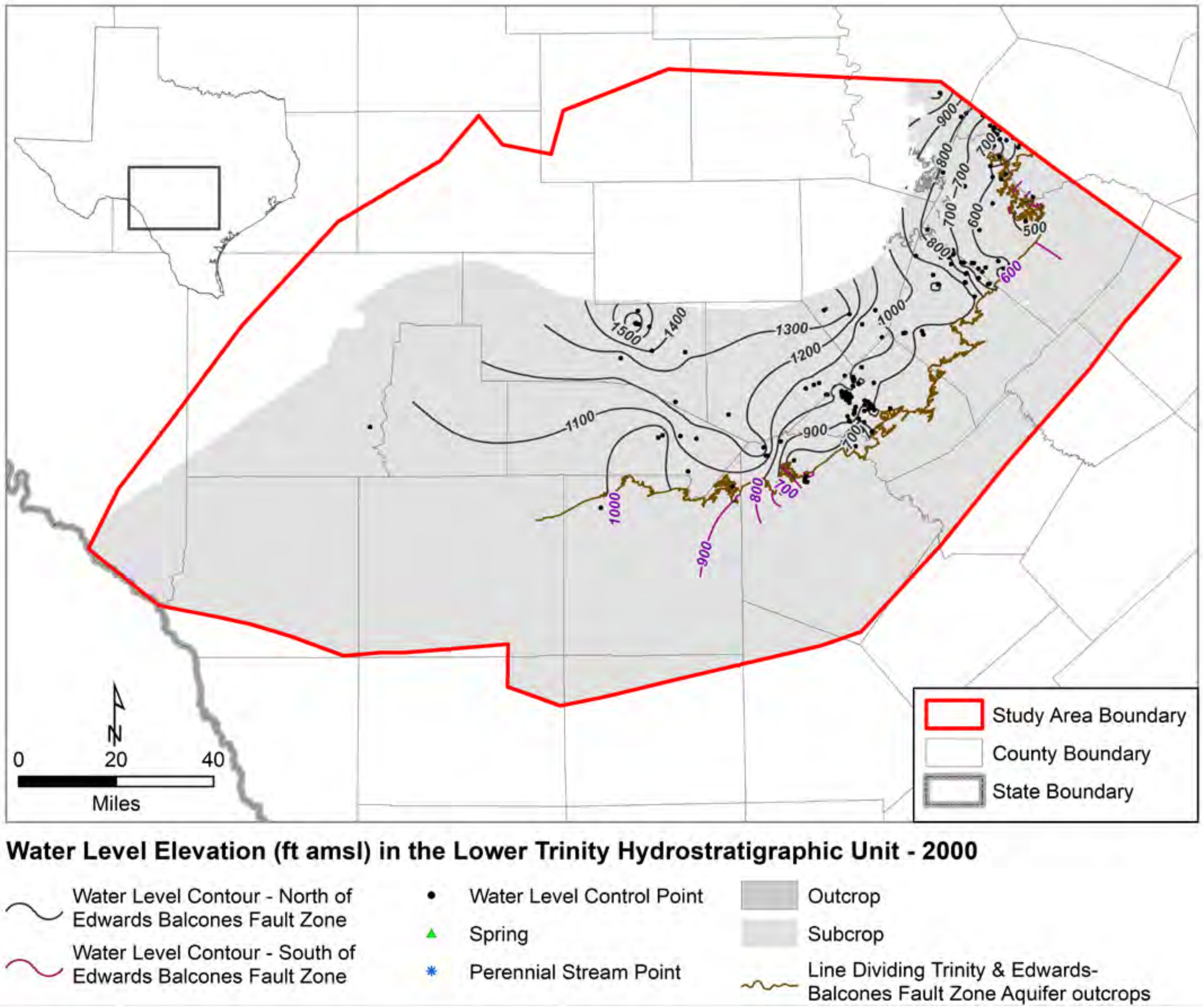

Figure 4.2.22 Estimated water-elevation contours in ft above mean sea level in the Lower Trinity hydrostratigraphic unit in 2000.

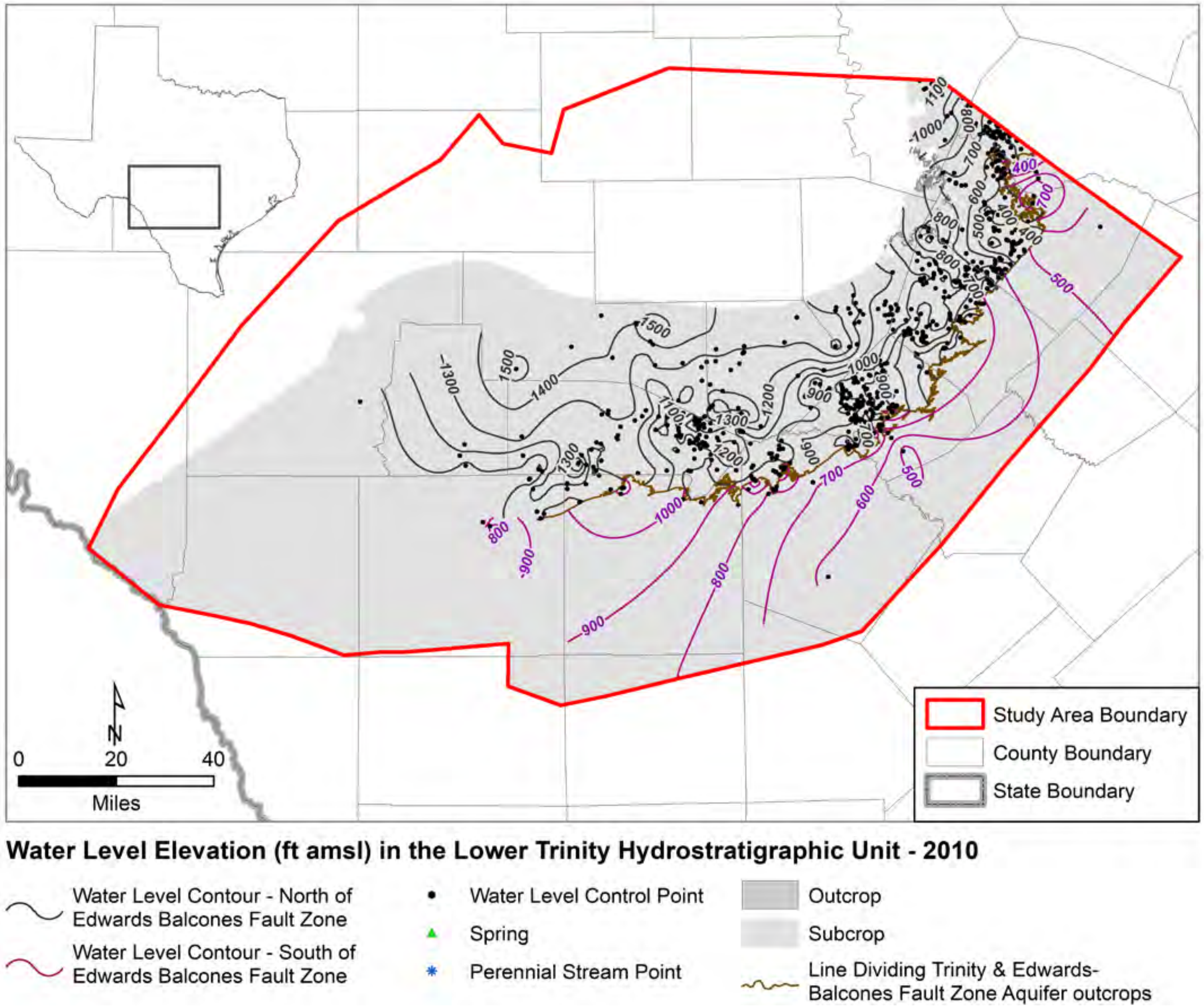

Figure 4.2.23 Estimated water-elevation contours in ft above mean sea level in the Lower Trinity hydrostratigraphic unit in 2010

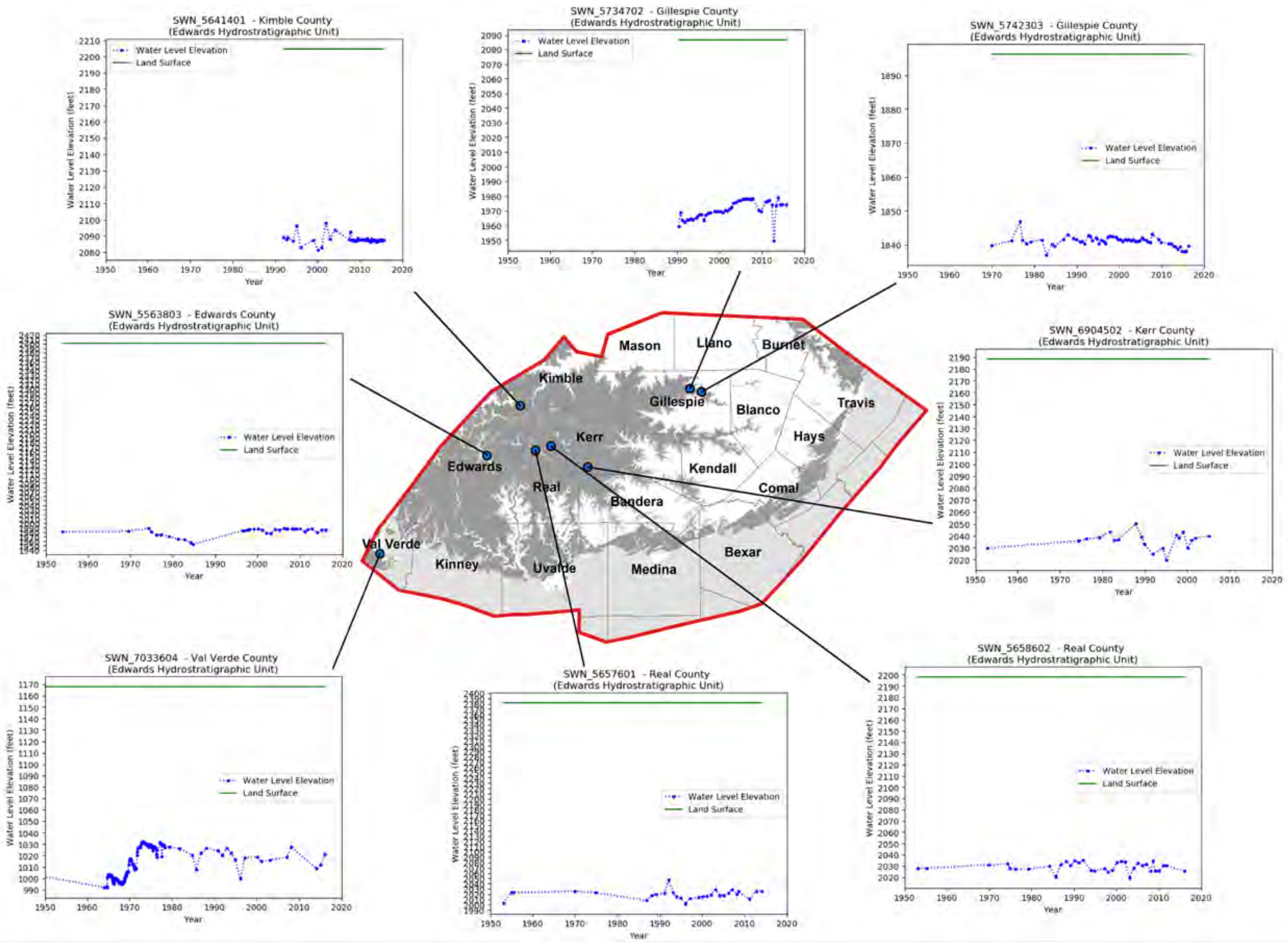

Figure 4.2.24 Select hydrographs for the Edwards hydrostratigraphic unit in the Edwards-Trinity Plateau region.

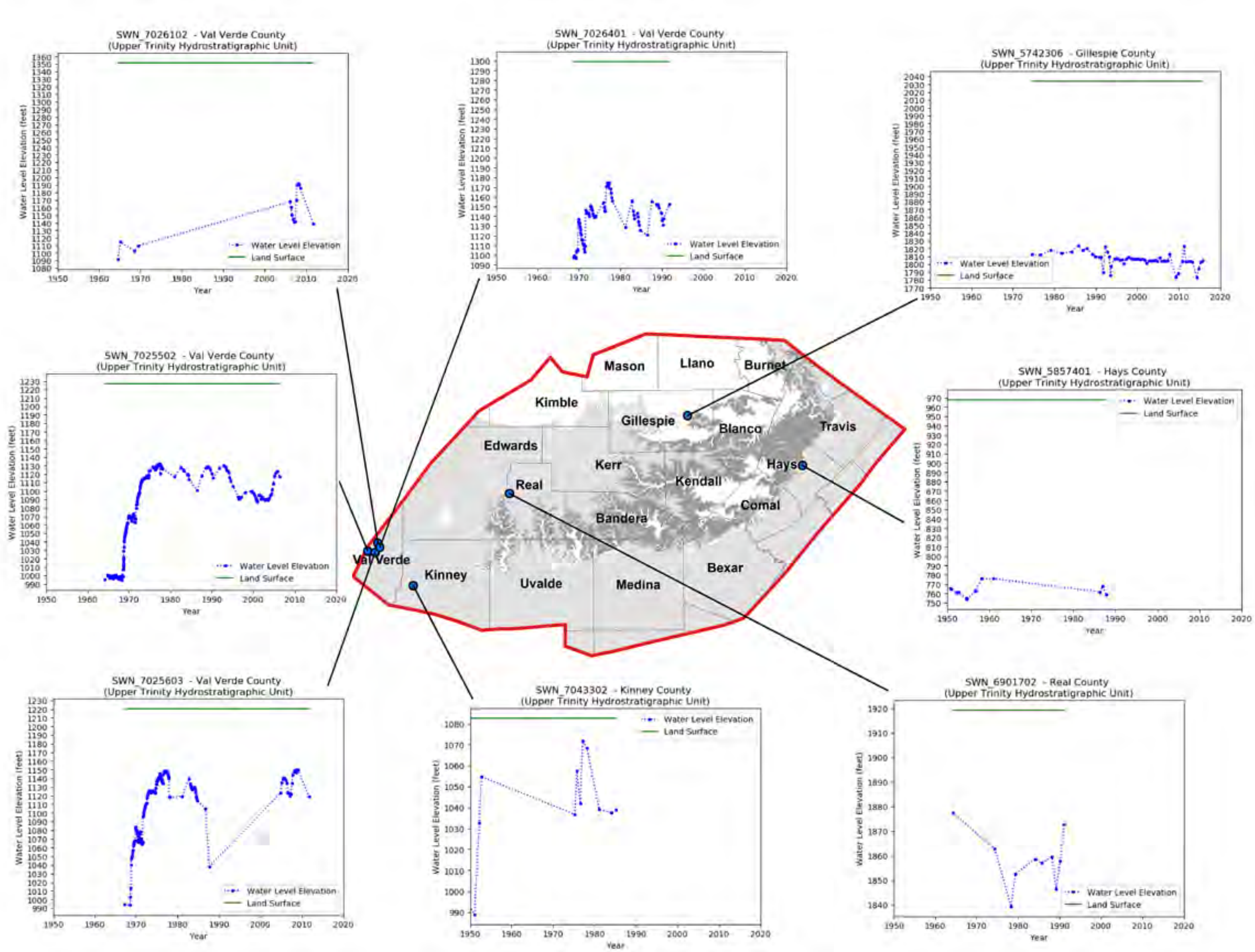

Figure 4.2.25 Select hydrographs for the Upper Trinity hydrostratigraphic unit.

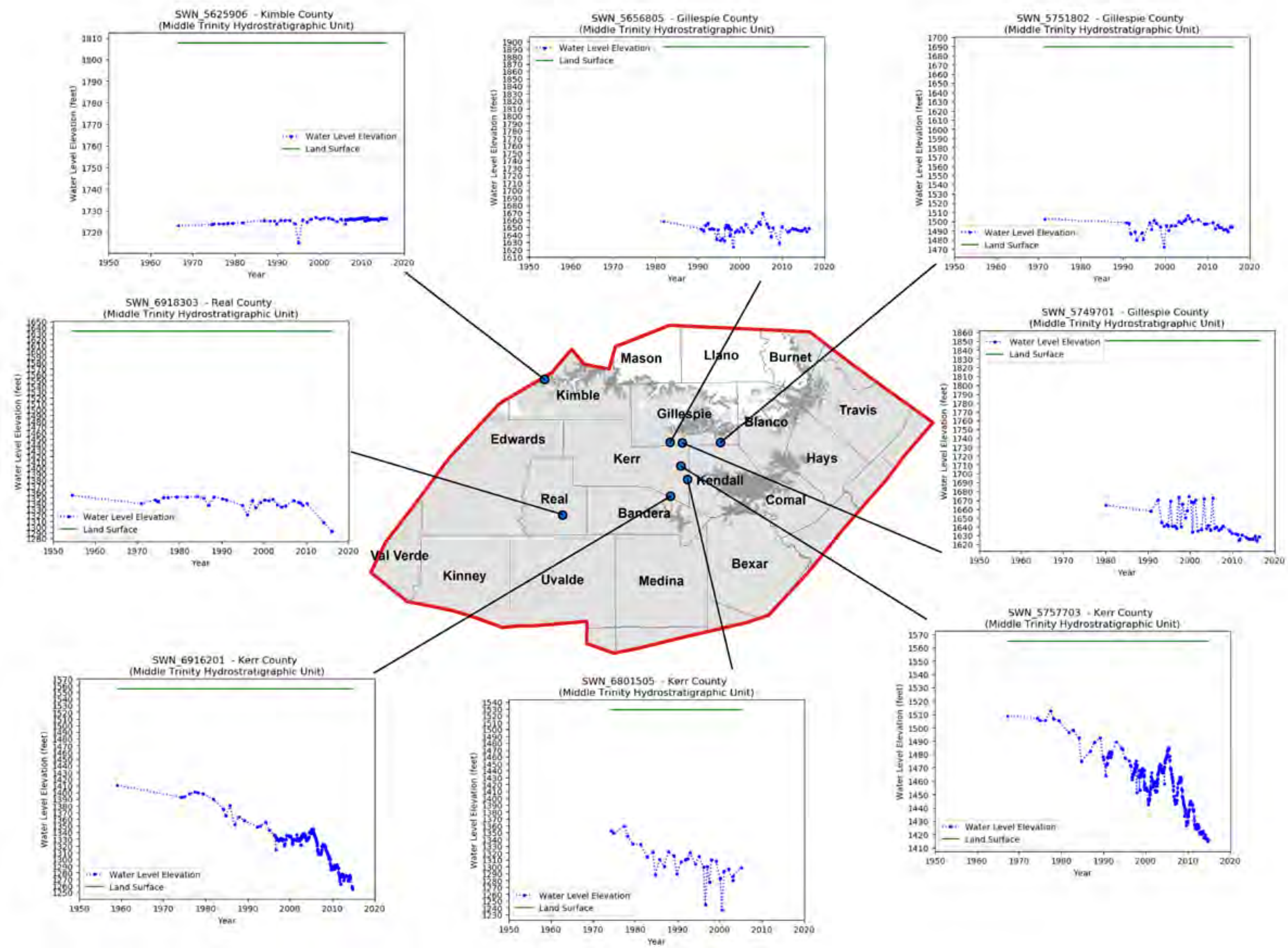

Figure 4.2.26 Select hydrographs for the Middle Trinity hydrostratigraphic unit in the west and west-central portions of the study area.

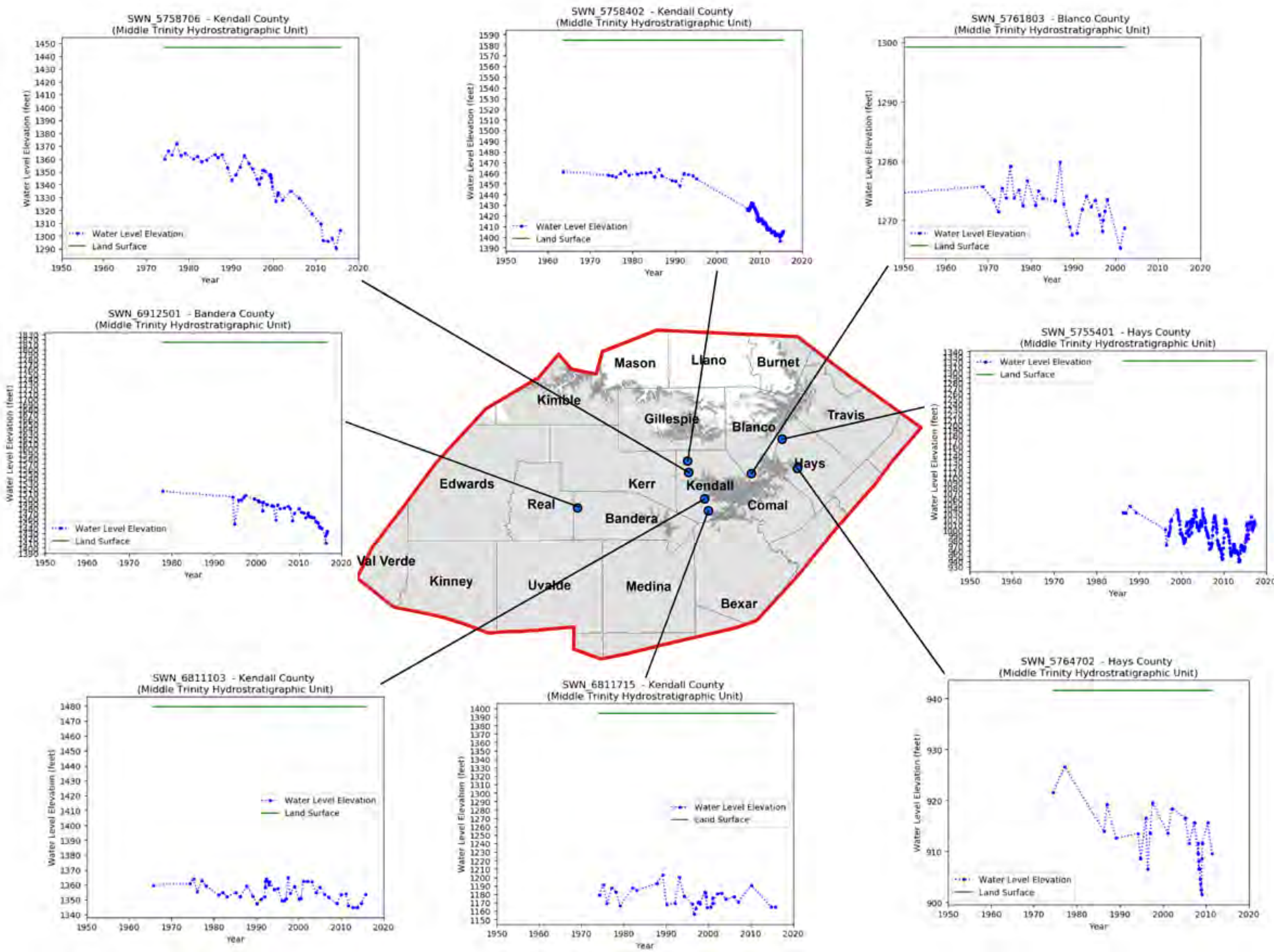

Figure 4.2.27 Select hydrographs for the Middle Trinity hydrostratigraphic unit in the east and east-central portions of the study area.

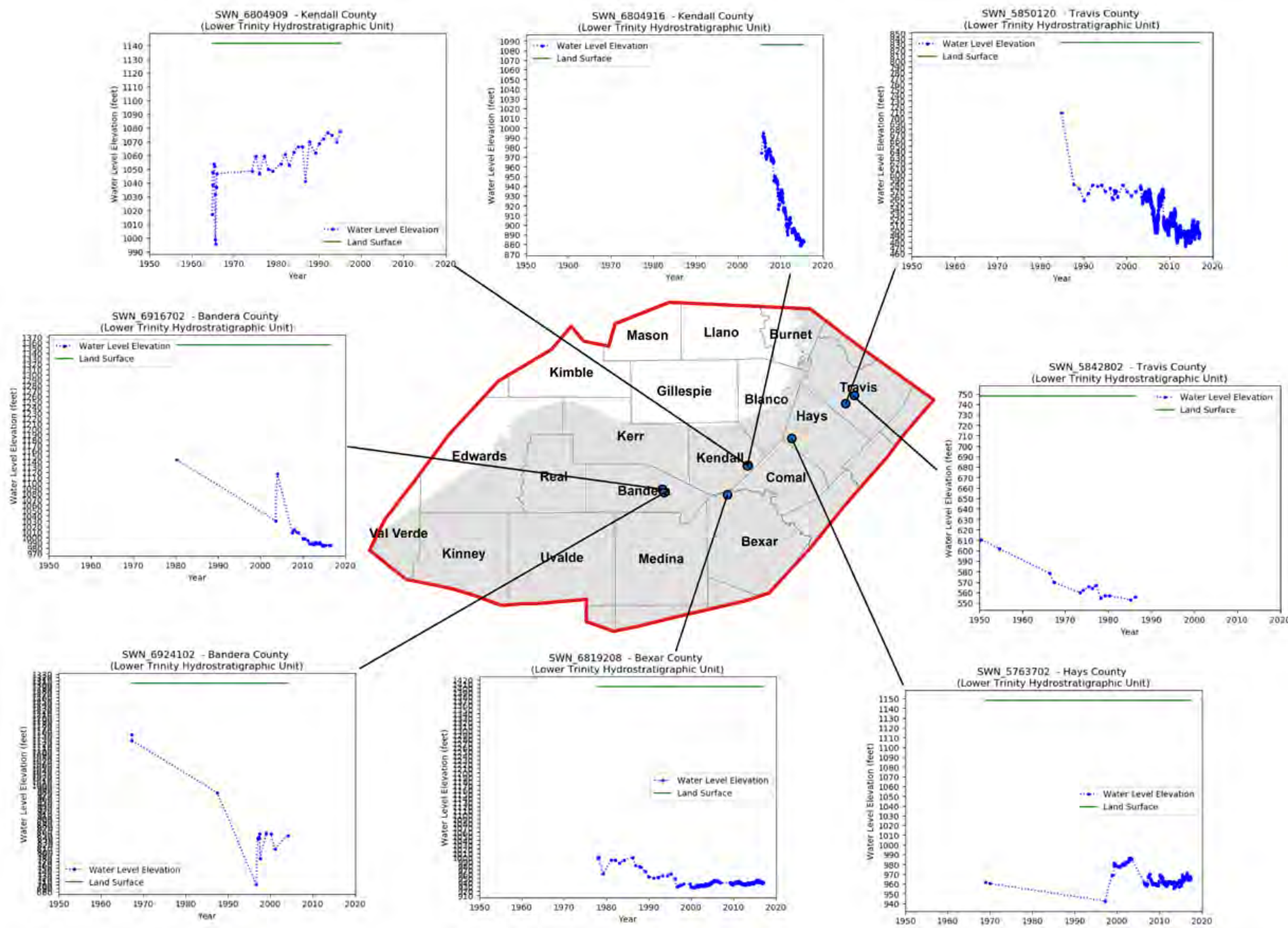

Figure 4.2.28 **Select hydrographs for the Lower Trinity hydrostratigraphic unit in the study area.**

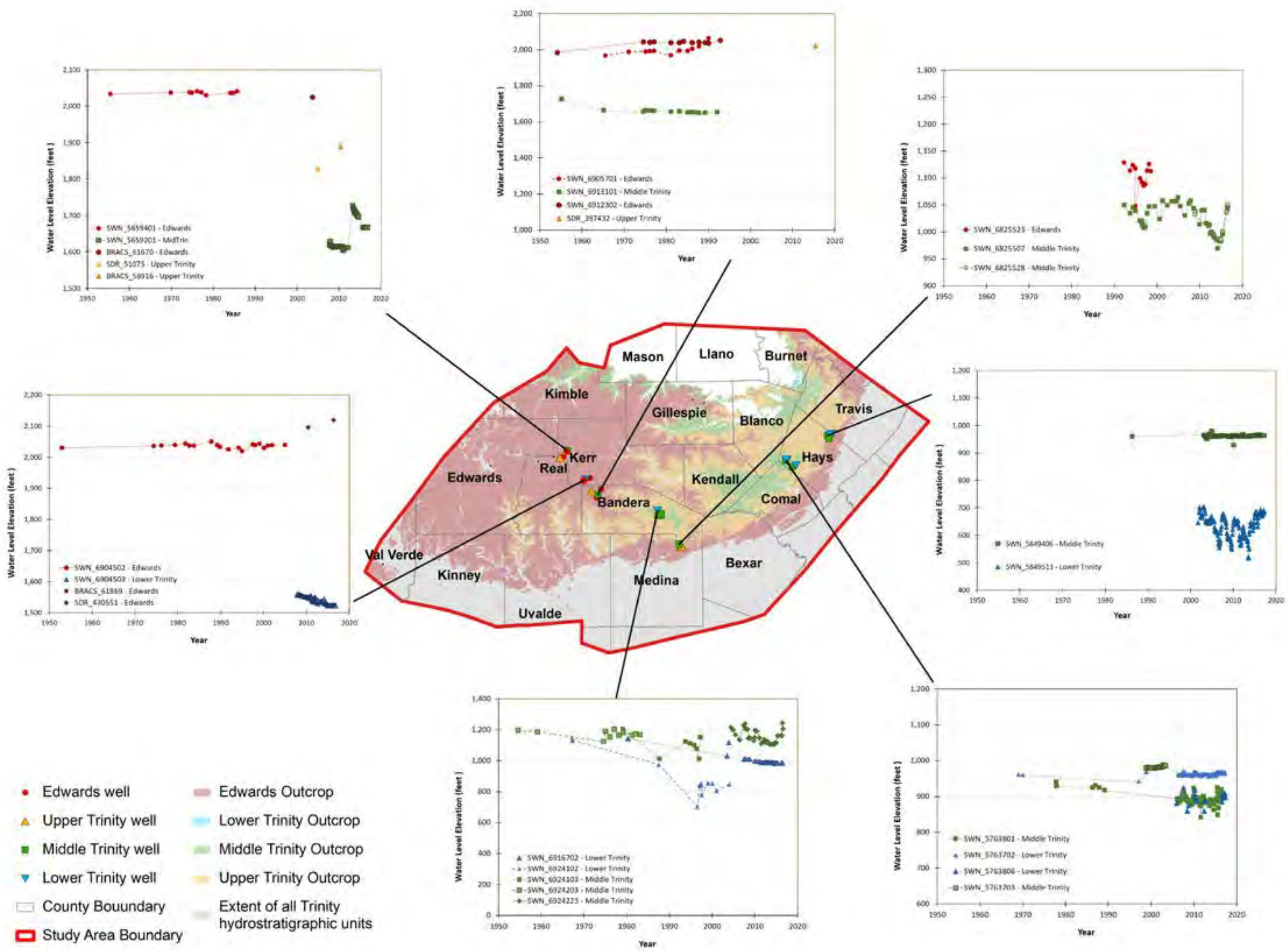

Figure 4.2.29 Comparison of Water elevations between different hydrostratigraphic units.

4.3 Recharge

This section discusses the conceptual approach for estimating recharge in the HCT conceptual model study area. Recharge to the Hill Country occurs as diffuse recharge in the upland areas and as focused recharge typically in river and stream channels. Although this is a fundamental question in the development of the conceptual model, there remains significant uncertainty as to the relative distribution of diffuse and focused recharge. Much of past investigation of recharge in the model domain targeted the Edwards Aquifer recharge zone; however, this body of work is relevant to recharge of the HCT Aquifer recharge zone because virtually all factors that influence recharge of the Edwards Aquifer are directly applicable to the HCT Aquifer. These include precipitation frequency and intensity, rock and soil type, vegetation, and climate. Seminal work by Puente (1978) has been relied on for the past four decades as the basis of the relative proportions of diffuse and focused recharge in the Edwards Aquifer recharge zone.

Investigation of recharge in the contributing zones of the Barton Springs (Hauwert, 2011) and the San Antonio (Fratesi et al., 2015) segments of the Edwards Aquifer explored the relative contributions of diffuse and focused recharge. A similar approach was used in the HCT conceptual model to provide a tool to estimate the spatial and temporal distribution of recharge.

This discussion details the development of a simple Excel-spreadsheet-based tool that stores the relevant hydrologic parameters and performs calculations to spatially and temporally distributed recharge in the HCT conceptual model study domain.

4.3.1 Diffuse Recharge

Diffuse recharge from precipitation was calculated by an analytical Excel-spreadsheet-based model. Once added to the future numerical model, diffuse recharge will flow through the subsurface in response to the hydraulic conductivity field and the hydraulic gradient. This approach makes it feasible to replicate the temporal lag between the time of precipitation and the time at which the recharge event was transmitted as a hydraulic impulse through the aquifer. The Excel-workbook contains the monthly precipitation values for every 4-km by 4-km cell in the HCT study area. The Excel-spreadsheet is saved in the GAM data directory under \Recharge Model\ Recharge_v1_5-7-18.xlsx.

Recharge is calculated directly from precipitation data representative for the outcrop area of the HCT Aquifer. Parameter-elevation Relationships on Independent Slopes Model (PRISM) precipitation data acquired from the PRISM website (http://prism.oregonstate.edu/) are available for the study area ranging from 1980-2015. PRISM datasets utilized for this study include precipitation as well as maximum and minimum temperature. PRISM datasets are useful for determining the average precipitation over a 30-year period, considered to be the standard averaging period in order to describe the long-term climate of a given region. PRISM datasets are calculated using a climate–elevation regression for every digital elevation model (DEM) grid cell. For this regression, monitoring stations are assigned weights based primarily on the physiographic similarity of the station to the 4-km by 4-km grid cell. The factors considered in the regression are elevation, location, topographic facet orientation, topographic position, coastal proximity, vertical atmospheric layer, and orographic effectiveness of the terrain (PRISM Climate Group, 2014).

Monthly precipitation data from the Oregon State Prism Climate Group was downloaded for the period of January 1980 to March 2015. The monthly precipitation raster data sets were clipped for the project area. A polygon grid that corresponds to the prism raster cells for the study area was created (Figure 4.3.1). Each grid cell was assigned a pixel ID and a center-point shapefile was created for each pixel cell. Each cell was then assigned evaporation quadrant IDs and River/Stream basin IDs. The PRISM raster grid cells and the evaporation quadrangles are shown on Figure 4.3.1. The PRISM raster grid cells and the HUC-6 river basins are shown on Figure 4.3.2.

Precipitation for each precipitation pixel in the study area is converted to recharge using an algorithm implemented in Excel, accounting for antecedent moisture and seasonal variability. Recharge was calculated by multiplying moisture by the amount of precipitation less the amount of pan evaporation according to the following equation:

$$R_i \ = \sum_i^{i-5} \Phi_i(Min(P_i, MaxP) - aE_i)$$

where:

R_i = recharge during month i for pixel
P_i = precipitation during month i
E_i = average pan evaporation for month i
Φi = weighting factor for antecedent moisture for month i
a = Evapotranspiration scaling factor
i = month indicator
MaxP = Maximum monthly precipitation allowed to recharge the aquifer

This algorithm accounts for the fact that recharge is greater in the winter than in the summer due to decreased evapotranspiration during the winter. Losses due to evapotranspiration are calculated from time series data of monthly gross-lake evaporation rates obtained using TWDB data for the period 1980-2015. Data were downloaded for the study area in quadrangles 708, 709, 710, 807, 808, 809, and 810. Average lake evaporation by month varies from a high of 9 inches in July to a low of 2 inches in December and January. The average evaporation rate for each evaporation quadrangle is summarized in Figure 4.3.3. TWDB lake evaporation datasets were utilized to create a table of pan evaporation rates for every month and every quadrant for the period of January 1980 to March 2015 in every evaporation quadrant as delineated by the TWDB. Pan evaporation for each quadrant was calculated using this TWDB lake evaporation-rate, time-series data and dividing the value for each evaporation quadrant on a given month by the pan to lake evaporation coefficient. Pan evaporation is determined in the Excel spreadsheet for every cell and every month by a lookup table utilizing the evaporation quadrant ID assigned to every cell.

The antecedent moisture weighting factors are calibration parameters and should be adjusted during numerical model calibration. The initial antecedent weighting factors Excel-spreadsheet model has been populated with values extrapolated from the Edwards Aquifer Authority finite-element model (Table 4.3.1) (Fratesi et al., 2014). The initial antecedent weighting factors used in the Excel-spreadsheet model are provided in

Table 4.3.1. The antecedent weighting factors are independently set for each river/stream basin. The Excel spreadsheet allows a lookup to identify the factors to use in the calculation for each pixel. The amplitudes of these weighting factors are adjusted during calibration of the numerical model. The calibrated volume of recharge is a reflection of correct natural and anthropogenic discharge quantities.

Lastly, the temporal duration represented by the algorithm is adjusted so that the duration of recharge is commiserate with the duration of a precipitation event such that recharge is consistent with the "hydraulic memory" of the aquifer system in the contributing and recharge zones of the HCT Aquifer. Again, the temporal duration is independently set for each river/stream watershed basin. The Excel spreadsheet allows a lookup to identify the temporal duration factors to use in the calculation for each pixel. The default temporal duration factors used in the Excel-spreadsheet model are provided in

Table 4.3.1.

Increased precipitation losses to surface runoff during large storms or periods of intense rainfall are accounted for by capping the amount of precipitation allowed to be applied as recharge during any single month. To accomplish this, a maximum threshold for monthly precipitation is be applied. The default maximum threshold is 8.0 inches for all watersheds. Using the PRISM precipitation data with the assigned seasonal and antecedent weighting factors, recharge for each month is calculated by the excel spreadsheet for each 4-km by 4-km pixel in the study area as an example. The distribution of recharge in the study area for two selected months, representing the lowest recharge and the highest recharge, calculated by the analytical model are shown in Figure 4.3.4 and Figure 4.3.5.

4.3.2 Focused Recharge

Focused recharge from precipitation was calculated by a separate analytical Excel-spreadsheet-based model. The focused recharge Excel-workbook contains the monthly precipitation values for every 4-km by 4-km prism cell in the HCT study area that is within catchments that recharge the Trinity aquifer formations. The Excel-spreadsheet is saved in the GAM data directory under \Recharge Model\FocusedRecharge_v1.xlsx.

The PRISM polygon grid described in Section 4.3.1 was clipped to the extent of the HCT study area that is within catchments that recharge the Trinity Aquifer formations (Figure 4.3.6). A derivative polygon feature class was created where major streams and rivers in the study area intersect PRISM cells. Cell centers for each grid feature were converted to points. Using the *NEAR* geoprocessing tool in ArcGIS a matrix of distances from PRISM cells to nearest streamnode was created.

Precipitation for each precipitation pixel in the study area is converted to focused recharge using an algorithm implemented in Excel, accounting for antecedent moisture and seasonal variability. Recharge was calculated by multiplying moisture by the amount of precipitation less the amount of pan evaporation according to the following equation:

$$R_i \;=\; \sum_1^n \left(Min(P_n, MaxP) * (\%focused\ at\ Cell_n * IDW\ \right)$$

where:

R_i = focused recharge during month i for stream pixel
P_n = precipitation during month i for each PRISM pixel associated with stream node
% focused = % of P_n destined for focused recharge set for each basin or each cell
IDW = Distance Weighting = 1 – (Distance $Cell_n$/Max Basin Distance)
i = month indicator
MaxP = Maximum monthly precipitation allowed to recharge the aquifer

This algorithm accounts for the fact that a fraction of precipitation runoff will report to streams and rivers where it may enter the groundwater system as focused recharge. The percentage of precipitation reporting to the stream cell from any given PRISM cell is determined by the percentage of focused precipitation factor and the distance between the PRISM cell and the stream cell. The percentage of focused precipitation is set on a basin by basin basis and should be adjusted during calibration. The distribution of focused recharge in the study area for two selected months, representing the lowest recharge and the highest recharge, calculated by the analytical model are shown in Figure 4.3.7 and Figure 4.3.8.

Table 4.3.1. Default Weighting factors, Φi, Max P, and a to account for antecedent moisture and evaporation

Basin	Φ_i	Max P (inches)	a
Middle Colorado-Concho	0.2	8	0.4
Middle Colorado-Llano	0.33	8	0.4
Little	0.2	8	0.6
Lower Colorado	0.2	8	0.6
Lower Brazos	0.2	8	0.6
Devils	0.2	8	0.4
Guadalupe	0.363	8	0.4
Nueces	0.2	8	0.4
San Antonio	0.11	8	0.4
Rio Grande-Falcon	0.2	8	0.4
Rio Grande-Amistad	0.2	8	0.4

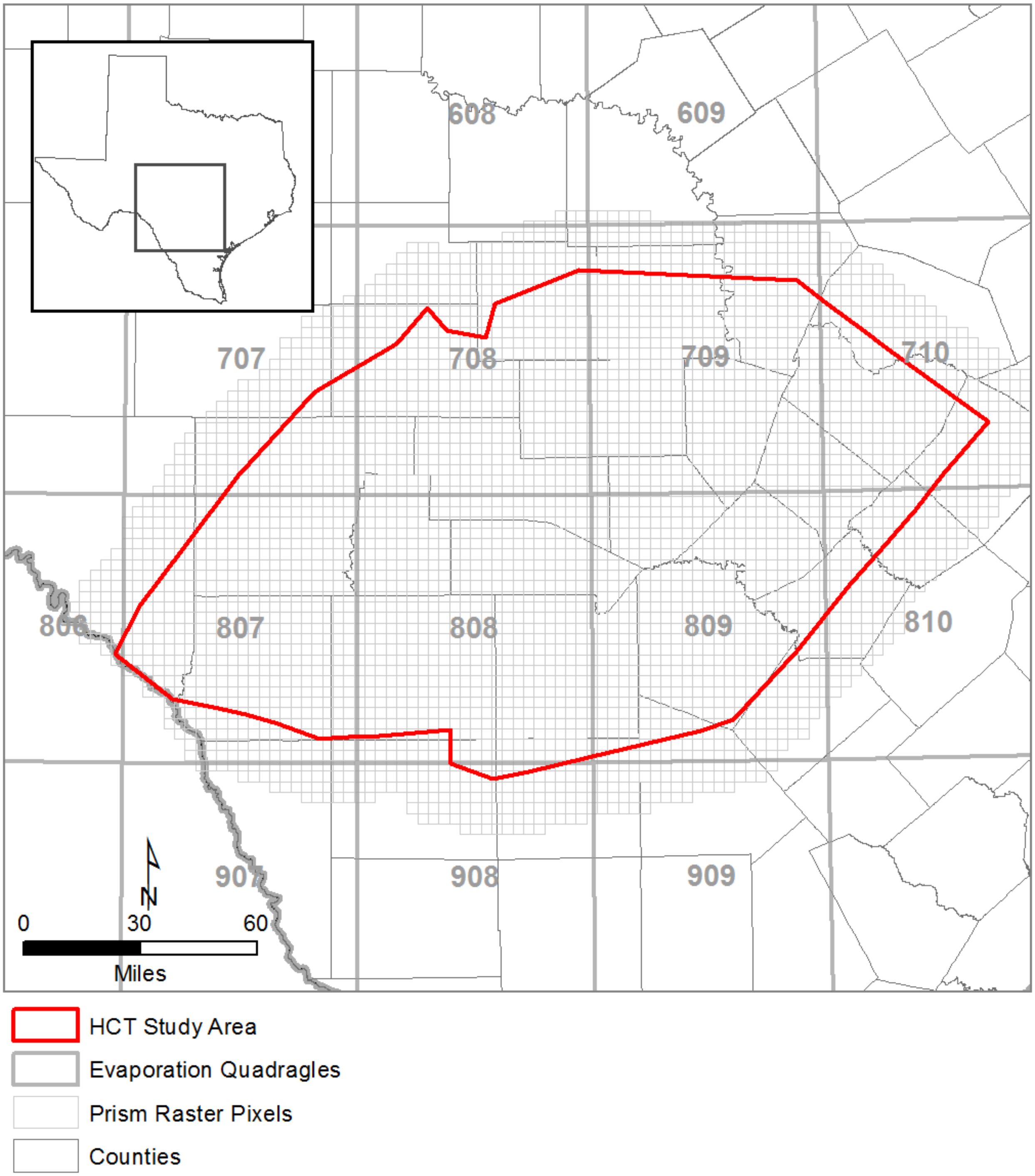

Figure 4.3.1. Map showing the location of the evaporation quadrangles and PRISM precipitation raster pixels used to calculate diffuse recharge within the conceptual model study area.

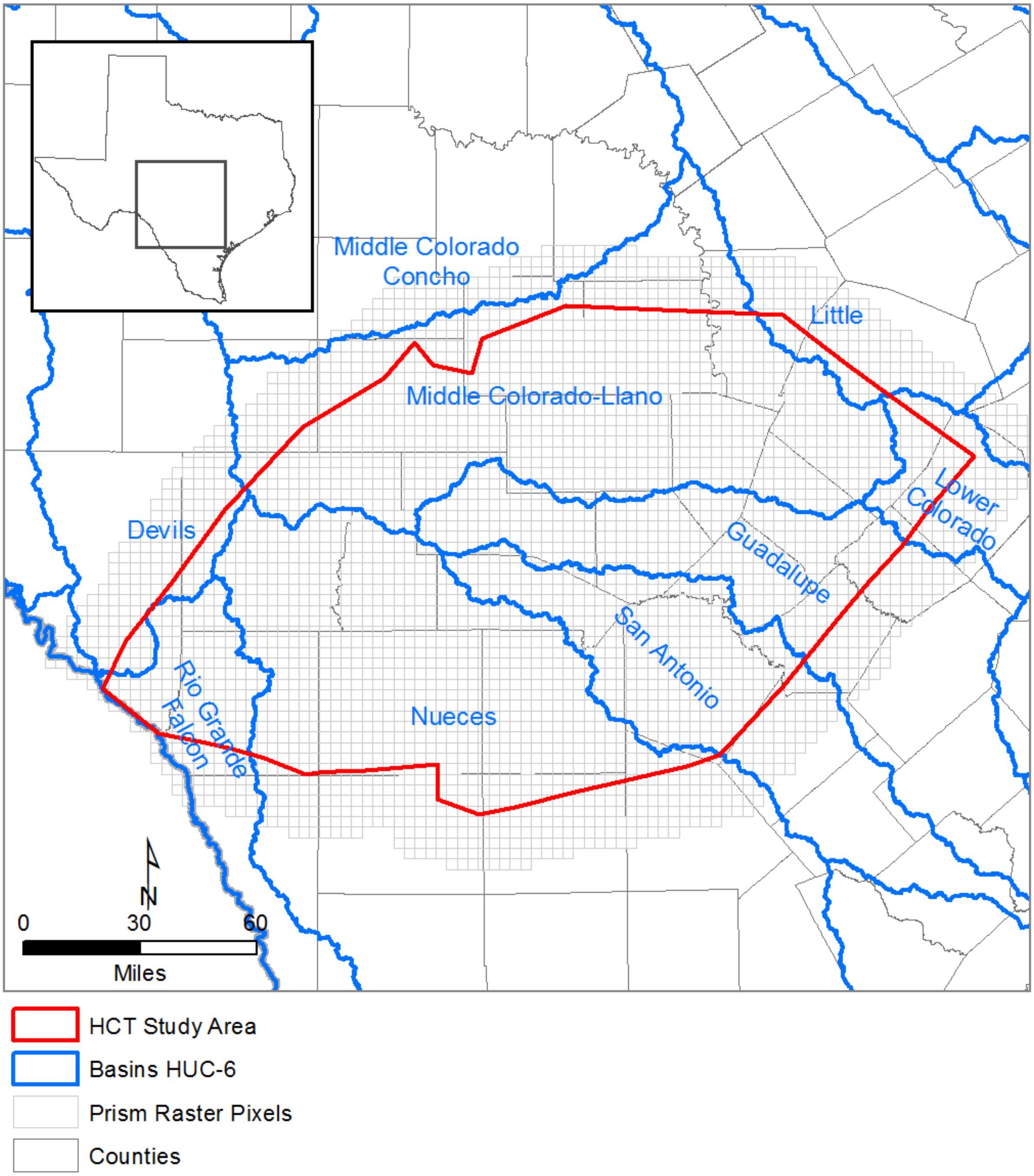

Figure 4.3.2. Map showing the locations of PRISM raster pixels and the HUC-6 basins they fall within.

Figure 4.3.3. **Average annual lake evaporation for each quadrangle in the study area. Average annual lake evaporation for each month in each quadrangle is shown in the respective graph.**

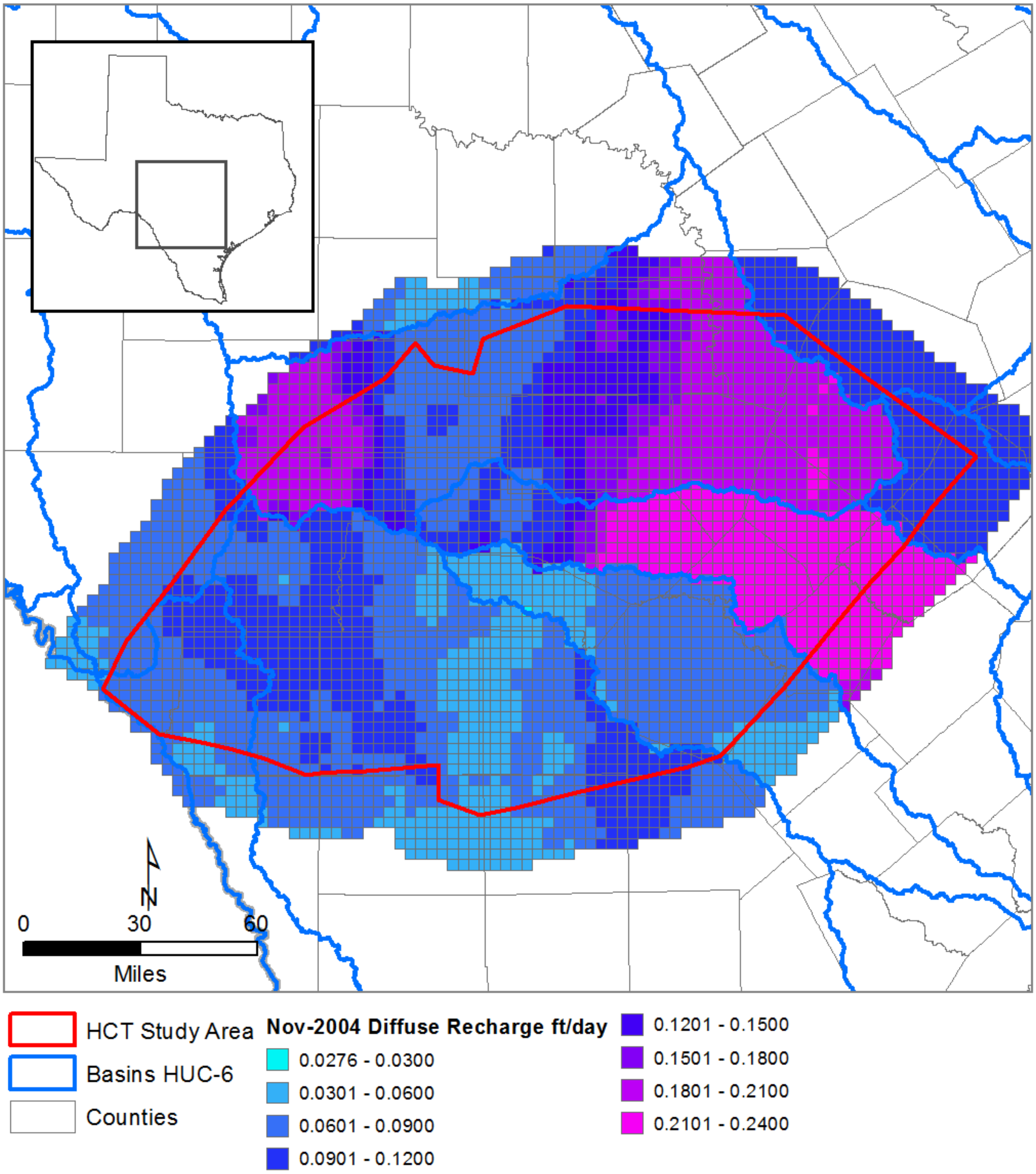

Figure 4.3.4. **Distribution of recharge in November 2004 calculated using the Excel Analytical Model populated with default values.**

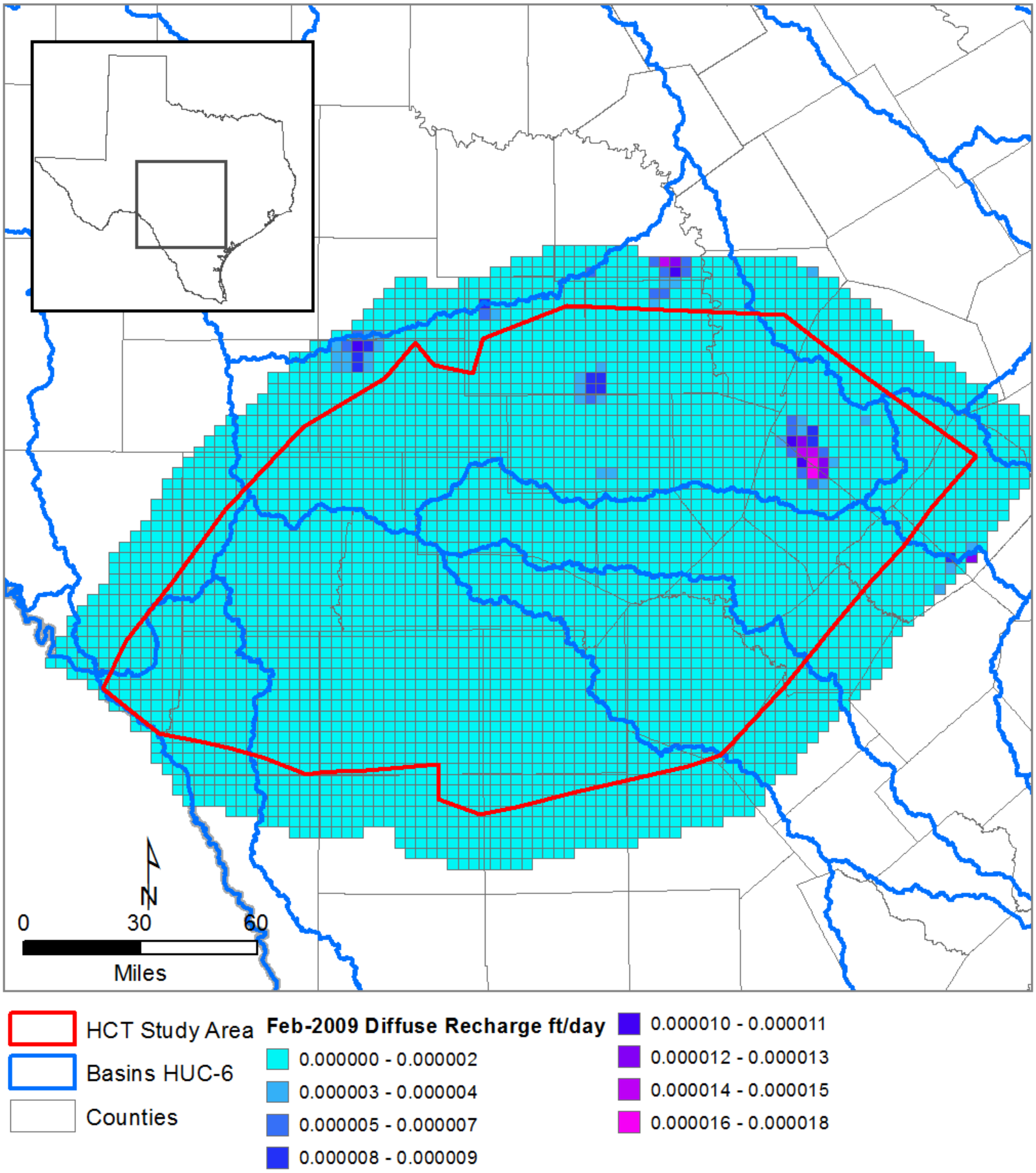

Figure 4.3.5. Distribution of diffuse recharge in February 2009 calculated using the Excel Analytical Model populated with default values.

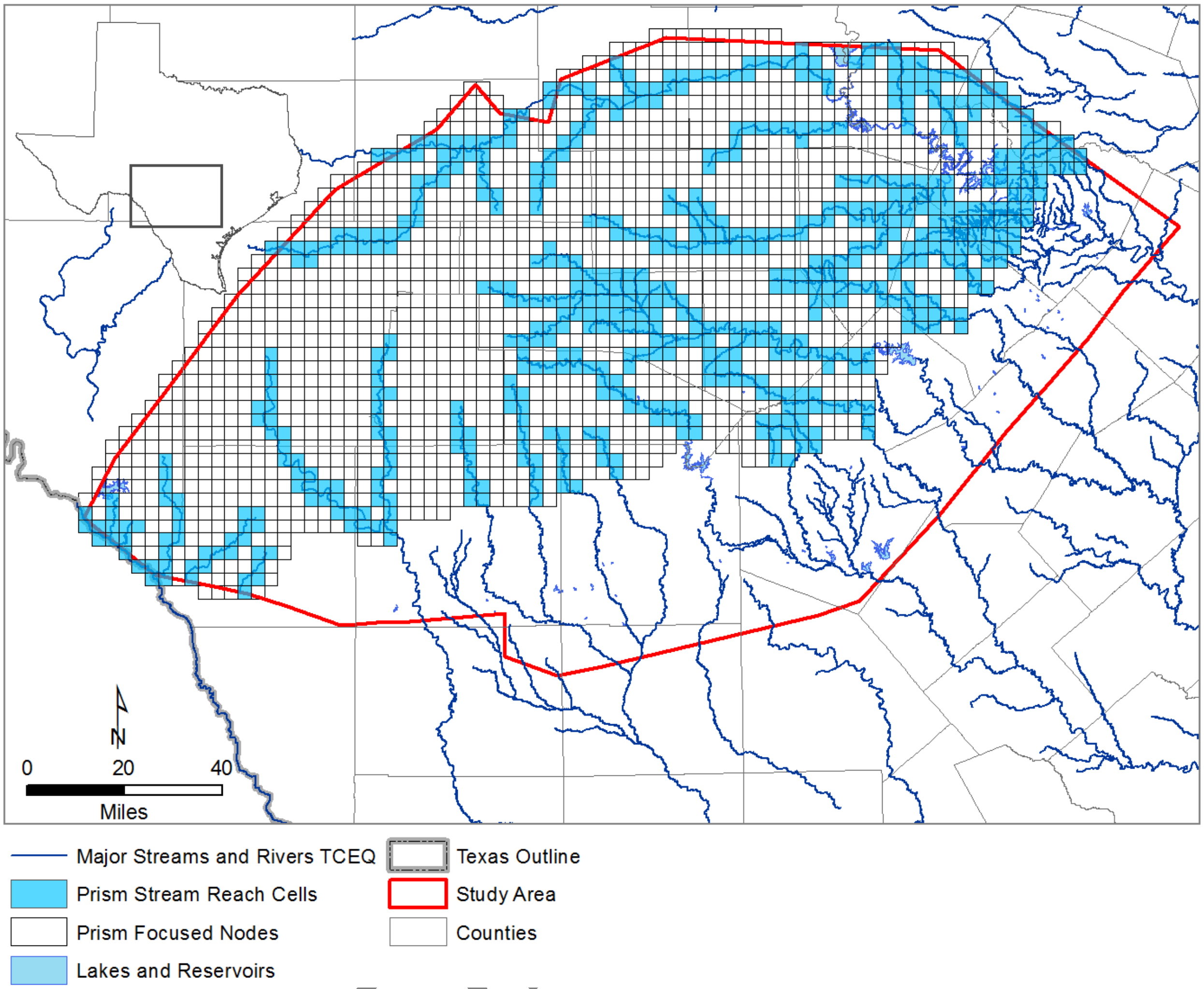

Figure 4.3.6 PRISM pixel cells used to calculate focused recharge in outcrop area of HCT study area. The unshaded cells are cells where precipitation is scaled and assigned to stream cells shaded in blue.

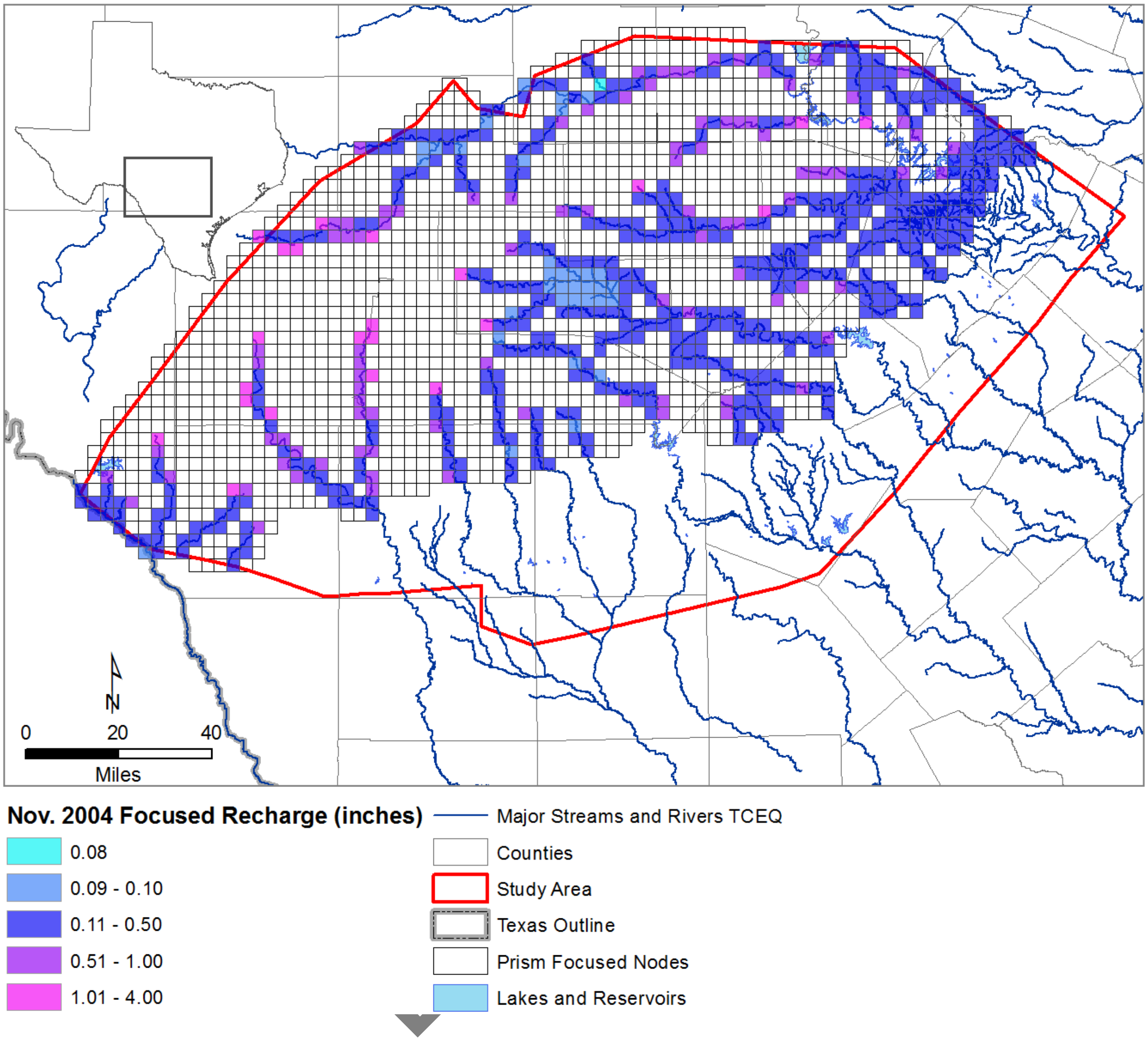

Figure 4.3.7 **Calculated Focused recharge using 2% of precipitation at every PRISM cell directed to the nearest major stream or river and scaled according to its distance from the stream. November 2004 selected since it is the wettest month in the period 1980 to 2015.**

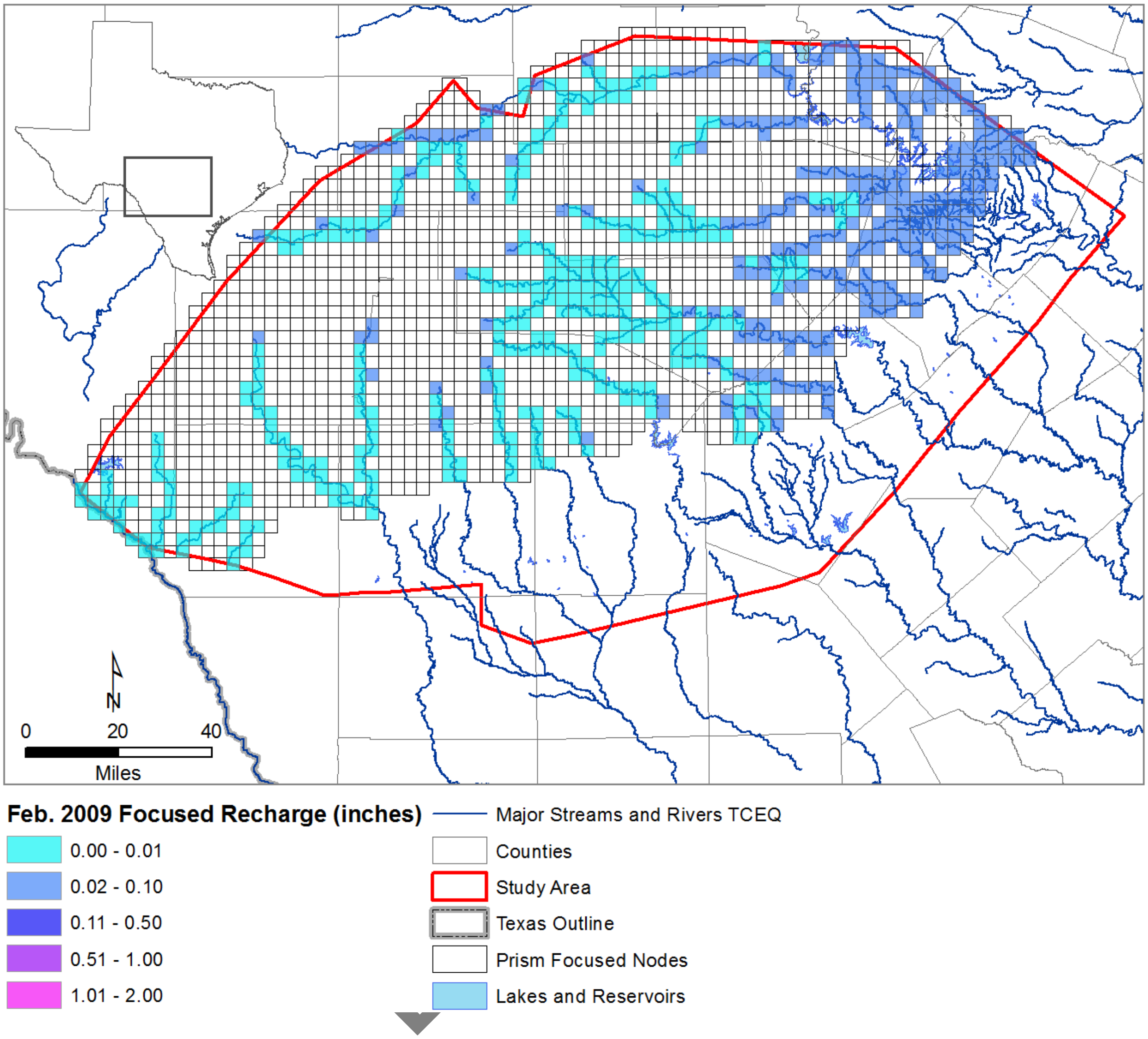

Figure 4.3.8 **Calculated Focused recharge using 2% of precipitation at every PRISM cell directed to the nearest major stream or river and scaled according to its distance from the stream. February 2009 selected since it is the dryest month in the period 1980 to 2015.**

4.4 Rivers, Streams, and Lakes

Surface water/groundwater interaction occurs primarily where surface water intersects aquifer outcrops. At these intersections, flow is between rivers and streams, springs, and lakes, and the aquifer. Direction of flow (i.e. flow from the surface water system into the aquifer or vice versa) depends on the relative hydraulic head of groundwater and surface water, with water flowing from relatively high to relatively low hydraulic head.

4.4.1 Rivers and Streams

Interactions between rivers and streams and groundwater depend on the relative elevation of the stream stage of the river or stream and the elevation of the water table in the aquifer. For gaining streams, the elevation of the water table in the aquifer is higher than the stream-stage elevation and therefore water flows from the aquifer to the stream. For losing streams, the stream-stage elevation is higher than the elevation of the water table in the aquifer and therefore water flows from the stream into the aquifer.

The major rivers and streams in the HCT Aquifer study area and the locations of USGS gauges on the rivers are shown in Figure 4.4.1. Hydrographs of key gauging stations are presented in Figure 4.4.2. Daily-stream flow data have been extracted from the USGS National Water Information System (NWIS) website (USGS, 2018). Streamflow contains stormflow from overland flow and groundwater contributions. The groundwater contribution is reported as the baseflow to the stream. An automated empirical method for estimating the baseflow fraction of the total streamflow was applied to each gauging station dataset. The automated method, called Baseflow, was developed by Arnold et al. (1996, 1999) and relies on a recursive digital filter to separate baseflow from streamflow-recession slopes after storm events. The software code Baseflow was acqired from the Texas A&M University soil and water-assessment tool website (TAMU, 2018). Hydrographs presented in Figure 4.4.2 have both total daily streamflow and second-pass baseflow fractions calculated using the baseflow filter software reported. Parameters for each gauging location calculated with the automated baseflow-separation method are summarized in Table 4.4.1. Baseflow fractions reported are useful to constrain the amount of aquifer recharge in each stream's contributing watershed. The baseflow timeseries data are useful as model calibration targets given that the majority of discharge in the HCT Aquifer study area occurs as springflow to streams and rivers.

The headwaters of the major rivers in the HCT Aquifer study area arise along the eastern margin of the Edwards Plateau and descend with a steep gradient into the Hill Country (Figure 4.4.1). Many of these streams have upper reaches contained within narrow canyons and broaden into flat-bottomed valleys farther downstream (Barker and Ardis, 1996). Four major drainage basins—the Nueces, San Antonio, Guadalupe, and Middle Colorado-Llano rivers—traverse the study area and funnel flow toward the southeast. These rivers are interpreted to be hydraulically connected to the regional-flow system (Kuniansky, 1990).

Historically, the major rivers in the Hill Country have been classified as gaining in the upland area and losing in the recharge zone. The upland areas have been shown to be more complex than this observation, although, there may be a general tendency for spring discharge to cause rivers to gain in upland areas (Hauwert, 2009, 2011) . Gain/loss measurements for the HCT Aquifer study area provide insight into this classification. Data from multiple gain/loss studies that were summarized by Slade et al. (2002) were collected at different times and do not represent synoptic studies (Figure 4.4.3). This factor obfuscates the database because of the variable nature of stream flow in the Hill Country. Repeat streamflow measurements in the Hill Country illustrate that stream and river changes can change between gaining and losing when observed during different hydrologic conditions.

The major rivers in the study area are typically perennial, although certain reaches may lose surface flow particularly when flowing across areas with significant recharge. Lower reaches of most of the streams lose significant quantities of flow where they cross the recharge zone of the Edwards (BFZ) aquifer (Barker et al., 1994). For example, the lower reach of the Nueces River where it crosses the Edwards Aquifer recharge zone has no baseflow (Fratesi et a., 2014). Lower reaches of Cibolo Creek lose flow between Boerne and Bulverde where the creek flows over the lower member of the Glen Rose Limestone (Ashworth, 1983). Conversely, Cibolo Creek gains water where it flows over the upper member of the Glen Rose Limestone (Guyton and Associates, 1958, 1970; Espey, Huston and Associates, 1982; LBG-Guyton Associates, 1995; Mace et al., 2000). Many perennial rivers have had brief episodes of no flow during droughts (Figure 4.4.2).

Useful in understanding gain/loss on rivers in the study area are synoptic streamflow measurements of the Nueces and Blanco rivers undertaken by a collaboration of the Edwards Aquifer Authority and the University of Texas Jackson School of Geosciences that was conducted as part of the Edwards Aquifer Authority Interformational Flow program (Figure 4.4.4 and Figure 4.4.5). Flow in the Nueces River (Figure 4.4.4) differs from flow in the Blanco River (Figure 4.4.5). The Blanco River is losing from its upland area until western Comal County. From that point downstream, the river is gaining. The transition occurs along a reach where the Upper Glen Rose Formation is absent and the riverbed overlies the Lower Glen Rose Formation. The Blanco River is mostly gaining over the remaining reach located within the HCT Aquifer study domain. The Nueces River is more complex. It varies between gaining and losing over the entire reach where is was measured (Figure 4.4.4). Part of the variability in flow measurements is due to difficulty in obtaining accurate flow measurements due to the large quantity of gravel and alluvium present in the bed of the Nueces River.

4.4.2 Lakes and Reservoirs

Lakes and reservoirs in the area include Lake Buchanan, Inks Lake, Lake Travis, Lake Walter E. Long, Canyon Lake, Medina Lake, Calaveras Lake, Braunig Lake, and Amistad Reservoir (Figure 4.4.6). None of the lakes are naturally occurring. All are reservoirs that result from the damming of rivers. The largest reservoirs are gauged allowing the elevation of the water elevation to be recorded over time. Daily water elevations for the lakes in the study area that have historical measurements are included in Figure 4.4.7. Canyon Lake and Lake Travis have maintained approximately constant levels (+/- 20 ft) although Lake Travis had large declines during the drought of the 1950s and again in the mid-1960s (fig. 36). Lake Medina has much more variation in levels and has nearly been dry on a couple occasions (Espey, Huston, and Associates, 1989).

Table 4.4.1 **Summary statistics for automated baseflow separation filter. The baseflow fraction values are the fraction of the total long term discharge that is contributed by baseflow in the watershed upstream of the gauge location.**

USGS Station	Baseflow Fraction Pass One	Baseflow Fraction Pass Two	Baseflow Fraction Pass Three	Number of Recessions Used	Baseflow Recession Constant	Baseflow Days
810464660	0.54	0.38	0.31	4	0.149	15.484
8148500	0.67	0.54	0.48	14	0.021	108.249
8150000	0.91	0.86	0.82	5	0.007	320.871
8150700	0.83	0.74	0.67	6	0.011	214.947
8150800	0.72	0.57	0.47	8	0.026	86.980
8151500	0.69	0.56	0.5	54	0.023	102.302
8152000	0.46	0.29	0.23	32	0.086	26.681
8152900	0.62	0.48	0.42	36	0.031	74.919
8153500	0.58	0.43	0.37	24	0.051	45.091
8154700	0.57	0.4	0.33	47	0.035	66.079
8155200	0.64	0.47	0.38	37	0.037	61.972
8155240	0.64	0.47	0.38	29	0.039	58.854
8158700	0.66	0.45	0.32	8	0.020	113.734
8158810	0.62	0.46	0.37	35	0.034	66.941
8158840	0.69	0.51	0.4	4	0.050	45.730
8158920	0.39	0.22	0.15	12	0.110	20.906
8165300	0.8	0.68	0.6	2	0.054	42.952
8165500	0.7	0.58	0.51	4	0.008	308.169
8166000	0.75	0.66	0.61	26	0.012	190.732
8166140	0.82	0.72	0.66	8	0.022	102.888
8166200	0.79	0.69	0.64	23	0.016	143.243
8167000	0.8	0.68	0.61	10	0.016	142.605
8167500	0.74	0.6	0.52	53	0.019	123.108
8167800	0.71	0.58	0.49	52	0.010	227.493
8171000	0.78	0.65	0.56	30	0.015	150.403
8178585	0.46	0.23	0.12	3	0.274	8.389
817887350	0.8	0.68	0.59	3	0.008	284.656
8178880	0.77	0.63	0.54	10	0.019	123.426
8179520	0.82	0.7	0.61	2	0.006	396.733
8180586	0.74	0.56	0.45	2	0.028	82.741
8181400	0.44	0.22	0.14	8	0.133	17.325
8183850	0.57	0.38	0.29	7	0.053	43.428
8183890	0.65	0.49	0.42	3	0.023	99.368

Table 4.4.1 Continued.

USGS Station	Baseflow Fraction Pass One	Baseflow Fraction Pass Two	Baseflow Fraction Pass Three	Number of Recessions Used	Baseflow Recession Constant	Baseflow Days
8183900	0.63	0.47	0.4	19	0.046	50.587
818999010	0.92	0.87	0.83	3	0.005	427.889
8190000	0.77	0.62	0.52	11	0.010	225.016
8195000	0.83	0.71	0.63	34	0.009	258.244
8196000	0.68	0.53	0.46	67	0.016	141.018
8198000	0.73	0.58	0.48	4	0.022	107.184
8200000	0.67	0.5	0.42	57	0.021	110.687
8200977	0.56	0.35	0.25	2	0.100	23.053
8201500	0.76	0.6	0.5	9	0.033	70.599
8202450	0.58	0.36	0.25	2	0.060	38.401

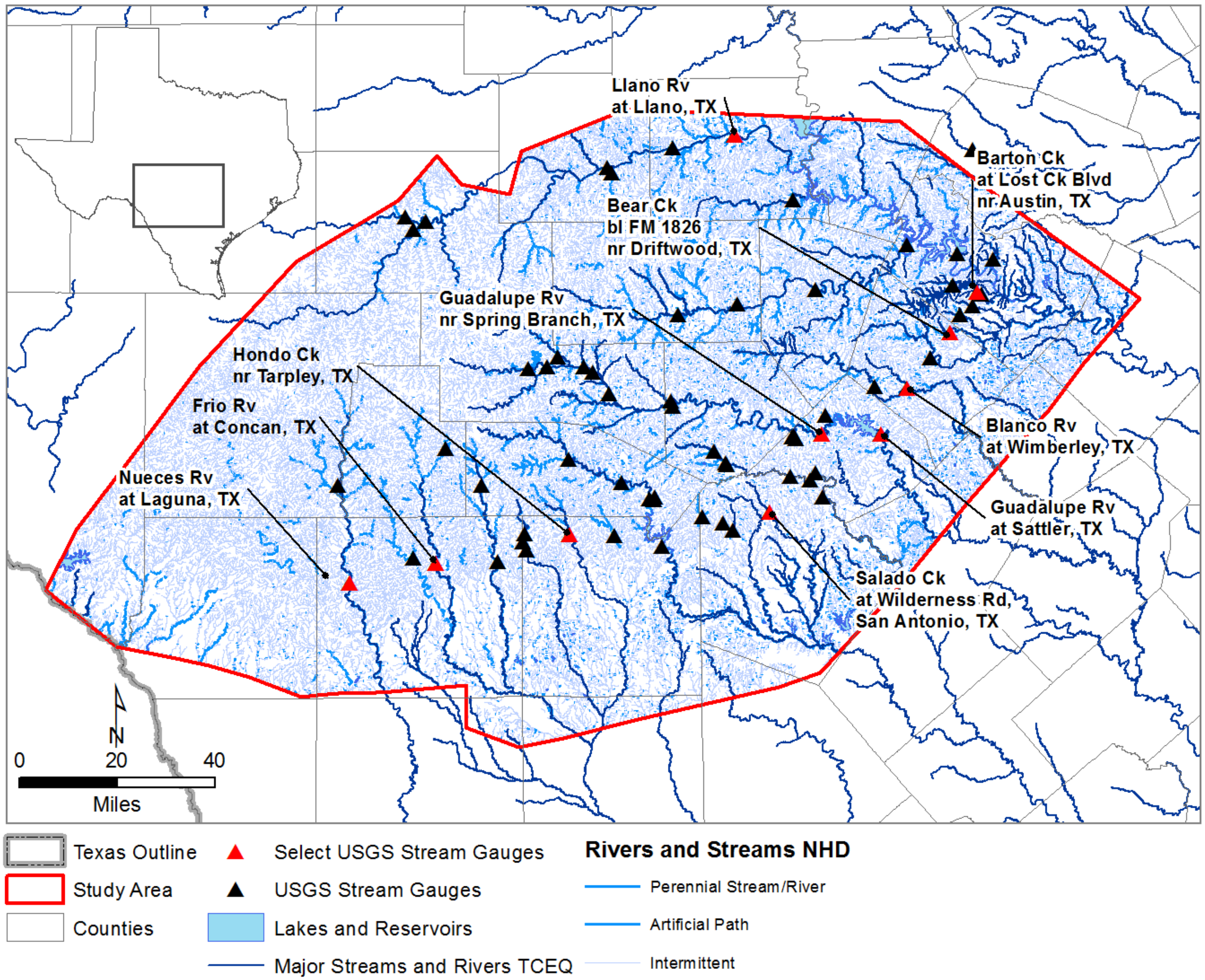

Figure 4.4.1 **Locations of USGS Stream Gages in the study area. Gage locations with Hydrographs appearing in this report are indicated in red.**

8151500 Llano River at Llano, TX

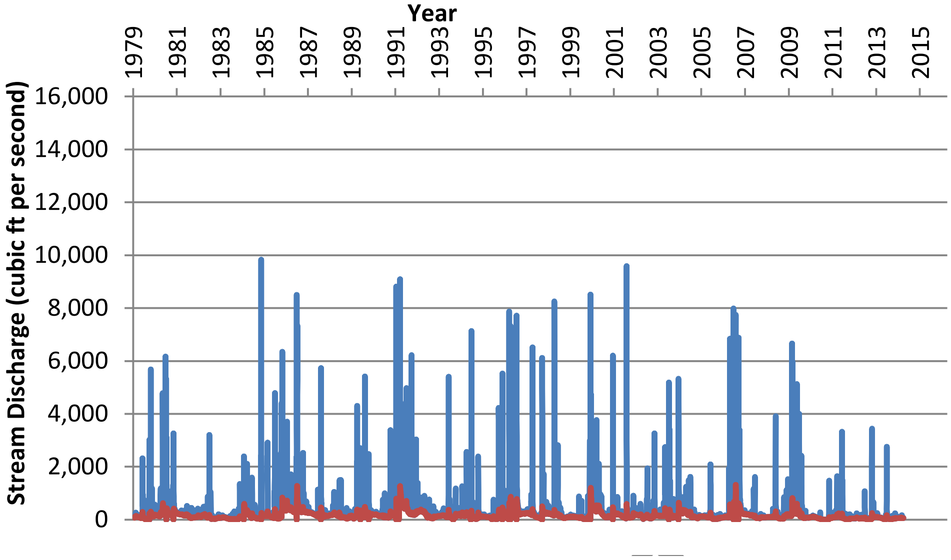

8155240 Barton Ck at Lost Ck Blvd nr Austin, TX

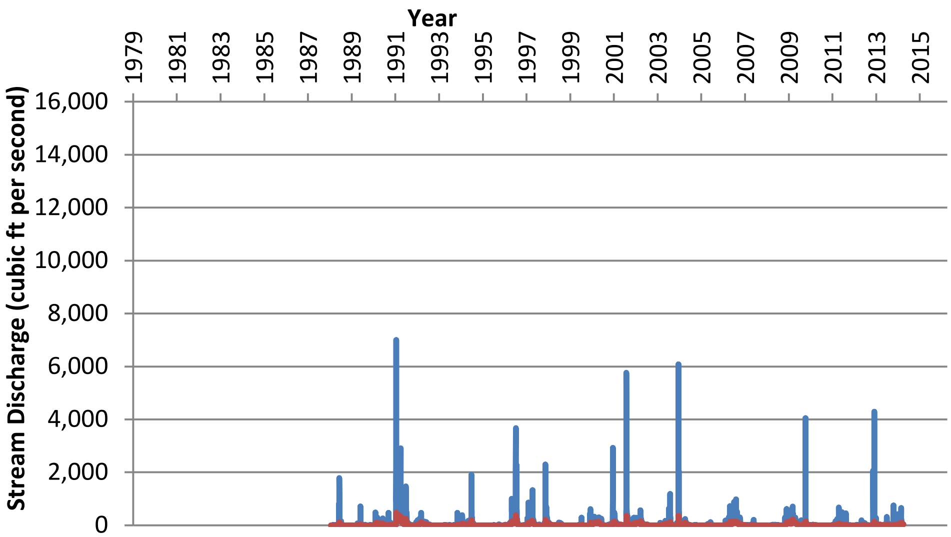

Figure 4.4.2 **Stream Discharge hydrographs for selected gauging sites in the HCT study area. Blue lines indicate total stream discharge. Red line indicates baseflow fraction of discharge.**

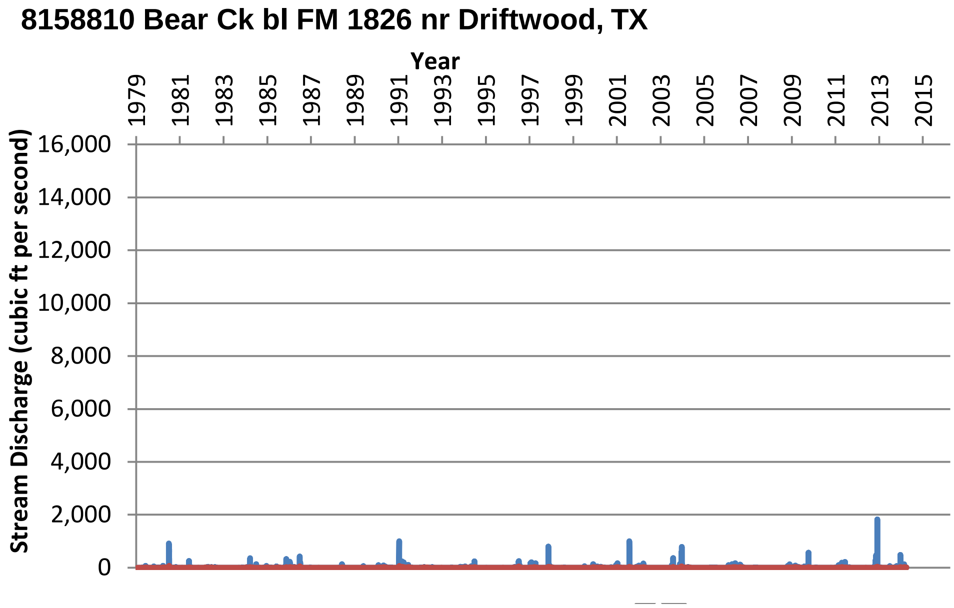

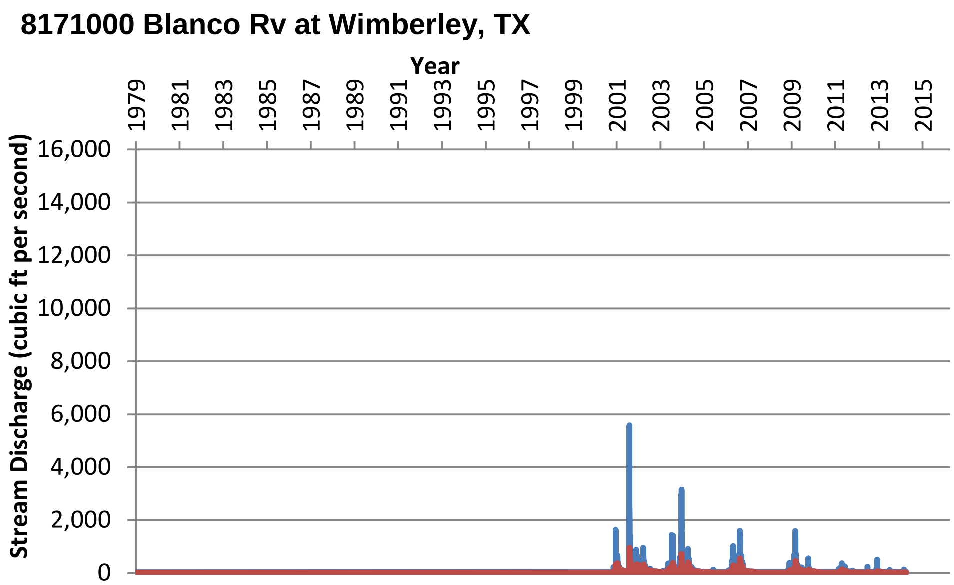

Figure 4.4.2 Continued.

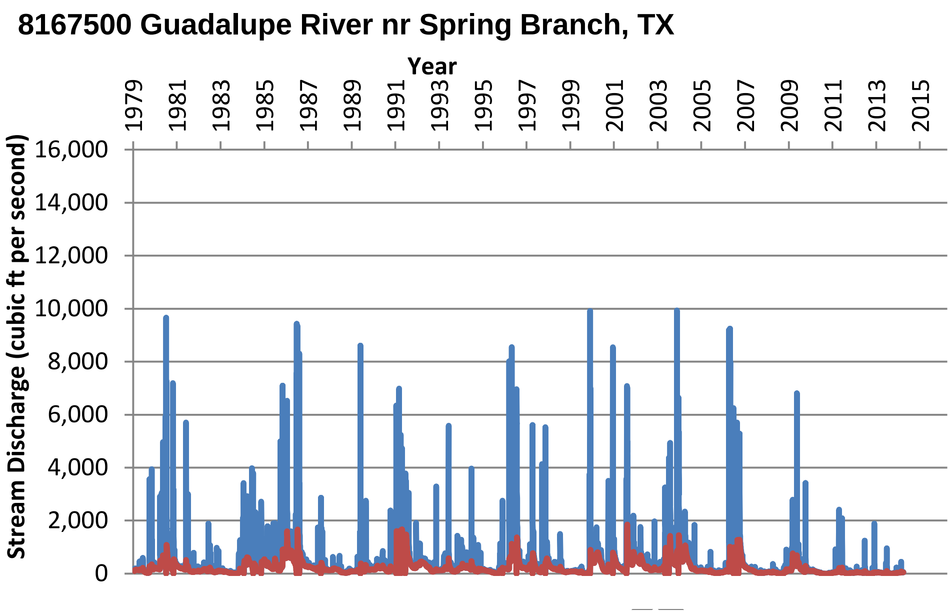

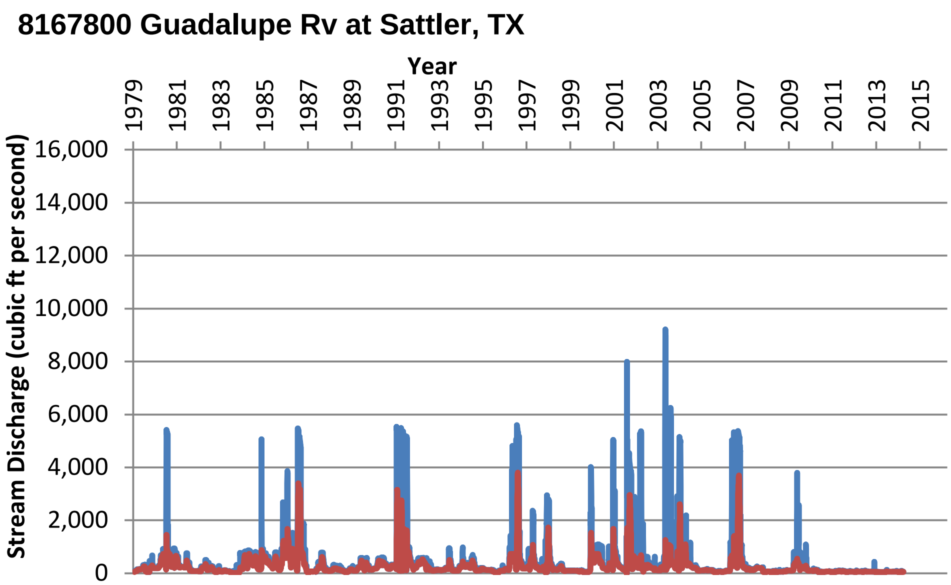

Figure 4.4.2 Continued.

8178585 Salado Ck at Wilderness Rd, San Antonio, TX

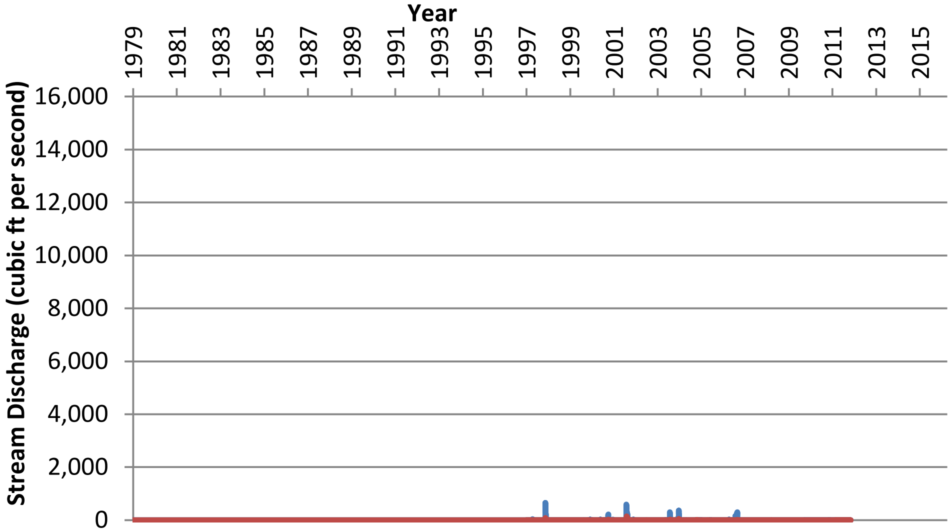

8200000 Hondo Ck nr Tarpley, TX

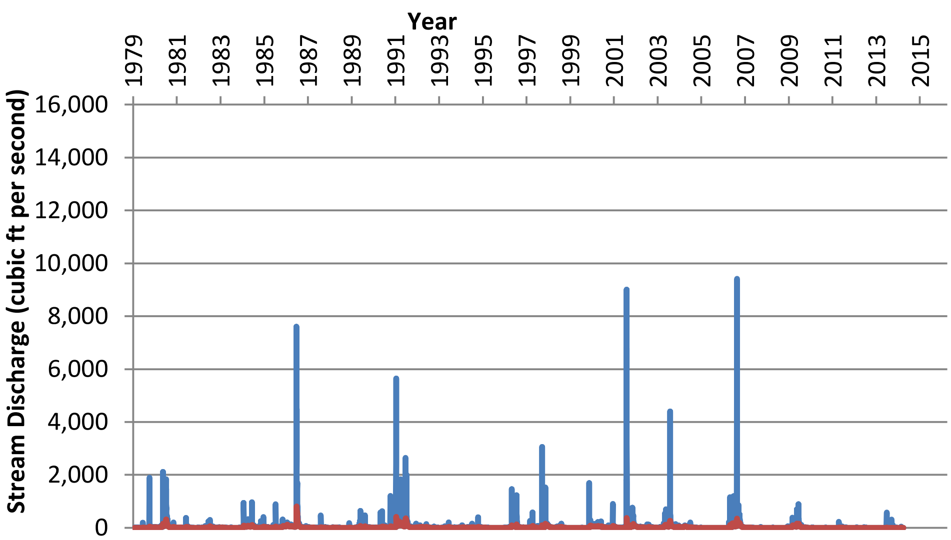

Figure 4.4.2 Continued.

8190000 Nueces River at Laguna, TX

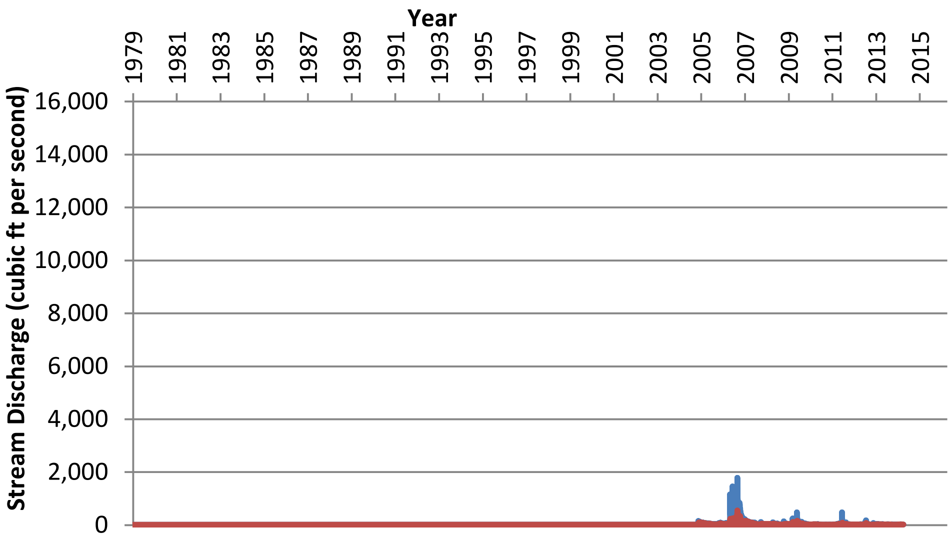

8195000 Frio Rv at Concan, TX

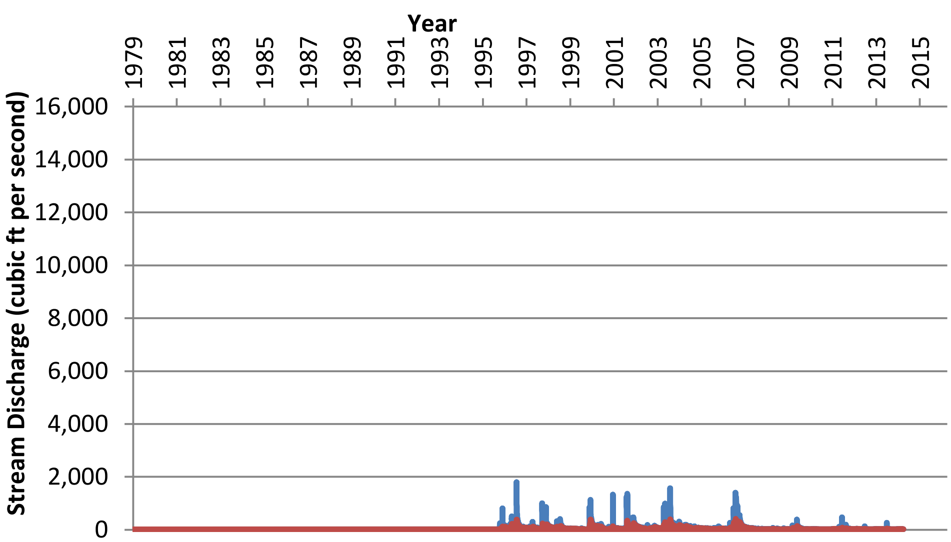

Figure 4.4.2 Continued.

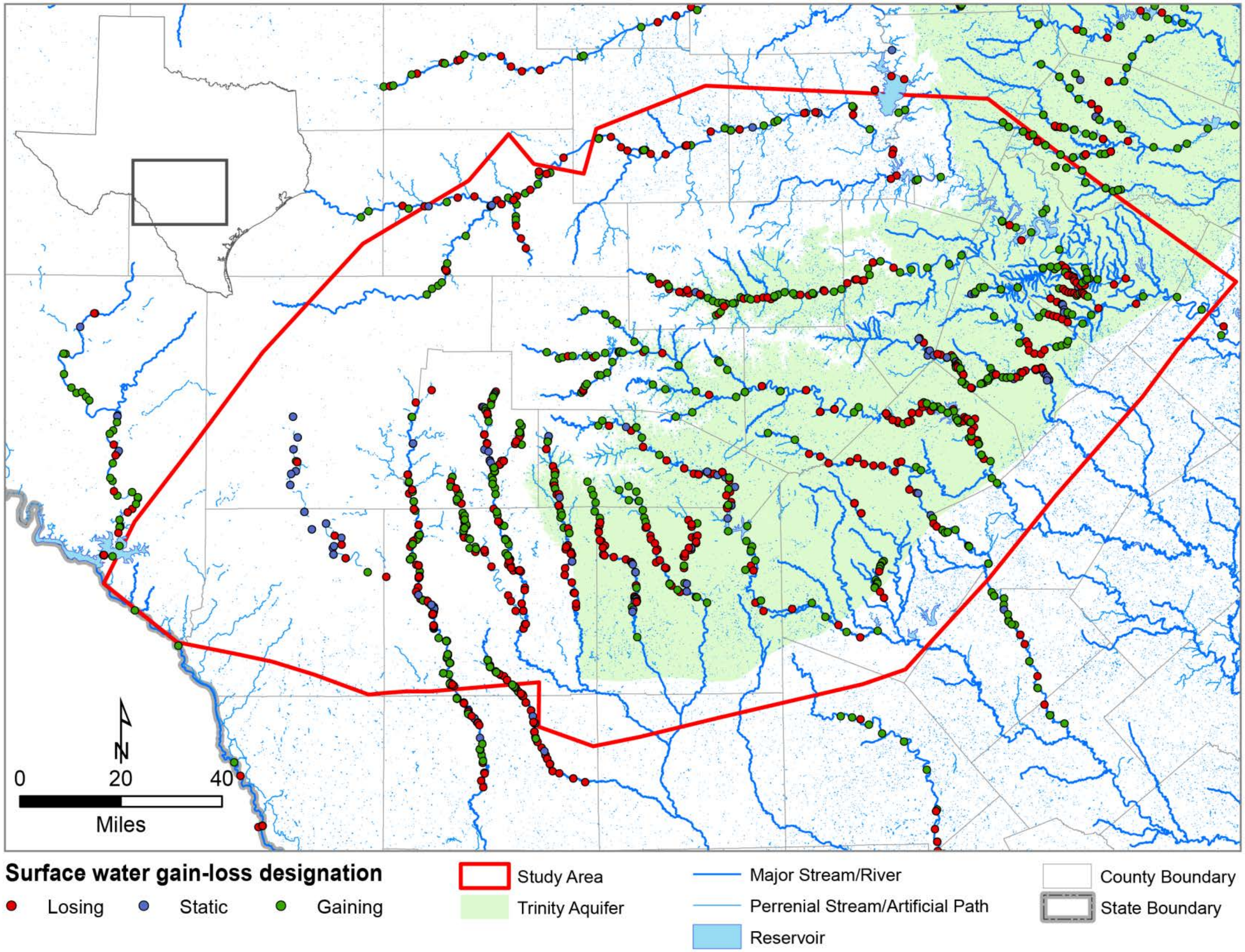

Figure 4.4.3 Gain/loss measurements in the study area (Slade et al., 2002 and Gary, 2018).

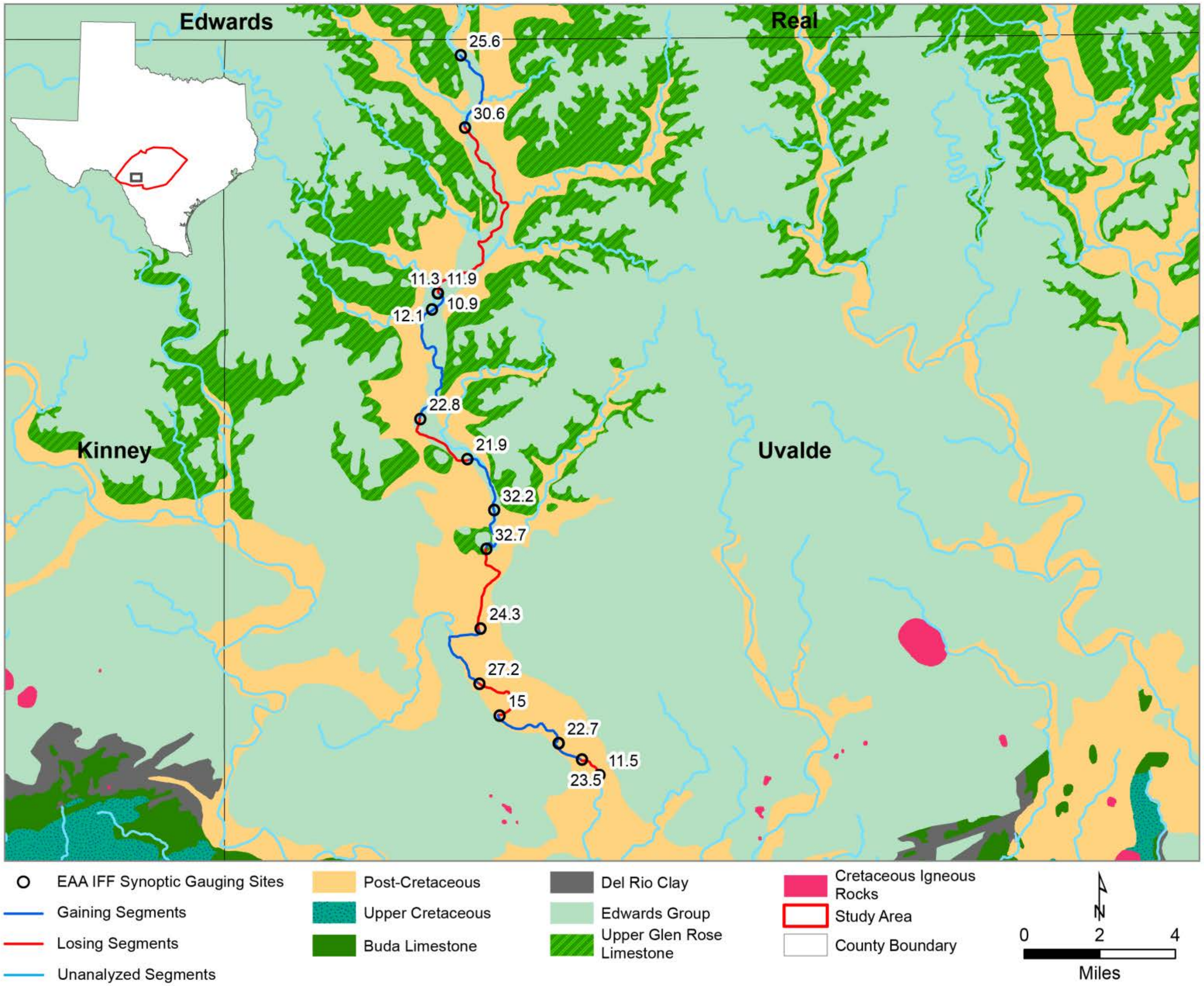

Figure 4.4.4 **Synoptic gain/loss measurements of the Nueces River (Gary, 2018).**

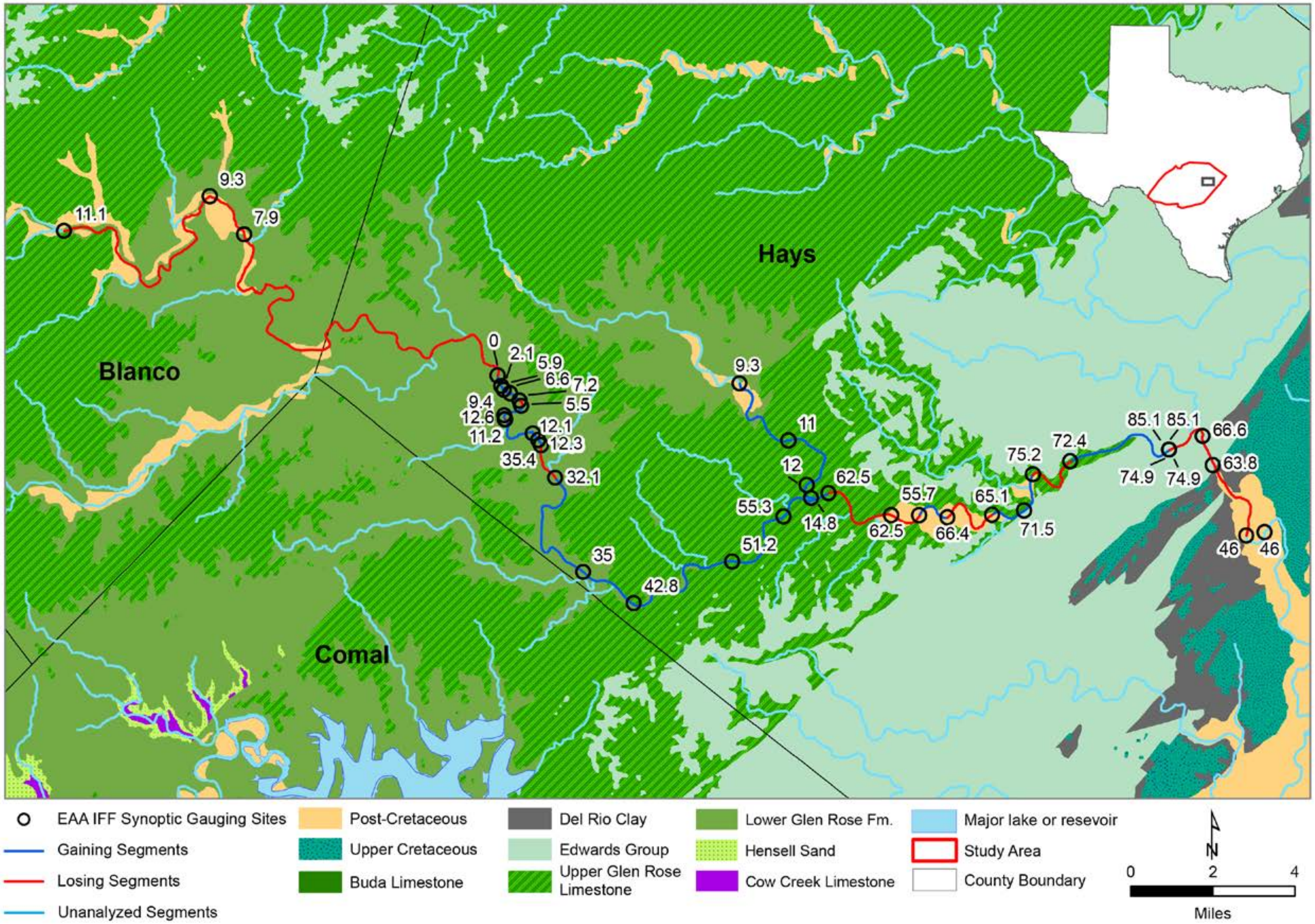

Figure 4.4.5 Synoptic gain/loss measurements of the Blanco River (Gary, 2018).

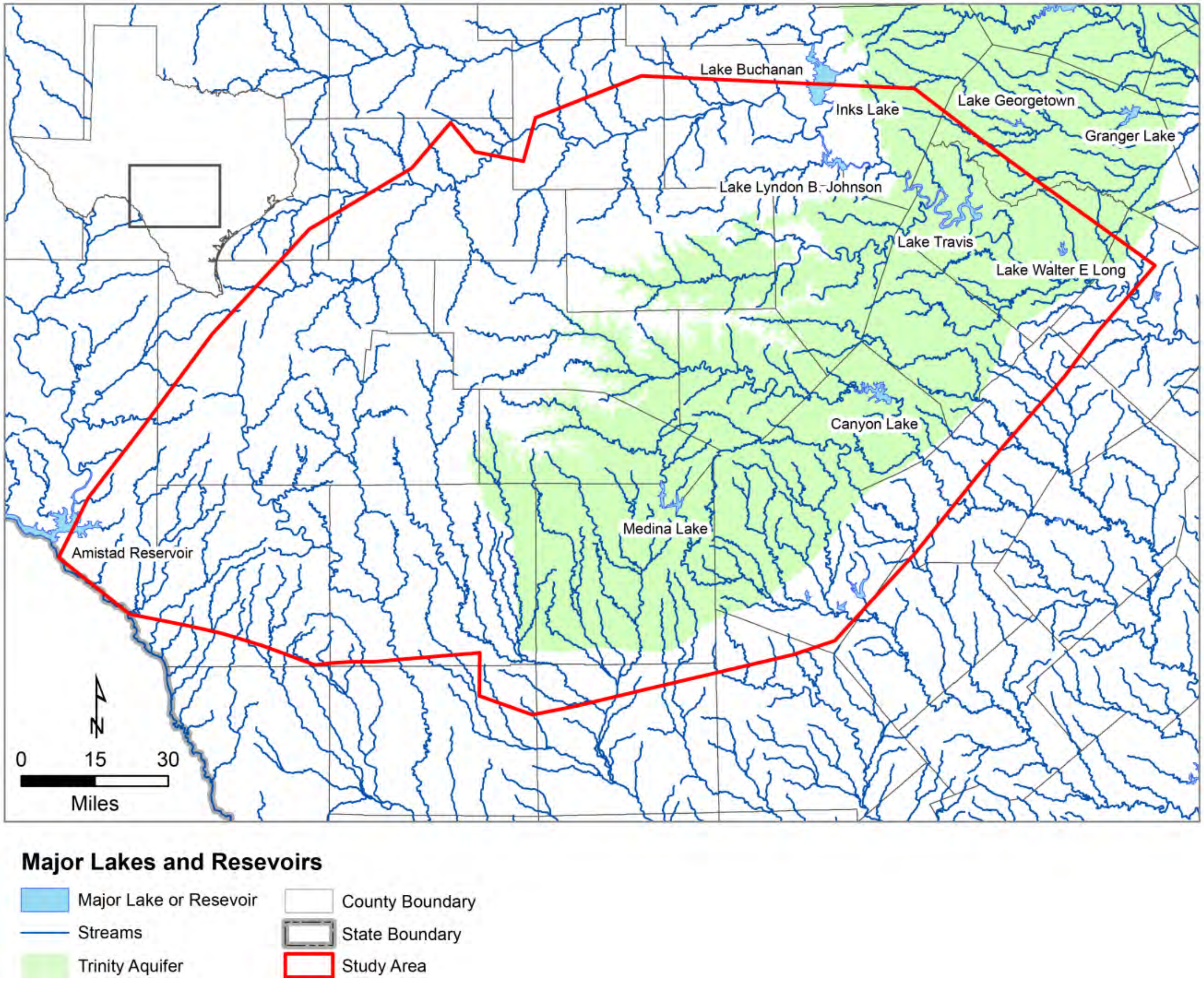

Figure 4.4.6 Major lakes and reservoirs in the study area.

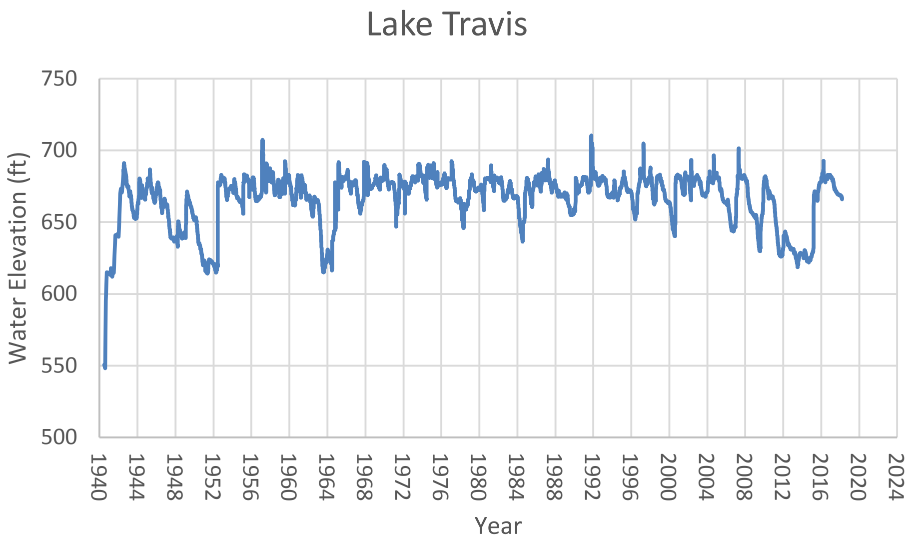

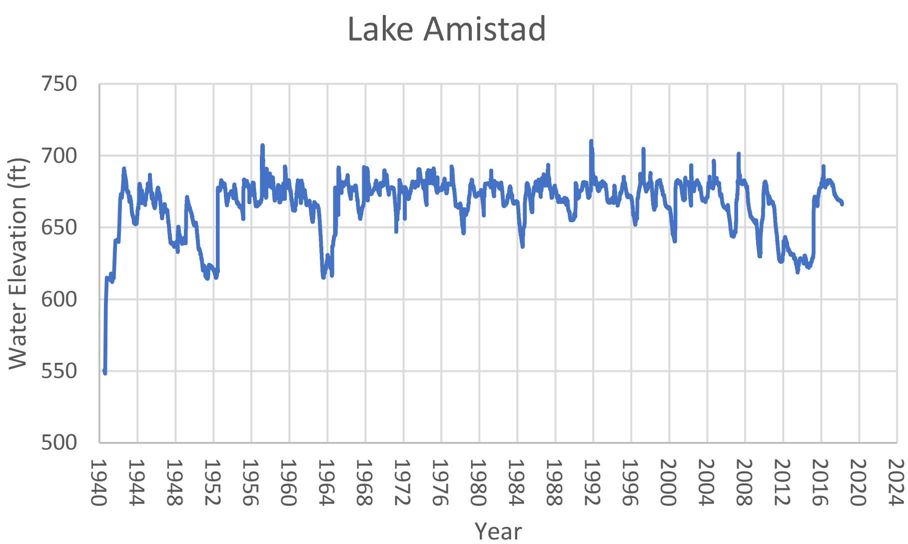

Figure 4.4.7 Hydrographs of Major Lakes in the Study Area 1940-2018.

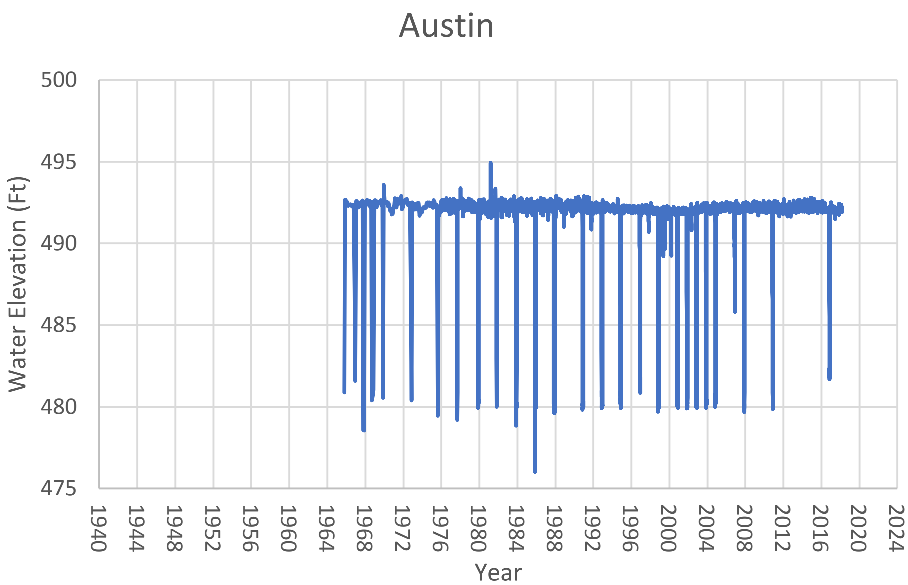

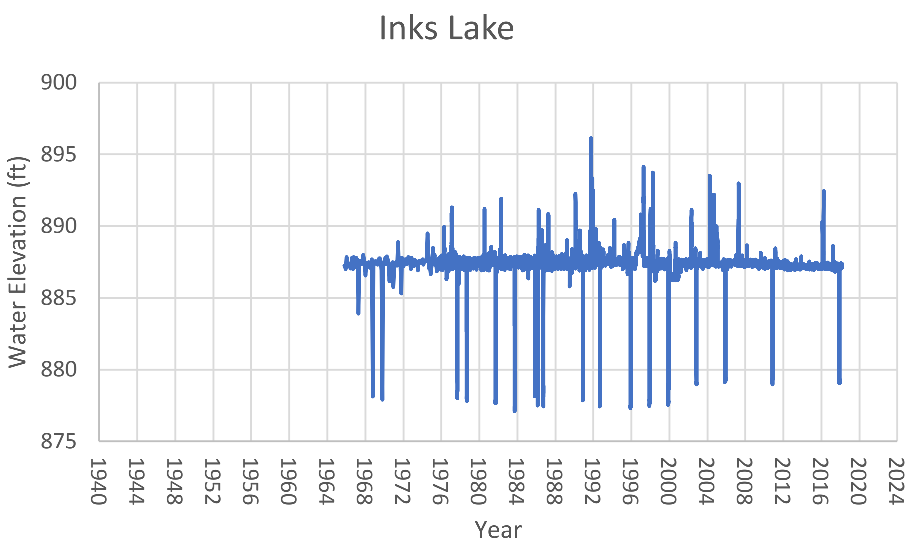

Figure 4.4.5 Continued.

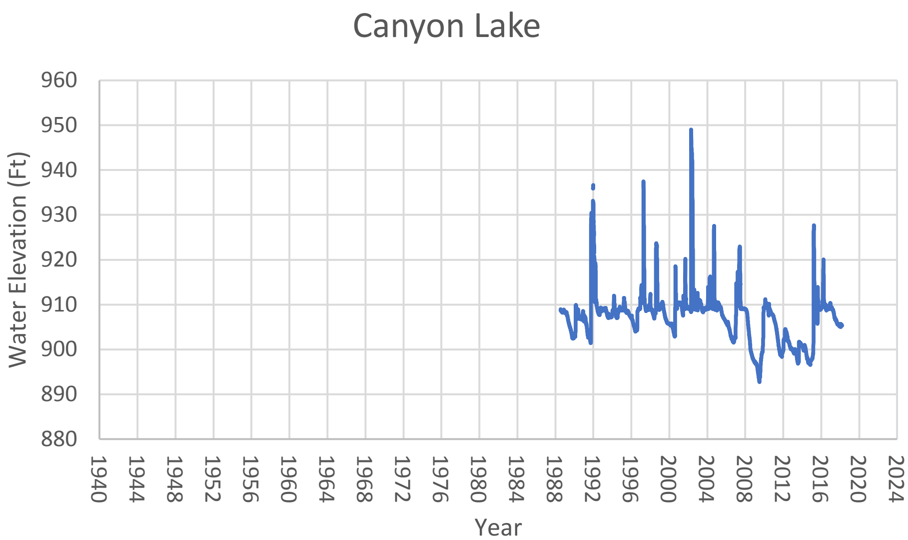

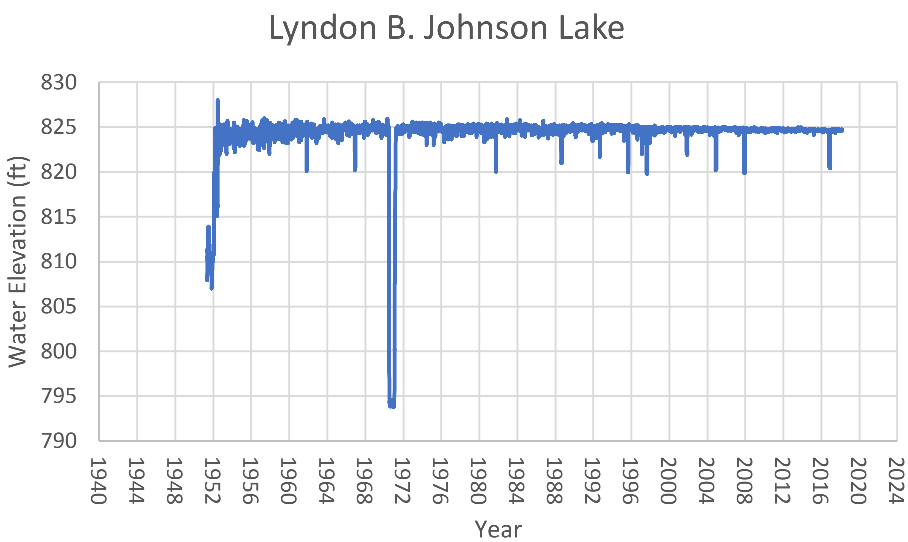

Figure 4.4.5 Continued.

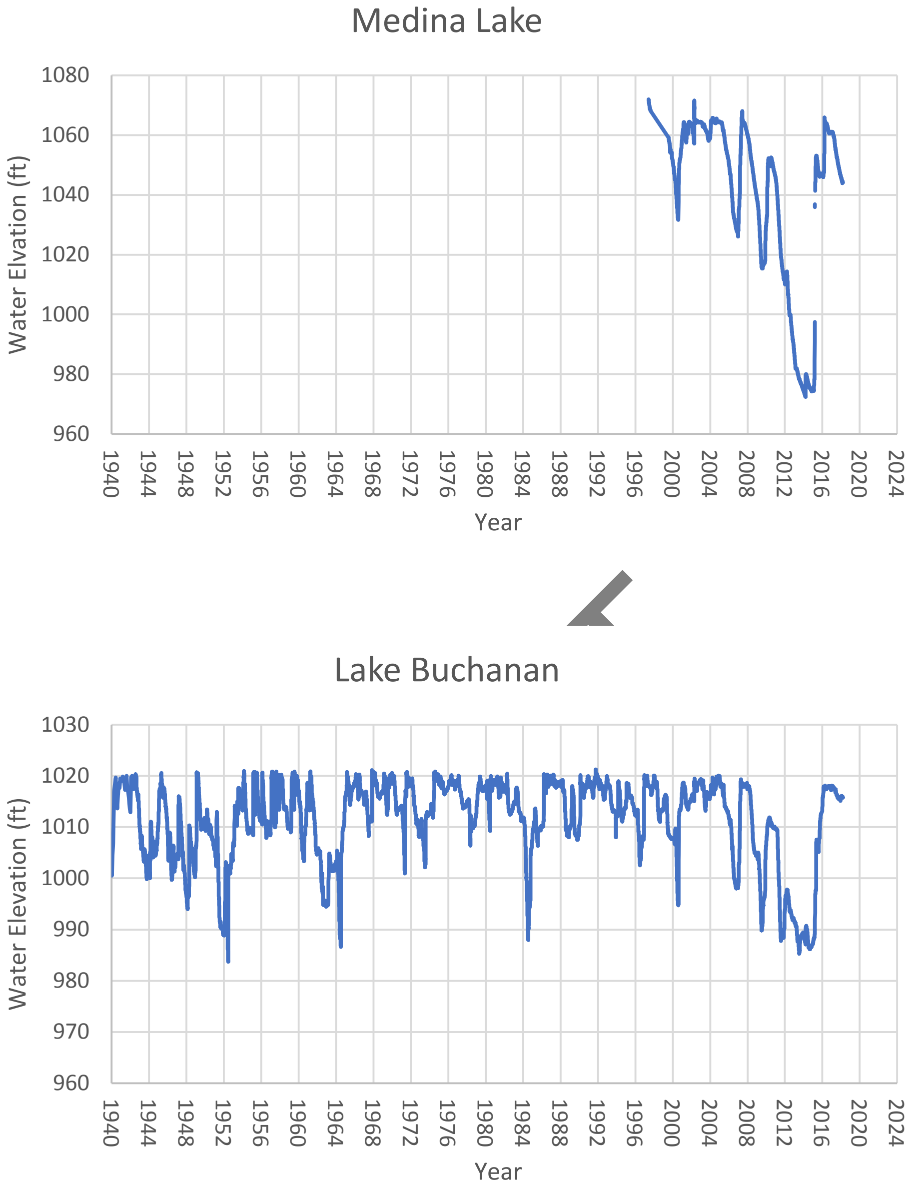

Figure 4.4.5 **Continued.**

4.5 Hydraulic Properties

Hydraulic properties, which describe the ability of an aquifer to transmit and store groundwater, can vary greatly depending on the individual characteristics of an aquifer. Several hydraulic properties are used to describe groundwater flow in aquifers. The properties discussed here are hydraulic conductivity, transmissivity, specific capacity, storativity, specific storage and specific yield. Each of these terms is briefly described below.

Hydraulic Conductivity – The measure of the ease with which groundwater can flow through an aquifer. Higher hydraulic conductivity indicates that the aquifer will allow more water movement under the same hydraulic gradient. Units for hydraulic conductivity may be expressed in ft/day or gpd per square foot.

Transmissivity – This term is closely related to hydraulic conductivity and refers to the product of the hydraulic conductivity times the effective aquifer thickness. Transmissivity describes the ability of groundwater to flow through the entire thickness of an aquifer. As the thickness of the aquifer increases, the transmissivity increases for a given hydraulic conductivity. Units for transmissivity may be expressed in ft^2/day or gpd/ft.

Specific Capacity – The rate of water that can be produced from a well per unit length of drawdown. This parameter depends on both the efficiency of a well and the productivity of the aquifer. Specific capacity is expressed in terms of gallons per minute per foot (gpm/ft) of drawdown in the well.

Storativity – The volume of water that an aquifer releases from storage under a unit decline in hydraulic head. For a confined aquifer, the storativity is equal to the product of specific storage and aquifer thickness. In an unconfined aquifer, the aquifer storativity is equal to the sum of the specific yield and the product of specific storage and aquifer thickness. Storativity can be expressed as a dimensionless parameter, or storage coefficient.

Specific Yield – The measure of the amount of water that an unconfined aquifer releases from storage per unit surface area of aquifer per unit decline in water table due to the drainage of the pore spaces in the aquifer by gravity. Specific yield is a dimensionless parameter.

Specific Storage – The measure of the amount of water that a unit volume of a confined aquifer releases from storage per unit decline in head, due to changes in the density of the water from reduced hydraulic pressure and to changes in the arrangement and bulk density of the aquifer matrix. Specific storage can be influenced by lithology and depth of burial. Specific storage can be expressed per foot, or units of ft^{-1}.

The assignment of values for aquifer hydraulic properties is an important aspect in numerical modeling because adjusting those values is typically an integral part of model calibration. Values for the hydraulic properties of the HCT Aquifer were obtained from the literature and estimated from observed data. The following subsections describe the data sources and summarize the data from those sources, the estimation of hydraulic conductivity from specific capacity measurements, the estimated spatial distribution of transmissivity and horizontal hydraulic conductivity, vertical hydraulic conductivity, and specific yield.

4.5.1 Data Sources for Transmissivity and Specific Capacity Measurements

Multiple sources were queried for transmissivity and specific capacity measurement data for the Trinity hydrostratigraphic units in the current study area. The compiled point measurements were assigned to the current report's hydrostratigraphic units based on their well depth and screen information, where available. Well assignments were made according to the methodology described in Section 4.2. Data sources for point measurements of transmissivity and specific capacity measurements included:

- TWDB compilations of pumping test analyses based on data in the TWDB database (Myers, 1969; Christian and Wuerch, 2012)
- A compilation of pumping tests from county groundwater availability studies (Daniel B. Stephens and Associates, 2006)
- Pumping test data received from GCDs in the study area, including individual records and a compilation of aquifer tests from Barton Springs Edwards Aquifer Conservation District (Hunt et al., 2010)
- The Edwards-Trinity Plateau GAM (Anaya and Jones, 2009) database, which includes aquifer test data from the TWDB groundwater database and the Texas Commission on Environmental Quality (TCEQ) database.
- Drawdown, yield, and duration data for specific capacity tests from the TWDB groundwater database remarks table (TWDB, 2017b) and the TWDB submitted drillers' report database (2017d) and the TWDB BRACS database (TWDB, 2017a).

Two TWDB publications that compiled and analyzed aquifer test data in Texas (Myers, 1969; Christian and Wuerch, 2012) were queried. The Myers (1969) dataset includes 22 tests and the Christian and Wuerch (2012) dataset includes 30 tests for wells within the study area. These wells were assigned to the current report's hydrostratigraphic units based on their well depth and screen information.

Daniel B. Stephens and Associates (2006) compiled subdivision pumping tests conducted in 12 counties, most of which fall wholly or partially within the current study area. This dataset includes 72 aquifer tests, mostly from counties that require Groundwater Availability Studies (GwAS) as part of the subdivision platting process. Of these, about sixty aquifer tests fell within the study area and could be assigned to hydrostratigraphic units based on their well depth and screen information. An additional three aquifer tests fall within the study area but do not have location information and so could not be assigned to the current report's hydrostratigraphic units.

The Edwards-Trinity Plateau Aquifer GAM (Anaya and Jones, 2009) database includes 7 TWDB pumping tests that fall within the current study area. Of these, four wells overlap with the Christian and Wuerch (2012) dataset. The database also includes about 400 hydraulic conductivity values derived from specific capacity test data that fall within the current study area. These specific capacity values were not considered as a separate dataset, as they overlapped with the specific capacity dataset created for the current study using the TWDB groundwater database remarks table (TWDB, 2017b)(see below).

The Edwards-Trinity Plateau Aquifer GAM (Anaya and Jones, 2009) database also includes an additional 700 hydraulic conductivity values calculated from specific capacity data in Texas Commission on Environmental Quality well records. These values are shown in Figure 4.5.1 by

Texas Commission on Environmental Quality grid-block**.** Note that, if more than one well is present in a grid-block, the value represents the geometric mean of those wells. The figure only shows values for wells assigned to the Trinity model layer in the Edwards-Trinity Plateau Aquifer GAM. These hydraulic conductivity values could not otherwise be used directly in the current analysis as they do not include the aquifer in which the wells are completed and locations are identified only at the Texas Commission on Environmental Quality grid-block level, which is a 2.5-minute by 2.5-minute area. Therefore, the locations of these wells were considered too uncertain to re-assign them to the current project's hydrostratigraphic units.

Barton Springs Edwards Aquifer Conservation District compiled aquifer test data in Hays and Trinity counties (Hunt et al., 2010). This dataset includes about 96 tests compiled from County Water Availability Studies, district hydrogeologic reports and the TWDB groundwater well database. About 23 of these tests appear to be duplicates of the Daniel B. Stephens and Associates (2006) dataset. Several recent documents for individual aquifer tests were also provided by Barton Springs Edwards Aquifer Conservation District and Blanco-Pedernales GCD. This yielded about 25 additional data values.

The TWDB groundwater database (TWDB, 2017b), the TWDB submitted drillers' report database (TWDB,2017d) and the TWDB BRACS database (TWDB, 2017a) were queried for drawdown, yield, and duration data for specific capacity tests. Wells were not included if test data was missing, drawdown was zero, or if the well was bailed. This yielded over 3,000 total specific capacity data values in the current study area.

4.5.2 Literature Sources for Transmissivity and Hydraulic Conductivity Values

In addition to sources of hydraulic property measurements, other literature sources were also reviewed, including previous groundwater models. These did not yield additional data values but were useful for determining reasonable hydraulic property ranges for the current study. Barker and Ardis (1996) provide insight into hydraulic property trends in the study area. They note that hydraulic conductivity changes spatially within each Trinity hydrostratigraphic unit. In general, they note that downgradient subcrops become less permeable due to stable mineral evolution, whereas upgradient outcrops become more permeable due to evaporite leaching and unstable carbonate constituents. Examples of these permeable features include cavernous areas and sinkholes in the Glen Rose Limestone outcrop and shallow subcrop (particularly in northern Bexar and southwestern Comal counties), highly permeable quartzose clastic facies in the updip portion of the Hensell Sand and dissolution pores in the Cow Creek Limestone outcrop areas (Barker and Ardis, 1996).

A groundwater model in North Medina County (Young et al., 2005) produced a calibrated hydraulic conductivity value of 0.5 ft/day for the Upper Trinity hydrostratigraphic unit and a hydraulic conductivity distribution that averaged 1.6 ft/day for the Middle Trinity hydrostratigraphic unit. The Edwards-Trinity Plateau GAM (Anaya and Jones, 2009) used an initial hydraulic conductivity value of 2.5 ft/day in the southern part of the Trinity model layer that overlaps the current study area. A re-calibration of this GAM (Young et al., 2010) produced calibrated hydraulic conductivities of 2.1 ft/day in the southern part of the Trinity model layer that overlaps the current study area. A groundwater availability model of the Lower Trinity Aquifer in Bandera County (LBG-Guyton Associates, 2008) produced a calibrated hydraulic conductivity range of 15 ft/day in the Lower Trinity hydrostratigraphic unit in the Kerrville area, 0.16 ft/day near the City of Bandera and 0.1 ft/day in the area between them. The previous HCT

GAM (Jones et al., 2011) produced calibrated hydraulic conductivity values that averaged 10.4 ft/day for the Upper Trinity hydrostratigraphic unit, 8.8 ft/day for the Middle Trinity hydrostratigraphic unit, and 4.4 ft/day for the Lower Trinity hydrostratigraphic unit.

4.5.3 Analysis of Transmissivity Data

Hydraulic property data values were only considered in the current analysis if there was sufficient information for them to be assigned to the current study's hydrostratigraphic units. Well assignments were made according to the methodology described in Section 4.2 and were only used for the current analysis if they were fully completed in only one hydrostratigraphic unit. Table 4.5.1 summarizes the hydraulic property data available for each hydrostratigraphic unit. As illustrated by the table, while hydraulic conductivity and transmissivity data are scarce, specific capacity data are abundant. The spatial distribution of available transmissivity measurements from long-term pumping tests is shown in Figure 4.5.2 by hydrostratigraphic unit. Many of these fall in Hays County, which is fast-growing and requires water availability studies for new subdivisions. While most of the counties in the eastern portion of the study area have at least a few pumping tests for the Trinity hydrostratigraphic units, the western portion of the study area has only one test in Kimble County.

The spatial distribution of available specific capacity estimates is shown in Figure 4.5.3 by hydrostratigraphic unit. The majority of the available specific capacity data are for the Middle Trinity hydrostratigraphic unit in the central portion of the aquifer in Kerr, Kendall, Comal, Hays, Travis, eastern Bandera counties and the northern portion of Uvalde, Medina and Bexar counties. Upper Trinity specific capacity values are less common in the central portion of the study area, although there is a cluster near the Edwards Balcones Fault Zone in Comal County. Most of the specific capacity data available in the Edwards-Trinity Plateau region, including western Kerr County and Real, Edwards, and Val Verde counties, are in the Upper Trinity hydrostratigraphic unit. Lower Trinity specific capacity values are mostly located in the central portion of the study area, with most clustered near the Balcones Fault Zone, especially in Comal County.

4.5.4 Calculation of Transmissivity from Specific Capacity

Field-scale hydraulic conductivity can be estimated from various types of aquifer performance tests, including slug tests (local near-well estimate), specific capacity tests (relatively near-well estimate), and multi-hour to multi-day aquifer pumping tests (integrated estimate over radius of influence, the size of which depends on the duration of the test). The results from aquifer pumping tests are most appropriate for estimating hydraulic conductivity for use in regional groundwater models as they stress a larger area of the aquifer than do slug and specific capacity tests. In addition, results from specific capacity tests are dependent on the efficiency of the well as well as properties of the aquifer, making them less useful than pumping tests for parameterization of regional-scale groundwater models. However, specific capacity is relatively easy to measure, requiring only the pumping rate and drawdown, and is commonly reported for wells. Aquifer pumping tests, on the other hand, are much more time consuming and expensive to conduct and interpret than are specific capacity tests.

Because high-quality data from multi-day aquifer pumping tests are scarce for the HCT Aquifer, but a large volume of specific capacity data are available, a methodology was developed to estimate transmissivity from the specific capacity data. An aquifer-specific relationship between transmissivity and specific capacity can be developed using both types of data from a single well. Using paired transmissivity/specific capacity measurements, Mace (2001) developed empirical relationships for the Glen Rose and Cow Creek formations (representing fractured carbonate) and for the Hensell and Hosston formations (representing sandstone). Figure 4.5.4**,** Figure 4.5.5, and Figure 4.5.6 show the transmissivity/specific capacity pairs available for the Upper Trinity, Middle Trinity and Lower Trinity hydrostratigraphic units, respectively, compared to the Mace (2001) empirical relationships for the Glen Rose/Cow Creek and the Hensell/Hosston formations. Due to the limited sample size, it is not clear which of the Mace (2001) empirical relationships provides the best fit to the transmissivity/specific capacity pairs.

Because the comparison of the data for each hydrostratigraphic unit to existing empirical relationships for other aquifers did not provide a definitive match, the analytical approach presented in Mace (2001) was used to estimate transmissivity from the available specific capacity for the aquifer. According to Mace (2001), the preferred analytical approach for establishing a relationship between specific capacity and transmissivity is based on the Theis non-equilibrium equation (Theis et al., 1963):

$$S_c = \frac{4\pi T}{\left[ln\left(\frac{2.25Tt}{r^2 S}\right)\right]} \qquad (4.5.1)$$

where:

S_c = specific capacity,
T = aquifer transmissivity,
t = pumping time,
r = well radius, and
S = aquifer storativity.

Equation 4.5.1 cannot be solved directly for transmissivity, so it was solved iteratively using Microsoft Excel. For wells with no reported well radius, an assumed well radius was used. This value was calculated from the wells with a reported well radius and was about 2.5 inches for the Upper Trinity hydrostratigraphic unit and 3 inches for the Middle and Lower Trinity hydrostratigraphic units. As suggested by Mace (2001), data for wells with no recorded pumping duration and wells where the type of specific capacity test was recorded as “bailed” were not used. Aquifer storativity for the calculation was assumed to be 1.2 x 10^{-5} for the Upper Trinity, 2.0 x 10^{-4} for the Middle Trinity, and 1.3 x10^{-4} for the Lower Trinity hydrostratigraphic unit based on literature values (Section 4.5.7).

If only a small portion of the aquifer thickness is screened, the resulting transmissivity value calculated from Equation 4.5.1 will not be representative of the entire aquifer thickness (Mace, 2001). This “partial penetration” can be addressed through mathematical methods that correct for the short screen or by only considering wells that are screened over a large percentage of the aquifer thickness. However, implementing these methods require that both the screen length and the aquifer thickness at wells be known. Unfortunately, many wells in this specific capacity dataset lack screen information. Rather than introduce more uncertainty by trying to correct for an uncertain value, no additional mathematical corrections were added to account for partially penetrating wells. There was also no attempt to filter the well dataset using a ratio of screen length to aquifer thickness, again due to the lack of screen information.

The calculated transmissivity values for the entire specific capacity dataset are shown in Figure 4.5.4, Figure 4.5.5, and Figure 4.5.6. In the figures, the transmissivity values calculated for wells with a reported well radius are plotted separately from the values calculated for wells with an assumed well radius. As shown, the transmissivity values calculated for all Trinity hydrostratigraphic units from specific capacity using Equation 4.5.1 are consistent with the Mace (2001) empirical relationship developed for the Hensell and Hosston formations. For this reason, the transmissivity values used in the current analysis were calculated directly from this relationship, rather than from the Theis analysis. This simplifies the calculation and eliminates the need to assume values for well radius and storativity.

Because of the many assumptions and simplifications involved in calculating transmissivity from specific capacity, the calculated transmissivity values are considered more uncertain than values determined from aquifer pumping tests. However, the available data from aquifer pumping tests are insufficient to develop a distribution of transmissivity across most of the study area. Therefore, using the specific capacity data greatly improves coverage and is useful for providing a general idea of relative transmissivity values in the aquifer.

For the purposes of this analysis, the few wells with calculated transmissivity values of greater than 15,000 ft^2/day and/or with reported yields greater than 500 gpm were not considered representative of Trinity hydrostratigraphic units. In the Upper Trinity, transmissivities with greater than 1,000 ft^2/day were also discarded, as they appear anomalous when compared to other nearby Upper Trinity wells. These anomalies could potentially be due to partial screens in other units, particularly the Edwards hydrostratigraphic unit, and so are considered unreliable.

4.5.5 Spatial Distribution of Transmissivity and Horizontal Hydraulic Conductivity

The transmissivity values calculated from specific capacity data using the Mace (2001) empirical relationship and the aquifer pumping test transmissivity values compiled from the literature are shown in Figure 4.5.7, Figure 4.5.8, and Figure 4.5.9 for the Upper Trinity, Middle Trinity, and Lower Trinity hydrostratigraphic units, respectively. In general, the highest transmissivities in the Upper Trinity hydrostratigraphic unit occur in the western portion of the study area in Edwards, Real and Val Verde counties. The highest transmissivities in the Middle Trinity hydrostratigraphic unit occur in the central portion of the study area, generally clustered around outcrop areas in Hays, Comal, Kendall, Bandera, and Gillespie counties. The highest transmissivities in the Lower Trinity hydrostratigraphic unit occur in Kerr and Bandera counties and along the Comal/Hays county boundary. High values also occur in central Comal and northern Medina counties, but as these are surrounded by values of much lower transmissivity, these may be anomalies and not be representative of actual conditions.

In a confined aquifer, hydraulic conductivity can be calculated as the transmissivity divided by the aquifer thickness. Using the aquifer thickness based on the structural surfaces developed for this project and the transmissivity values shown in Figure 4.5.7, Figure 4.5.8, and Figure 4.5.9, estimated hydraulic conductivities for the aquifer were generated. Note that this calculation assumes that wells are screened over the entire aquifer thickness. The resultant distribution of estimated horizontal hydraulic conductivity for the Upper Trinity, Middle Trinity, and Lower Trinity are shown in Figure 4.5.10, Figure 4.5.11, and Figure 4.5.12, respectively. In general, the spatial distribution of hydraulic conductivity is consistent with the spatial distribution of transmissivity discussed earlier. Note that neither the transmissivity nor hydraulic conductivity values were interpolated. This was to prevent emphasizing potentially misleading anomalies caused by high variability in densely spaced point values. Values derived from the range and statistical distribution of the point values are more likely to be representative of actual regional aquifer properties.

Representative values for transmissivity and hydraulic conductivity derived from the point values are presented in Table 4.5.2 and Table 4.5.3. The median transmissivity value for the Upper Trinity hydrostratigraphic unit is 28 ft^2/day and the median hydraulic conductivity is 0.07 ft/day. A histogram of the horizontal hydraulic conductivity estimates for the Upper Trinity hydrostratigraphic unit is shown in Figure 4.5.13a. The median transmissivity value for the Middle Trinity hydrostratigraphic unit is 73 ft^2/day and the median hydraulic conductivity is 0.2 ft/day. A histogram of the horizontal hydraulic conductivity estimates for the Middle Trinity hydrostratigraphic unit is shown in Figure 4.5.13b. The median transmissivity value for the Lower Trinity hydrostratigraphic unit is 57 ft^2/day and the median hydraulic conductivity is 0.2 ft/day. A histogram of the horizontal hydraulic conductivity estimates for the Lower Trinity hydrostratigraphic unit is shown in Figure 4.5.13c.

4.5.6 Vertical Hydraulic Conductivity

At very small scales, the vertical and horizontal hydraulic conductivity of an aquifer may differ by very little. However, on a regional scale, the differences between the vertical and horizontal hydraulic conductivities can be very large. In areas where the aquifer is thought to be largely structurally intact, the vertical hydraulic conductivity is limited by the hydraulic conductivity of lower permeability units. For instance, a continuous low permeability clay layer in the middle of a sandy aquifer could greatly impede vertical flow in what would otherwise be a high permeability system. This could create a difference of several orders of magnitude between vertical and horizontal hydraulic conductivity.

Within the Trinity Aquifer as a whole, this vertical anisotropy is evident in observed groundwater behavior. As discussed in Barker and Ardis (1996), the tight low-permeability interbeds in the upper and middle parts of the Trinity Aquifer severely restrict vertical flow so that groundwater moves laterally along impermeable bedding (often discharging from seeps and springs) rather than percolating into lower portions of the aquifer. One study in North Bexar County estimated that the vertical hydraulic conductivity of these confining units of the Trinity Aquifer, including the Hammett Shale, Bexar Shale, and the clays and marls of upper member of the Glen Rose Limestone, was only around 0.0001 to 0.003 ft/day (W.E. Simpson Company and William F. Guyton Associates, 1993). This effectively separates the permeable units of Trinity Aquifer into distinct hydrostratigraphic units with low interformational leakage. Anaya and Jones (2009) also considered the effect of this stratification on groundwater flow in the HCT region compared to other portions of the Edwards-Trinity Plateau Aquifer. They note that the shale, sand, and limestone transgressive-regressive sequence represented by the Upper, Middle and Lower Trinity sediments introduces significant vertical anisotropy compared to the thinner, but more homogenous Trinity Sands in the northwest portion of the Edwards-Trinity Plateau Aquifer (Anaya and Jones, 2009).

Because vertical groundwater flow in the Trinity Aquifer and Edwards-Trinity Plateau Aquifer is dominated by the presence of underlying or overlying low-permeability units, there is little discussion in the literature about vertical anisotropy within individual hydrostratigraphic units themselves. The exception is the Upper Trinity hydrostratigraphic unit which contains the low-permeability clays and marls of upper member of the Glen Rose Limestone discussed in the

North Bexar County report mentioned above (W.E. Simpson Company and William F. Guyton Associates, 1993). Kuniansky and Ardis (2004) noted that water in flat-lying sedimentary aquifers, such as "the cyclic depositional environments of the Edwards–Trinity aquifer," generally flows more readily horizontally than vertically and cited observed horizontal plant growth along hillsides as evidence. Jones et al. (2011) make a similar assumption that "vertical hydraulic conductivities are likely to be much lower than horizontal hydraulic conductivities" and assumes starting anisotropy ratios of 1:10 (that is, vertical hydraulic conductivity values are one-tenth the value of horizontal hydraulic conductivity values).

4.5.7 Storage Properties

The most representative storage properties are determined through analysis of observation well data from aquifer pumping tests. The compilation of transmissivity measurements (Section 4.5.1) yielded several pumping test records that also contained calculated storativity values. The distribution of available storativity data is shown in Figure 4.5.14. Representative values from these tests are shown in Table 4.5.4. The median storativity value from the compiled point measurements is $2x10^{-4}$ for the Middle Trinity hydrostratigraphic unit and $8x10^{-5}$ for the Lower Trinity hydrostratigraphic unit. There were no values available for the Upper Trinity hydrostratigraphic unit. These calculated values are very sparse, as many aquifer test reports include estimated values or literature values rather than calculated values from pumping test data (Hunt et al., 2010). For this reason, additional literature sources and calibrated groundwater models were also queried for estimates of storage properties.

<u>Literature Sources for Unconfined Specific Yield Values</u>

The groundwater availability model for the Edwards-Trinity High Plains Aquifer (Anaya and Jones, 2009) included a Trinity model layer that could be considered equivalent to a combination of the Upper, Middle, and Lower Trinity hydrostratigraphic units discussed in the current report. Calibrated specific yield values in that model were 0.03 for the area roughly corresponding to the HCT Aquifer outcrop. For the rest of the study area, calibrated specific yield ranged from 0.0003 to 0.003. A re-calibration of this GAM (Young et al., 2010) produced calibrated specific yield values in the Trinity Aquifer that ranged from 0.05 to 0.1, with a median value of 0.08. The groundwater availability model for the HCT Aquifer (Jones et al., 2011) produced calibrated specific yield values of 0.0005 for the Upper Trinity Aquifer, 0.0008 for the Middle Trinity Aquifer, and 0.0008 for the Lower Trinity Aquifer.

<u>Literature Sources for Confined Storativity Values</u>

Walker (1979) compiled hydraulic parameters from aquifer tests in the "Lower Cretaceous Aquifer" in the Edwards-Trinity Plateau Aquifer region. The compilation includes a Hensell (Middle Trinity hydrostratigraphic unit) aquifer test in Gillespie County with a storage coefficient of $7x10^{-5}$ and five Hosston and Sligo (Lower Trinity hydrostratigraphic unit) aquifer tests in Kerrville with storage coefficients ranging from $2\ x10^{-5}$ to $5\ x\ 10^{-5}$. These are presumably the same aquifer tests discussed in Ashworth (1983) which provides six storage coefficients from aquifer tests in the HCT Aquifer. The storage coefficients from four wells completed in Sligo and Hosston sediments (Lower Trinity hydrostratigraphic unit) ranged from $2\ x\ 10^{-5}$ to $5\ x\ 10^{-5}$. The storage coefficient for one well completed in the Hensell Sand (Middle Trinity hydrostratigraphic unit) was $7x10^{-5}$ and the storage coefficient for another well completed in

Cow Creek, Sligo and Hosston sediments (combination of Middle and Lower Trinity hydrostratigraphic units) was 7.4×10^{-4}.

The pumping test database associated with the groundwater availability model for the Edwards-Trinity High Plains Aquifer (Anaya and Jones, 2009) contained several pump test records with calculated storativity values. Eight of these wells were classified as Trinity wells and have a median storage coefficient of 3×10^{-4}. However, none of these wells fell in the current study area.

The Barton Springs Edwards Aquifer Conservation District compiled pumping tests conducted in Hays and Trinity counties (Hunt et al., 2010). Storativity values calculated from pumping tests in the Upper Trinity Aquifer ranged from 1×10^{-5} to 1.3×10^{-5} with a median value of 1.2×10^{-5}. Storativity values calculated from pumping tests in the Middle Trinity Aquifer ranged from 1.85×10^{-6} to 3.4×10^{-2} with a median value of 5×10^{-5}. Storativity values calculated from pumping tests in the Lower Trinity Aquifer ranged from 4×10^{-6} to 5×10^{-3} with a median value of 5×10^{-5}.

When calculated field storativity values are scarce, calibrated groundwater models can also provide additional data. In a groundwater model of the Edwards-Trinity Plateau, Edwards Balcones Fault Zone and Trinity aquifers (Kuniansky and Ardis, 2004), the storage coefficients for the Trinity Aquifer above the Hammett confining unit (Upper and Middle Trinity hydrostratigraphic units) range from 1×10^{-3} to 1×10^{-5}. The storage coefficient for the Trinity Aquifer below the Hammett confining unit (Lower Trinity hydrostratigraphic unit) was 1×10^{-5}. A groundwater availability model of the Lower Trinity Aquifer in Bandera County (LBG-Guyton Associates, 2008) produced a calibrated storativity range of 5×10^{-6} to 8×10^{-5} in the Lower Trinity hydrostratigraphic unit. The groundwater availability model for the Edwards-Trinity High Plains Aquifer (Anaya and Jones, 2009) included a Trinity model layer that could be considered equivalent to a combination of the Upper, Middle, and Lower Trinity hydrostratigraphic units discussed in the current report. Calibrated specific storage values in that model ranged from 10^{-5} ft^{-1} in an area roughly corresponding to the HCT Aquifer outcrop to 10^{-7} ft^{-1} in an area roughly corresponding to the HCT Aquifer subcrop under the Edwards Balcones Fault Zone. For the rest of the study area, calibrated specific storage in the Trinity Aquifer layer was 10^{-6} ft^{-1}. A re-calibration of that GAM (Young et al., 2010) produced calibrated specific storage values in the portion of the Trinity Aquifer roughly equivalent to the current study area that ranged from 2.9×10^{-6} to 9.7×10^{-6} ft^{-1} with a median value of 9.2×10^{-6} ft^{-1}. The groundwater availability model for the HCT Aquifer (Jones et al., 2011) produced calibrated specific storage values of 1.0×10^{-6} ft^{-1} for the Upper Trinity Aquifer, 1.0×10^{-7} ft^{-1} for the Middle Trinity Aquifer, and 1.0×10^{-7} ft^{-1} for the Lower Trinity Aquifer.

Table 4.5.1 Transmissivity values from compiled pump tests and calculated from specific capacity data

	Number of Data Values		
	Transmissivity (ft^2/day)	**Hydraulic Conductivity (ft/day)**	**Specific Capacity (gpm/ft)**
Upper Trinity	1	0	231
Middle Trinity	59	38	878
Lower Trinity	17	7	398
mixed Trinity	24	16	168
All Trinity	101	61	1675

Table 4.5.2 Transmissivity values from compiled pump tests and calculated from specific capacity data

Hydrostratigraphic unit	**Transmissivity values from Aquifer Pumping Tests (ft^2/day)**				**Transmissivity values calculated from Specific Capacity (ft^2/day)**				**All Transmissivity values from aquifer pumping tests and calculated from specific capacity (ft^2/day)**			
	Count	**25th Percentile**	**Median**	**75th Percentile**	**Count**	**25th Percentile**	**Median**	**75th Percentile**	**Count**	**25th Percentile**	**Median**	**75th Percentile**
Upper Trinity	1	--	199	--	217	7	28	70	218	8	28	70
Middle Trinity	58	41	159	521	821	26	70	185	879	28	73	200
Lower Trinity	17	142	214	317	385	35	54	127	402	35	57	147

Table 4.5.3 Hydraulic conductivity values from compiled pump tests and calculated from specific capacity data

Hydrostratigraphic unit	Hydraulic conductivity values calculated from Aquifer Pumping Tests(ft/day)				Hydraulic conductivity values calculated from Specific Capacity (ft/day)				All Hydraulic conductivity values calculated from aquifer pumping tests and specific capacity (ft/day)			
	Count	25th Percentile	Median	75th Percentile	Count	25th Percentile	Median	75th Percentile	Count	25th Percentile	Median	75th Percentile
Upper Trinity	1	--	0.4	--	217	0.02	0.07	0.2	218	0.02	0.07	0.2
Middle Trinity	58	0.1	0.5	2	821	0.05	0.2	0.5	879	0.06	0.2	0.6
Lower Trinity	17	0.2	0.5	0.8	385	0.1	0.1	0.4	402	0.1	0.2	0.4

Table 4.5.4 Storativity values available from compiled aquifer pump tests

Formation	Storativity	Storativity Value		
		Min	Median	Max
Upper Trinity	0	--	--	--
Middle Trinity	28	0.00001	0.0002	0.149
Lower Trinity	6	0.00001	0.00008	0.0045
mixed Trinity	13	0.00001	0.00009	0.0004
All Trinity	47	0.00001	0.0002	0.149

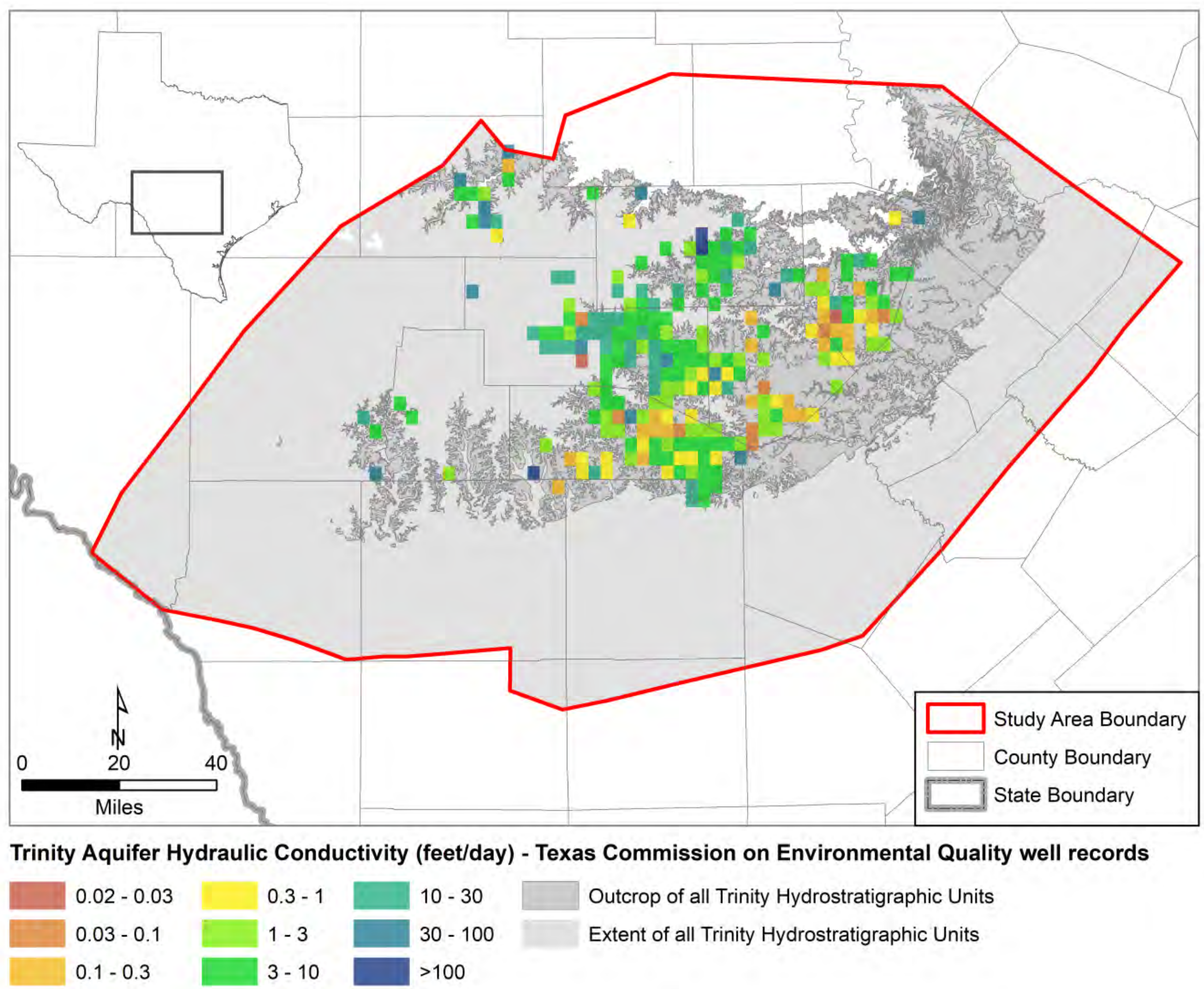

Figure 4.5.1 **Distribution of horizontal hydraulic conductivity calculated from Texas Commission on Environmental Quality well records, based on the Edwards-Trinity Plateau GAM database (Anaya and Jones, 2009).**

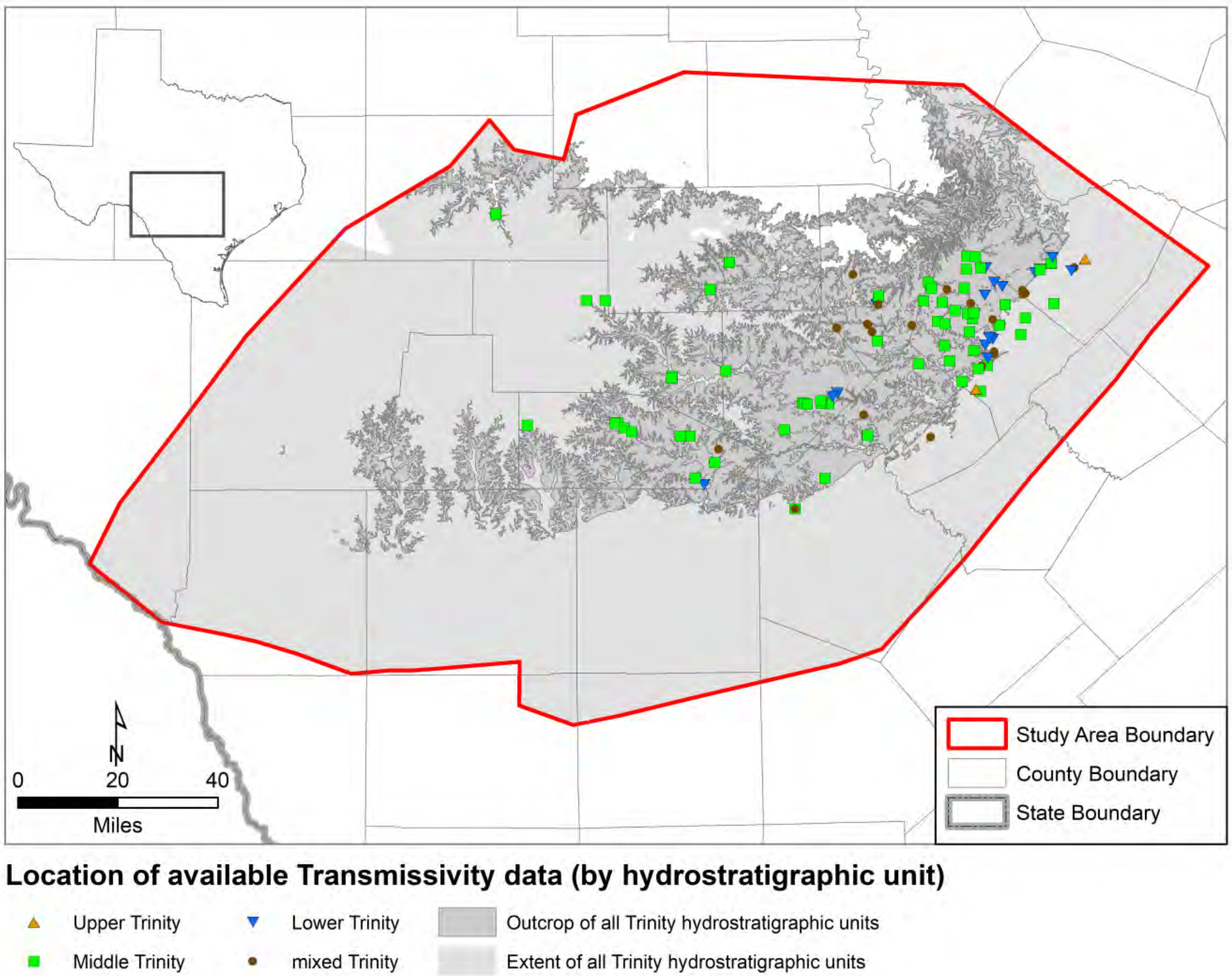

Figure 4.5.2 Location of available transmissivity data by hydrostratigraphic unit in the study area.

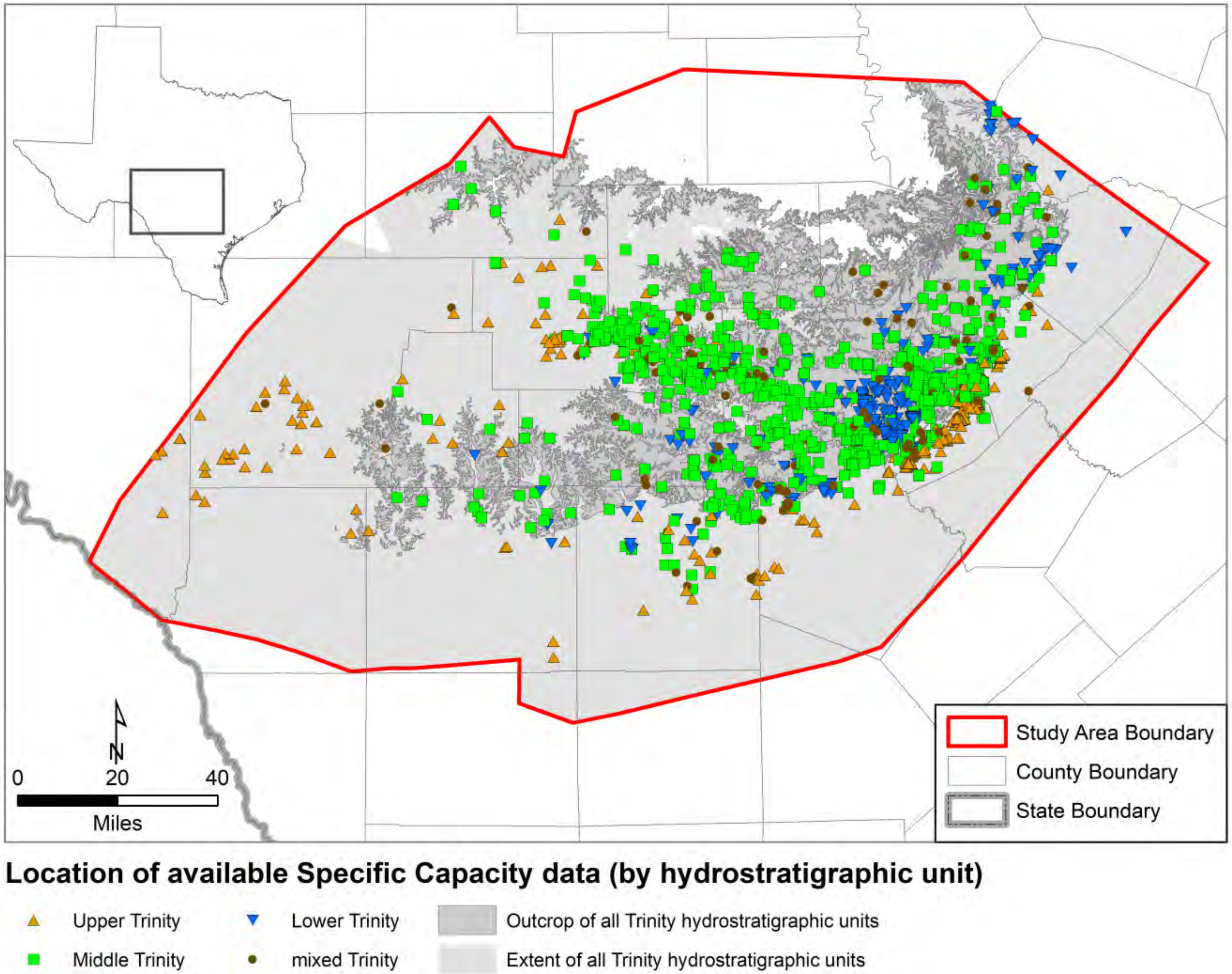

Figure 4.5.3 Location of available specific capacity data by hydrostratigraphic unit in the study area.

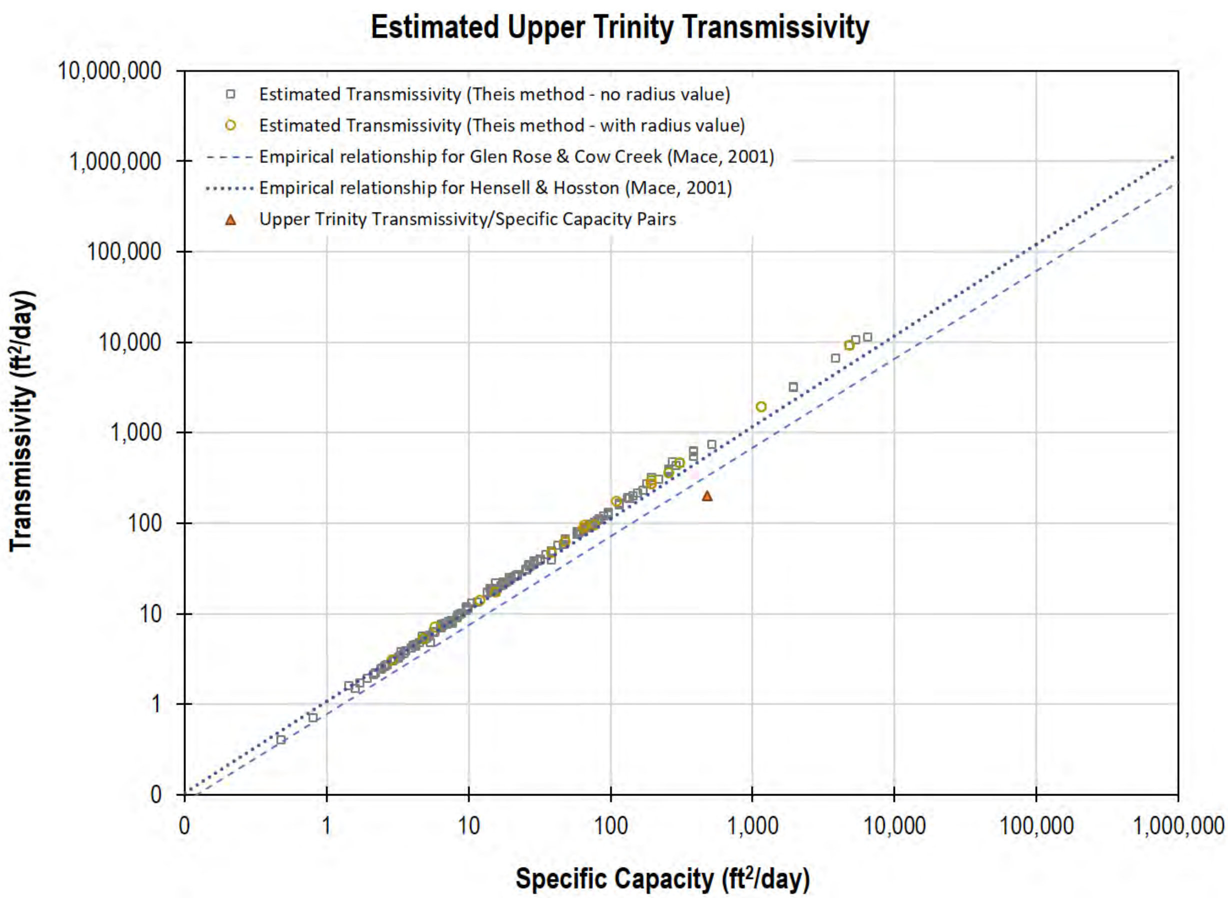

Figure 4.5.4 **Upper Trinity transmissivity – specific capacity measurement pairs compared to transmissivity values calculated by Mace (2001) methods (empirical relationship and Theis method).**

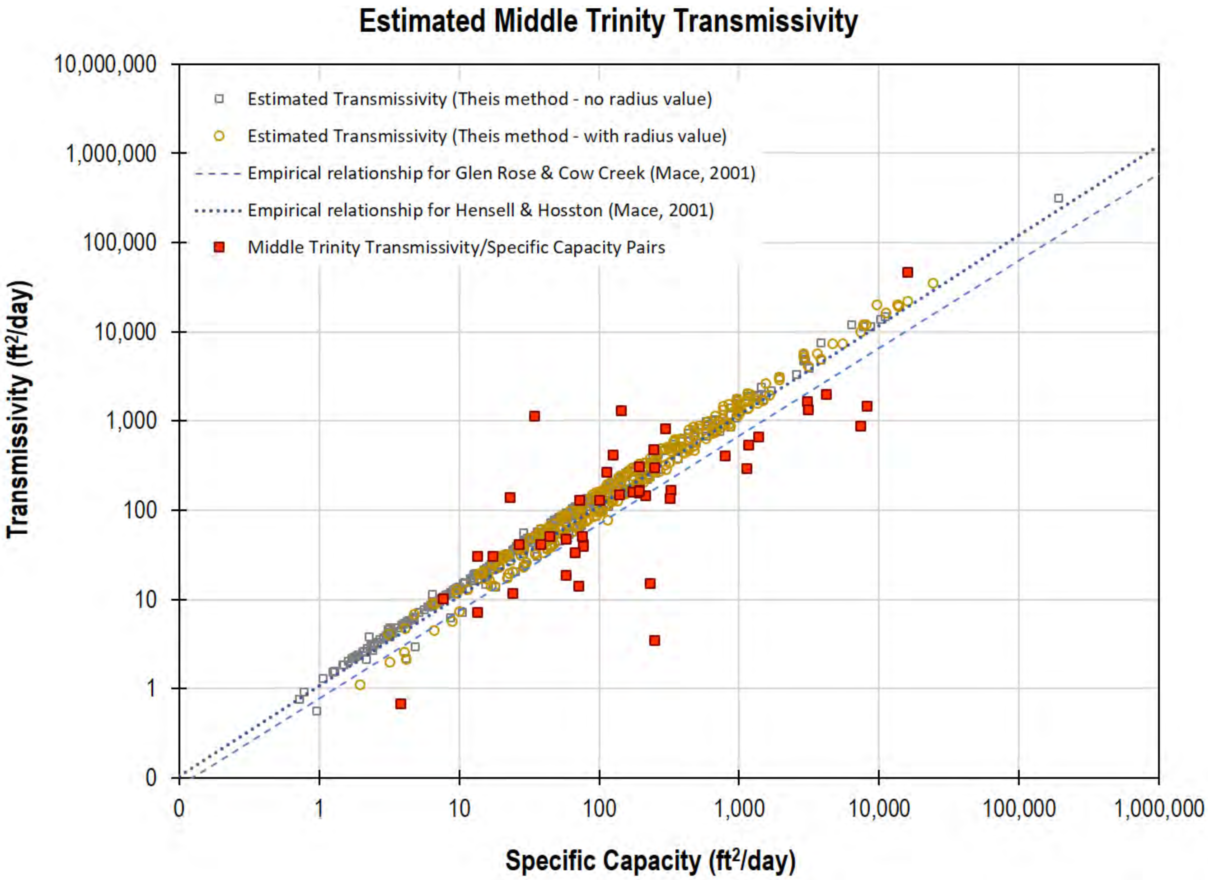

Figure 4.5.5 Middle Trinity transmissivity – specific capacity measurement pairs compared to transmissivity values calculated by Mace (2001) methods (empirical relationship and Theis method).

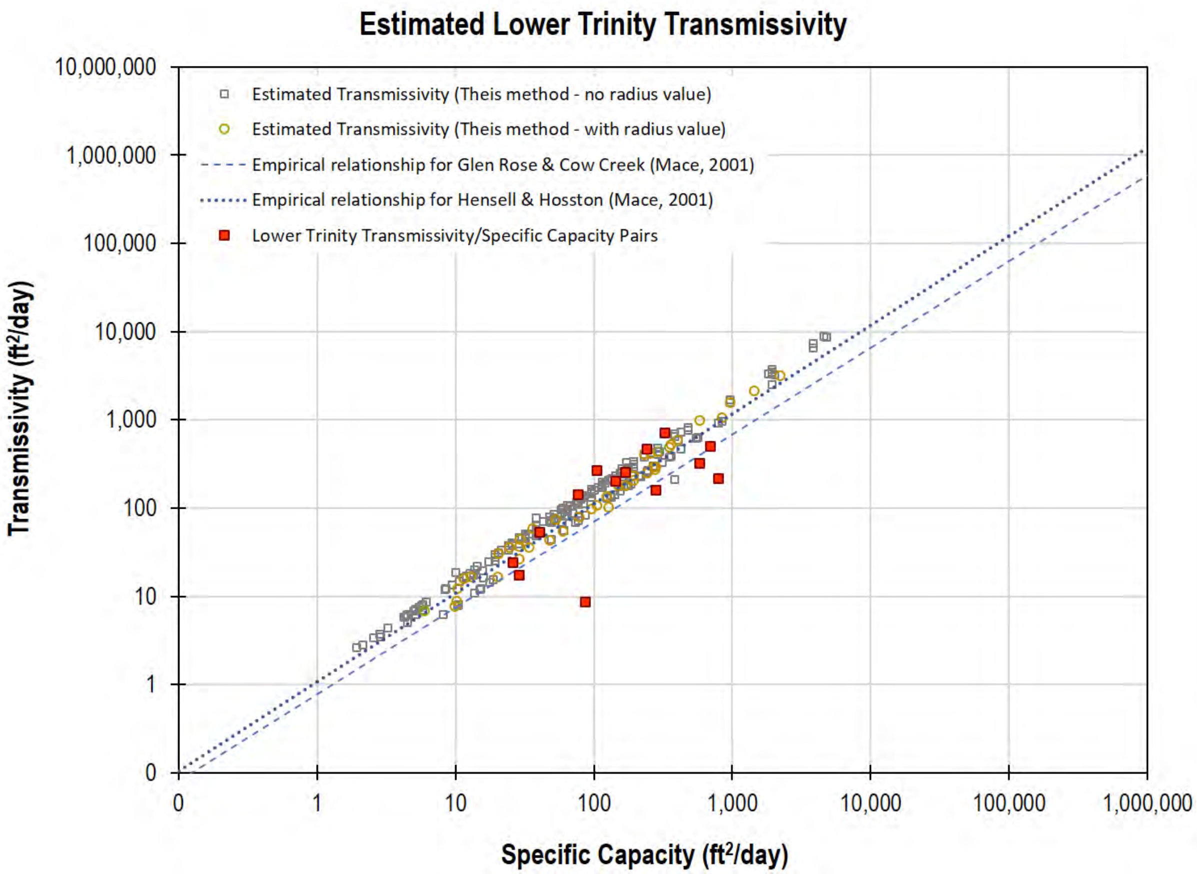

Figure 4.5.6 **Lower Trinity transmissivity – specific capacity measurement pairs compared to transmissivity values calculated by Mace (2001) methods (empirical relationship and Theis method)**

.

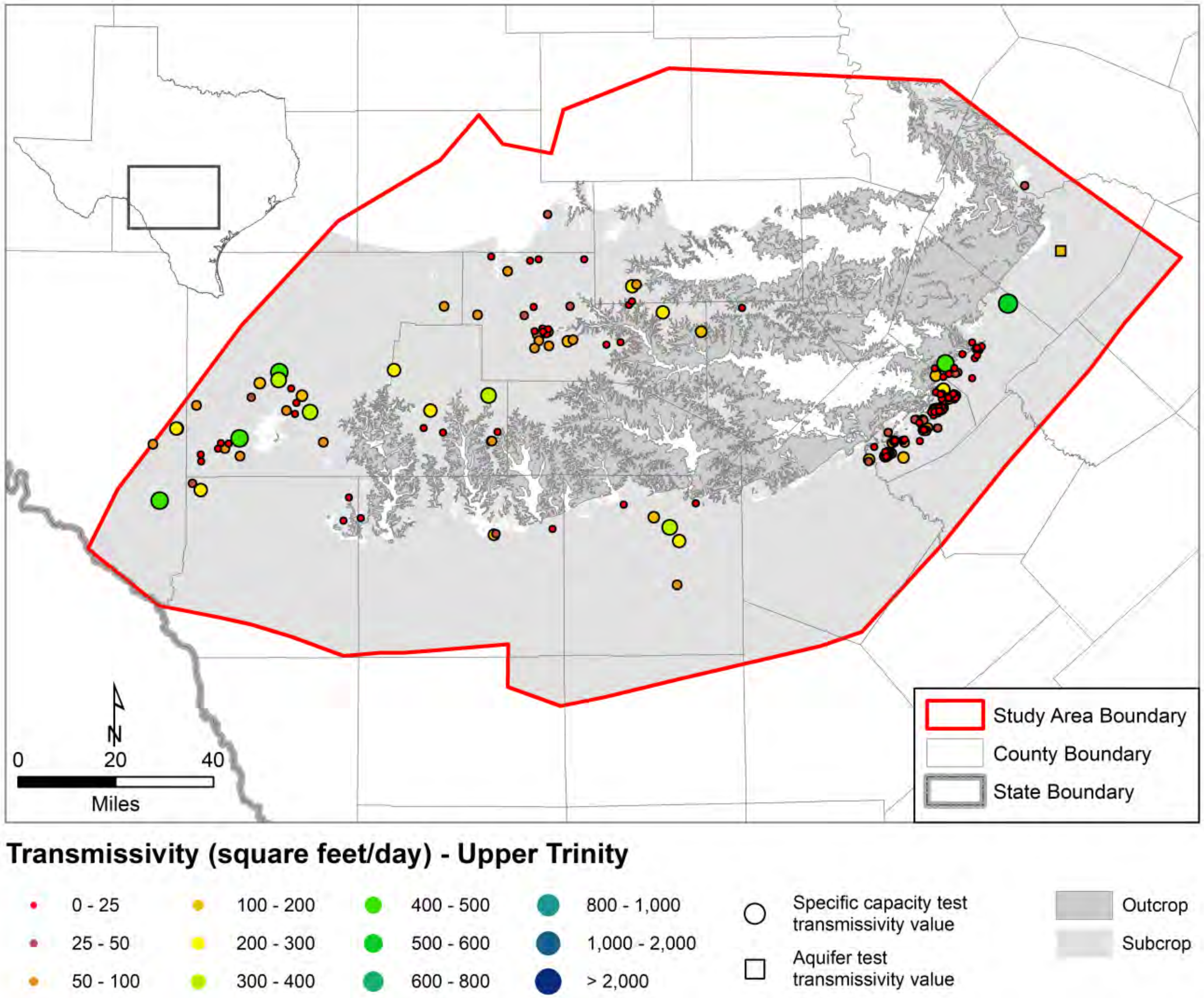

Figure 4.5.7 Spatial distribution of transmissivity values for the upper Trinity hydrostratigraphic unit.

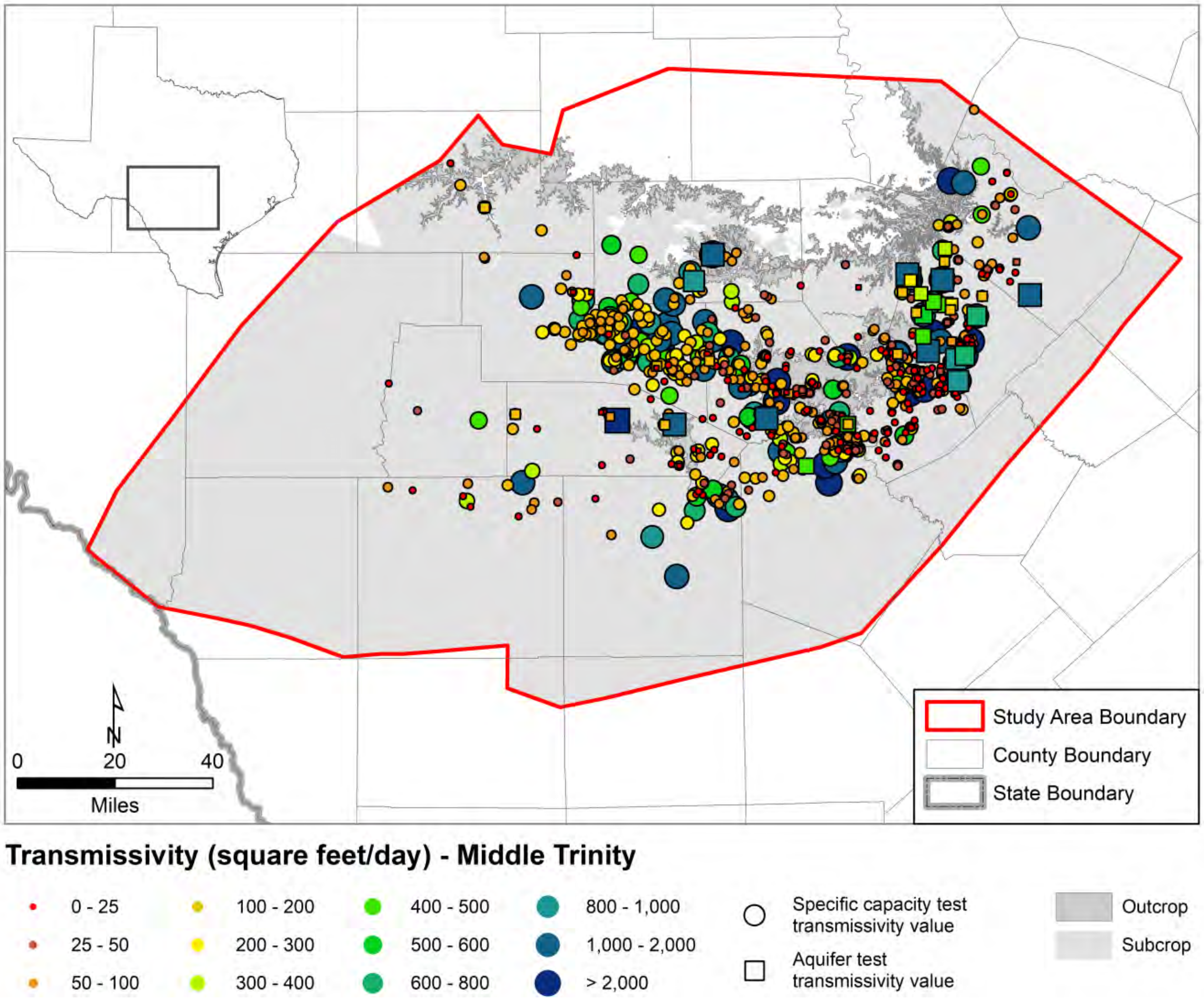

Figure 4.5.8 Spatial distribution of transmissivity values for the Middle Trinity hydrostratigraphic unit.

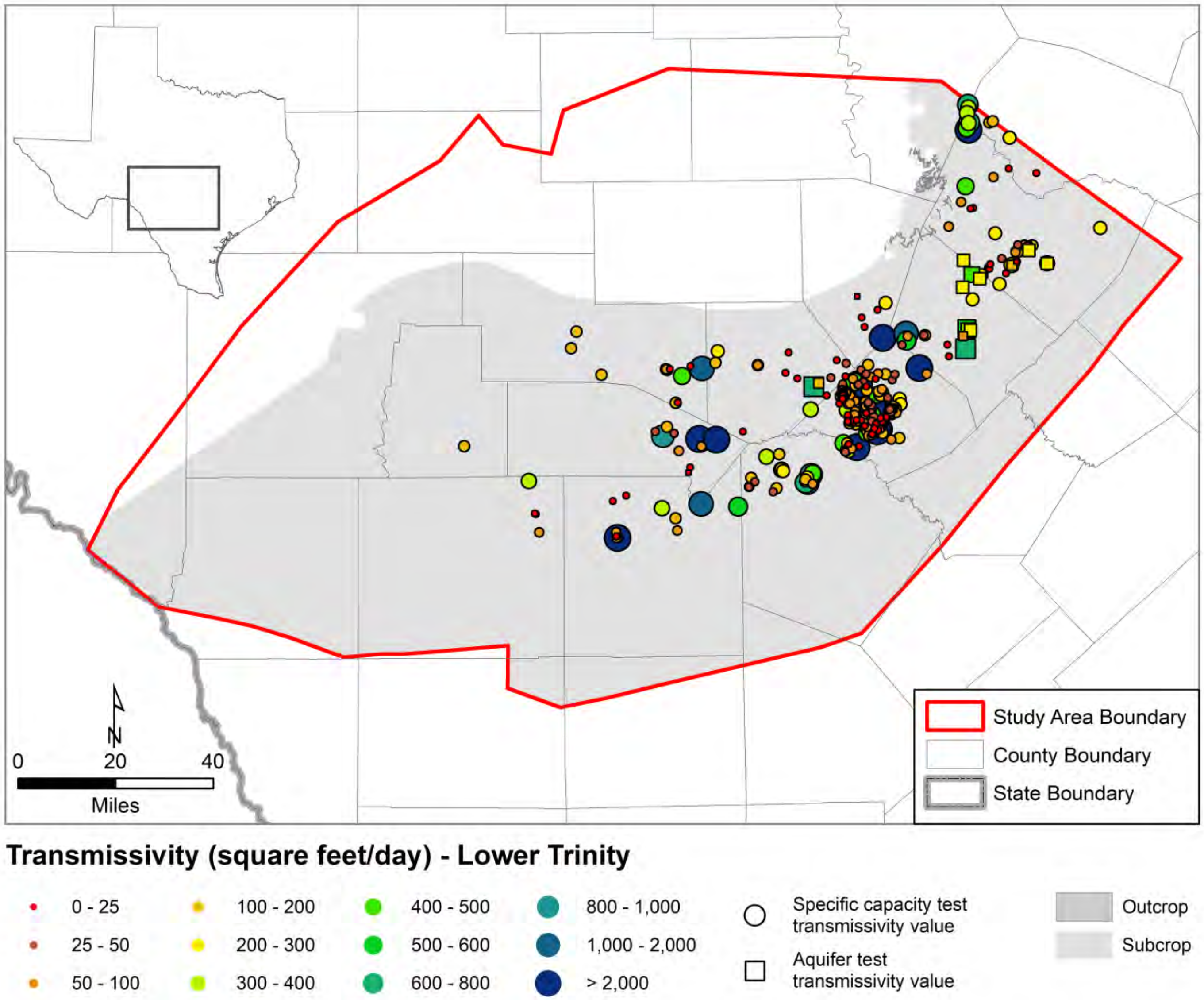

Figure 4.5.9 Spatial distribution of transmissivity values for the Lower Trinity hydrostratigraphic unit.

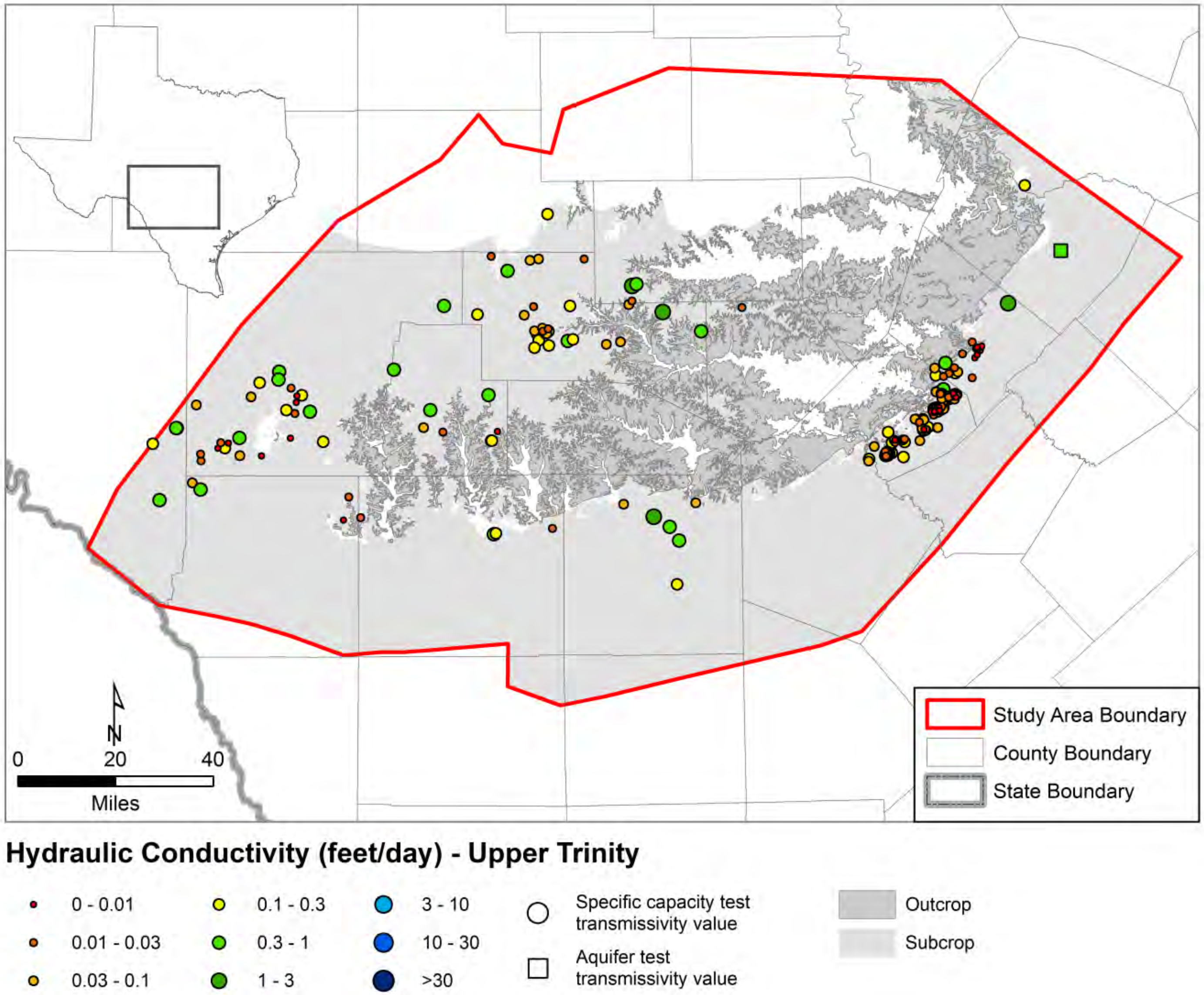

Figure 4.5.10 Spatial distribution of horizontal hydraulic conductivity values for the Upper Trinity hydrostratigraphic unit.

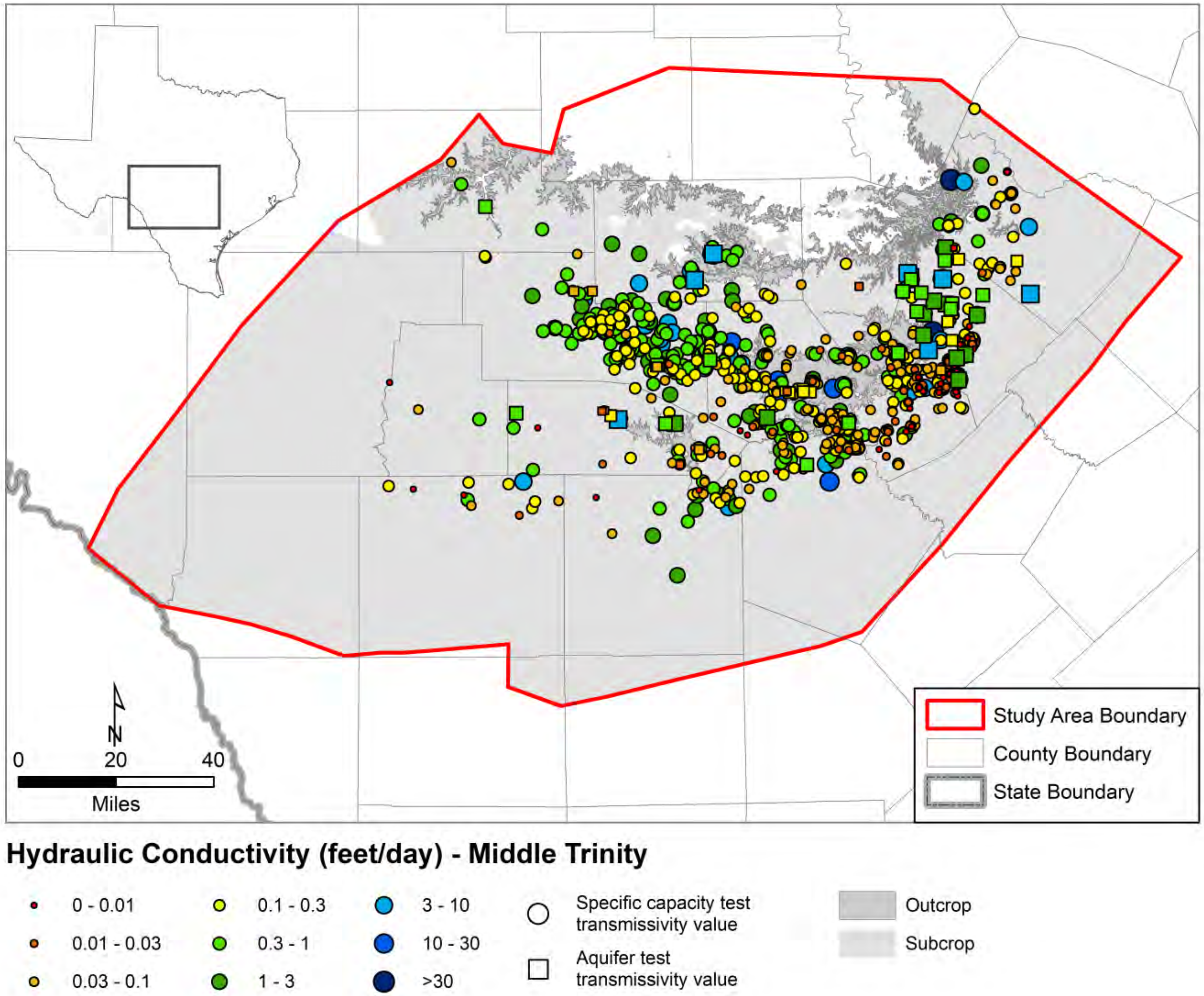

Figure 4.5.11 Spatial distribution of horizontal hydraulic conductivity values for the Middle Trinity hydrostratigraphic unit.

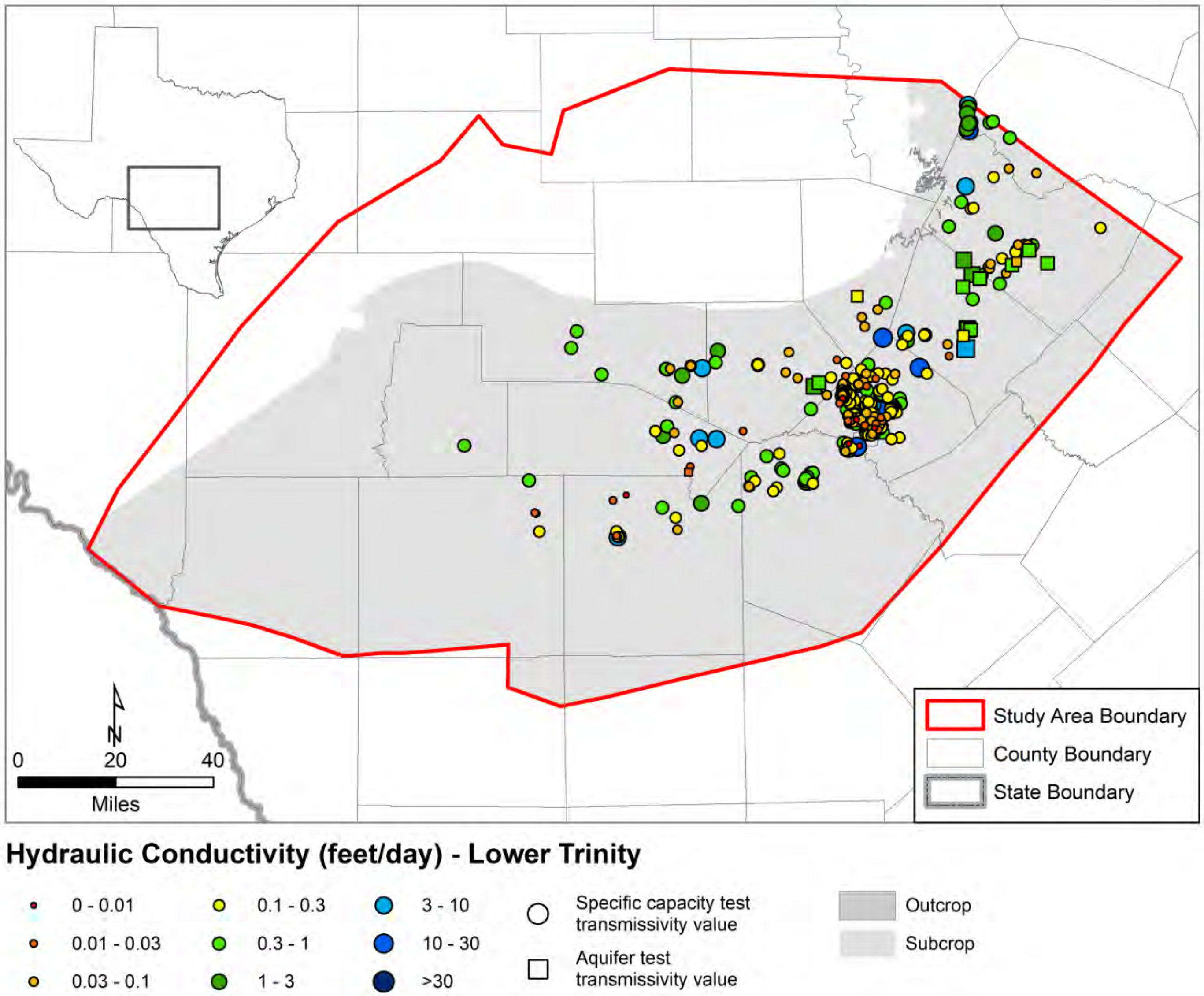

Figure 4.5.12 Spatial distribution of horizontal hydraulic conductivity values for the Lower Trinity hydrostratigraphic unit.

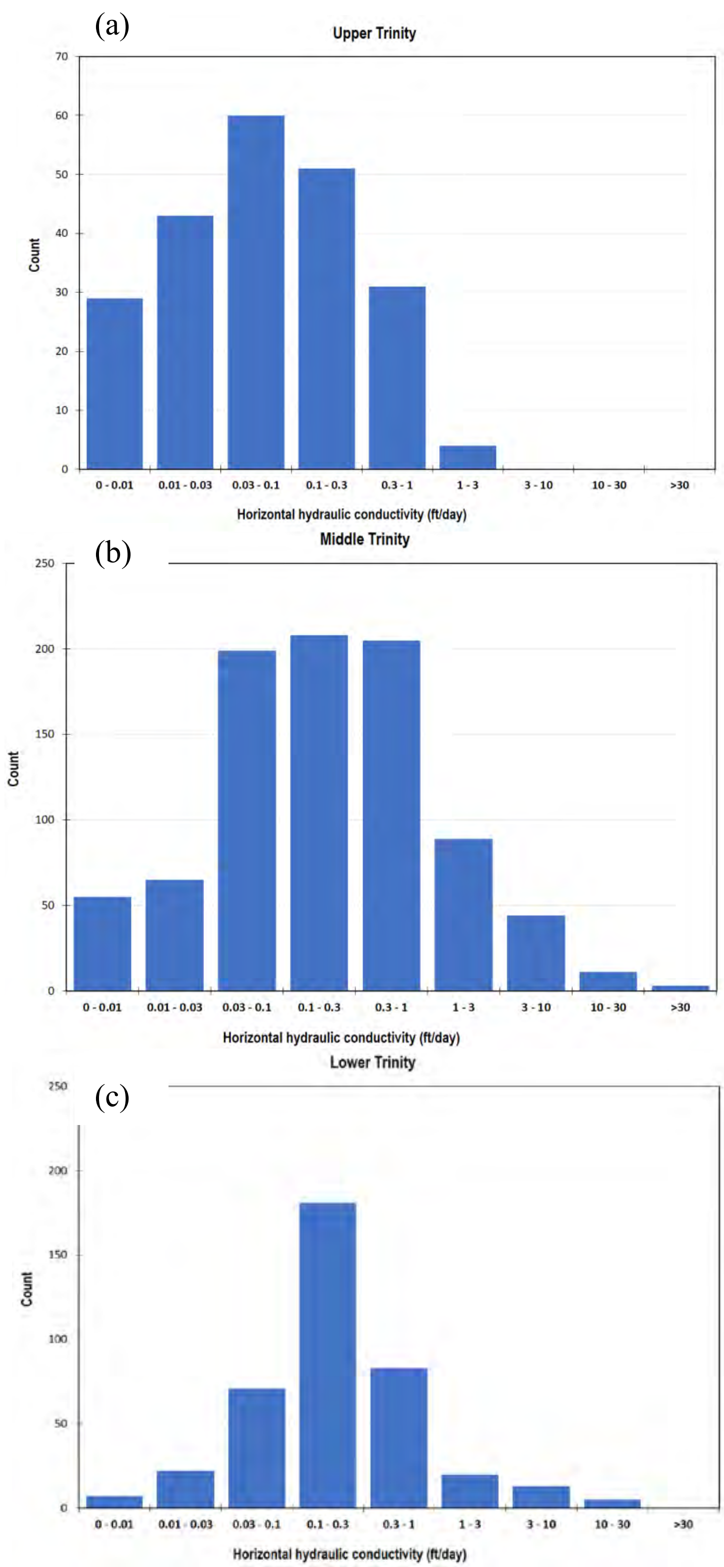

Figure 4.5.13 Histogram of horizontal hydraulic conductivity in ft/day for (a) Upper Trinity hydrostratigraphic unit, (b) Middle Trinity hydrostratigraphic unit, and (c) Lower Trinity hydrostratigraphic unit.

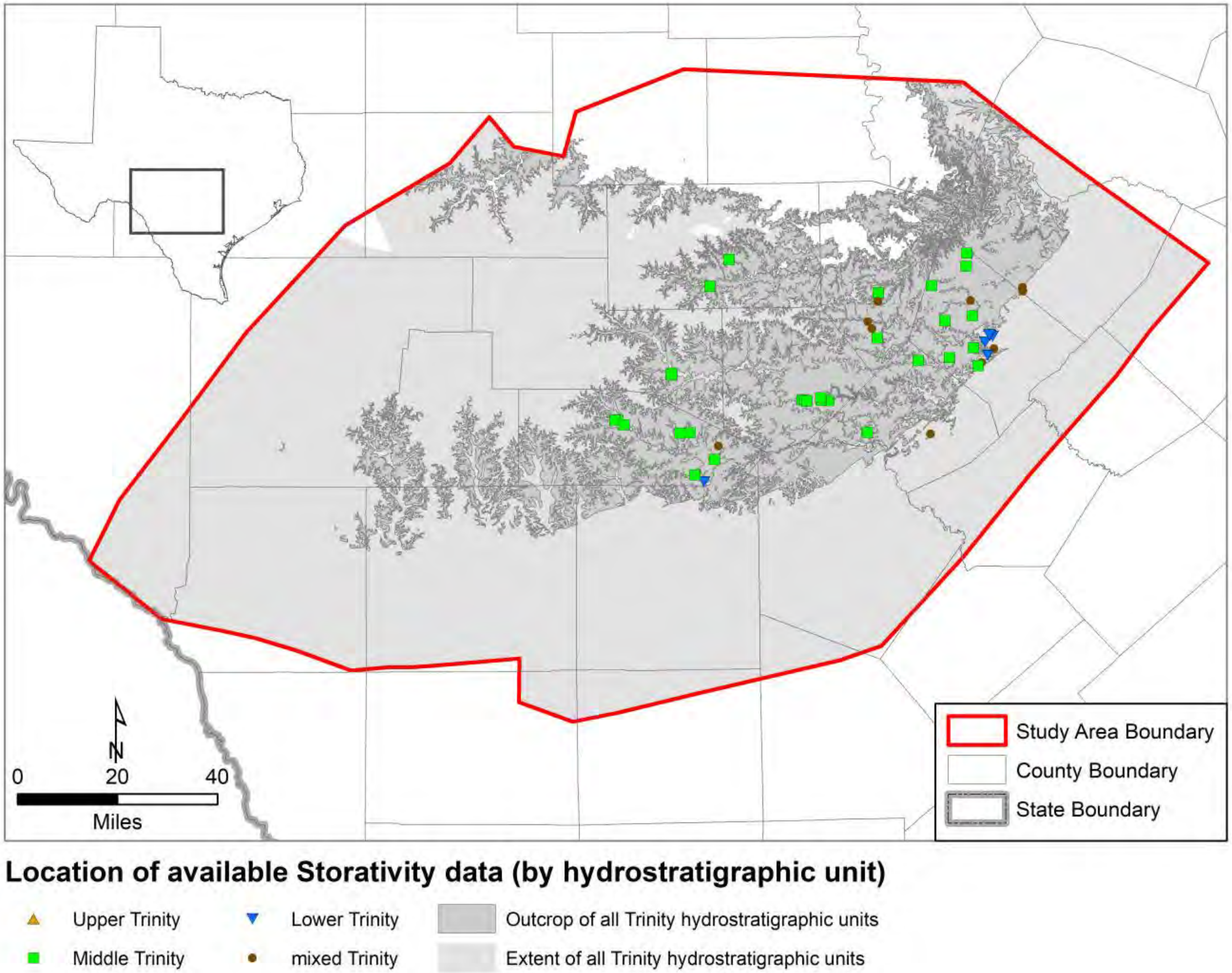

Figure 4.5.14 Location of available storativity data by hydrostratigraphic unit in the study area

4.6 Discharge

Discharge from the HCT occurs by: (i) spring discharge; (ii) interformational flow; and (iii) pumping. The first two are naturally occurring, the third is obviously not.

4.6.1 Springs

Springs present in the model domain are described in this section (Figure 4.6.1, Figure 4.6.2). Virtually all river baseflow within the HCT Aquifer domain is derived from springs discharging into river channels. Springs with significant flow are named (Figure 4.6.1, Figure 4.6.2). Most springs in river channels in the HCT Aquifer units are not named. With the exception of Jacob's Well, the named springs in the study area discharge from the Edwards group. Given the lack of springflow measurements, stream baseflow measurements are often used as a surrogate for spring discharge (Figure 4.4.2). This is particularly useful if a sufficient number of stream gain/loss measurements allow for accurate attribution of how much spring discharge occurs in a particular stream reach.

Representation of the springs as singular features in the model can be challenging because springs tend to have multiple points of discharge with different elevations. As a result, different points of discharge can cease flowing as groundwater-elevations drop. Elevations used for guidance are referred to as reference elevations due to this physical ambiguity.

The composition of source water for spring systems can be useful when determining the capture area of the spring, however, minimal data on the chemistry of spring discharge are available. Parsing out source areas using tools such as water chemistry, tracer experiments, and water-budget analyses has proven to be useful in characterizing these systems (Hauwert, 2009). Identification of source areas can become more complicated if the sources of discharge vary with stage (Doctor et al., 2006). These complications appear to be more common in larger spring systems, such as Comal, San Marcos, and Barton springs. Smaller spring systems with a limited number of discharge points or even a single point of discharge are more easily conceptualized. Within the study area, Pinto, Las Moras, San Pedro, San Antonio, Pleasant Valley, and Hueco springs are conceptualized as systems of limited complexity due to a relatively simple source area and a limited extent of discharge points, however, in reality, these springs may also have multiple points of discharge.

4.6.2 Aquifer Discharge through Pumping

Estimates of pumping discharge from the Trinity hydrostratigraphic units in the study area were developed for each county for the time period from 1980 through 2015. The following subsections describe (1) sources of historical pumping data, (2) approach to estimating rural domestic pumping, (3) estimates of specific historical pumping data for the Trinity hydrostratigraphic units, (4) a summary of historical pumping data for 1980 through 2015, (5) a discussion of water uses of the Trinity hydrostratigraphic units, and (6) the estimated spatial distribution of pumping.

4.6.2.1 Historical Pumping Data Sources

A search was conducted to identify sources of historical pumping estimates for the HCT Aquifer. This search included a literature survey, a request of water-use survey data from the TWDB, and requests of production data from GCDs. An additional source of historical pumping data was the calculation of rural domestic pumping from census block data and estimated per capita water use, discussed in Section 4.6.2.2.

4.6.2.1.1 Literature Review Results

Several sources describing historical pumping from the Trinity hydrostratigraphic units in the study area were identified through the literature review. These include historical county reports documenting groundwater resources (Livingston, 1947; George, 1947; Reeves, 1967; Reeves, 1969; Alexander and Patman, 1969; Follett, 1973; Reeves and Small, 1973) and historical public water supply reports (Sundstrom et al.,1949; Broadhurst et al., 1950; Broadhurst et al., 1951). These literature values were of limited use for the current analysis. When pumping values are included in these sources, typically, only a one-time measurement, rather than a time series, is included. Most sources only include expected yields or water uses from a particular hydrostratigraphic unit. Some units are only described as “Trinity,” so it is difficult to assign pumping to the hydrostratigraphic units used in the current report. However, these literature sources are helpful in developing a probable timeline for the start of groundwater pumping from the Trinity hydrostratigraphic units in the current study area. Table 4.6.1 summarizes the year(s) of first recorded pumping, the hydrostratigraphic unit(s) associated with the pumping data, and the groundwater-use type associated with the pumping. As shown, pumping from the Trinity hydrostratigraphic units in Bandera, Bexar, Kerr and Kimble counties dates back to the 1940s and there is even a record of a Trinity well drilled in 1928 in Edwards County. While these literature sources can indicate a nominal start of pumping from the Trinity hydrostratigraphic units, it is difficult to extrapolate this information into usable data about the temporal and spatial distribution of pumping over the rest of the historical time period, for which little to no other data exists. Therefore, this information was used only indirectly in the current analysis. For instance, it was used in choosing the time period for pre-development water-elevation contours (Section 4.2)

4.6.2.1.2 TWDB Water Use Survey Data

Estimates of historical pumping for 1980 and 1984 through 2015 are available from the TWDB historical groundwater pumpage database (TWDB, 2018a). These values are available for municipal, manufacturing, mining, power, irrigation, and livestock water-use categories by TWDB aquifer designation. These estimates have been developed by the TWDB as a water-use survey database to support state water planning and the TWDB Groundwater Availability Model program and are considered the most reliable source of historical pumping information available. These are the primary data used in previous groundwater models in the study area (Mace et al., 2000; Anaya and Jones, 2009; Jones et al., 2011). A formal request for specific pumping data on a per-well basis was made to the TWDB. In response to that request, TWDB provided a dataset of water-use survey data with groundwater-use estimates for 1980 through 2015 that provides water-use estimates by well and by aquifer for all counties in the current study area (TWDB, 2017e).

Since they are derived from the same water-use survey data, the total values for these county-level (TWDB, 2018a) and well-specific (TWDB, 2017e) datasets are generally consistent post-2000. From 2000 onwards, both datasets include “non-surveyed estimates” for all water uses, in addition to the surveyed estimates. Since there is some uncertainty inherent in survey-reliant data, these non-surveyed estimates can help account for pumping that is unreported or under-reported in the survey data. However, while the county-wide pumping data (TWDB, 2018a) includes pre-2000 non-survey estimates, the per-well estimates (TWDB, 2017e) do not. For this reason, the county-wide pumping total values are considered more representative of county-wide pre-2000 pumping. An additional difference between the two datasets is that the per-well dataset (TWDB, 2017e) include values for the years 1981 through 1983 whereas the county-wide pumping dataset (TWDB, 2018a) does not. The current analysis therefore uses a combination of these two datasets to fill in data gaps as necessary.

In addition to the post-1980 groundwater pumpage database, TWDB also provides datasets for historical municipal and historical industrial water intake that provide data by water user from the 1950’s onwards (TWDB, 2018b). However, these data are provided by water-use location rather than the location of actual groundwater pumpage. For this reason, pumping values from this dataset were only considered if the listed water supplier was in the study area, not if the water user was in the study area. In addition, because industrial water users often use public or municipal suppliers, there is overlap between the industrial and municipal datasets. For this reason, only “self-supplied” industrial users could be considered. While less complete than the groundwater pumpage datasets (TWDB, 2017e, 2018a), the benefit of the historical municipal data (TWDB, 2018b) is the long historical record available. This database helps establish pumping start dates and some counties have data available over nearly 70 years. However, these data are not consistently available for all counties. Some county records appear to be incomplete, as they start much later than the expected start date of pumping based on the county reports and public water supply reports discussed in the previous section. Some records even start after the post-1980 historical groundwater pumpage database (TWDB, 2017e, 2018a) begins. For this reason, these data were not used to create pre-1980 groundwater pumping trends across the region, as they were considered much less certain than the post-1980 water-use survey datasets. A summary of the information available from this dataset is included in Table 4.6.1**,** as it could be helpful for investigating pumping of individual counties. Note that the start date from this dataset was not included if it occurred post-1980.

4.6.2.1.3 GCD Data

The study area intersects twenty-three GCDs (Figure 2.0.5). During stakeholder meetings and other outreach efforts for the current project, all districts were invited to submit relevant pumping data. A few districts were able to provide pumping records. In general, because most GCDs only recently began monitoring activities, or in some cases, only recently were formed, GCD data pertains to recent pumping within the past five to ten years, rather than historical records. A few datasets were only available as district-wide estimates or as limited numbers of individual well records and so could not be readily compared with the county-level data available from TWDB. In addition, pumping data at particular wells could not be used in most cases since there was not enough well location or completion information to assign these wells to the current project's hydrostratigraphic units. Since major water users are required to report to the TWDB water-use survey program as well as to local GCDs, it is assumed that much of the information received from GCDs is already incorporated in the TWDB historical groundwater pumpage database (TWDB, 2017e, 2018a). For this reason, the current analysis focuses on the TWDB datasets, and only indirectly uses pumping data received from GCDs to check those values.

4.6.2.2 Calculated Rural Domestic Pumping

Estimates of rural domestic pumping for the years 1990, 2000, and 2010 were developed using census block data from these years and an assumed per capita water use. Census block data for 1990, 2000, and 2010 were obtained from the IPUMS National Historical Geographic Information System (Manson et al., 2017) in the format of tables linked to a census-block geographic information system (GIS) coverage. These data include the total population, as well as the rural and urban population by census block. The rural-domestic water use in each census block was calculated as the rural population times an estimated per capita water use. The per capita use was assumed to be 110 gallons per day (pgd) (0.1232 acre-ft per year) based on the approximate median per capita water use in Texas between 1980 and 1997 (Hamlin and Anaya, 2006).

For the purposes of this analysis, water used for rural domestic purposes was assumed to be supplied solely by groundwater. This was assumed because the high treatment cost associated with surface water for human consumption is likely to make groundwater the most common source of rural-domestic pumping. This analysis also assumed that rural domestic pumping in each hydrostratigraphic unit was confined to the outcrop of that unit and that all water used for rural domestic purposes in the outcrop area is supplied by groundwater solely from that hydrostratigraphic unit. This was assumed because rural-domestic wells are typically only drilled to the shallowest permeable unit to minimize drilling costs. The exception to this is the Upper Trinity hydrostratigraphic unit. Since this unit has low permeability and is thin throughout much of the HCT region, eighty percent of the pumping in this outcrop was assumed to actually be sourced from the Middle Trinity hydrostratigraphic unit. The census block coverage was clipped to the extent of the hydrostratigraphic unit outcrop. The ratio of the census-block area within the hydrostratigraphic unit outcrop to the total census-block area was considered equivalent to the ratio of rural-domestic pumping within the hydrostratigraphic unit to the total rural-domestic pumping within the census block. This ratio was used to calculate a weighted amount of rural-domestic pumping for the clipped census block. The weighted rural-domestic pumping in all clipped census blocks in a hydrostratigraphic unit in a county were summed to get the total rural-domestic pumping within the hydrostratigraphic unit for that county. This calculation of groundwater for rural domestic purposes by year and by hydrostratigraphic unit can be summarized as:

$$RD_{HU} = \sum RurPop_{CB} \bullet AreaRatio_{\frac{out}{CB}} \bullet PerCapitaUse \quad (4.6.1)$$

where:

RD_{HU} = groundwater use from the hydrostratigraphic unit for rural domestic purposes (acre-ft per year),

$RurPop_{CB}$ = total rural population per census block

$AreaRatio_{out/CB}$ = ratio of the area of the census block falling within the hydrostratigraphic unit outcrop to the total census block area, and

PerCapitaUse = per capita water use (acre-ft per year)

The estimated rural domestic pumping from each hydrostratigraphic unit for the years 1990, 2000, and 2010 were calculated using Equation 4.6.1. Figure 4.6.3, Figure 4.6.4, and Figure 4.6.5 show distributions of rural-domestic pumping as acre-ft per year per census block in 1990, 2000, and 2010, respectively. Census blocks with no rural population are excluded from this analysis and appear as blank areas in the figures. In the western portion of the study area, these blank areas generally indicate census blocks with no recorded population at all. In the eastern portion of the study area, these blank areas generally indicate the presence of cities. There are a few inconsistencies between years, reflecting minor changes in the census block extents or census methodology. However, in general, there is a trend of declining rural population over time in the study area. As shown, the Trinity hydrostratigraphic units contribute little to no rural domestic pumping in the western portion of the study area, as the Edwards hydrostratigraphic unit outcrops in this region. The exception is an area of Middle Trinity outcrop in Kimble County. In the HCT region, the Upper and Middle Trinity hydrostratigraphic units provide most of the rural-domestic pumping. As the Lower Trinity hydrostratigraphic unit is deeper and does not outcrop anywhere except a small area in Travis and Burnet counties, this unit is assumed to provide very little of the rural-domestic pumping in the area.

Rural population estimates by census block were not available for non-census years or for 1980. For the purposes of this analysis then, rural domestic pumping for the years 1980 through 1995 were assumed to be the same as the estimated rural domestic pumping from 1990. Rural domestic pumping for the years 1996 through 2005 were assumed to be the same as the estimated rural domestic pumping from 2000. Rural domestic pumping for the years 2006 through 2015 were assumed to be the same as the estimated rural domestic pumping from 2010.

4.6.2.3 Estimation of Historical Pumping Data by Hydrostratigraphic Unit

Total annual pumping values by aquifer and by county for 1980 and 1984 through 2015 were sourced from the TWDB historical groundwater pumpage county-level database (TWDB, 2018a). The TWDB well-specific water-use survey data (TWDB, 2017e) does provide estimates for the years 1981,1982, and 1983. However, these estimates are likely incomplete, as they are much lower than values in 1980 and 1984 provided in the county-level dataset (TWDB, 2018a). Therefore, to fill in missing data in the years 1981,1982, and 1983, pumping was assumed to increase or decrease linearly between 1980 and 1984 pumping values from the county-level dataset (TWDB, 2018a). The one exception is Bexar County, where TWDB well-specific water-use survey data (TWDB, 2017e) indicated higher pumping values than this linear estimate.

Therefore, the values from the TWDB well-specific water-use survey data (TWDB, 2017e) were used to fill in the missing years in Bexar County.

The estimated historical pumping data obtained from TWDB (2017e,2018a) provide groundwater use by TWDB aquifer designation. The Upper, Middle, and Lower Trinity hydrostratigraphic units discussed in the current report are not officially-recognized TWDB aquifers. Rather they comprise portions of two TWDB-designated major aquifers: the Trinity Aquifer and the Edwards-Trinity Plateau Aquifer. Therefore, it was necessary to determine what portion of pumping from these aquifers comes from the Upper, Middle and Lower hydrostratigraphic units.

Total pumping from the Edwards-Trinity Plateau Aquifer by county and by year was distributed to the Edwards, Upper Trinity, Middle Trinity and Lower Trinity hydrostratigraphic units by percentages based on number of wells. For each hydrostratigraphic unit, this percentage was determined by the number of wells completed fully in that hydrostratigraphic unit compared to the total number of wells completed fully in any of the component hydrostratigraphic units of the Edwards-Trinity Plateau Aquifer. For counties intersecting both the Edwards-Trinity Plateau Aquifer and the Trinity Aquifer, only wells falling in the footprint of the Edwards-Trinity Plateau Aquifer were considered, rather than total wells in the county. For each year, this calculation only includes wells constructed during or before that particular year. At the beginning of the record, if there were no wells counted for a year, but pumping was reported, the distribution from the earliest year with well counts was used. This distribution of Edwards-Trinity Plateau Aquifer pumping by year and by hydrostratigraphic unit in a particular county can be summarized as:

$$Pump_{HU(ETP)} = WellRatio_{\frac{HU}{ETP}} \cdot Pump_{ETP} \qquad (4.6.2)$$

where:

$Pump_{HU(ETP)}$ = total annual pumping sourced from the hydrostratigraphic unit (acre-ft per year) in the extent of the Edwards-Trinity Plateau Aquifer in the county,
$WellRatio_{HU/ETP}$ = ratio of the wells completed fully in the hydrostratigraphic unit to the total number of wells completed fully in any of the component hydrostratigraphic units of the Edwards-Trinity Plateau Aquifer, and
$Pump_{ETP}$ = total pumping sourced from the Edwards-Trinity Plateau Aquifer (acre-ft per year) in the county.

Total pumping from the Trinity Aquifer by county and by year was distributed to the Upper Trinity, Middle Trinity and Lower Trinity hydrostratigraphic units by percentages based on number of wells. For each hydrostratigraphic unit, this percentage was determined by the number of wells completed fully in that hydrostratigraphic unit compared to the total number of wells completed fully in any of the component hydrostratigraphic units of the Trinity Aquifer. For counties intersecting both the Edwards-Trinity Plateau Aquifer and the Trinity Aquifer, only wells falling in the footprint of the Trinity Aquifer were considered, rather than total wells in the county. For each year, this calculation only includes wells constructed during or before that particular year. At the beginning of the record, if there were no wells counted for a year, but pumping was reported, the distribution from the earliest year with well counts was used. This distribution of Trinity Aquifer pumping by year and by hydrostratigraphic unit in a particular county can be summarized as:

$$Pump_{HU(T)} = WellRatio_{\frac{HU}{T}} \bullet Pump_T \qquad (4.6.3)$$

where:

$Pump_{HU(T)}$ = total annual pumping sourced from the hydrostratigraphic unit (acre-ft per year) in the extent of the Trinity Aquifer in the county,
$WellRatio_{HU/T}$ = ratio of the wells completed fully in the hydrostratigraphic unit to the total number of wells completed fully in any of the component hydrostratigraphic units of the Trinity Aquifer, and
$Pump_T$ = total pumping sourced from the Trinity Aquifer (acre-ft per year) in the county.

Bandera, Blanco, Gillespie, Kendall, Kerr, Real, Uvalde counties intersected both the Edwards-Trinity Plateau and Trinity aquifers. For these counties, the total pumping from each hydrostratigraphic unit was considered to be the sum of the pumping sourced from the hydrostratigraphic unit from both the Edwards-Trinity Plateau and Trinity aquifer extents. This calculation can be summarized as:

$$Pump_{HU} = Pump_{HU(ETP)} + Pump_{HU(T)} \qquad (4.6.4)$$

where:

$Pump_{HU}$ = total annual pumping sourced from the hydrostratigraphic unit (acre-ft per year) in the county,
$Pump_{HU(ETP)}$ = total annual pumping sourced from the hydrostratigraphic unit (acre-ft per year) in the extent of the Edwards-Trinity Plateau Aquifer in the county,
$Pump_T$ = total pumping sourced from the Trinity Aquifer (acre-ft per year) in the county.

This methodology does assume that every well constructed before a certain date remains in operation at that date. This may erroneously include some wells that were plugged or retired over time. This methodology also does not account for wells screened over multiple hydrostratigraphic units or for differences in transmissivity between hydrostratigraphic units that can control the productivity of individual wells. However, because early wells would have preferentially been drilled in the most transmissive units, the number of wells drilled in each hydrostratigraphic unit over time are considered a reasonable proxy for the transmissivity-controlled production from each hydrostratigraphic unit over time. Table 4.6.2 provides the calculated percentages of county-wide Trinity Aquifer and Edwards-Trinity Plateau Aquifer pumping sourced from each hydrostratigraphic unit by decade.

4.6.2.4 Summary of Historical Pumping Estimates for 1980 through 2015

The historical pumping estimates calculated from TWDB water-use survey data (Section 4.6.2.1) were combined with the calculated rural domestic pumping estimates (Section 4.6.2.2) to obtain an estimate of total historical pumping for the time period from 1980 through 2015.

Table 4.6.3 provides the estimated amount of historical pumping in acre-ft from each Trinity hydrostratigraphic unit by county for the years 1980, 1990, 2000, and 2010. Figure 4.6.6 and Figure 4.6.7 show time series of the estimated amount of historical sourced from the Trinity hydrostratigraphic units for counties in the western/west-central portion and eastern/east-central portion of the study area, respectively. Each chart shows the division of pumping between the Trinity hydrostratigraphic units only. Values for counties in the extent of the Edwards-Trinity Plateau Aquifer exclude any Edwards-Trinity Plateau Aquifer pumping that is sourced from the

Edwards hydrostratigraphic unit. The years on the x-axis for all charts are 1980 to 2015. The scale on the y-axis is the same for charts in the same figure except for Bexar County which had much higher pumping than the rest of the counties in the study area. Each chart also indicates whether the total pumping was derived from TWDB estimates for the Edwards-Trinity Plateau Aquifer, the Trinity Aquifer, or a combination of both.

In the western portion of the study area, very little county pumping is sourced from the Trinity hydrostratigraphic units. This is due to both low overall pumping in these counties as well as the fact that most of the Edwards-Trinity Plateau Aquifer pumping in this region is sourced from the shallow and more permeable Edwards hydrostratigraphic unit rather than the underlying Trinity hydrostratigraphic units. Of the pumping from the Trinity hydrostratigraphic units, the earliest pumping was sourced from the Upper Trinity hydrostratigraphic unit, likely because it is the shallowest and easiest to access beneath the Edwards hydrostratigraphic unit. This remains the main source of Trinity pumping in Edwards and Kinney counties. Over time, the amount of pumping sourced from the Middle Trinity and Lower Trinity hydrostratigraphic units has increased slightly in Uvalde and Real counties, reflecting increasing numbers of wells drilled into these deeper units. The Middle Trinity hydrostratigraphic unit has been the main source of Trinity pumping in Kimble and Medina counties over time, likely because it is shallower and outcrops in that area. Most of the counties in the region show at least some increase in groundwater pumping during the 2011 drought.

County pumping sourced from the Trinity hydrostratigraphic units increases from west to east, as more of each county intersects the Trinity Aquifer rather than the Edwards-Trinity Plateau Aquifer. Bandera, Blanco, Kendall, Kerr, and Gillespie counties intersect both aquifers and show much higher pumping from Trinity hydrostratigraphic units than western counties that only intersect the Edwards-Trinity Plateau Aquifer. The Middle Trinity hydrostratigraphic unit is the main source of Trinity pumping in these counties. However, the amount of pumping from the Lower Trinity hydrostratigraphic unit has increased in Kendall, Blanco, Kerr and Bandera counties, particularly after about 2005. Kerr and Gillespie counties also saw an increase in the pumping sourced from the Upper Trinity hydrostratigraphic unit around the same time period. All counties in this region show a spike in groundwater pumping during the 2011 drought.

County pumping sourced from the Trinity hydrostratigraphic units is highest in the eastern portion of the study area, with the highest total county pumping in Bexar and Travis counties. These values reflect the high demand from populations near the large cities of San Antonio in Bexar County and Austin in Travis County. Comal and Hays counties, which fall in the fast-developing area between these two cities, also show increasing pumping values over time that reflect the high population growth in that region. The Middle Trinity hydrostratigraphic unit is the main source of Trinity pumping in these counties. However, the amount of pumping from the Lower Trinity hydrostratigraphic unit has increased over time, particularly after about 2005. This proportion has increased most dramatically in Comal County, where the amount of recent pumping sourced from the Lower Trinity hydrostratigraphic is as much or more than the amount sourced from the Middle Trinity hydrostratigraphic unit. All counties in this region show a spike in groundwater pumping during the 2011 drought.

4.6.2.5 Historical Pumping Estimates for 1980 through 2015 by Water Use

The TWDB historical groundwater pumping dataset (TWDB, 2018a) provides county pumping estimates by water use and by TWDB aquifer designation. Water uses include municipal, mining, manufacturing, steam electric power, irrigation, and livestock. As mentioned previously, the Upper, Middle, and Lower Trinity hydrostratigraphic units discussed in the current report are not officially-recognized TWDB aquifers. Rather they comprise portions of two TWDB-designated major aquifers: the Trinity Aquifer and the Edwards-Trinity Plateau Aquifer. For the purposes of this analysis, it was assumed that each Trinity hydrostratigraphic unit had the same water-use divisions as the major aquifer of which it was a component. The TWDB datasets do not provide estimates for rural domestic pumping. These values are based on the estimates from the current analysis (Section 4.6.2.2).

Stacked bar charts of pumping by use category were developed for all counties for the time period 1980 through 2015. Figure 4.6.8 and Figure 4.6.9 show time series of the water uses of pumping sourced from the Trinity hydrostratigraphic units for counties in the western/west-central portion and eastern/east-central portion of the study area, respectively. The charts do not show divisions between the Trinity hydrostratigraphic units, so pumping values represent all combined pumping from the Trinity hydrostratigraphic units. The legend for each chart shows the water-use categories. The years on the x-axis for all charts are 1980 to 2015. The scale on the y-axis is the same for charts in the same figure except for Bexar County which had much higher pumping than the rest of the counties in the study area.

In the western counties of the study area, the majority of groundwater pumped from the Trinity hydrostratigraphic units is used for municipal, rural-domestic and livestock purposes. Very little Trinity groundwater is used for irrigation, except in Kinney County and small amounts in Real, Gillespie and Kimble counties. This is likely due to the Edwards hydrostratigraphic unit being shallower, more accessible and less saline than the Trinity hydrostratigraphic units in that region. There has been some increase in municipal pumping over time in Medina, Uvalde, and Real counties. In general, the increase in groundwater pumping during the 2011 drought in all counties in the region is driven by increases in municipal pumping in all counties in the region, with some increase in irrigation and livestock pumping in Gillespie County.

In the central counties of the study area that intersect both the Edwards-Trinity Plateau Aquifer and the Trinity Aquifer, the majority of groundwater pumped from the Trinity hydrostratigraphic units is used for municipal and rural-domestic purposes, with small amounts used for irrigation and livestock purposes. In general, the increase in groundwater pumping during the 2011 drought in all counties in the region is driven by increases in municipal pumping in all counties.

In the eastern counties of the study area, the majority of groundwater pumped from the Trinity hydrostratigraphic units is used for municipal and rural-domestic purposes. These values reflect the high demand from the large cities of San Antonio in Bexar County and Austin in Travis County. Comal and Hays counties, which fall in the fast-developing area between these two cities, also show large municipal and rural-domestic values that reflect the high population growth in that region. The Trinity hydrostratigraphic units also provide significant amounts of pumping for manufacturing and mining purposes in Bexar County. In general, the increase in groundwater pumping during the 2011 drought in all counties in the region is driven by increases in municipal pumping and less so by minor increases in irrigation and livestock use.

4.6.2.6 Spatial Distribution of Pumping by Water Use

In order to incorporate pumping into a numerical groundwater model, estimated historical pumping must be distributed spatially so that the volume of groundwater withdrawal from each grid block can be defined over time. The spatial distribution of pumping in each water-use category is assumed to be coincident with the location of wells for which the primary water-use matches the pumping category. However, while pumping from water-use categories with large individual users (municipal, industrial, power) can reasonably be assigned to actual well locations, there is great uncertainty in well locations for pumping from water-use categories with smaller and decentralized users (livestock, irrigation, rural-domestic). The following section provides recommendations for distributing pumping values spatially by water-use category.

Figure 4.1.10 shows the locations of municipal and industrial wells in the study area. Wells were considered municipal if they had a public water supply source number (from the Texas Commission on Environmental Quality), if the stated water use was "public supply" or "institution", or if a city was listed as the owner. Wells were assumed to be industrial if the stated water use was "commercial" or "industrial." This may not be a comprehensive dataset, as some well uses may be unlisted or listed erroneously in the source datasets. Wells that could be linked to the TWDB well-specific pumping dataset (TWDB, 2017e) are circled in the map. This is not a comprehensive dataset, as there were wells in the well-specific pumping dataset that could not be definitively matched with well locations either by public water supply source number or owner name. Therefore, additional information will likely be needed during model development to spatially assign pumping.

Land cover datasets from the National Land Cover Dataset are available for the years 1992, 2001, 2006, and 2011 (Vogelmann et al., 2001; Homer et al., 2007; Fry et al., 2006; Homer et al., 2015). Figure 4.1.11, Figure 4.1.12, and Figure 4.1.13

show the distribution of rangeland and irrigated cropland for 1992, 2001, and 2011, respectively. Developed and urban areas are also included in the figures for reference. For the current analysis, rangeland was assumed to be a combination of the extents of the "shrubland" and "herbaceous" land-use categories. Irrigated cropland was assumed to be a combination of the extents of the "pasture/hay" and "cultivated crops" land-use categories. The category names are different for 1992 land cover dataset than for later datasets. For the 1992 dataset, rangeland was assumed to be a combination of the extents of the "shrubland" and "grassland/herbaceous" land-use categories. Irrigated cropland was assumed to be a combination of the extents of the "pasture/hay", "orchards/vineyards", "row crops" and "fallow" land-use categories. Note that more detailed land coverages, such as the National Agricultural Statistics Service crop data layers, are available in the area. However, these are generally only available for the past five to ten years and so, the National Land Cover Dataset coverages, while less detailed, are considered more useful since they are available for a longer time period.

The recommended spatial distribution for rural domestic pumping was discussed previously and shown in Figure 4.6.3**,** Figure 4.6.4, and Figure 4.6.5 for the years 1990, 2000, and 2010, respectively. This spatial distribution strategy is based on the rural population by census block falling within the outcrop of each hydrostratigraphic unit.

4.6.3 Interformational Flow

Natural groundwater discharges from the HCT Aquifer also occurs as interformational flow to other units which may transmit water from the HCT Aquifer to locations outside of the study domain. As illustrated in vertical cross sections A-A', B-B', and C-C' (Figure 2.2.5, Figure 2.2.6, and Figure 2.2.7) the greatest potential for interformational flow occurs in the Balcones Fault Zone where fault displacement is the greatest and the juxtaposition of the HCT Aquifer with other aquifers allows for the conveyance of groundwater from the HCT Aquifer out of the model domain.

Table 4.6.1 Initial reference elevation, calibrated elevation and calibrated conductivity of springs and points of discharge. Locations and elevations taken from TWDB GWDB for all springs except Pleasant Valley Spring. Pleasant Valley Spring location was extracted from a georeferenced Barton Springs Central Texas Water Map (BSEACD, 2017) and elevation was extracted from the DEM used in this study.

Spring Name	Latitude	Longitude	Elevation (ft, msl)
San Marcos Spring	29.893	-97.93	570
Comal Springs	29.7129	-98.1378	582.8
Hueco Springs	29.7593	-98.1408	660
Pleasant Valley Springs	30.0152	-98.2071	924
San Antonio Springs	29.4661	-98.4686	685
San Pedro Springs	29.4452	-98.5019	660
Las Moras Springs	29.3094	-100.4206	1105
Barton Springs	30.2635	-97.7713	462.34
Jacob's Well	30.0355	-98.1297	922.84
Cold Springs	30.0916	-98.403	1280

Table 4.6.2 Summary of early recorded groundwater use from the Trinity hydrostratigraphic units in the study area.

	County Report			Public Water Supply Report		TWDB Historical Municipal & Industrial Estimates (TWDB, 2018b)	
County	First record of pumping	Trinity Water Source (HSU*)	Water Use+	First record of pumping from "Trinity Group"	Water Use	First record of pumping from "Trinity Aquifer"	Water Use
Bandera	--	--	--	1940[8]	MUN	1955	MUN
Bexar	1947[1]	Travis Peak (MT)	--	--	--	1958	IND
Blanco	1973[2]	Upper Glen Rose (UT) Lower Glen Rose (MT) Travis Peak (MT)	-- IRR MUN	--	--	1955	MUN
Comal	1947[3]	Upper Glen Rose (UT) Lower Glen Rose (MT) Hensell (MT)	-- -- DOM & STK	--	--	--	--
Edwards	--	--	--	1928[9]	MUN		
Gillespie	--	--	--	--		1955	IND
Hays	--	--	--	--		1965	MUN
Kendall	1967[4]	Glen Rose (UT) Glen Rose (MT) Hensell (MT) Cow Creek (MT)	-- -- -- --	--		1955	MUN & IND
Kerr	1969[5]	Hosston/Sligo (LT)	MUN	1940[10]	MUN	1958	MUN
Kimble	1964[6]	Hensell (MT)	--	1946[10]	MUN		
Travis	--			--		1955	MUN
Val Verde	1973[7]	Glen Rose (UT?)	STK	--			

** HSU = Hydrostratigraphic unit. Abbreviation key: UT = Upper Trinity; MT = Middle Trinity; LT = Lower Trinity*
+ Water use abbreviation key: DOM = domestic; IRR = irrigation; IND = industrial; MUN = Municipal; STK = livestock
[1] Livingston (1947) *[2] Follet (1973)* *[3] George (1947)*
[4] Reeves (1967) *[5] Reeves (1969)* *[6] Alexander and Patman (1969)*
[7] Reeves and Small (1973) *[8] Broadhurst et al. (1950)* *[9] Broadhurst et al. (1951)*
[10] Sundstrom et al. (1949)

Table 4.6.3 Percentage of county-wide Trinity Aquifer and Edwards-Trinity Plateau Aquifer pumping sourced from each Trinity hydrostratigraphic unit by decade.

County	Year	Percent of Edwards-Trinity Plateau Aquifer pumping sourced from each hydrostratigraphic unit			Percent of Trinity Aquifer pumping sourced from each hydrostratigraphic unit		
		Upper Trinity	Middle Trinity	Lower Trinity	Upper Trinity	Middle Trinity	Lower Trinity
Bandera	1980	6.3%	12.5%	--	1.1%	83.0%	16.0%
Bandera	1990	6.3%	12.5%	--	0.7%	83.5%	15.8%
Bandera	2000	5.6%	11.1%	--	0.5%	82.0%	17.5%
Bandera	2010	13.0%	34.8%	4.3%	0.2%	77.4%	22.3%
Bexar	1980	--	--	--	--	94.3%	5.7%
Bexar	1990	--	--	--	--	90.4%	9.6%
Bexar	2000	--	--	--	--	91.0%	9.0%
Bexar	2010	--	--	--	0.1%	86.6%	13.3%
Blanco	1980	25.0%	75.0%	--	--	97.4%	2.6%
Blanco	1990	25.0%	75.0%	--	--	97.6%	2.4%
Blanco	2000	25.0%	75.0%	--	--	97.2%	2.8%
Blanco	2010	8.3%	83.3%	8.3%	0.4%	85.6%	14.0%
Burnet	1980	--	--	--	14.3%	57.1%	28.6%
Burnet	1990	--	--	--	11.1%	55.6%	33.3%
Burnet	2000	--	--	--	11.1%	55.6%	33.3%
Burnet	2010	--	--	--	3.3%	56.9%	39.8%
Comal	1980	--	--	--	--	79.8%	20.2%
Comal	1990	--	--	--	--	82.3%	17.7%
Comal	2000	--	--	--	--	77.9%	22.1%
Comal	2010	--	--	--	0.1%	46.7%	53.2%
Edwards	1980	8.5%	0.9%	0.4%	--	--	--
Edwards	1990	8.4%	0.8%	0.4%	--	--	--
Edwards	2000	7.1%	0.6%	0.3%	--	--	--
Edwards	2010	14.9%	2.0%	0.7%	--	--	--
Gillespie	1980	11.9%	8.3%	--	2.7%	97.3%	--
Gillespie	1990	10.5%	16.7%	--	1.5%	98.5%	--
Gillespie	2000	10.1%	20.2%	--	1.2%	98.8%	--
Gillespie	2010	20.4%	27.8%	--	0.5%	99.5%	--
Hays	1980	--	--	--	--	88.1%	11.9%
Hays	1990	--	--	--	--	86.3%	13.7%
Hays	2000	--	--	--	--	80.9%	19.1%
Hays	2010	--	--	--	0.3%	67.1%	32.6%
Kendall	1980	--	100.0%	--	0.4%	96.0%	3.6%

County	Year	Percent of Edwards-Trinity Plateau Aquifer pumping sourced from each hydrostratigraphic unit			Percent of Trinity Aquifer pumping sourced from each hydrostratigraphic unit		
		Upper Trinity	Middle Trinity	Lower Trinity	Upper Trinity	Middle Trinity	Lower Trinity
Kendall	1990	--	100.0%	--	0.4%	95.7%	4.0%
Kendall	2000	--	100.0%	--	0.3%	94.2%	5.5%
Kendall	2010	13.5%	83.8%	--	0.3%	86.6%	13.1%
Kerr	1980	8.3%	46.7%	--	--	95.0%	5.0%
Kerr	1990	9.1%	55.8%	--	--	95.8%	4.2%
Kerr	2000	13.0%	50.0%	--	--	96.3%	3.7%
Kerr	2010	18.0%	48.7%	1.3%	0.2%	91.4%	8.4%
Kimble	1980	4.9%	46.2%	--	--	--	--
Kimble	1990	4.8%	46.5%	--	--	--	--
Kimble	2000	6.9%	40.8%	--	--	--	--
Kimble	2010	7.3%	43.2%	--	--	--	--
Kinney	1980	11.1%	--	--	--	--	--
Kinney	1990	11.1%	--	--	--	--	--
Kinney	2000	10.3%	--	--	--	--	--
Kinney	2010	6.7%	--	--	--	--	--
Mason	1980	--	--	--	--	--	--
Mason	1990	--	--	--	--	--	--
Mason	2000	--	--	--	--	--	--
Mason	2010	--	50.0%	--	--	--	--
Medina	1980	--	--	--	--	100.0%	--
Medina	1990	--	--	--	--	100.0%	--
Medina	2000	--	--	--	--	100.0%	--
Medina	2010	--	--	--	1.1%	83.1%	15.7%
Real	1980	5.9%	5.9%	--	--	100.0%	--
Real	1990	23.8%	4.8%	--	--	100.0%	--
Real	2000	24.0%	4.0%	--	--	100.0%	--
Real	2010	27.1%	33.9%	2.3%	--	100.0%	--
Travis	1980	--	--	--	0.4%	70.7%	28.9%
Travis	1990	--	--	--	0.7%	68.9%	30.3%
Travis	2000	--	--	--	1.0%	67.6%	31.4%
Travis	2010	--	--	--	0.3%	60.2%	39.4%
Uvalde	1980	--	--	--	--	100.0%	--
Uvalde	1990	--	--	--	--	100.0%	--
Uvalde	2000	20.0%	--	--	--	75.0%	25.0%
Uvalde	2010	10.3%	55.1%	6.4%	2.0%	72.5%	25.5%
Val Verde	1980	21.9%	1.4%	--	--	--	--

County	Year	Percent of Edwards-Trinity Plateau Aquifer pumping sourced from each hydrostratigraphic unit			Percent of Trinity Aquifer pumping sourced from each hydrostratigraphic unit		
		Upper Trinity	Middle Trinity	Lower Trinity	Upper Trinity	Middle Trinity	Lower Trinity
Val Verde	1990	21.3%	1.3%	--	--	--	--
Val Verde	2000	19.3%	1.2%	--	--	--	--
Val Verde	2010	5.3%	0.3%	--	--	--	--
Williamson	1980	--	--	--	16.7%	41.7%	41.7%
Williamson	1990	--	--	--	11.1%	33.3%	55.6%
Williamson	2000	--	--	--	8.7%	26.1%	65.2%
Williamson	2010	--	--	--	3.2%	20.3%	76.5%

Table 4.6.4 Summary of pumping in acre-ft from Trinity hydrostratigraphic units by county for the years 1980, 1990, 2000, and 2010.

County	Year	Pumping by hydro-stratigraphic unit (excluding rural domestic)			Estimated Rural domestic pumping by hdyro-stratigraphic unit			Total pumping (all water uses) by hydro-stratigraphic unit		
		Upper Trinity	Middle Trinity	Lower Trinity	Upper Trinity	Middle Trinity	Lower Trinity	Upper Trinity	Middle Trinity	Lower Trinity
Bandera	1980	17	1050	200	162	961	--	179	2011	200
Bandera	1990	18	1533	289	162	961	--	180	2494	289
Bandera	2000	21	2336	495	274	1599	--	295	3935	495
Bandera	2010	31	2797	797	325	1870	--	356	4667	797
Bexar	1980	--	1284	78	223	1074	--	223	2358	78
Bexar	1990	--	6290	672	223	1074	--	223	7364	672
Bexar	2000	--	7253	721	250	1169	--	250	8422	721
Bexar	2010	21	13403	2051	171	735	--	192	14138	2051
Blanco	1980	--	364	10	71	508	1	71	872	11
Blanco	1990	--	455	11	71	508	1	71	963	12
Blanco	2000	1	421	12	96	709	2	96	1130	14
Blanco	2010	5	1214	199	116	902	1	121	2115	200
Burnet	1980	169	678	339	52	483	39	222	1161	378
Burnet	1990	116	580	348	52	483	39	168	1063	387
Burnet	2000	143	716	430	31	289	67	174	1005	497
Burnet	2010	69	1208	846	39	366	82	108	1574	928
Comal	1980	--	1512	384	199	1578	--	199	3090	384
Comal	1990	--	1482	319	199	1578	--	199	3060	319
Comal	2000	--	2255	640	252	2166	--	252	4421	640
Comal	2010	2	1148	1309	436	3598	--	438	4745	1309
Edwards	1980	111	11	6	18	--	--	130	11	6
Edwards	1990	72	7	4	18	--	--	90	7	4
Edwards	2000	69	6	3	16	--	--	86	6	3
Edwards	2010	108	14	5	14	--	--	123	14	5
Gillespie	1980	41	1468	--	30	1485	--	72	2952	--
Gillespie	1990	27	1675	--	30	1485	--	57	3160	--
Gillespie	2000	58	1730	--	40	668	--	98	2397	--
Gillespie	2010	220	1871	--	51	784	--	271	2655	--
Hays	1980	--	1502	203	285	1257	0.1	285	2759	203
Hays	1990	--	1556	247	285	1257	0.1	285	2813	247
Hays	2000	--	1809	427	426	1894	2	426	3704	429
Hays	2010	14	3342	1623	572	2497	3	586	5840	1626
Kendall	1980	7	1681	63	256	1324	--	263	3005	63
Kendall	1990	8	2162	90	256	1324	--	264	3486	90
Kendall	2000	9	3223	186	205	1369	--	214	4592	186

County	Year	Pumping by hydro-stratigraphic unit (excluding rural domestic)			Estimated Rural domestic pumping by hdyro-stratigraphic unit			Total pumping (all water uses) by hydro-stratigraphic unit		
		Upper Trinity	Middle Trinity	Lower Trinity	Upper Trinity	Middle Trinity	Lower Trinity	Upper Trinity	Middle Trinity	Lower Trinity
Kendall	2010	24	4243	632	253	1922	--	277	6165	632
Kerr	1980	29	5261	268	460	1840	--	489	7101	268
Kerr	1990	28	2918	122	460	1840	--	487	4758	122
Kerr	2000	104	3820	131	181	726	--	285	4546	131
Kerr	2010	253	4441	363	224	897	--	477	5339	363
Kimble	1980	54	510	--	0.1	155	--	54	665	--
Kimble	1990	41	393	--	0.1	155	--	41	548	--
Kimble	2000	40	237	--	0.1	39	--	40	276	--
Kimble	2010	46	271	--	0.1	44	--	46	315	--
Kinney	1980	1065	--	--	0.4	--	--	1066	--	--
Kinney	1990	773	--	--	0.4	--	--	774	--	--
Kinney	2000	1107	--	--	0.3	--	--	1107	--	--
Kinney	2010	82	--	--	0.1	--	--	82	--	--
Mason	1980	--	--	--	--	2	--	--	2	--
Mason	1990	--	--	--	--	2	--	--	2	--
Mason	2000	--	--	--	--	2	--	--	2	--
Mason	2010	--	6	--	--	2	--	--	8	--
Medina	1980	--	68	--	27	--	--	27	68	--
Medina	1990	--	71	--	27	--	--	27	71	--
Medina	2000	--	42	--	46	--	--	46	42	--
Medina	2010	4	298	56	130	--	--	134	298	56
Real	1980	21	21	--	182	--	--	202	21	--
Real	1990	144	29	--	182	--	--	326	29	--
Real	2000	61	21	--	221	--	--	282	21	--
Real	2010	203	275	17	242	--	--	444	275	17
Travis	1980	11	1901	778	553	2509	3	564	4410	781
Travis	1990	23	2081	916	553	2509	3	576	4589	919
Travis	2000	20	1263	586	457	2263	5	476	3526	591
Travis	2010	29	5301	3470	480	2472	7	509	7773	3477
Uvalde	1980	--	--	--	37	--	--	37	--	--
Uvalde	1990	--	--	--	37	--	--	37	--	--
Uvalde	2000	82	37	12	42	--	--	125	37	12
Uvalde	2010	57	461	96	52	--	--	110	461	96
Val Verde	1980	367	23	--	--	--	--	367	23	--
Val Verde	1990	899	56	--	--	--	--	899	56	--
Val Verde	2000	3203	200	--	--	--	--	3203	200	--
Val Verde	2010	638	32	--	--	--	--	638	32	--
Williamson	1980	694	1735	1735	79	--	--	772	1735	1735

County	Year	Pumping by hydro-stratigraphic unit (excluding rural domestic)			Estimated Rural domestic pumping by hdyro-stratigraphic unit			Total pumping (all water uses) by hydro-stratigraphic unit		
		Upper Trinity	Middle Trinity	Lower Trinity	Upper Trinity	Middle Trinity	Lower Trinity	Upper Trinity	Middle Trinity	Lower Trinity
Williamson	1990	566	1698	2830	79	--	--	645	1698	2830
Williamson	2000	147	440	1099	121	--	--	268	440	1099
Williamson	2010	100	633	2383	167	--	--	267	633	2383

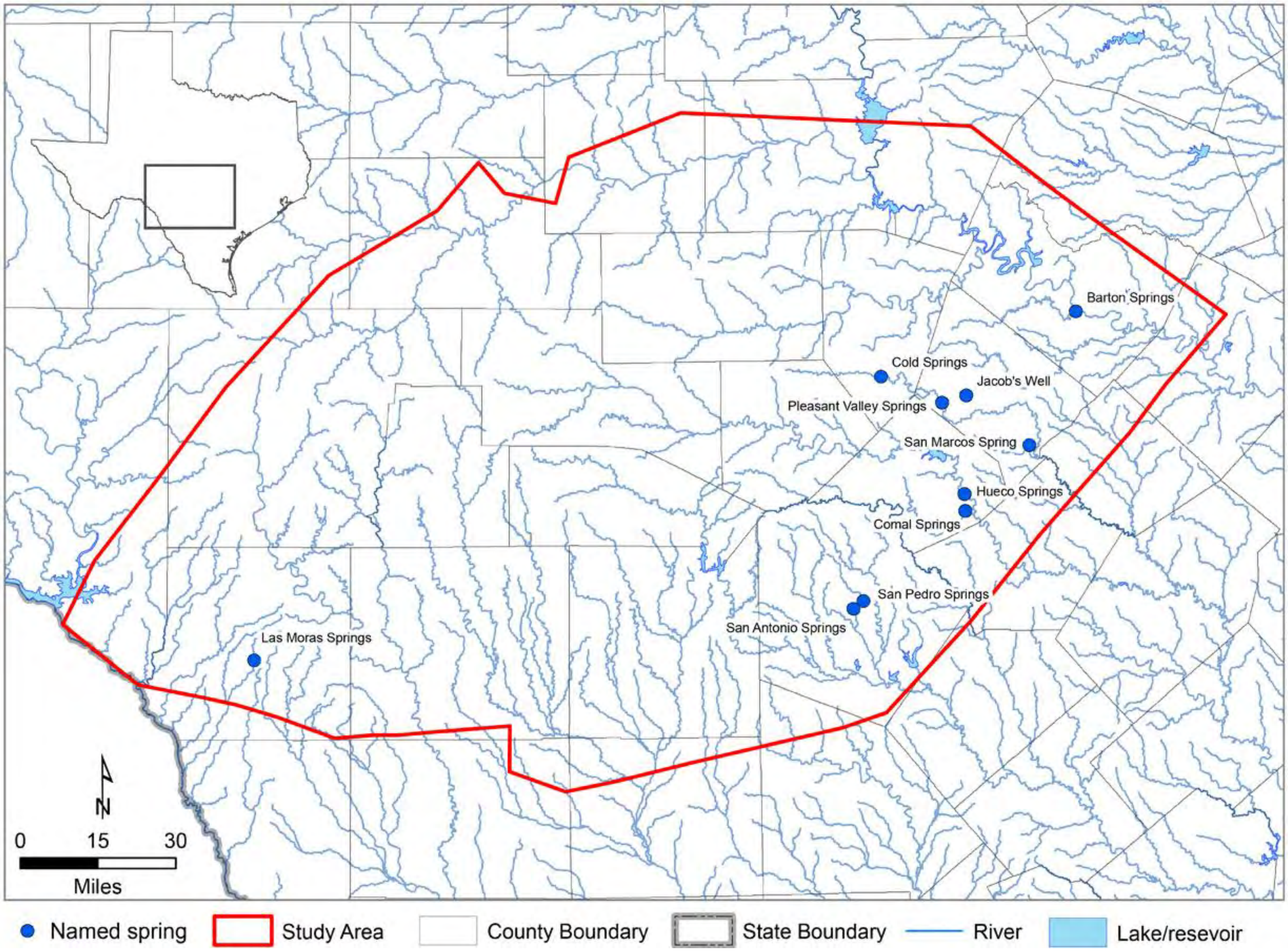

Figure 4.6.1 Selected named springs in the study area.

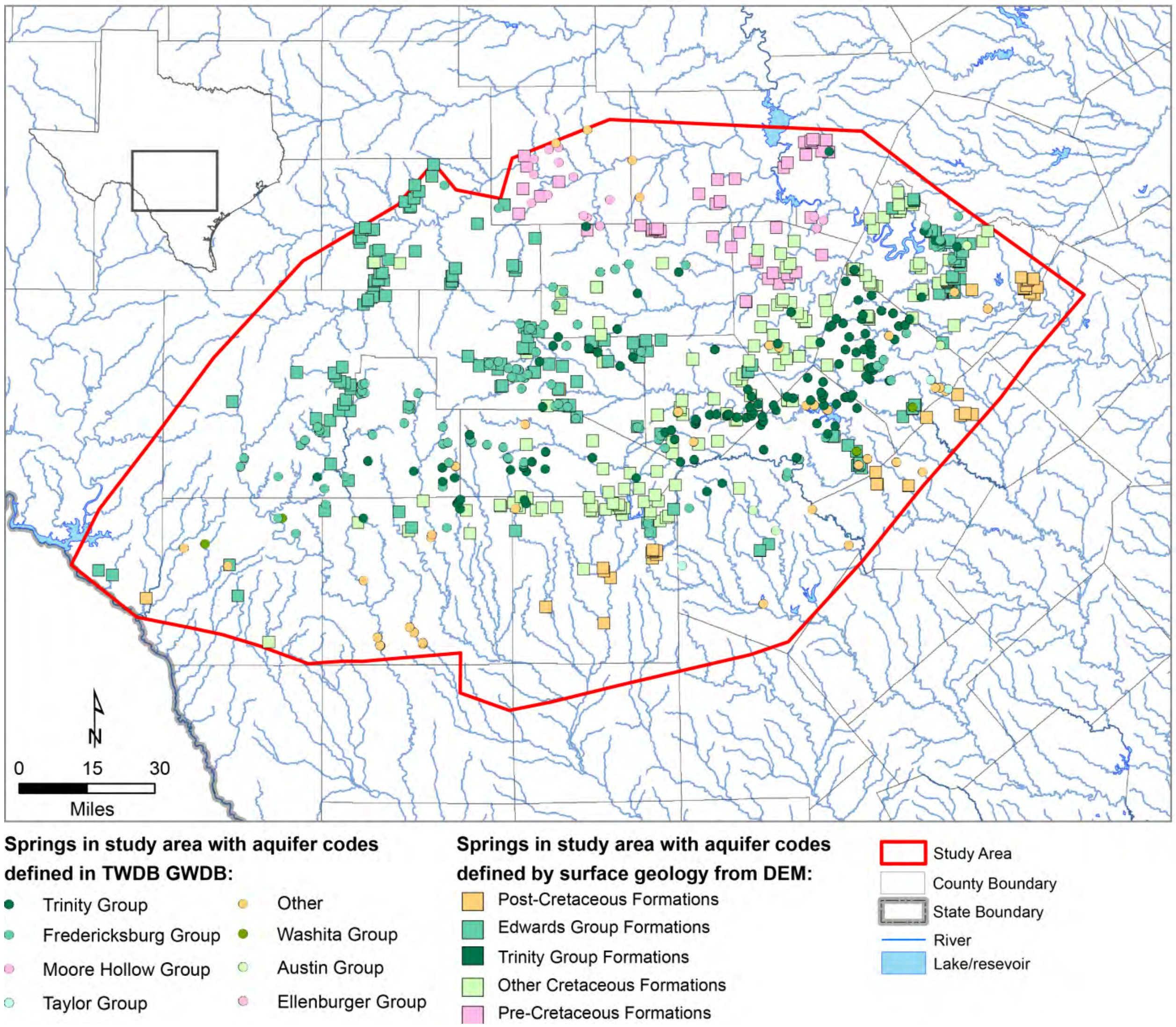

Figure 4.6.2 **Springs located in study area. Circle symbology indicates the geological group from which the spring discharges water as specified in the TWDB GWDB. Springs in the TWDB GWDB which did not have a discharge unit specified were assigned the unit of the surface geology at that location according to the GAT.**

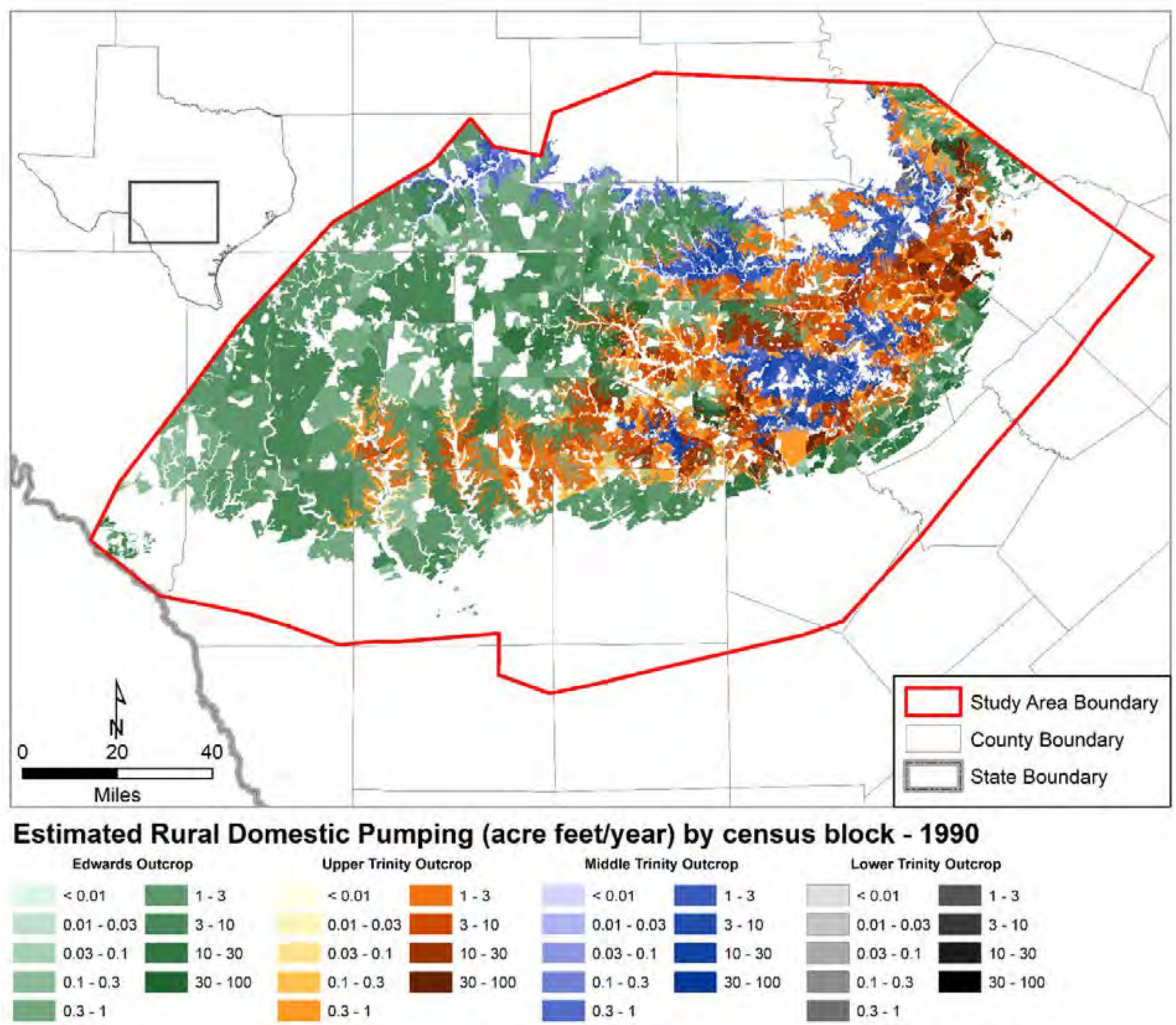

Figure 4.6.3 **Estimated rural domestic pumping by hydrostratigraphic unit outcrop in the study area, based on 1990 census block rural population data (Manson et al., 2017).**

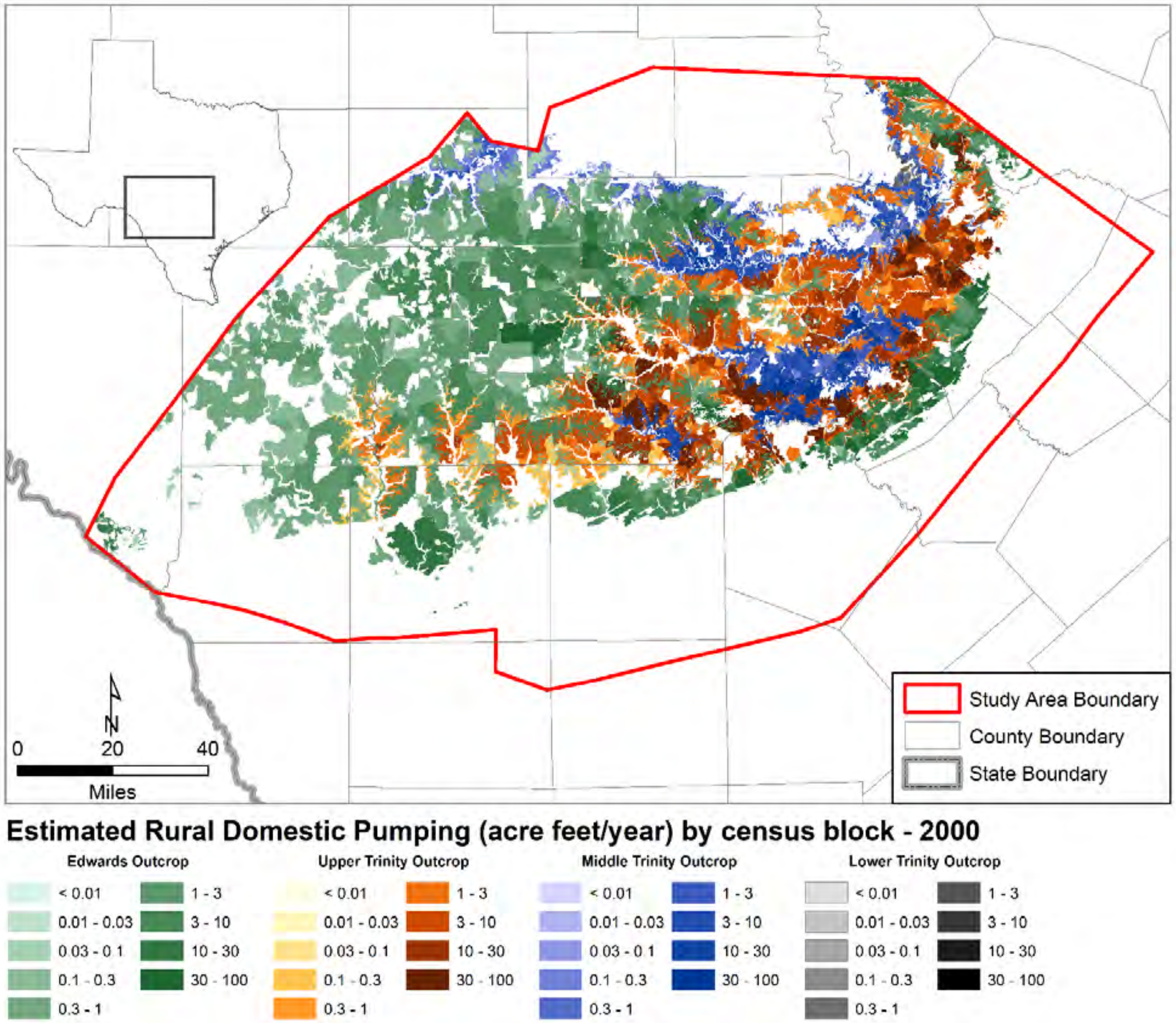

Figure 4.6.4 **Estimated rural domestic pumping by hydrostratigraphic unit outcrop in the study area, based on 2000 census block rural population data (Manson et al., 2017).**

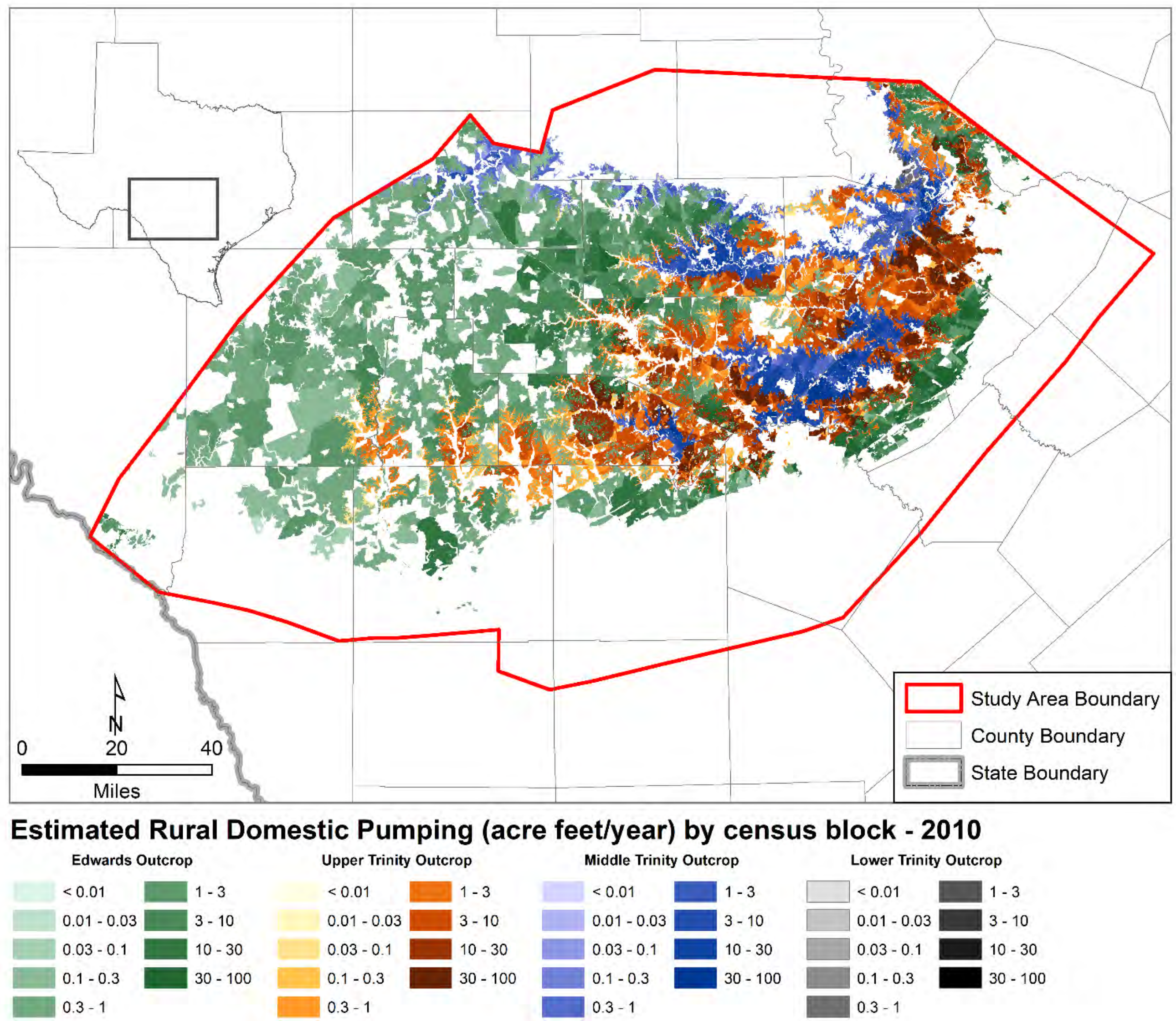

Figure 4.6.5 **Estimated rural domestic pumping by hydrostratigraphic unit outcrop in the study area, based on 2010 census block rural population data (Manson et al., 2017).**

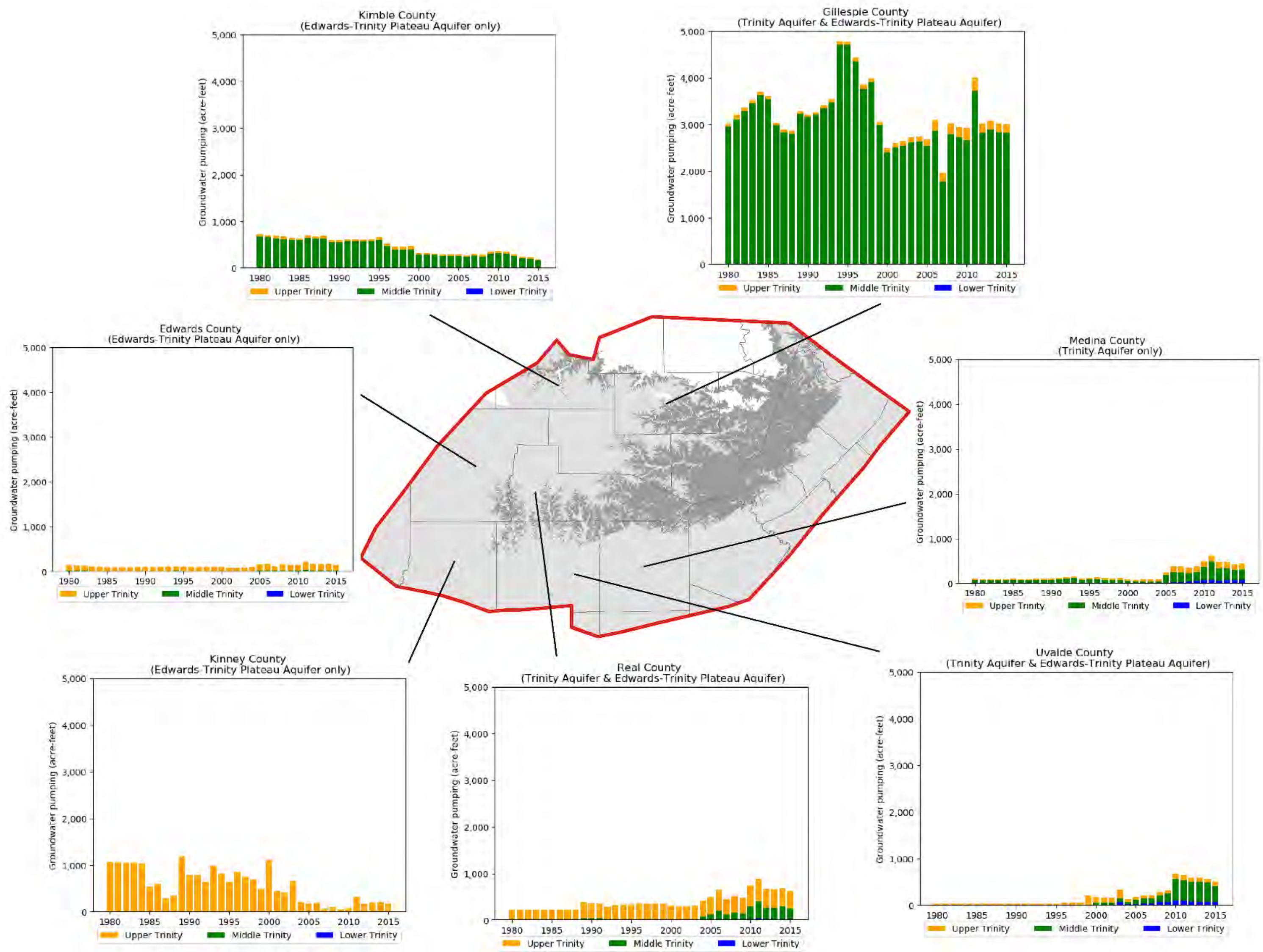

Figure 4.6.6 **Estimated total pumping by hydrostratigraphic unit in the western/west-central counties of the study area.**

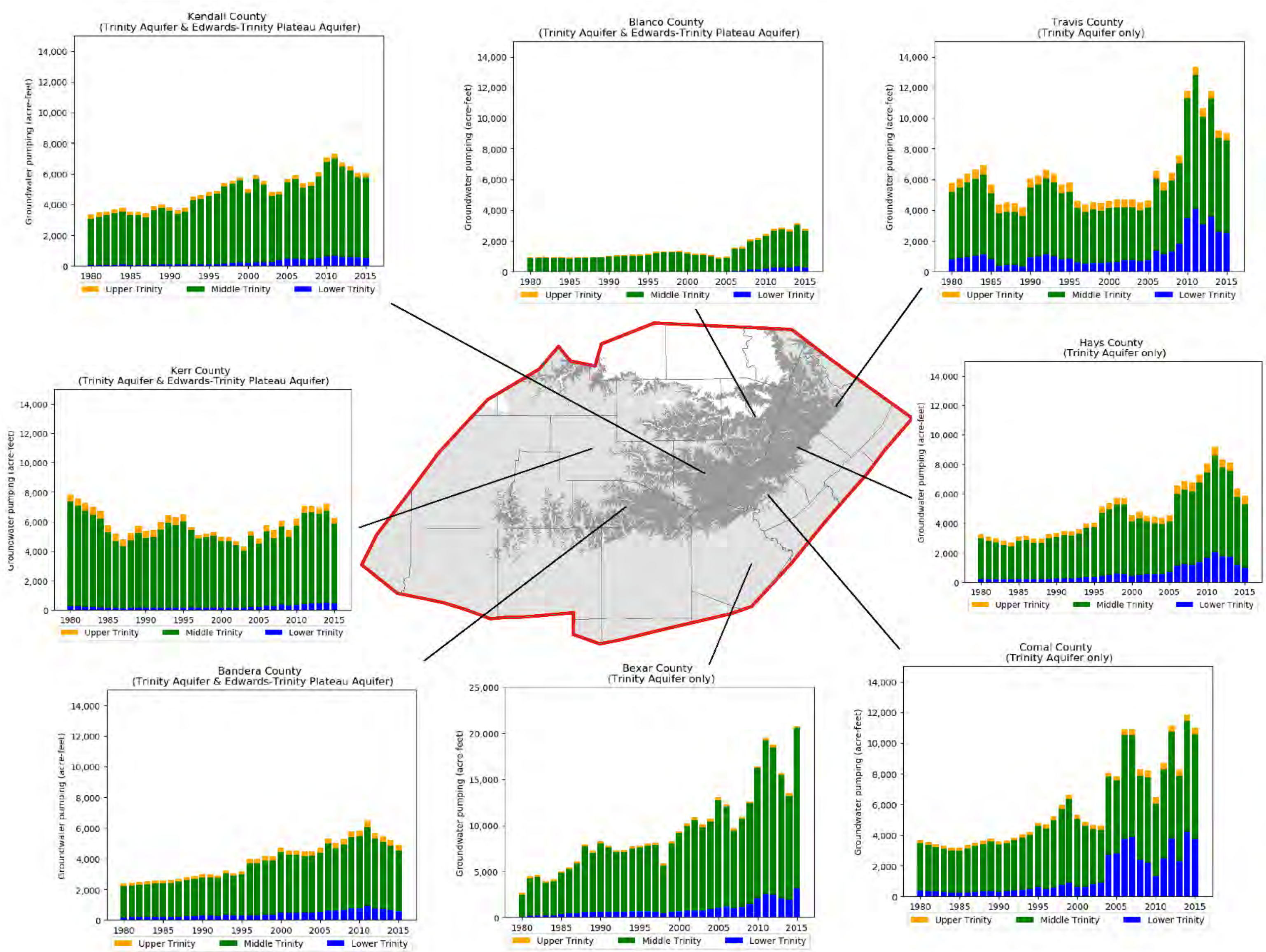

Figure 4.6.7 **Estimated total pumping by hydrostratigraphic unit in the eastern/east-central counties of the study area.**

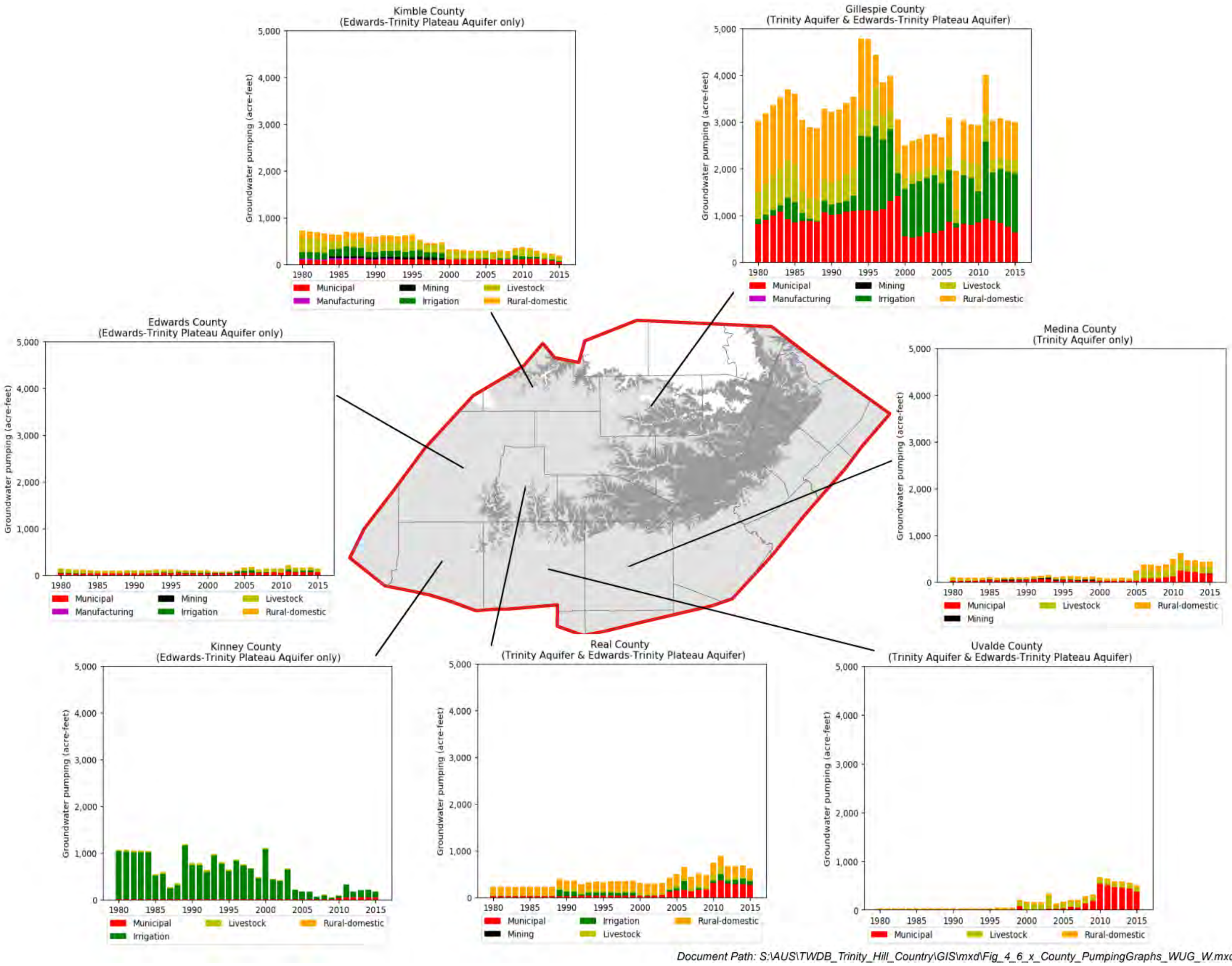

Figure 4.6.8 **Estimated total pumping by water-use category in the western/west-central counties of the study area.**

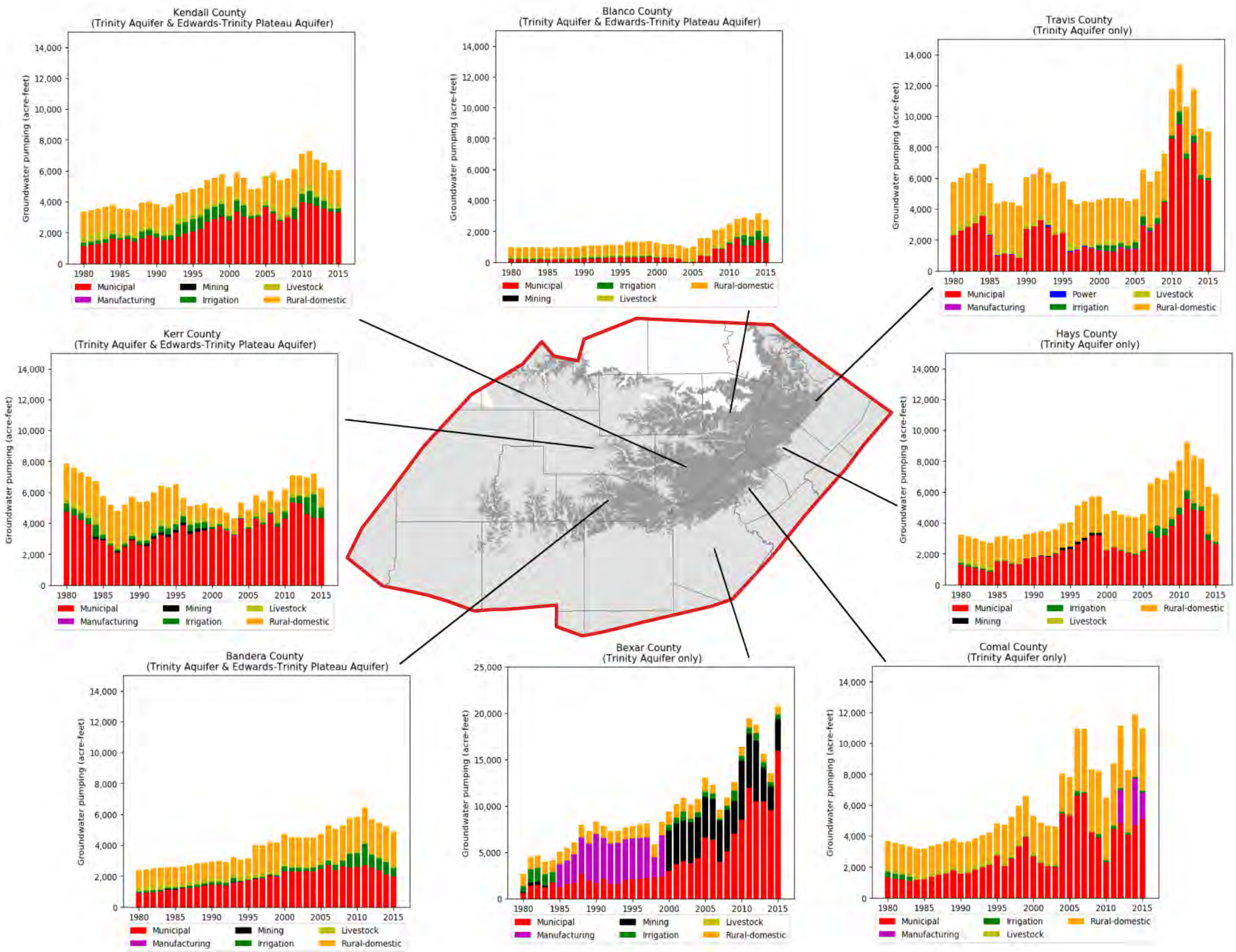

Figure 4.6.9 **Estimated total pumping by water-use category in the eastern/east-central counties of the study area.**

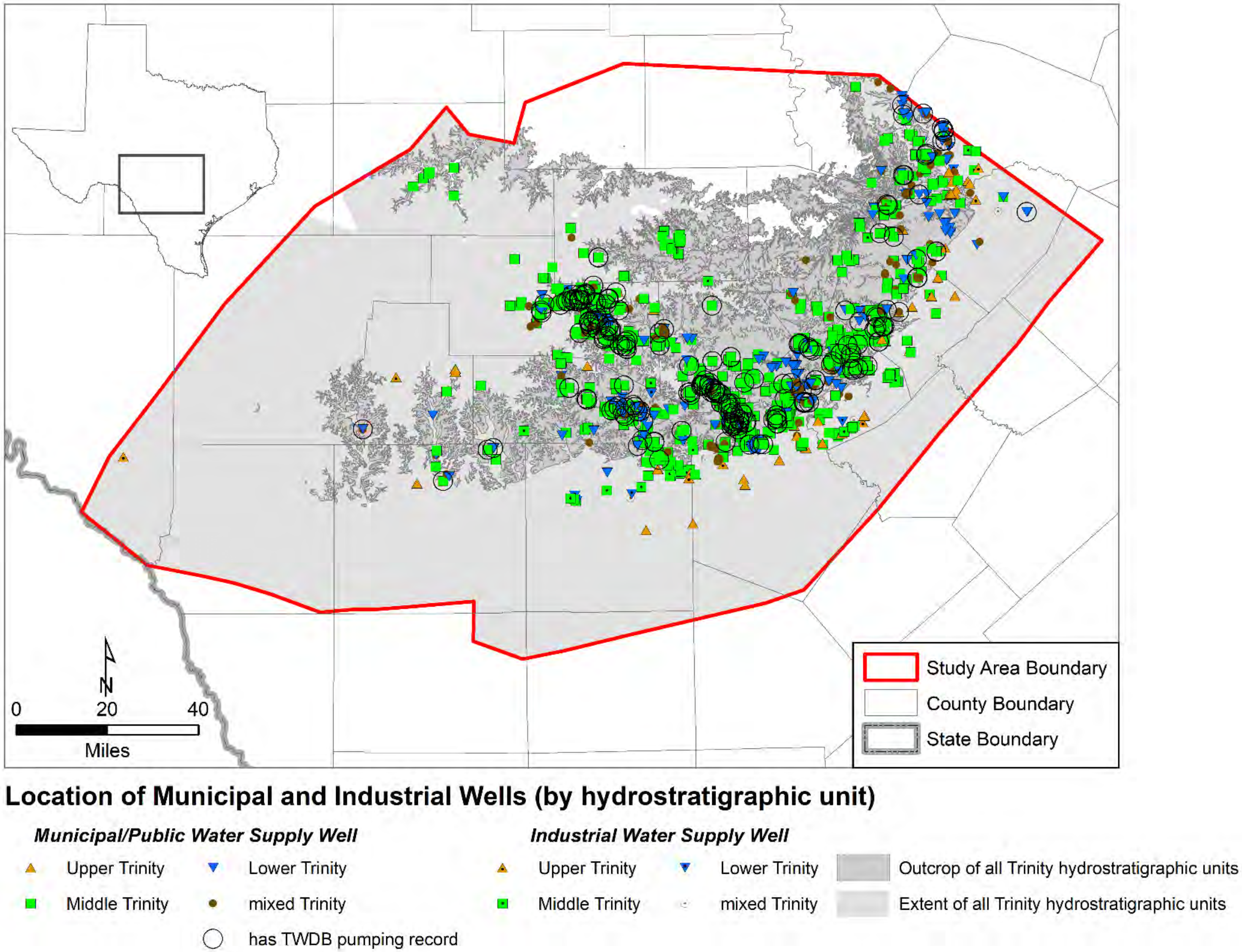

Figure 4.6.10 Locations of municipal and industrial wells in the study area by hydrostratigraphic unit

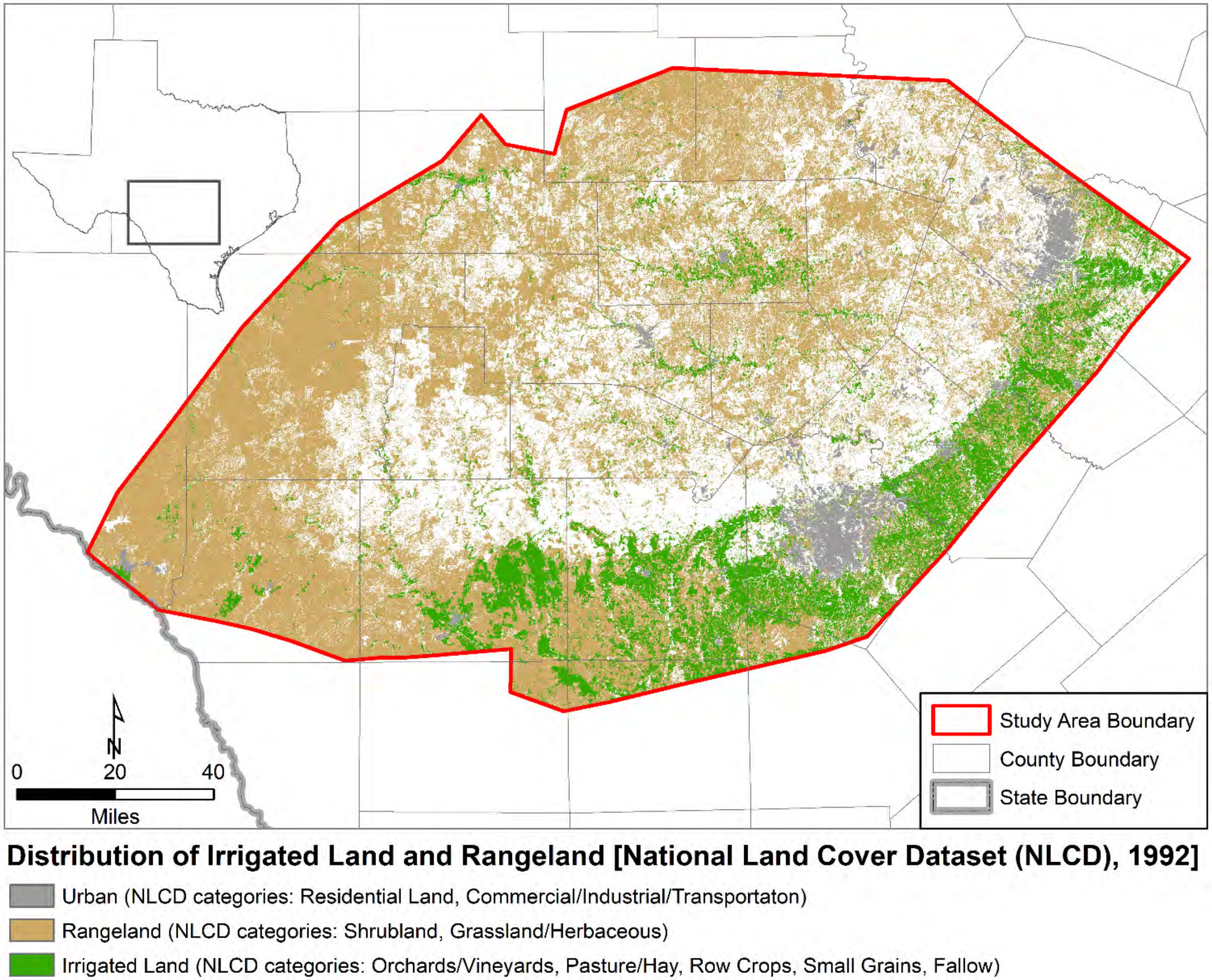

Figure 4.6.11 Estimated distribution of irrigated land and rangeland based on Vogelmann et al. (2001).

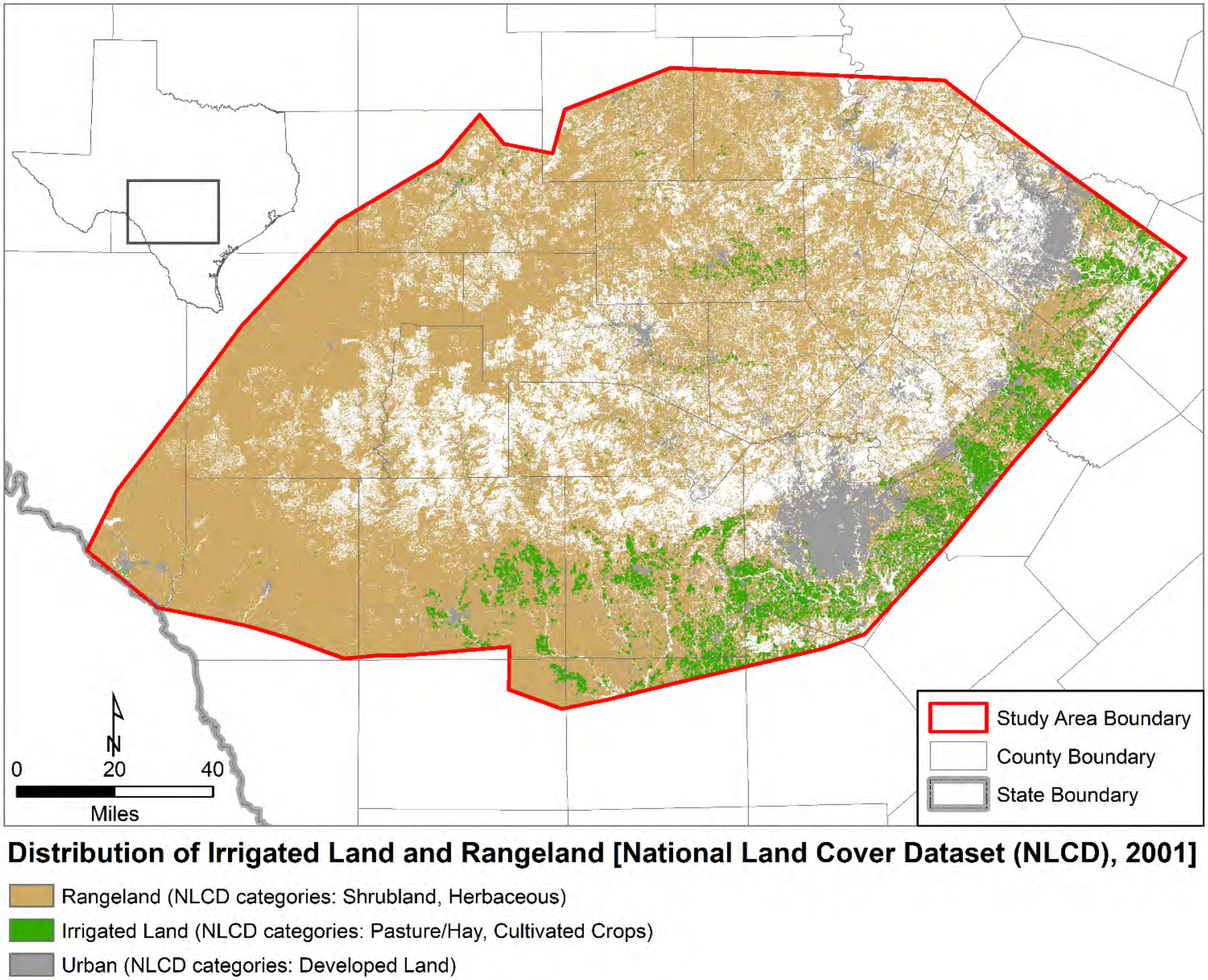

Figure 4.6.12 Estimated distribution of irrigated land and rangeland based on Homer et al. (2007).

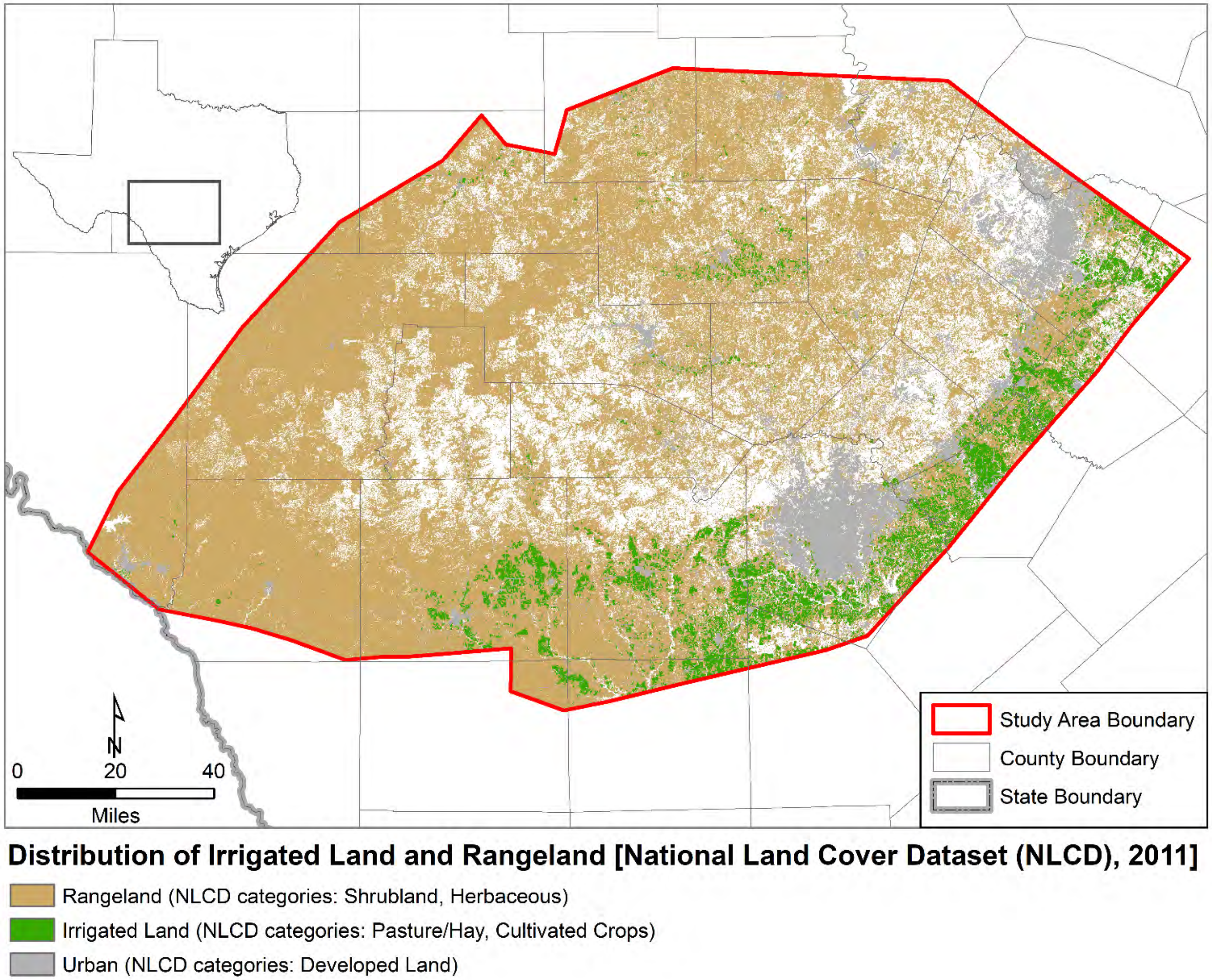

Figure 4.6.13 Estimated distribution of irrigated land and rangeland based on Homer et al. (2015).

4.7 Water Quality

This section describes the spatial and temporal trends of groundwater quality in the Trinity and Edwards-Trinity aquifers within the revised conceptual model area. Water quality data were extracted from the TWDB database (TWDB, 2018) and National Water Quality Monitoring Council database (WQP, 2018). The work builds on the analysis of spatial groundwater-quality trends described by Jones et al. (2011). Because the study area for the revised conceptual model includes areas west and south of those considered in Jones et al. (2011), the geochemical interpretations have been updated to include the expanded conceptual model study area.

4.7.1 General Water Quality

The description of water quality is based on water-chemistry characteristics for the following hydrostratigraphic units: Upper, Middle, and Lower Trinity Aquifer, Edwards-Trinity in the plateau region, and the Edwards and Trinity aquifers in the Balcones Fault Zone. The distribution of total dissolved solids (TDS) in the Trinity and Edward-Trinity is shown in Figure 4.7.1. Figure 4.7.2 through Figure 4.7.4 show TDS concentrations for the Upper, Middle, and Lower Trinity Aquifer, respectively. The TDS content of water in these hydrostratigraphic units is generally less than 500 mg/L in updip and western portions of the revised model area but increases downdip to the south and east. Figure 4.7.5 is a cumulative distribution plot of TDS by hydrostratigraphic unit. The median (50 percentile) TDS in the Upper and Middle Trinity, Edwards-Trinity Plateau region, and Edwards and Trinity aquifers in the Balcones Fault Zone is in the range of 300 to 500 mg/L. The TDS of water in the Lower Trinity is significantly more saline with TDS exceeding 1,000 mg/L in Comal, Blanco, Hays, and Travis counties. Water in the Edwards-Trinity Balcones area has a wide range of TDS with significantly higher TDS in the downdip areas where water may mix with saline water in the Edwards Aquifer (Figure 4.7.1).

Figure 4.7.6 shows a Piper diagram of the major ion composition of water in the Trinity Aquifer and Edwards-Trinity in the plateau region. The water composition ranges in type from calcium-magnesium carbonate in the updip and shallower portions of the Trinity Aquifer and in the Edwards-Trinity Plateau, to calcium-magnesium sulfate and sodium chloride in areas with the highest TDS. This relationship in the Trinity Aquifer is illustrated in Figure 4.7.7 which shows the sulfate and chloride concentrations in the Trinity Aquifer versus TDS. The sulfate concentration increases at nearly the rate as the TDS. The chloride concentration also generally increases with TDS although the trend is less consistent than that of sulfate. These trends are consistent with dissolution of dolostone and gypsum in the Glen Rose Limestone as well as mixing with sodium chloride brine in the deeper portions of the Trinity Aquifer, as noted by Jones et al. (2011). With one exception, a similar trend in increase sulfate and chloride with depth is not seen in the Edwards-Trinity Plateau area, as illustrated in Figure 4.7.8. The only exception is for the well with a depth of 753 ft with sulfate concentrations ranging from 1,300 to 1,600 mg/L. The chloride concentration in this well was relatively low suggesting that the water is locally affected by gypsum-bearing rocks. The well in the Edward-Trinity plateau region with the highest chloride concentration was only 74 ft deep and is probably affected by a local surface source of salty water.

4.7.2 Water Quality Trends

Trends in water quality were evaluated based on review of water-quality data from the Texas Water Development Board for wells with multiple data extending over at least 10 years. Figure 4.7.9 shows time histories of TDS for selected wells described as being completed in the Trinity Aquifer, Edwards-Trinity Plateau region, and Edwards-Trinity Balcones region. No significant trends were identified based on the available data. Given the increase in TDS with depth in the Trinity Aquifer and increasing water production from the Trinity Aquifer, TDS concentrations could increase in the future in areas of heavy groundwater use.

4.7.3 Contribution of Trinity Aquifer to the Edwards Aquifer Based on Water Chemistry

Upward leakage from the Trinity Aquifer into the Edwards Aquifer has been suggested as a potential source of elevated TDS in the Edwards Aquifer. Clark and Journey (2006) distinguished Trinity Aquifer water from Edwards Aquifer water along flow paths in Medina and Uvalde counties on the basis of Trinity Aquifer water being more mineralized than Edwards Aquifer water in these areas. Musgrove et al. (2010) conducted an analysis of groundwater-quality characteristics of the Edwards Aquifer and portions of the Trinity Aquifer in the San Antonio Segment of the Edwards Aquifer based on National Water-Quality Assessment Program (NAWQA) data from 1996 to 2006. They tentatively identified mixing of Trinity Aquifer water (as opposed to Edwards Aquifer Saline zone water) with Edwards Aquifer water on the basis of increasing magnesium-to-sodium and sulfate-to-chloride ratios, with these ratios increasing with increased contribution from the Trinity Aquifer. If correct, the Musgrove et al. (2010) interpretation would imply that the greatest contributions of Trinity Aquifer water to the Edwards Aquifer occur within the unconfined portion of the Edwards Aquifer within the San Antonio Segment (Figure 4.7.10). This finding may be attributed to the more intense faulting and vertical conduit development between the Trinity and Edwards Aquifer strata in the unconfined portion relative to the confined portion of the Edwards Aquifer. This interpretation is consistent with the general water-quality trend described in the preceding section that the TDS and salinity of the Trinity Aquifer water increase downdip and the finding by Clark and Journey (2006) that Trinity Aquifer water is more mineralized than Edwards Aquifer water in the Balcones Fault Zone.

Darling (2016) published findings of a geochemical investigation to elucidate interactions between the Trinity and Edwards aquifers in Travis, Hays, and Comal counties. The Darling study investigated trends in major ions and isotopic indicators as a means to identify inter-aquifer flow between the Trinity and Edwards aquifers. Darling concluded that the general similarity in major ion chemistry between Upper Trinity Aquifer water and Edwards Aquifer water in the study area would make identifying inter-aquifer flow based on major ion chemistry difficult or impossible. This conclusion conflicts with the findings of Musgrove et al. (2010) and Clark and Journey (2006) from the Balcones Fault Zone near San Antonio.

With respect to isotopic indicators, Darling (2016) found a significant overlap between the stable oxygen isotope ratios ($\delta^{18}O$) and stable hydrogen isotope ratios ($\delta^{2}H$) in water samples from the Upper Trinity and Edwards aquifer in his study area. He thus concluded that stable oxygen and hydrogen isotopes were not good indicators of flow between these aquifers. This is not surprising because groundwater in both aquifers originates from meteoric recharge with little difference in elevation and little opportunity for surface evaporation to modify the isotopic ratios.

Isotopic data reported by Fahlquist and Ardis (2004) for the Trinity and Edwards aquifers in south-central Texas west of the Darling (2016) study, showed more contrast in the stable oxygen and hydrogen isotopy for these two aquifers (Figure 4.7.11). As illustrated in Figure 4.7.11, a number of samples from the unconfined portion of the Edwards Aquifer fall below the meteoric water line and are isotopically heavier (less negative) than samples from the Trinity Aquifer, indicating that these stable isotopes could be indicators of interaction between the Trinity and Edwards aquifer, at least in the south-central portion of the revised Hill Country GAM study area. More data would be needed to confirm this conjecture.

Darling (2016) also investigated the use of strontium isotope ratios to distinguish between Trinity and Edwards aquifer water, but found the results inconclusive. Carbon-14 and Tritium age dating appeared to have more potential. In most areas along the downdip portion of the study area, groundwater in the Trinity Aquifer would be expected to be much older than more recently recharged water in the Edwards Aquifer. Thus, Trinity Aquifer water would be more depleted in Carbon-14 (half-life 5,730 years) than Edwards Aquifer water. Tritium (half-life 12.4 years) would be expected to be largely absent in deeper portions of the Trinity Aquifer, as indicated by tritium analyses reported by Fahlquist and Ardis (2004). Thus, finding lower than expected carbon-14 and tritium activities in Edwards Aquifer water could suggest a contribution from the Trinity Aquifer. However, unless the expected values in the unadulterated Edwards Aquifer were well known, using carbon-14 and tritium as indicators of contributions from the Trinity Aquifer would still be subject to large uncertainties.

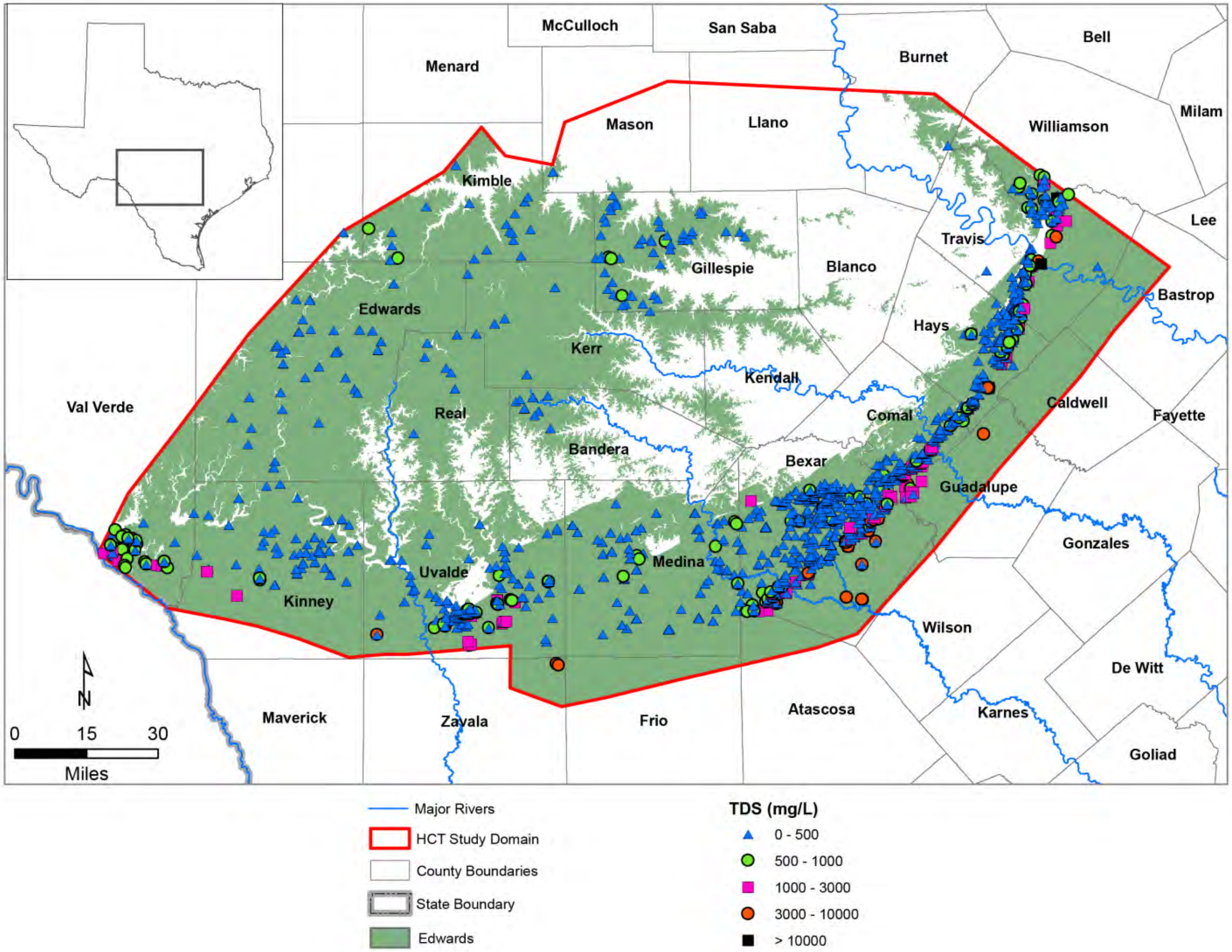

Figure 4.7.1 **Total Dissolved Solids (TDS) in the Trinity Aquifer and Edwards-Trinity Aquifer within the revised Hill Country GAM study area.**

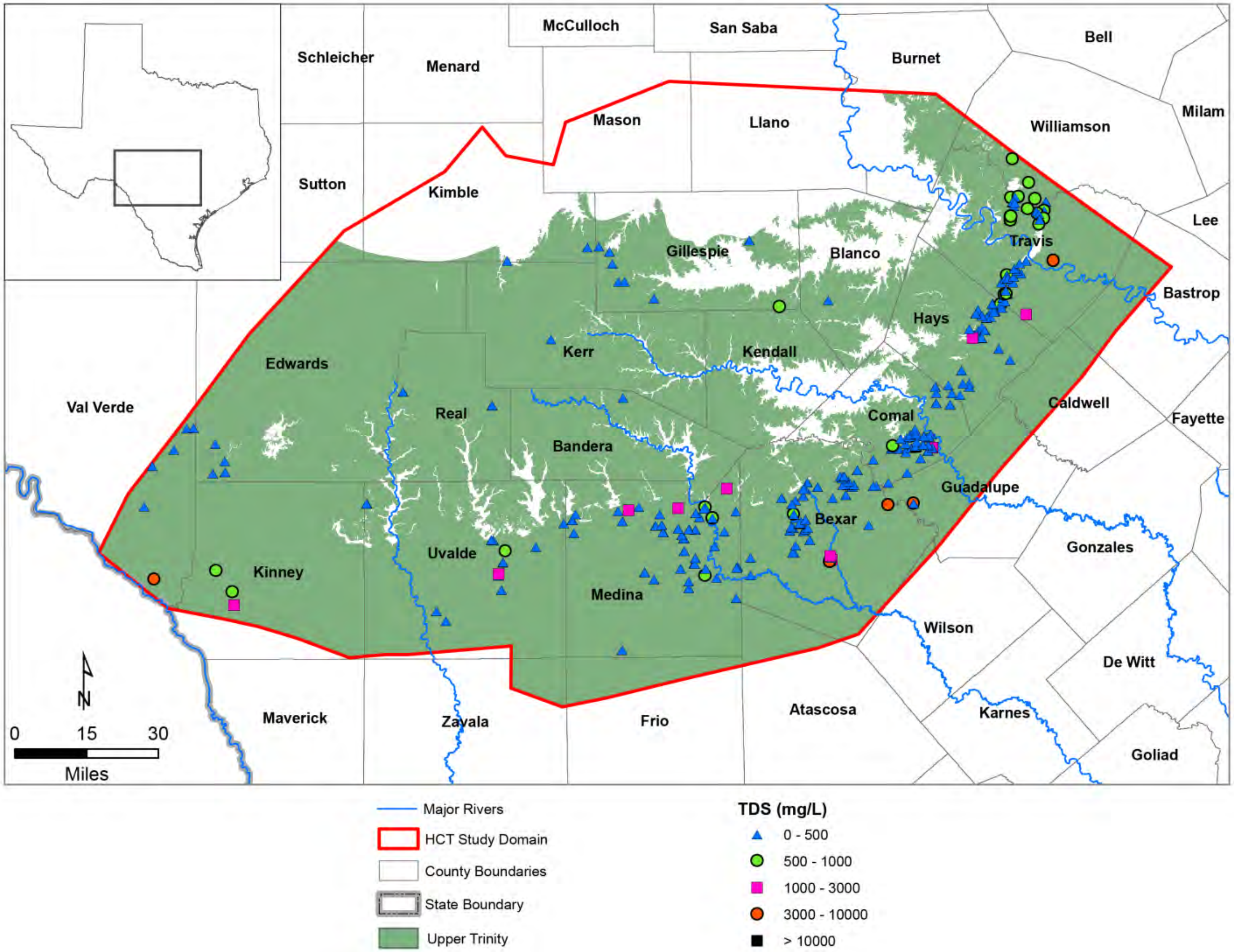

Figure 4.7.2 **Total Dissolved Solids (TDS) in the Upper Trinity within the revised Hill Country GAM study area.**

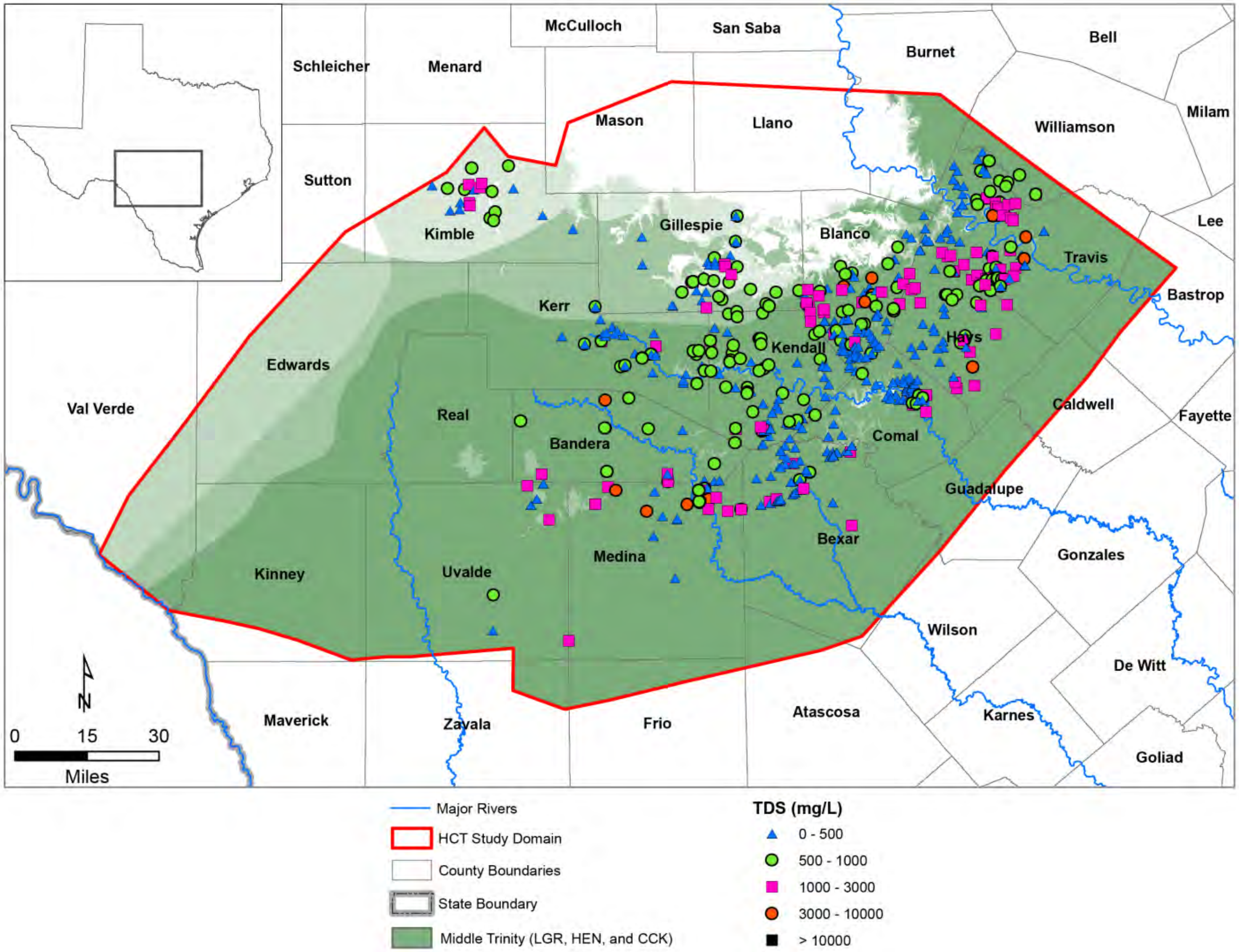

Figure 4.7.3 Total Dissolved Solids (TDS) in the Middle Trinity within the revised Hill Country GAM study area.

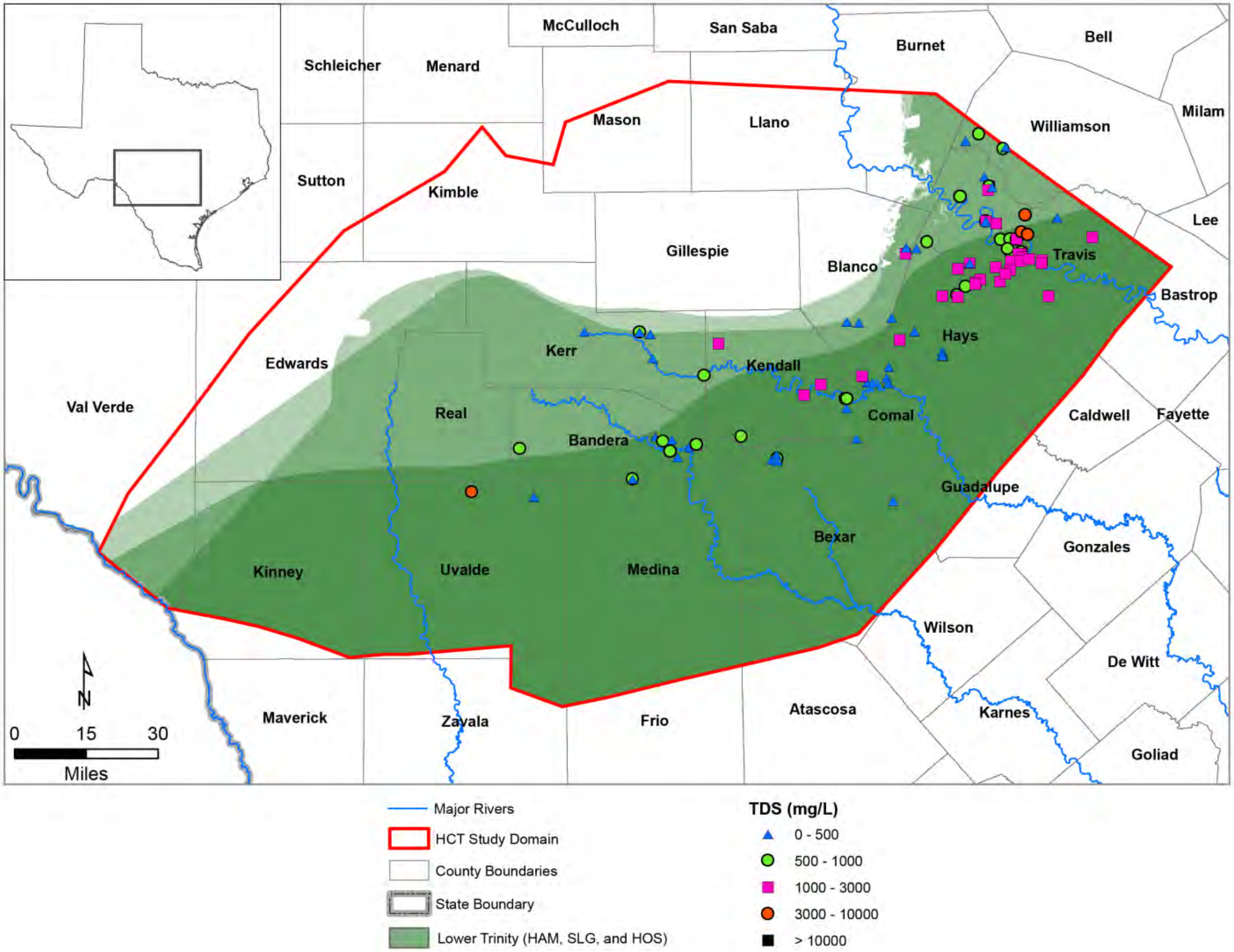

Figure 4.7.4 **Total Dissolved Solids (TDS) in the Lower Trinity within the revised Hill Country GAM study area.**

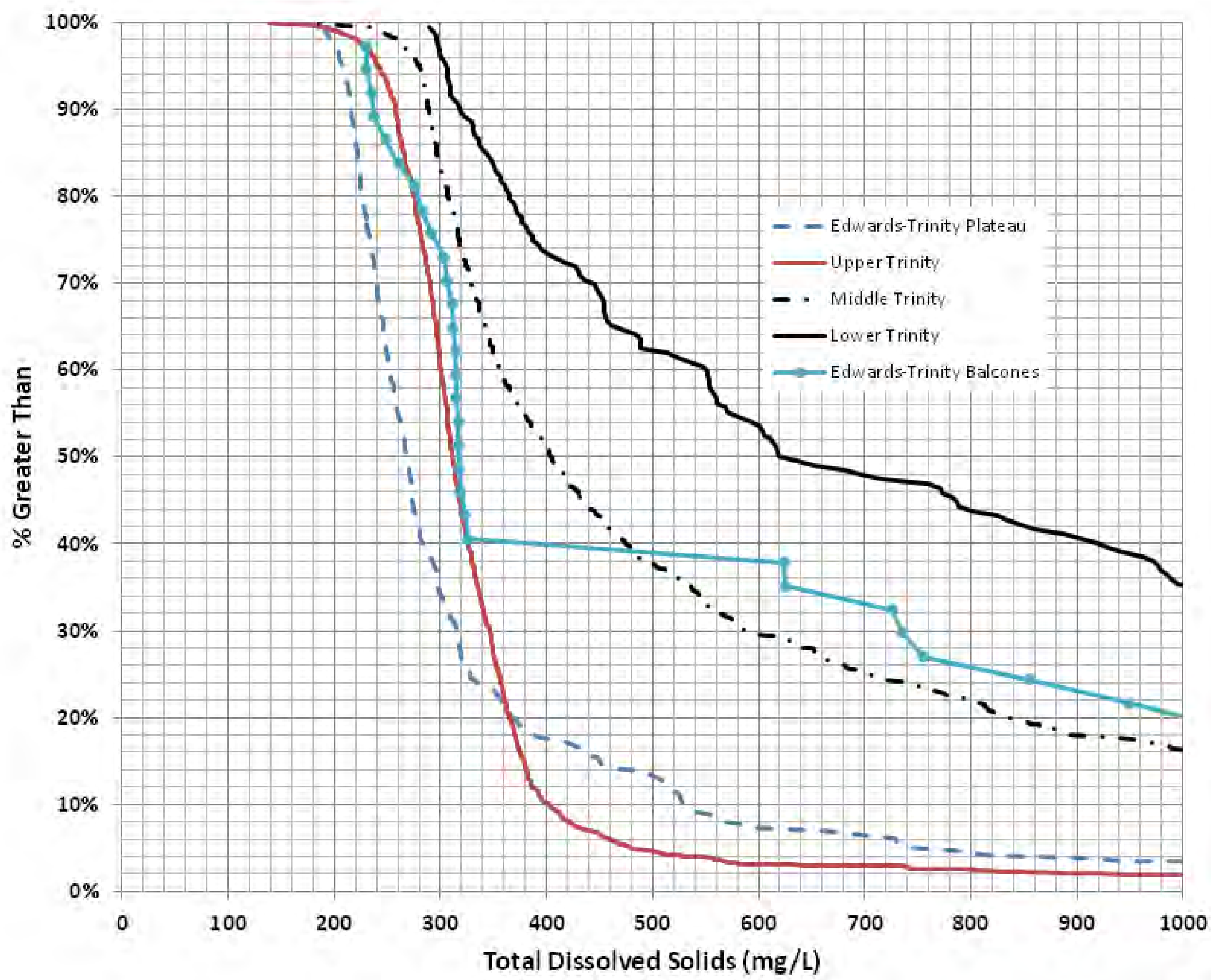

Figure 4.7.5 Cumulative Distribution of TDS in the Upper, Middle, and Lower Trinity Aquifer, Edwards-Trinity Plateau Region, and Edwards and Trinity aquifers in the Balcones Fault Zone.

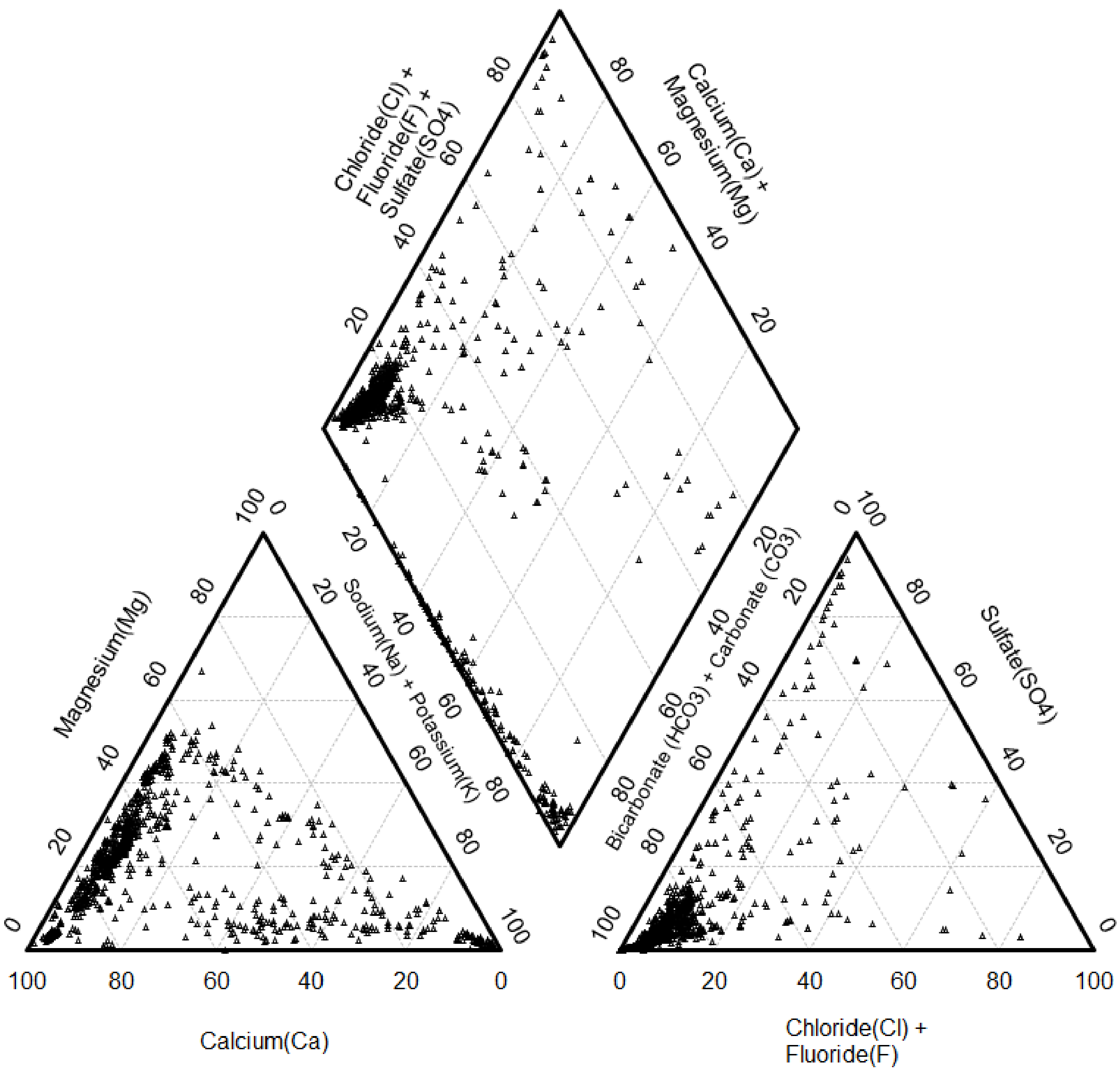

Figure 4.7.6 Piper diagram showcasing the major ion composition of groundwater in the Trinity Aquifer and Edwards-Trinity Plateau area.

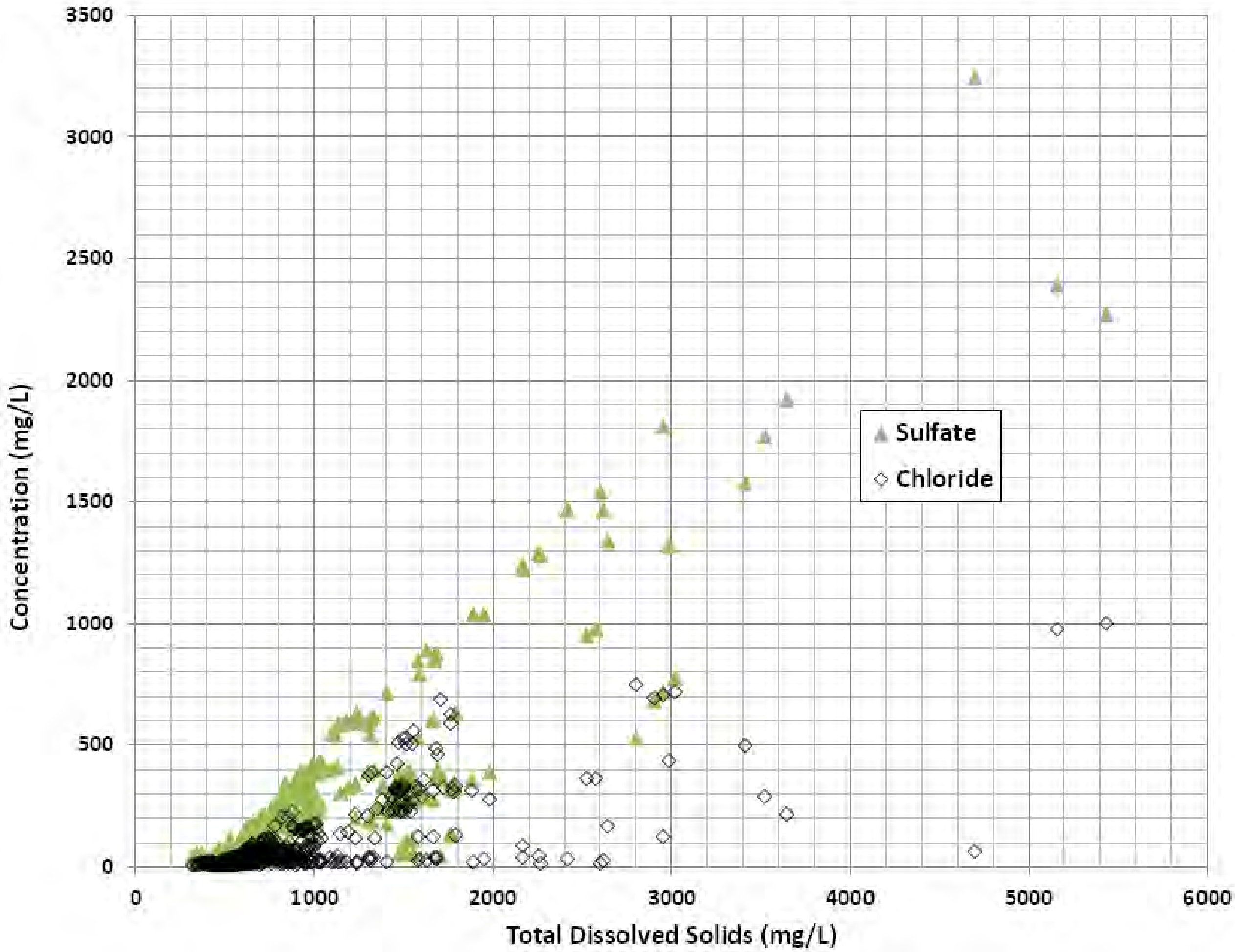

Figure 4.7.7 Sulfate and chloride concentrations versus Total Dissolved Solids in the Trinity Aquifer.

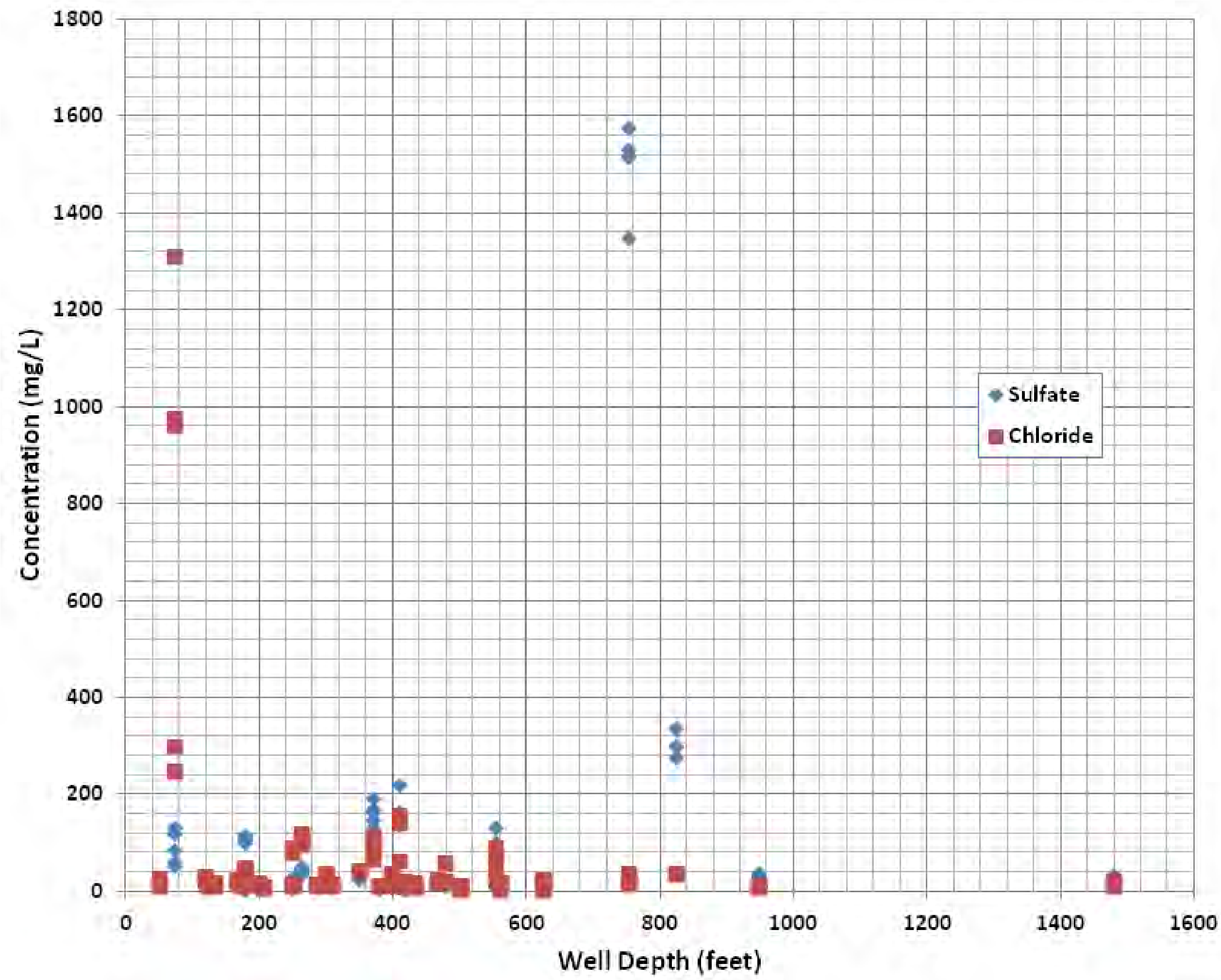

Figure 4.7.8 Sulfate and chloride concentrations versus depth in the Edwards-Trinity Plateau area.

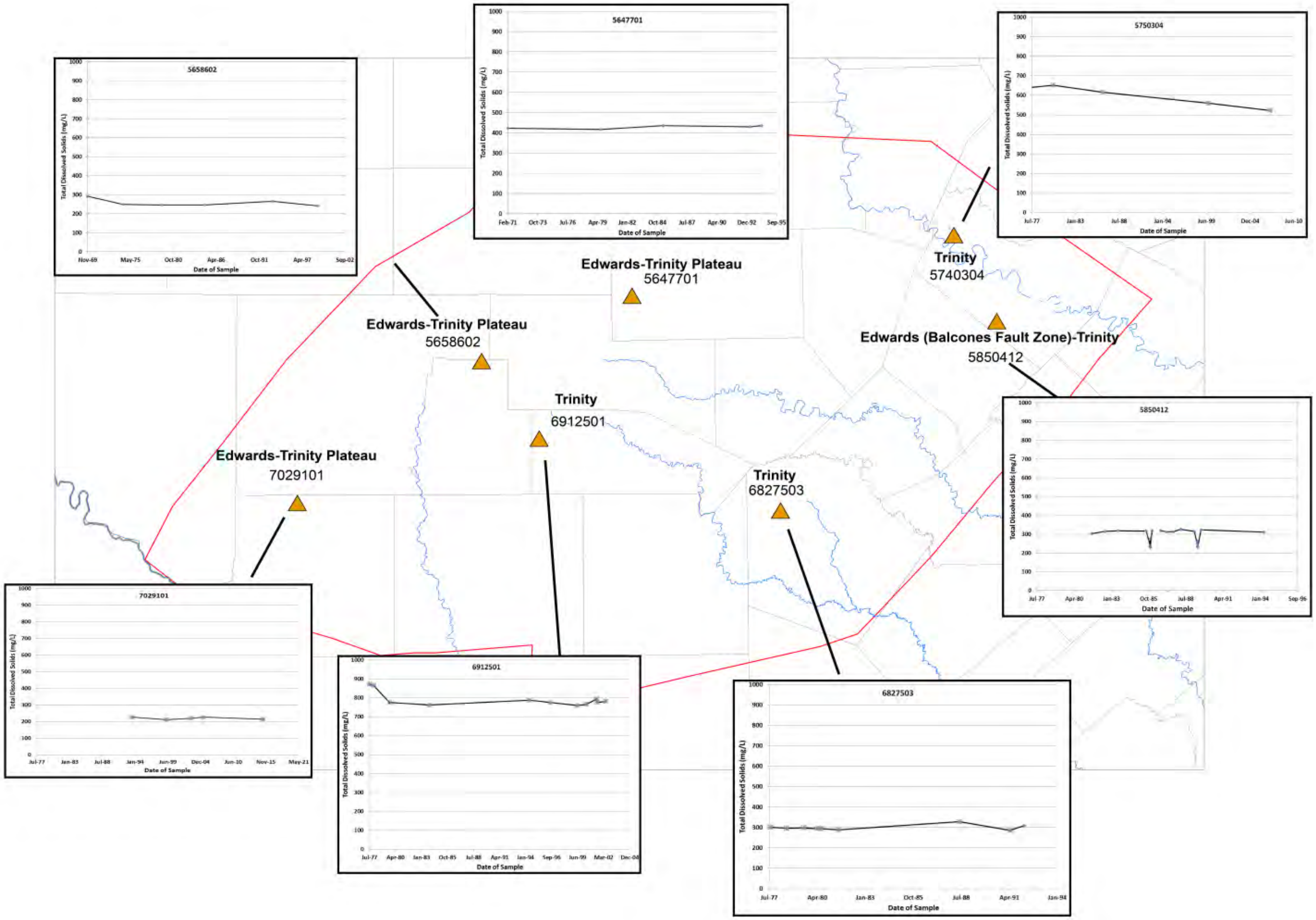

Figure 4.7.9 Time histories of TDS in selected wells within the revised Hill Country Model domain completed in the Trinity Aquifer, Edwards-Trinity Plateau Region, and Edwards and Trinity aquifers in the Balcones Fault Zone.

Geochemical Evolution Processes 25

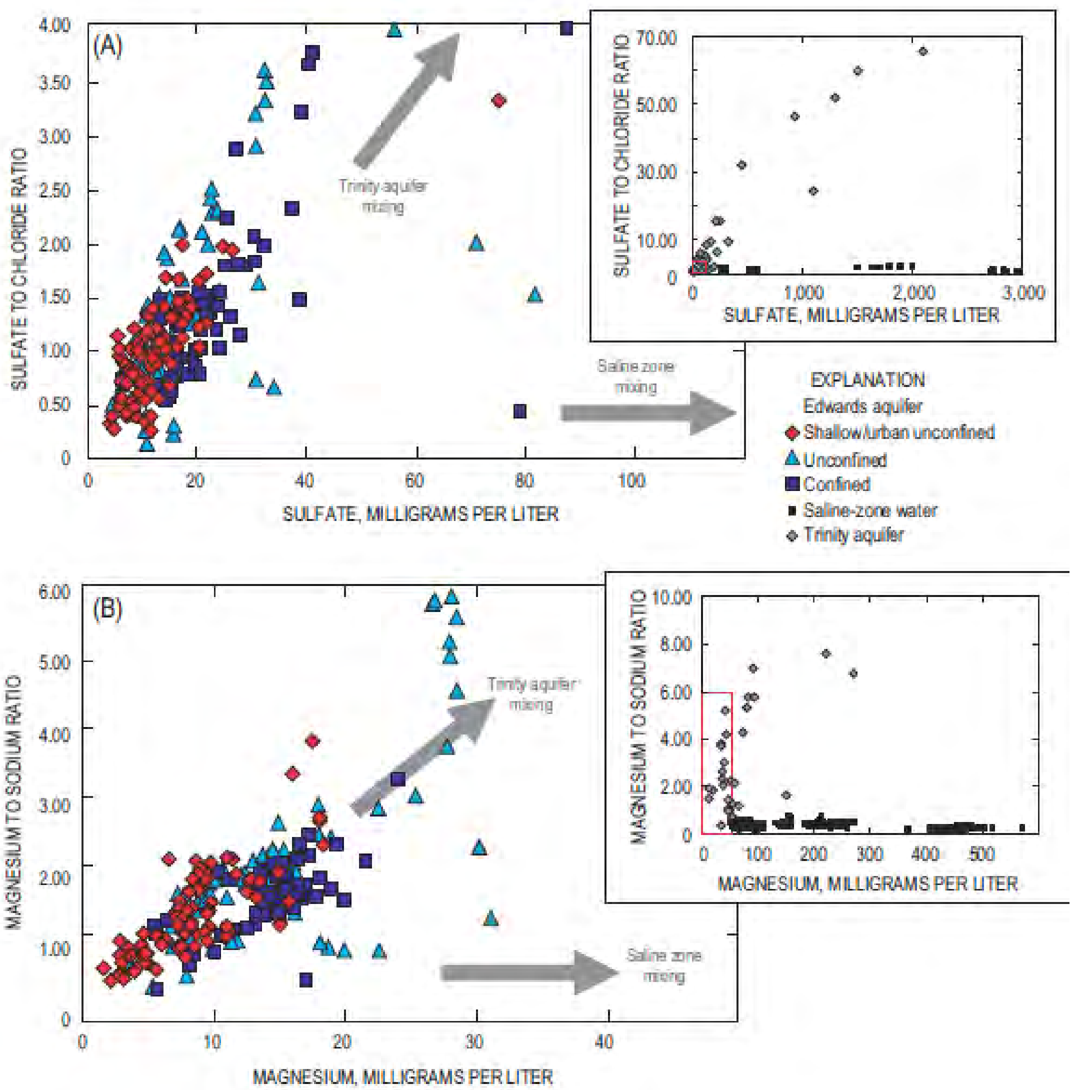

Figure 12. Relation between (A) sulfate to chloride ratio and sulfate concentration, and (B) magnesium to sodium ratio and magnesium concentration for groundwater samples collected from shallow/urban unconfined, unconfined, and confined parts of the San Antonio segment of the Edwards aquifer, south-central Texas, 1996–2006.

Trinity aquifer data from U.S. Geological Survey (2009) and saline-zone groundwater data from San Antonio Water System (Hydrogeologic Studies and Assessment Division, written commun., 2009). Red-bounded boxes in inserts denote scale expanded in (A) and (B). Arrows on (A) and (B) highlight mixing pathways with underlying Trinity aquifer groundwater (median sulfate to chloride ratio = 4.9; sulfate = 130 milligrams per liter (mg/L); magnesium to sodium ratio = 2.2; magnesium = 48 mg/L; n = 31) and downdip saline-zone groundwater in Bexar, Comal, and Hays Counties (median sulfate to chloride ratio = 1.04, n = 376; sulfate = 1,649 mg/L, n = 525; magnesium to sodium ratio = 0.34, n = 395; magnesium = 371 mg/L, n = 371).

Figure 4.7.10 Mixing between the Trinity Aquifer and Edwards Aquifer interpreted based on major ion ratios (taken from Musgrove et al., 2010).

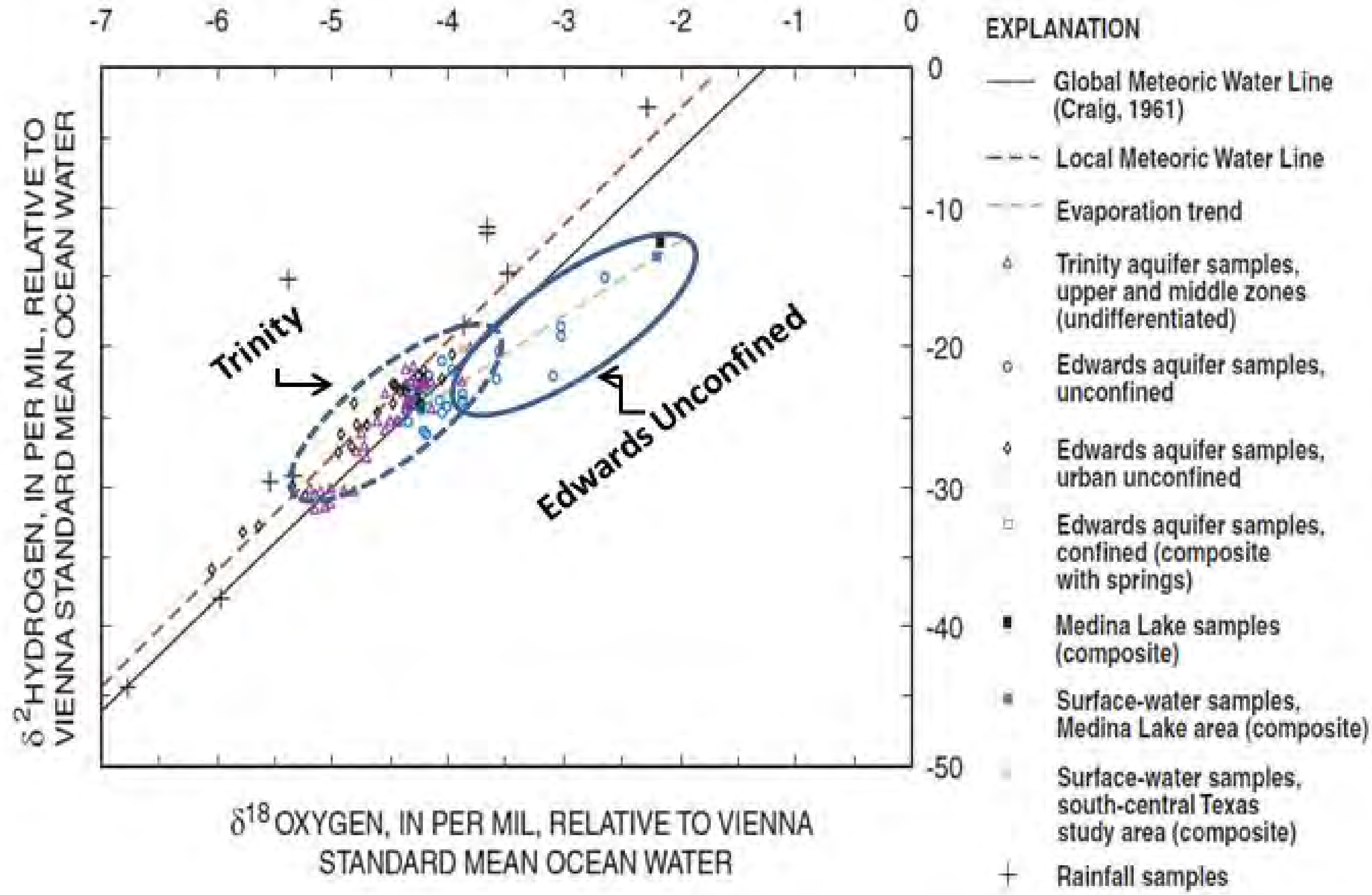

Figure 4.7.11 **Stable hydrogen and oxygen isotope ratios in water samples from wells in the Trinity and Edwards aquifers, and lakes in south-central Texas (taken from Fahlquist and Ardis, 2004).**

5.0 Conceptual Model of Flow in the Aquifer

The conceptual model of groundwater flow in the HCT Aquifer is based on the hydrogeologic setting described in Section 4.0. The conceptual model is a simplified representation of the hydrogeological features that govern groundwater flow in the aquifer. It includes the hydrostratigraphy, hydrogeologic framework, hydraulic properties, hydrologic boundaries, recharge, and discharge. Groundwater flow varies significantly with location across the aquifer. This variability results mostly from its complex geologic structure and changes in formation facies.

5.1 Overview

Conceptual models are developed to provide the best understanding of groundwater flow in the aquifer. When precipitation falls on areas that recharge the aquifers, much of the water either evapotranspires or runs off into local streams and eventually discharges through major streams out of the study area. However, some of the precipitation infiltrates into and recharges the underlying aquifer. Recharge to an aquifer can occur from several sources: (i) when precipitation falls within the confines of the aquifer (autogenic recharge), (ii) when precipitation falls outside of the confines of the aquifer, but then flows onto the aquifer where it provides recharge (allogenic recharge); or (iii) from interformational recharge in the subsurface. The HCT Aquifer is recharged by all three of these mechanisms. Allogenic recharge mostly occurs due to the fact that surface watersheds that overly the aquifer do not fully align with groundwater basins (Figure 5.1.1).

The HCT Aquifer extends across four geophysical provinces in central Texas; Edwards Plateau, Hill Country, Balcones Fault Zone, and Gulf Coast (Figure 5.1.2). The names of the formations that comprise the HCT Aquifer vary with geological province (Figure 2.2.1). Formations in the Balcones Fault Zone and the Gulf Coast provinces are similar and include, from older to younger, Hosston Formation, Sligo Formation, Pine Island Shale Member, Cow Creek Limestone Member, Bexar Shale Member, and Glen Rose Limestone. The Hill Country province is similar to the Balcones Fault Zone and the Gulf Coast provinces, but exhibits a facies change from Pine Island Shale in the Hill County province to Hammett Shale in the Balcones Fault Zone and Gulf Coast provinces. In addition, the Sycamore Sand in the Edwards Plateau province transitions to the Sligo Formation and the Hosston Formation in the other three provinces. As described in Section 4, the Trinity Formation thins to the north and west where several units pinch out, including the Glen Rose Limestone, Cow Creek Limestone, and Hammett Shale. As illustrated in three vertical cross sections, the Trinity Aquifer is absent where the Llano Uplift is exposed (Figure 5.1.3-5.1.8).

The designated boundaries of the HCT Aquifer in this study were modified from the HCT Aquifer boundaries previously defined by Mace et al. (2000) and Jones et al. (2011) to allow for more natural hydraulic boundaries to be assigned to both conceptual and numerical models of the aquifer. As described in Chapter 1, the TWDB required that the HCT Aquifer conceptual model include Groundwater Management Area 9. The study area boundaries delineated in Figure 5.1.9 were specified at the onset of project after consultation with staff from the TWDB. To the degree possible at that time, the study area contained what was thought to be the hydraulic boundaries of the HCT Aquifer. Refined HCT Aquifer conceptual model boundaries were identified and delineated during the course of this project. Both the HCT study domain and HCT conceptual model aquifer boundaries are illustrated in Figure 5.1.9. Following are descriptions of the deliberations that led to designation of the HCT Aquifer conceptual model boundaries. Note that no HCT Aquifer conceptual model boundary extends outside of the study domain designated at the onset of this project.

Similar to Mace et al. (2000) and Jones et al. (2011), the northeastern extent of the conceptual model of the aquifer abuts with the Northern Trinity Aquifer. The northeast boundary is aligned with the Colorado River from the Llano Uplift to the northwest to the 3,000 mg/L TDS contour of the Trinity Aquifer. The 3,000 mg/L TDS contour of the Trinity Aquifer defines the southern boundary of the HCT conceptual model (LBG-Guyton, 2003). A straight line has been extended from the western end of the 3,000 mg/L TDS contour line as defined by LBG-Guyton (2003) to the western boundary of the Nueces River watershed.

The western boundary of the HCT Aquifer conceptual model domain was extended to the Edwards-Trinity Aquifer, defined here by the western boundary of the watershed of the West Prong of the Nueces River. For the minor stretch of the boundary from the confluence of the West Prong of the Nueces River and the main branch of the Nueces River south to the 3,000 mg/L TDS contour line of the Trinity Aquifer, the western boundary of the Nueces River watershed is designated as the western boundary of the conceptual model.

The South Llano River watershed is included in the HCT Aquifer conceptual model domain, thus the South Llano River watershed northern boundary defines the northwest boundary of the HCT Aquifer conceptual model domain. The main branch of the Llano River is defined as the northern boundary for the segment spanning the stretch from the confluence of the North Llano and South Llano rivers to the Llano Uplift. The eastern segment of the northern boundary of the HCT Aquifer conceptual model domain aligns with the outcrop of the Llano Uplift.

Included in the map of the HCT Aquifer conceptual model domain (Figure 5.1.9) are the major watersheds that transecting the extent of the Trinity Aquifer. Because the upper reaches of several of these river watersheds extend upgradient from the HCT Aquifer recharge area, most notably the Colorado River watershed, there is the potential for allogenic recharge to the HCT Aquifer from this watershed.

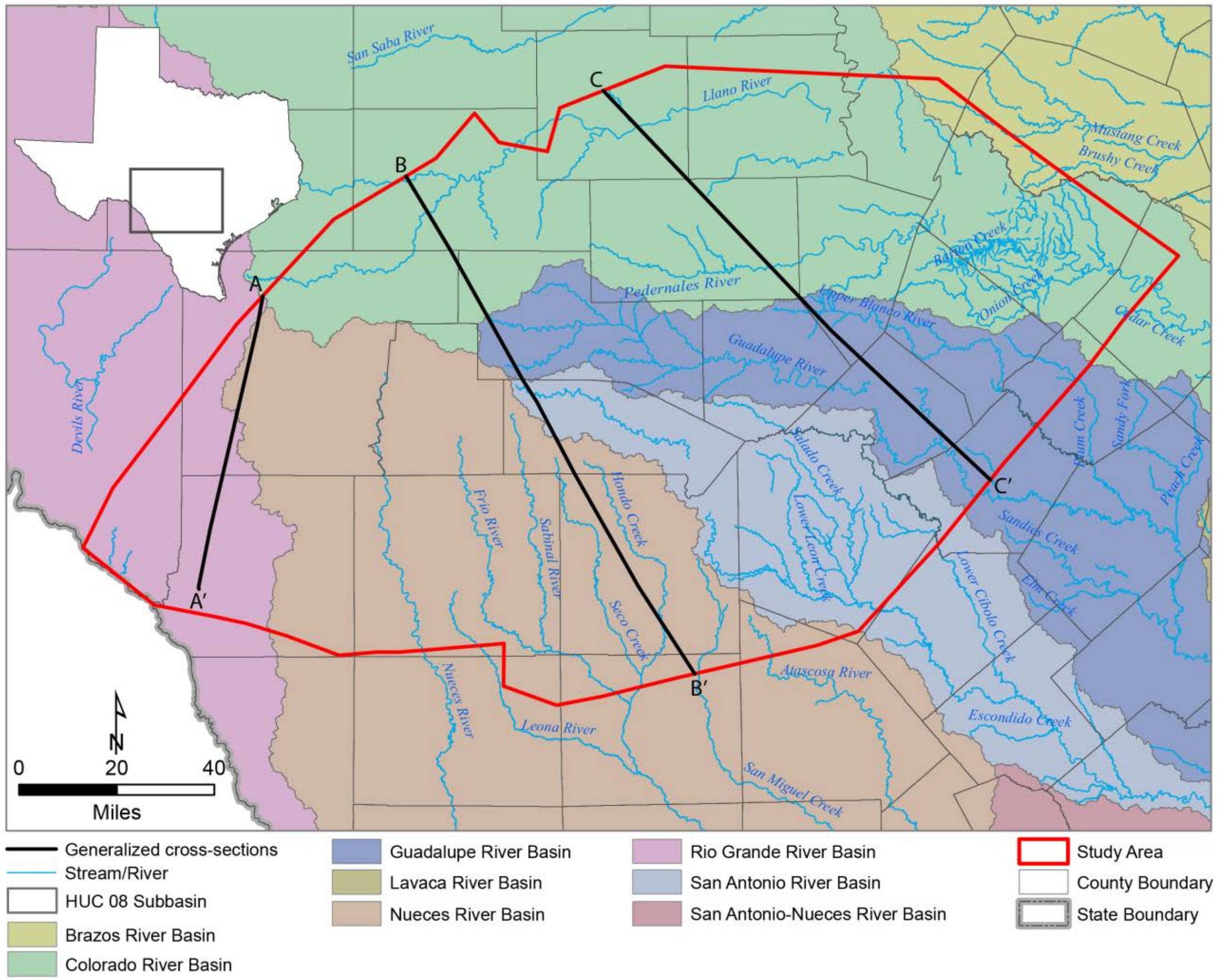

Figure 5.1.1 **Map of the study area with major river watersheds. Location of three cross-sections present in Figure 5.1.3, 5.1.5, and 5.1.7 are illustrated.**

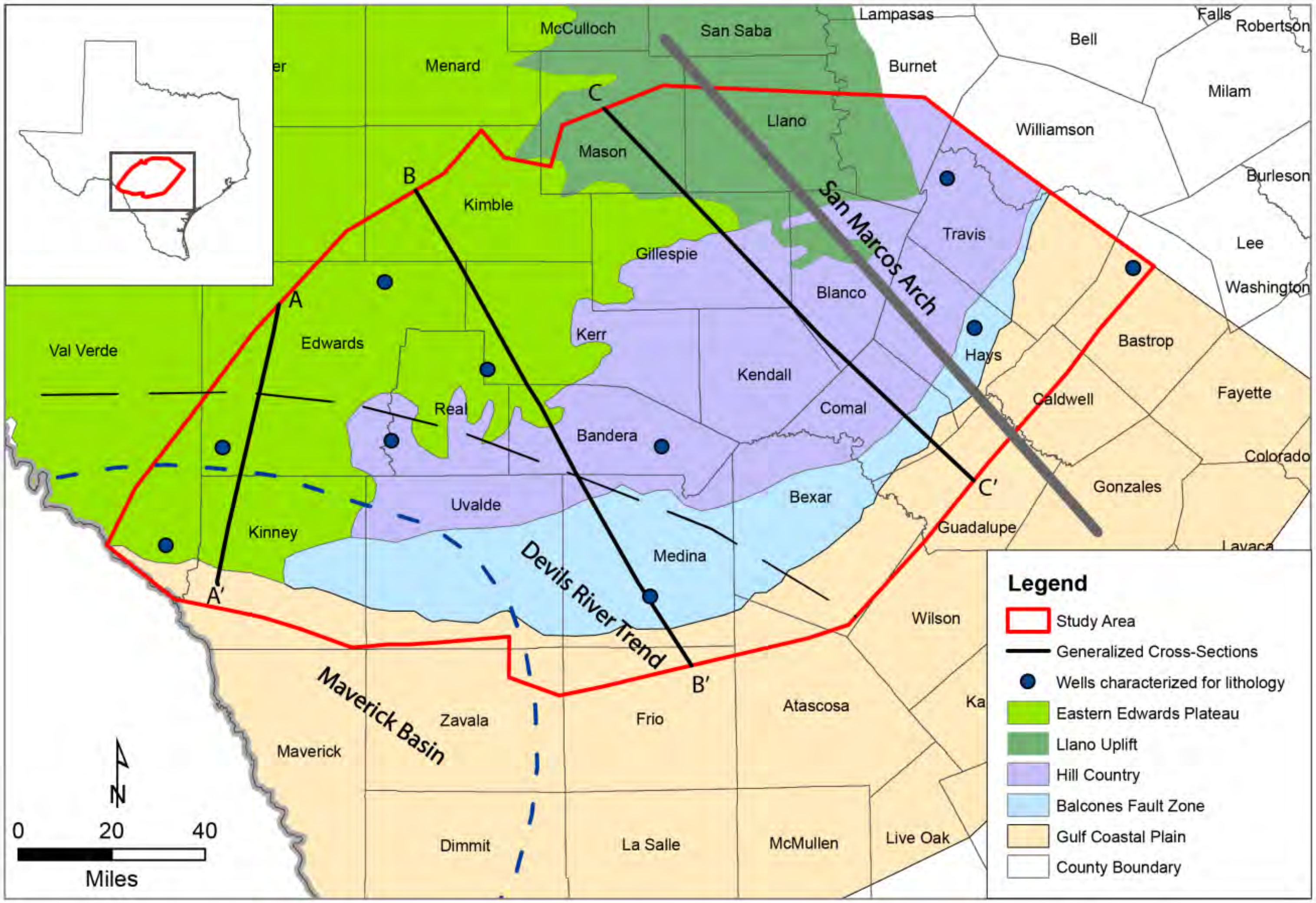

Figure 5.1.2 **Map of the study area with geologic provinces.**

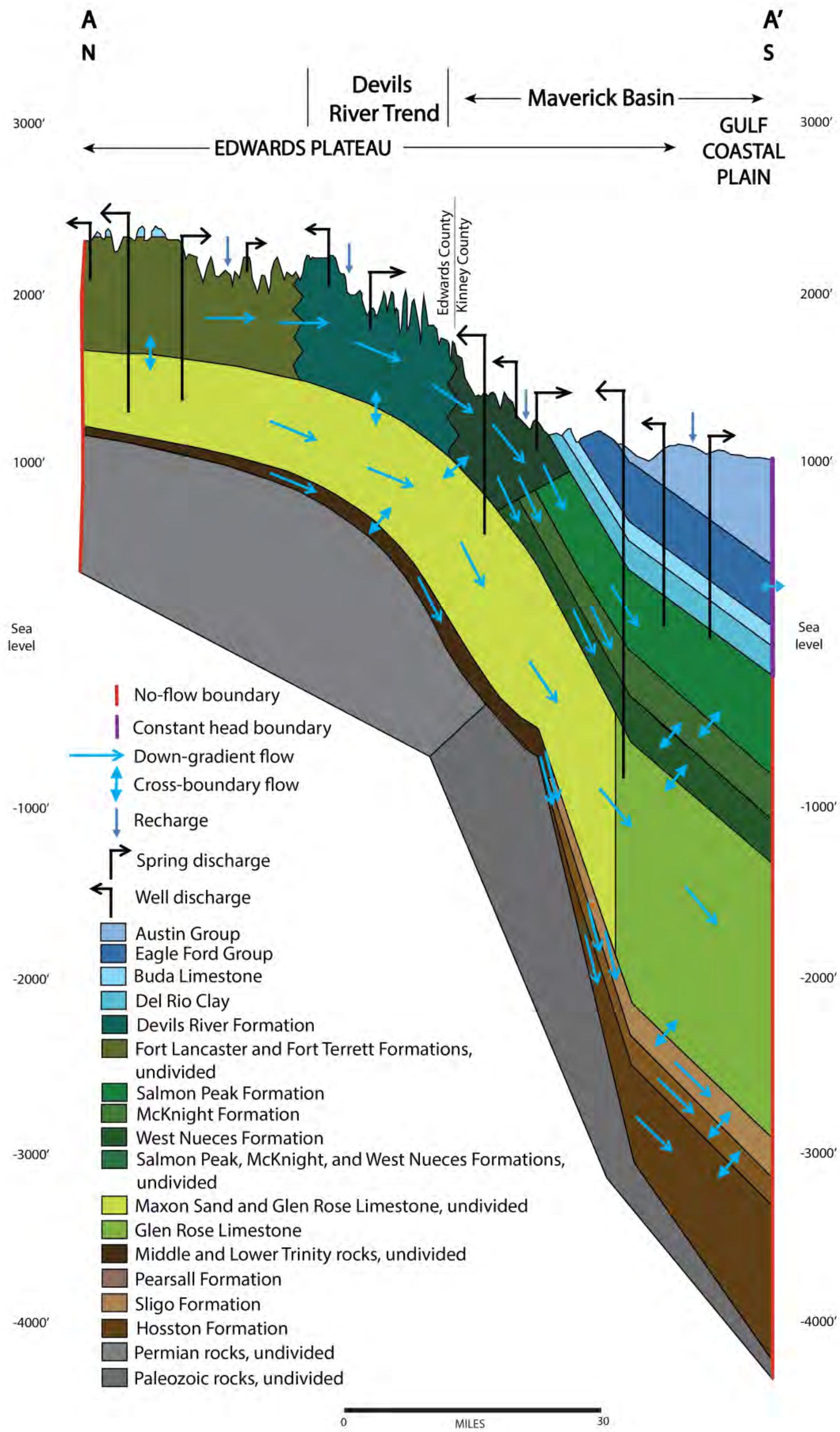

Figure 5.1.3 Hydrostratigraphic vertical cross section A-A' with flow between layers.

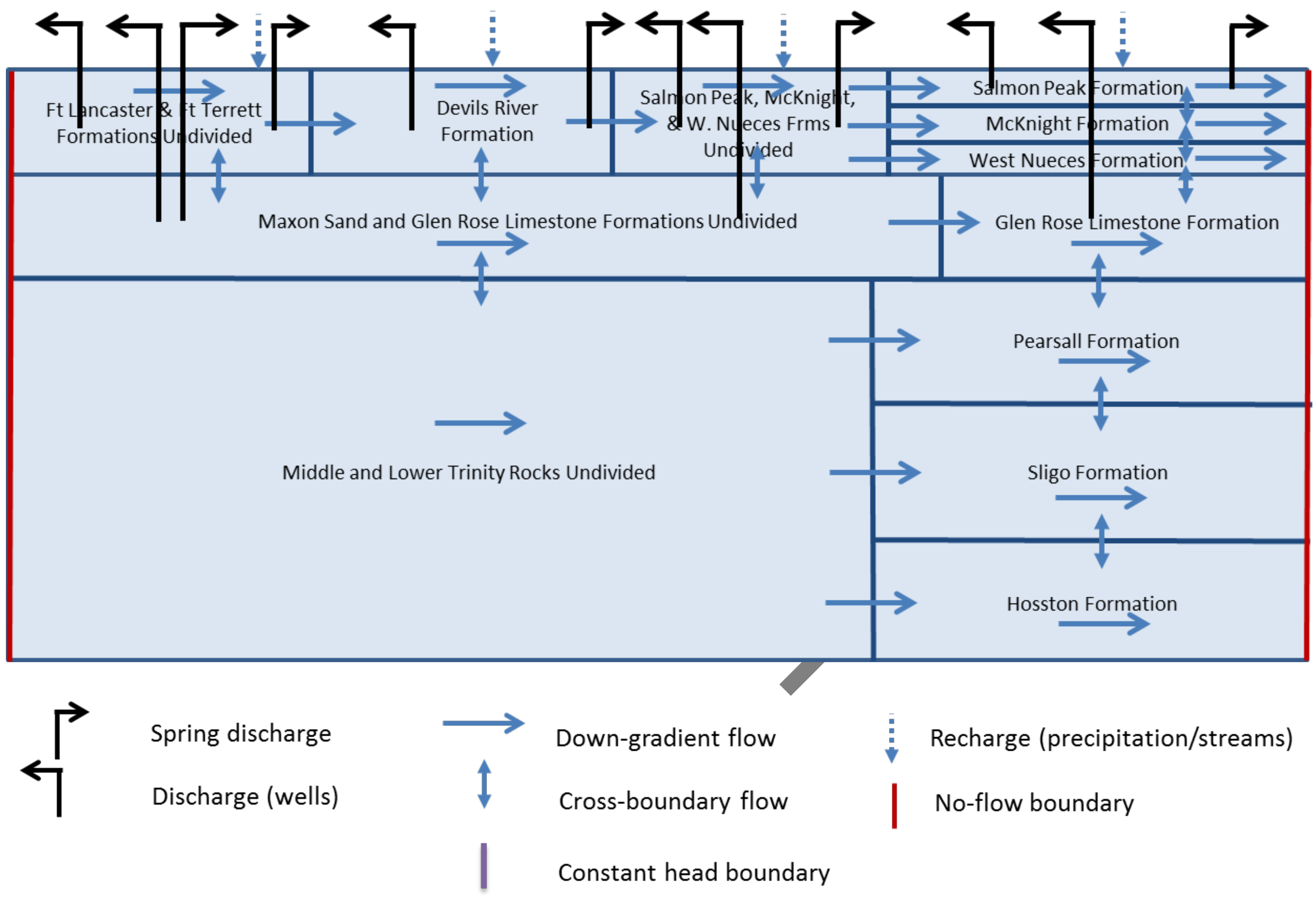

Figure 5.1.4 **Block diagram of A-A' transect illustrating how the conceptual model translates to the numerical model.**

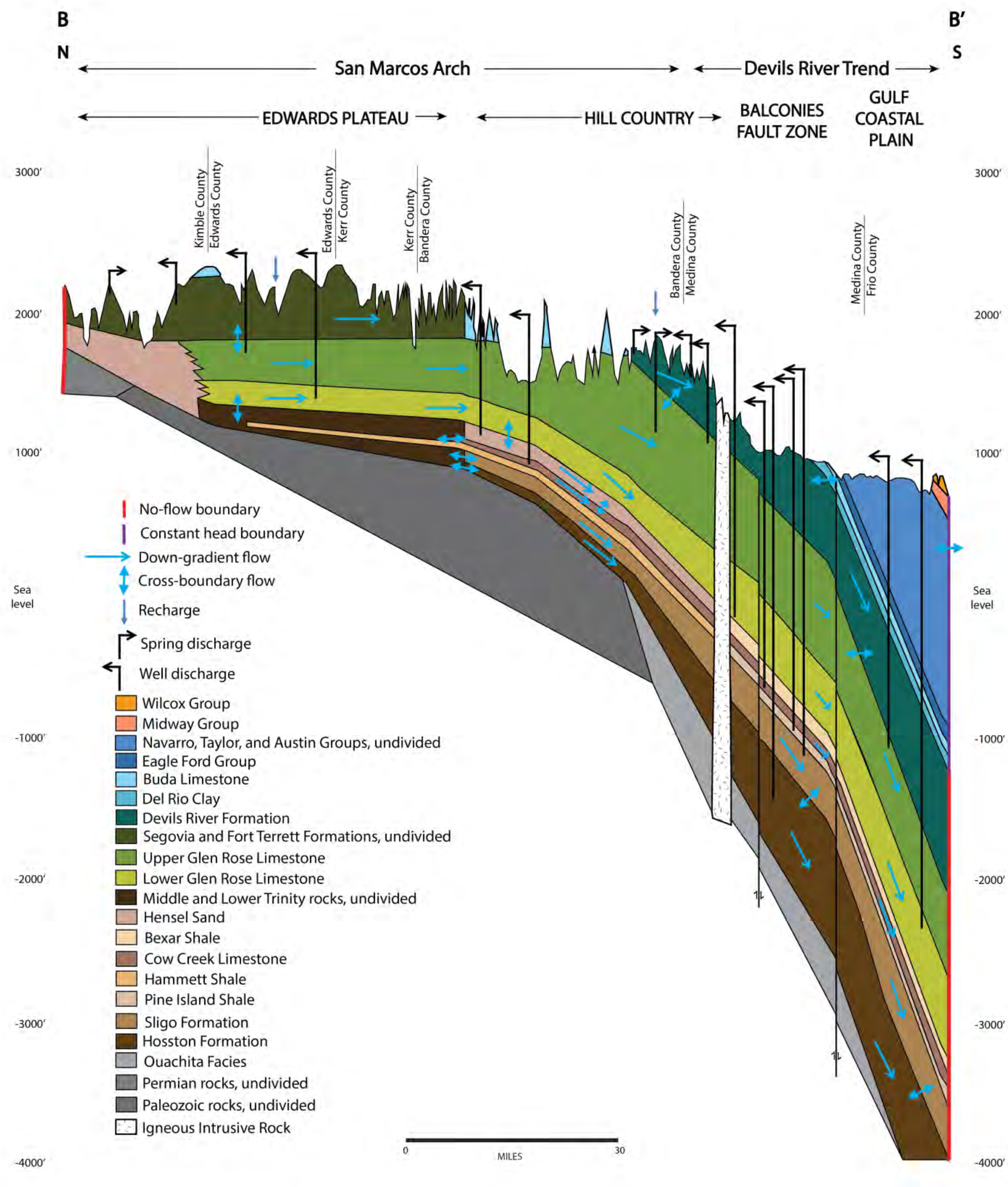

Figure 5.1.5 Hydrostratigraphic vertical cross section B-B' with flow between layers.

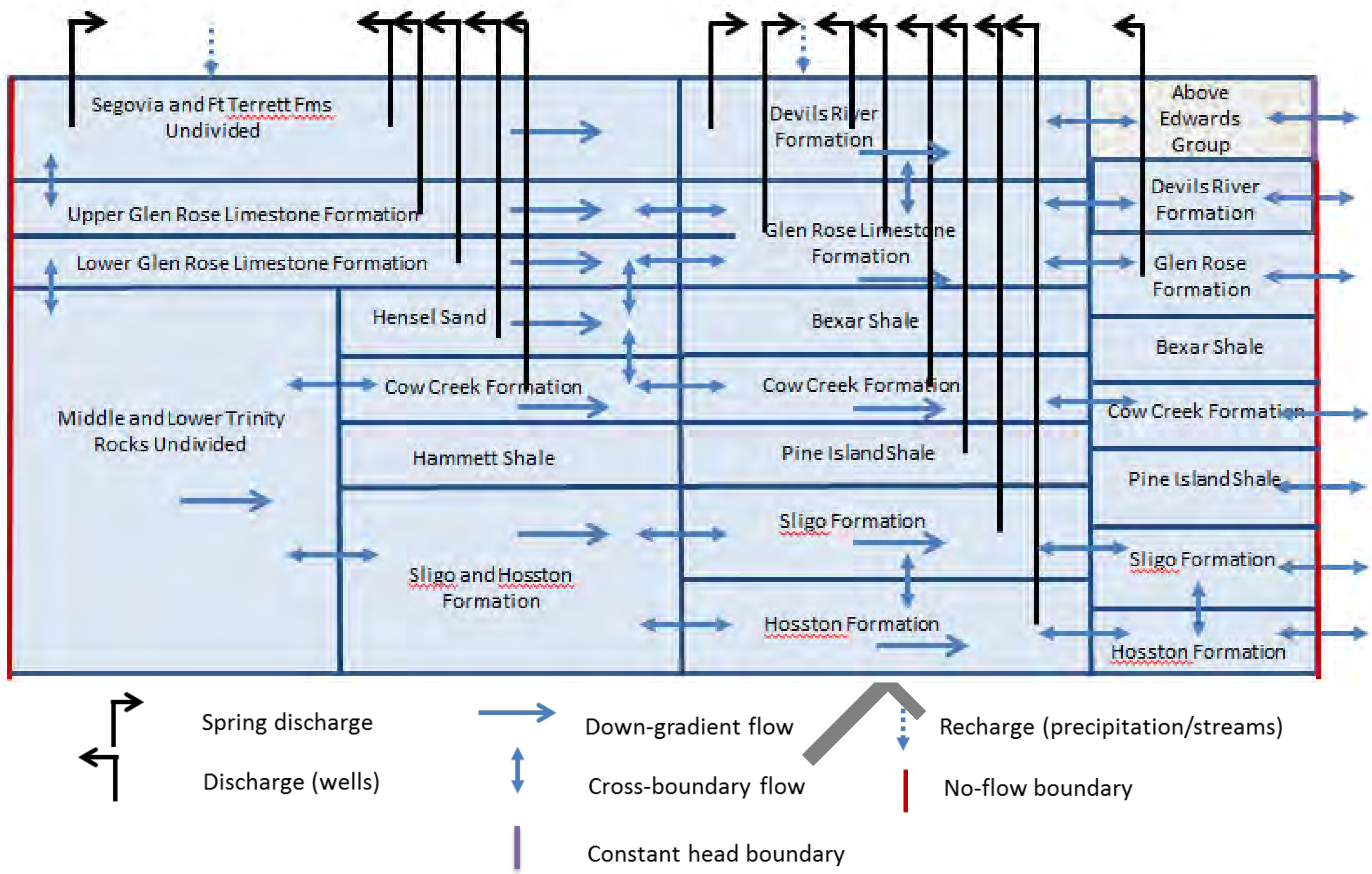

Figure 5.1.6 **Block diagram of B-B' transect illustrating how the conceptual model translates to the numerical model.**

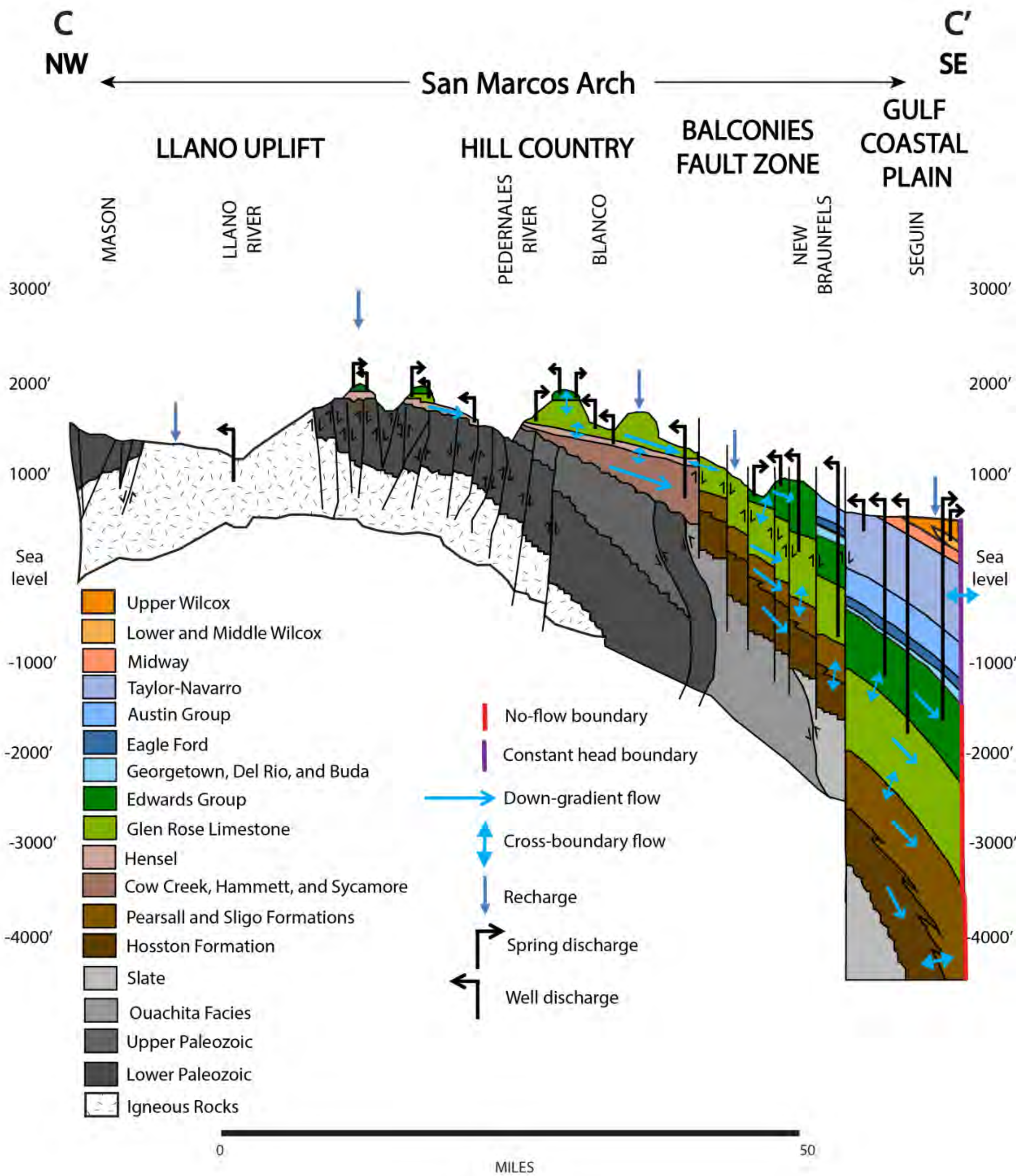

Figure 5.1.7 Hydrostratigraphic vertical cross section C-C' with flow between layers.

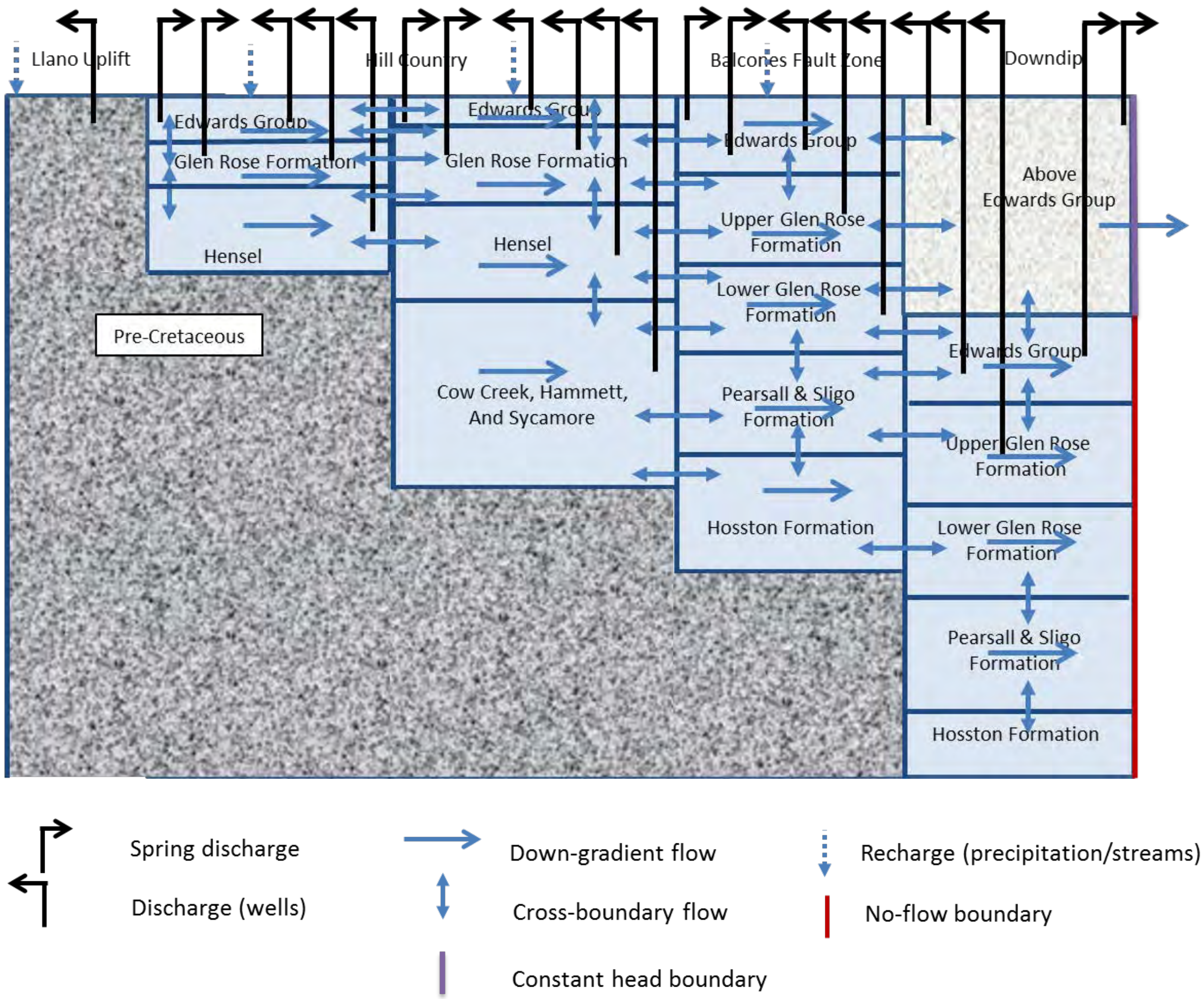

Figure 5.1.8 Block diagram of C-C' transect illustrating how the conceptual model translates to the numerical model.

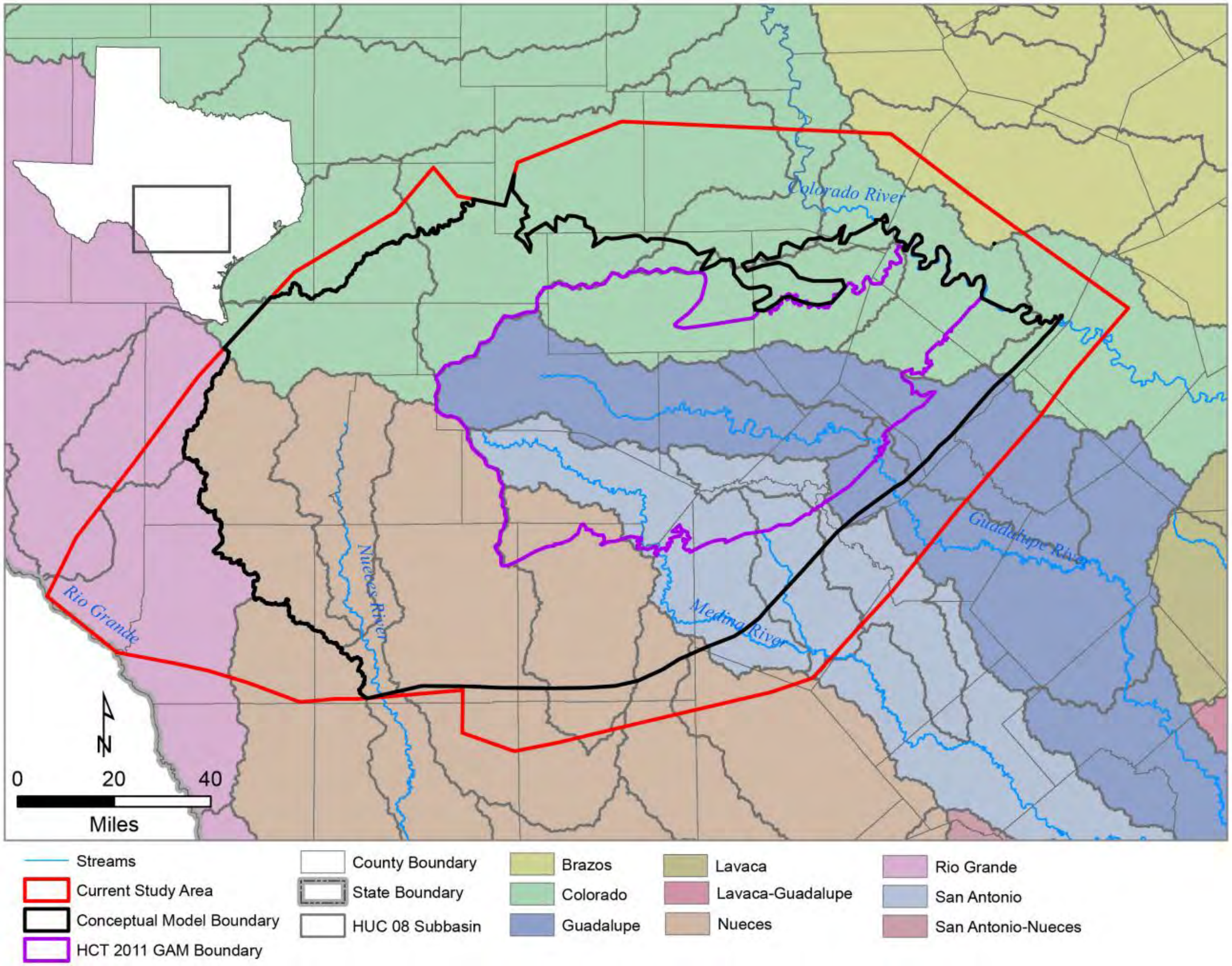

Figure 5.1.9 Map with study and model boundaries delineated.

5.2 Hydraulic Designation of HCT Conceptual Model Boundaries

The HCT Aquifer conceptual model boundaries are defined to reflect naturally occurring hydraulic conditions (Figure 5.1.9). This allows for many of the boundaries of the HCT Aquifer to be designated as no-flow. Boundaries not designated as no-flow are due to interformational hydraulic communication resulting from structural faulting and surface water flow into and out of the model domain. The hydraulic designation of each boundary segment is described and justified in the following paragraphs.

The interface between the HCT Aquifer and the Northern Trinity Aquifer is interpreted to have negligible hydraulic communication because groundwater flow along this boundary is interpreted to be parallel to the HCT Aquifer and Northern Trinity Aquifer interface. The boundary is located coincident with the Colorado River (Mace et al., 2000; Jones et al., 2011; Kelly et al., 2014). This boundary is considered a no-flow boundary.

Upland boundary conditions are designated in recognition that there is limited inter-basin hydraulic communication between adjoining unconfined aquifers. This phenomenon of negligible flow between adjoining watersheds has been observed elsewhere in the Edwards Plateau (Green et al., 2014; Toll et al., 2017) where hydraulic conditions are similar to the uplands of the HCT Aquifer. Under this hydraulic setting, the aquifers are near-surface, unconfined, and relatively thin (i.e., 100s ft). Inter-basin hydraulic communication under these conditions is minimal if not absent. Direction of groundwater flow under these conditions is typically parallel to watershed boundaries. The lack of inter-basin flow justifies designating the groundwater boundaries that are aligned with surface watershed boundaries as no-flow. Hydraulic communication between adjoining watersheds can become a factor in the downdip portion of the watersheds when the aquifer becomes thicker and more confined. Under these conditions, it is possible for water to transfer between adjoining watershed basins. As illustrated in Figure 5.1.9, the model domain was modified to align with surface watershed boundaries at two locations: (i) the western edge of the watershed of the West Prong of the Nueces River to the west and (ii) the northern edge of the watershed of the South Llano River to the north. These boundaries are specified as no-flow.

As illustrated in Figure 5.1.7, the northeastern boundary of the HCT Aquifer abuts the Pre-Cretaceous rocks of the Llano Uplift. These rocks are mostly comprised of fractured igneous intrusives with low primary and secondary permeability. Because the HCT Aquifer is absent in the Llano Uplift, the Llano Uplift was removed from the HCT Aquifer conceptual model domain. The permeability of the igneous rocks of the Llano Uplift is sufficiently low that interformational flow from the Llano Uplift to the HCT Aquifer is considered negligible (Figure 5.1.7-5.1.8). There is the potential for allogenic recharge by surface water flow from the Llano Uplift to the HCT Aquifer. Thus, the HCT Aquifer conceptual model boundary with the Llano Uplift is designated as no-flow, with the exception of allogenic recharge from watersheds on the Llano Uplift.

The downgradient (south) boundary was modified to align with the 3,000 mg/L TDS contour line in the Trinity Aquifer (LBG-Guyton, 2003). This boundary is designated as no-flow base on the premise that it is likely that groundwater flow will be parallel to contour lines aligned with major changes in groundwater salinity. There is the potential for discharge from the southern boundary via interformational flow in the Balcones Fault Zone from the HCT Aquifer to overlying aquifers (Figure 5.1.7-5.1.8).

There are two remaining short boundary segments in the model domain that require designation. On the northern boundary, there is a small gap between the confluence of the South Llano and North Llano rivers and the western edge of the Llano Uplift. This gap is filled by designating a no-flow boundary that is aligned with the Llano River. Although this segment is designated as no-flow, there is the potential for some groundwater flow from north of the Llano River to flow into the model domain. This boundary condition is a constant-head boundary with the head elevation set at the river elevation.

The second relatively short gap is the boundary designation located due south of the confluence of the West Prong of the Nueces River with the main branch of the Nueces River. The west side of the Nueces River watershed is designated as a no-flow boundary in this gap. Given that there may be inter-basin flow where the aquifer is deep and thick, such as along this segment, there may be interformational flow across this boundary.

The premises on which these boundary conditions were specified will need to be further evaluated during calibration of the numerical model. The hydraulic designation of any boundary can be modified during calibration if it is demonstrated that different hydraulic designation is warranted.

5.3 Discharge

Natural discharge from the model domain occurs via interformational flow or where surface water flows out of the model domain. Anthropogenic discharge occurs via pumping. Given the choice of natural boundaries of the HCT Aquifer for the model domain, there is no groundwater flow outside of the model domain via the HCT Aquifer. Naturally-occurring discharge from the HCT Aquifer, however, does occur via interformational flow through other aquifers. Idealized vertical cross sections were developed along three transects to graphically illustrate the complex hydrostratigraphy of the HCT Aquifer (Figure 5.1.3, Figure 5.1.5, Figure 5.1.7) . Three cross sections were prepared to depict the variability in geologic structure and facies for the western, central, and eastern sectors of the HCT Aquifer (Figure 5.1.2) (Figure 5.1.3, Figure 5.1.4, Figure 5.1.5, Figure 5.1.6, Figure 5.1.8). Two cross-sectional schematics were prepared for each transect. The schematics illustrate aquifer contact relationships including interformational flow, sources, and sinks of groundwater in the HCT Aquifer and overlying aquifers. The first cross section for each transect is the hydrostratigraphic cross section. The second cross section illustrates how the conceptual model translates to the numerical model.

As illustrated, flow among the formations segmented by geologic structure is complex (Figure 5.1.3-5.1.8). In particular, the hydraulic relationship between the Edwards and Trinity aquifers is of critical importance when conceptualizing the HCT Aquifer mostly due to fact that these two formations are prolific aquifers with significant hydraulic communication. Groundwater from the HCT Aquifer can discharge to the Edwards Aquifer in two ways: (i) as subsurface cross-formational inflow across the updip margin of the Balcones Fault Zone where the Trinity Aquifer is juxtaposed with the downfaulted Edwards Aquifer and (ii) as upward flow from the Trinity Aquifer into the Edwards Aquifer along faults, fractures, and dissolution enhanced conduits. In addition, there is water that enters the Edwards Aquifer recharge zone from the HCT Aquifer as surface flow. The volume of inflow and outflow from the HCT Aquifer as groundwater is difficult to determine and is typically estimated or constrained using numerical groundwater-flow models and water-balance calculations.

The vertical cross-section conceptual models (Figure 5.1.3-8) are our best understanding of groundwater flow in the HCT Aquifer. Discharge via springs that is illustrated in the vertical schematics Figure 5.1.4, Figure 5.1.6, and Figure 5.1.8 was determined using a correlation of spring location and surface geology (Figure 4.6.2). Discharge via pumping wells that is illustrated in the vertical schematics Figure 5.1.4, Figure 5.1.6, and Figure 5.1.8 was determined using a correlation of well location and well formation designation (Figure 5.3.2-5.3.15). Five databases were queried for well location and well formation information: (i) TWDB; (ii) Brackish Resources Aquifer Characterization System (BRACS) Database administered by the TWDB; (iii) Public Water Supply (PWS) database administered by the Texas Commission on Environmental Quality; (iv) Submitted Driller Reports (SDR) administered by the TWDB; and (v) U.S. Geological Survey. These databases are illustrated in five separate figures due to the high density of data (Figure 5.3.2-5.3.15). For wells with no formation designation, the depth of the well was used as a surrogate to estimate in which formation the well is set.

The STR and SFR2 packages in MODFLOW allow replication of spring discharge in river channels. These packages are applicable to rivers both within the HCT Aquifer and downgradient from the recharge zone of the HCT Aquifer. This will allow simulation of discharge from the HCT Aquifer that occurs as surface water (i.e., gaining river) and reaches where surface water infiltrates the subsurface (i.e., losing river). Drains in the STR and SFR2 packages are assigned an elevation and conductance. Drains discharge when the elevation of groundwater exceeds the specified elevation of the drain and receive water when surface water elevations exceed groundwater elevations. This designation is appropriate for an unconfined aquifer exposed in the riverbed. Spring discharge will only occur in a numerical model when the groundwater elevation is above the designated elevation of the drain. Thus, the drain will flow if groundwater elevation is higher than the drain elevation even when the topographic elevation at the drain is different from the drain elevation. This elevational discrepancy can occur when the grid size at the drain is too large to allow for small changes in topography to be accurately accommodated by relatively course grid size. It is noteworthy that this discrepancy is not an error in data assembly, nor is it a source of error in model calibration. It is simply a reflection of grid resolution and spatial changes in topography.

Drain discharge in a numerical model can be used to significantly improve a model during calibration. Spring discharge predictions can be calibrated to the stream-flow discharge observations, similar to those provided by the hydrographs in Chapter 4.5. Spring or stream discharge is calibrated by adjusting the drain elevation and conductance so that predicted spring discharge via drains matches observed spring hydrographs or, in the case that spring hydrographs are not available, baseflow calculations of stream hydrographs, which represent the accumulation of spring discharge (or recharge to drains accommodated with the stream-flow routing package) of all upstream springs. This additional step during calibration provides for increased constraints that would otherwise not be possible if the model is only calibrated to hydraulic heads. In this manner, the relative discharge from springs to stream baseflow (gaining streams) and the transfer of stream flow back to groundwater (losing streams) as documented in Figure 4.4.3 can be replicated during calibration. Previous experience with similar conceptual model development and implementation of an ensuing numerical model indicates that model calibration and performance are considerably more sensitive to designation of drain elevation and conductance than to hydraulic property assignment of the diffuse and conduit model grid cells.

There are two general types of springs in the HCT Aquifer model domain. Springs located in upland regions are mostly the result of groundwater issuing at ground surface where an impermeable surface is exposed at ground surface. As described in Section 4.5.6, the tight low-permeability interbeds, such as those found in the upper and middle parts of the Trinity Aquifer, severely restrict vertical flow so that groundwater moves laterally along impermeable bedding. This type of spring tends to be found in river and stream channels which are the points of the lowest local elevation. These springs are identified by the surface geologic formation at the spring location (Figure 4.6.2).

The second category is springs along the Balcones Fault Zone that are sourced from formations at depth. The most prominent of these springs are Comal, San Marcos, Hidden Valley, Hueco, Jacobs Well, San Pedro, San Antonio, and Las Moras springs (Figure 4.6.1). There are additional locations in stream and river beds in the Balcones Fault Zone where groundwater from depth issues at the surface. These water features are commonly referred to as blue holes and provide local perennial pools of water. Examples can be seen in Helotes Creek and Frio River (Green et al., 2008). Discharge at these pools is not significant. Inclusion of these features in water-budget analyses is not recommended.

The most challenging mechanism of discharge from the HCT Aquifer to determine is interformational flow. This quantity is rarely directly measured of even directly estimated. It will be necessary to first calibrate spring discharge in the model using spring and stream hydrographs and account for discharge by pumping before discharge via interformational flow can be calculated. The uncertainty in interformational flow determination will be a function of how well recharge, spring discharge, and discharge by pumping are known and how well they are accommodated in the model. A particular challenge is to estimate vertical hydraulic communication between the hydrostratigraphic units of the Trinity Aquifer at depth. There are limited data to clarify these hydraulic relationships. Several generalizations are possible. There is no vertical hydraulic communication between the Glen Rose Formation and the Cow Creek Formation where the Bexar Shale is present. Similarly, there is no vertical hydraulic communication between the Cow Creek Formation and the Sligo Formation where the Hammett Shale/Pine Island Shale is present. There is possible vertical hydraulic communication where these confining layers are absent. Differentiation among the Peasall, Sligo, and Hooston formations may not be feasible. It may be possible to lump these units together, particularly where data are sparse. Ultimately, interformational hydraulic communication between these formations in the numerical model at locations where data are sparse or missing will need to be determined during calibration.

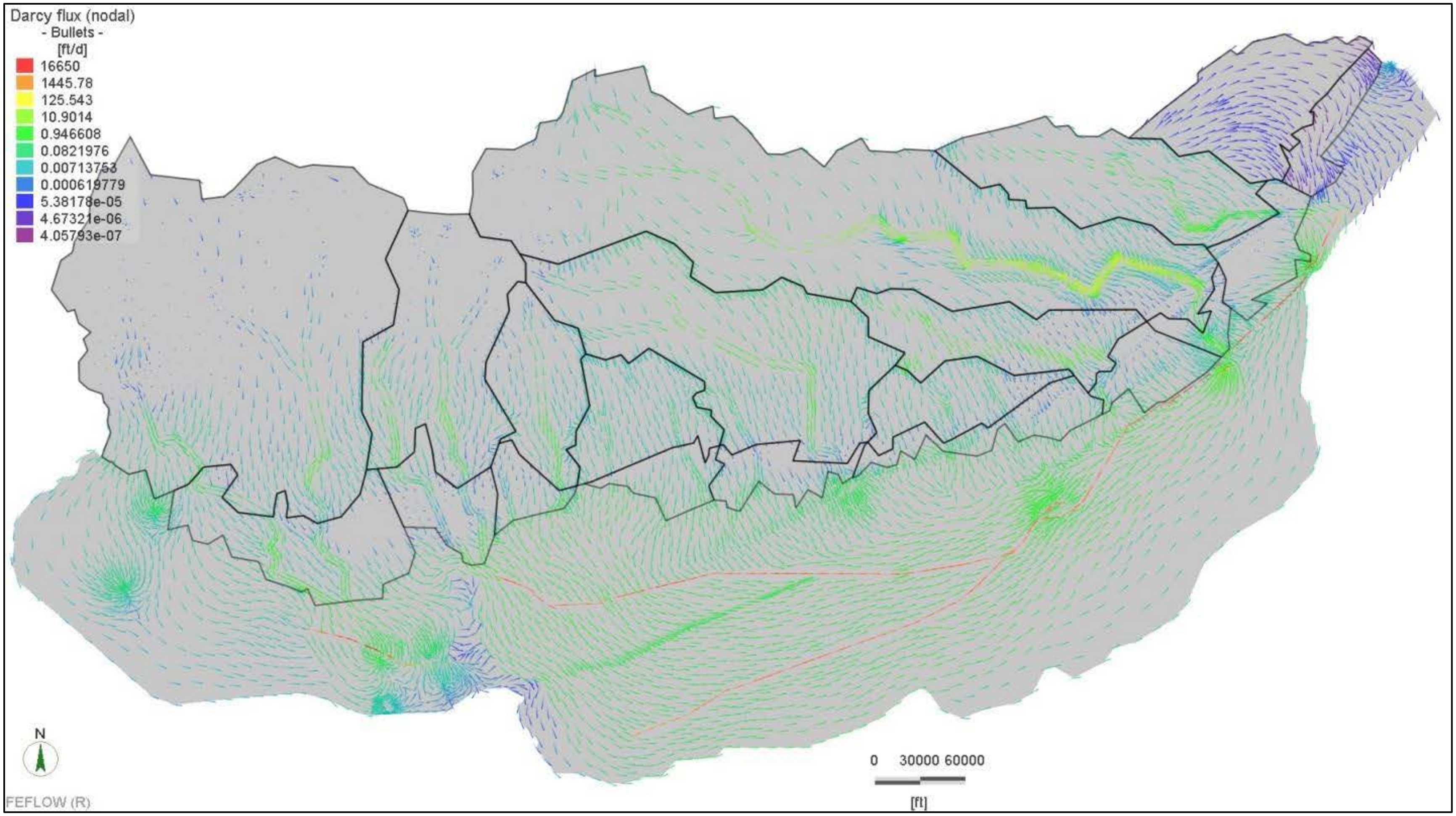

Figure 5.3.1 Direction of groundwater flow in the Edwards Aquifer (from Fratesi et al., 2015).

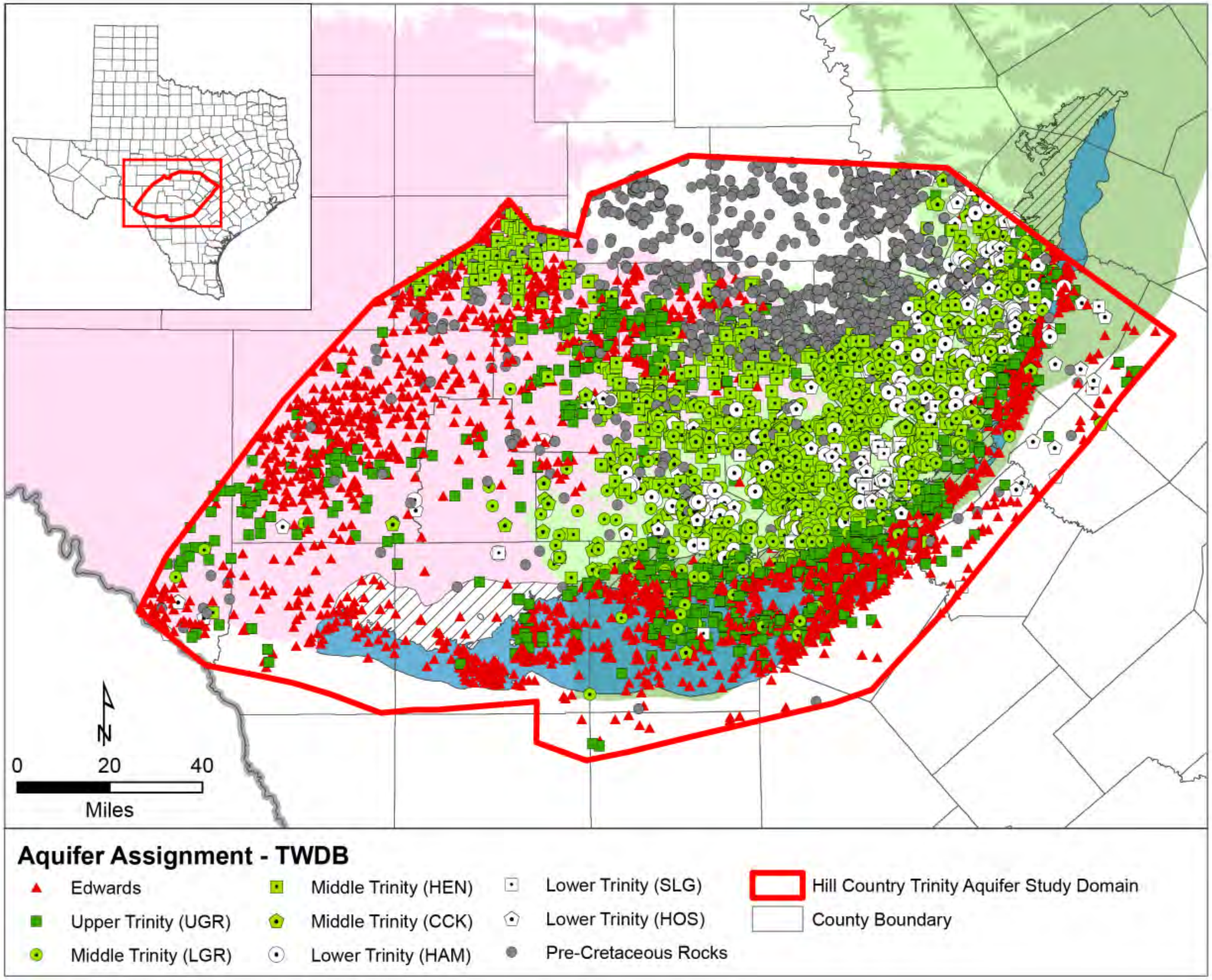

Figure 5.3.2 Water well locations designated by well formation from the TWDB.

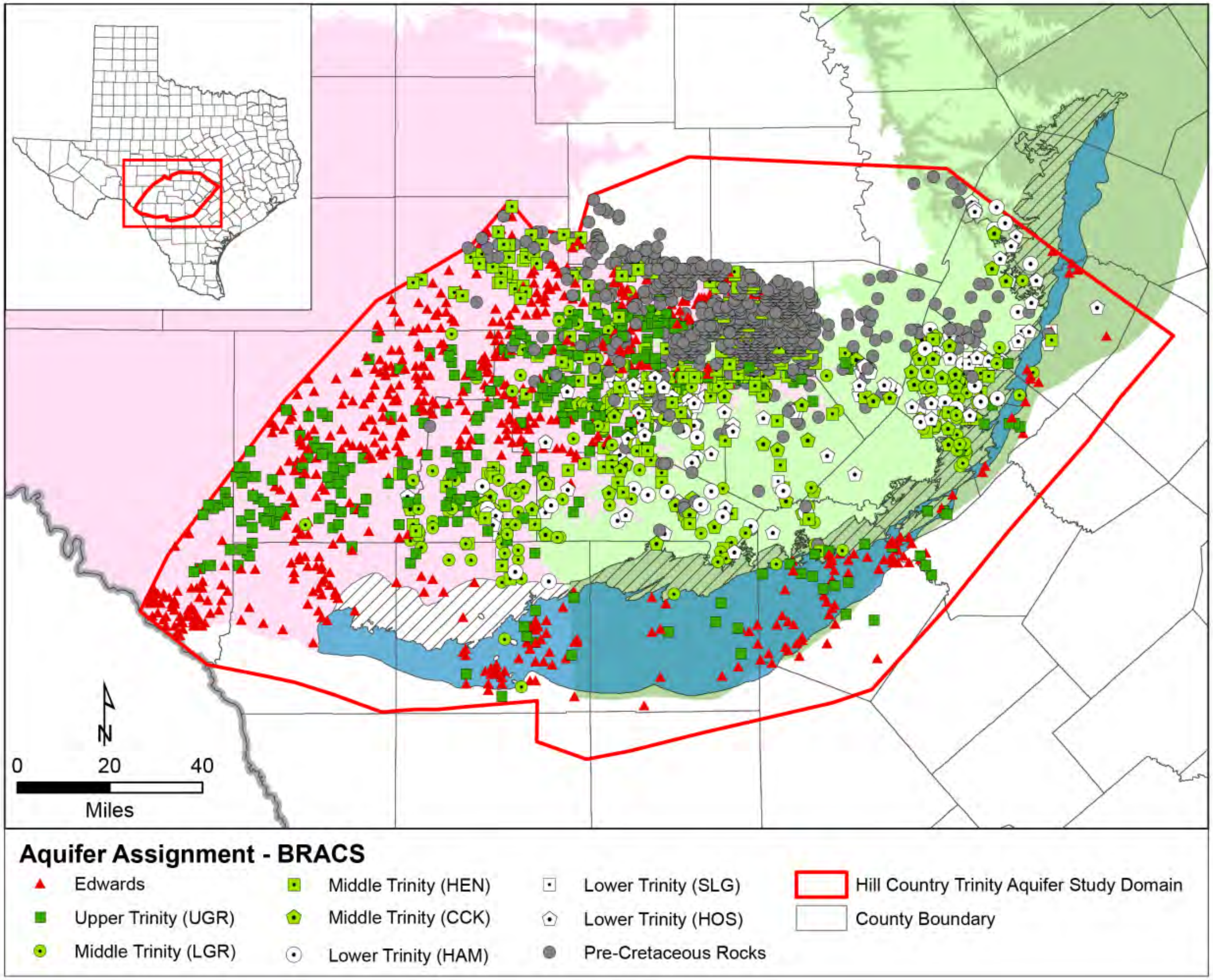

Figure 5.3.3 **Water well locations designated by well formation from the Texas Brackish Resources Aquifer Characterization System (BRACS) Database.**

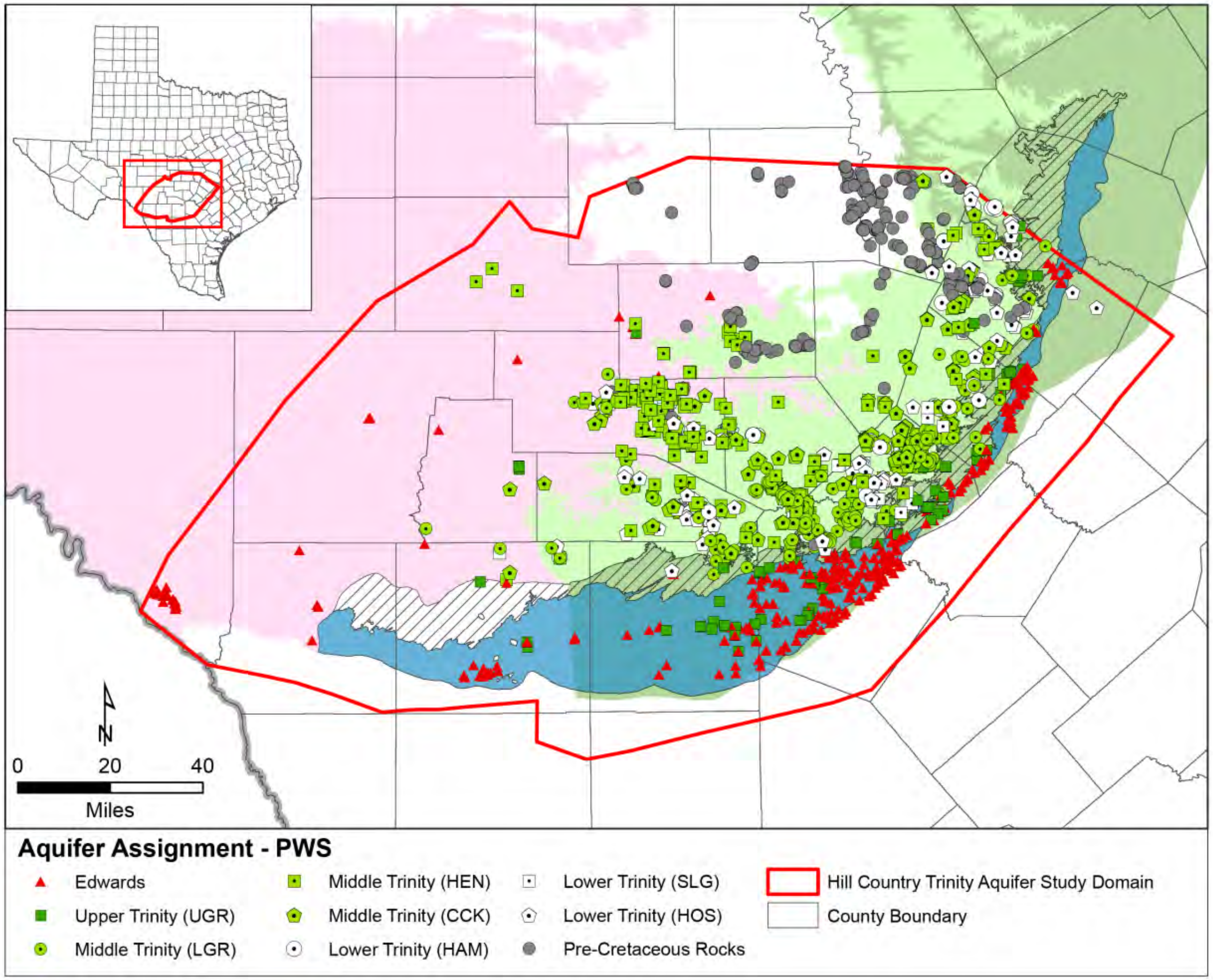

Figure 5.3.4 **Water well locations designated by well formation from the Public Water Supply (PWS) database administered by the Texas Commission on Environmental Quality.**

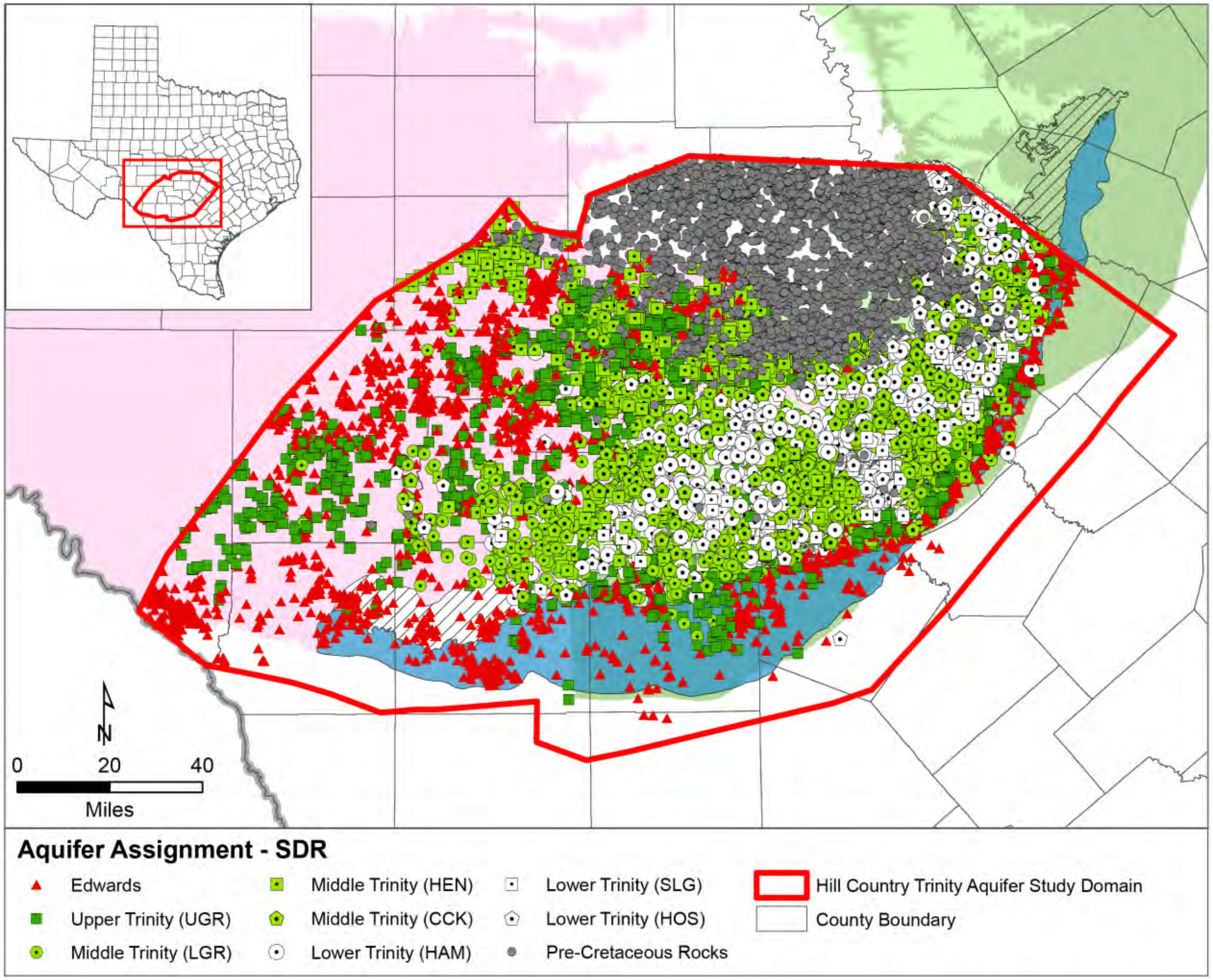

Figure 5.3.5 **Water well locations designated by well formation from the Submitted Driller Reports (SDR).**

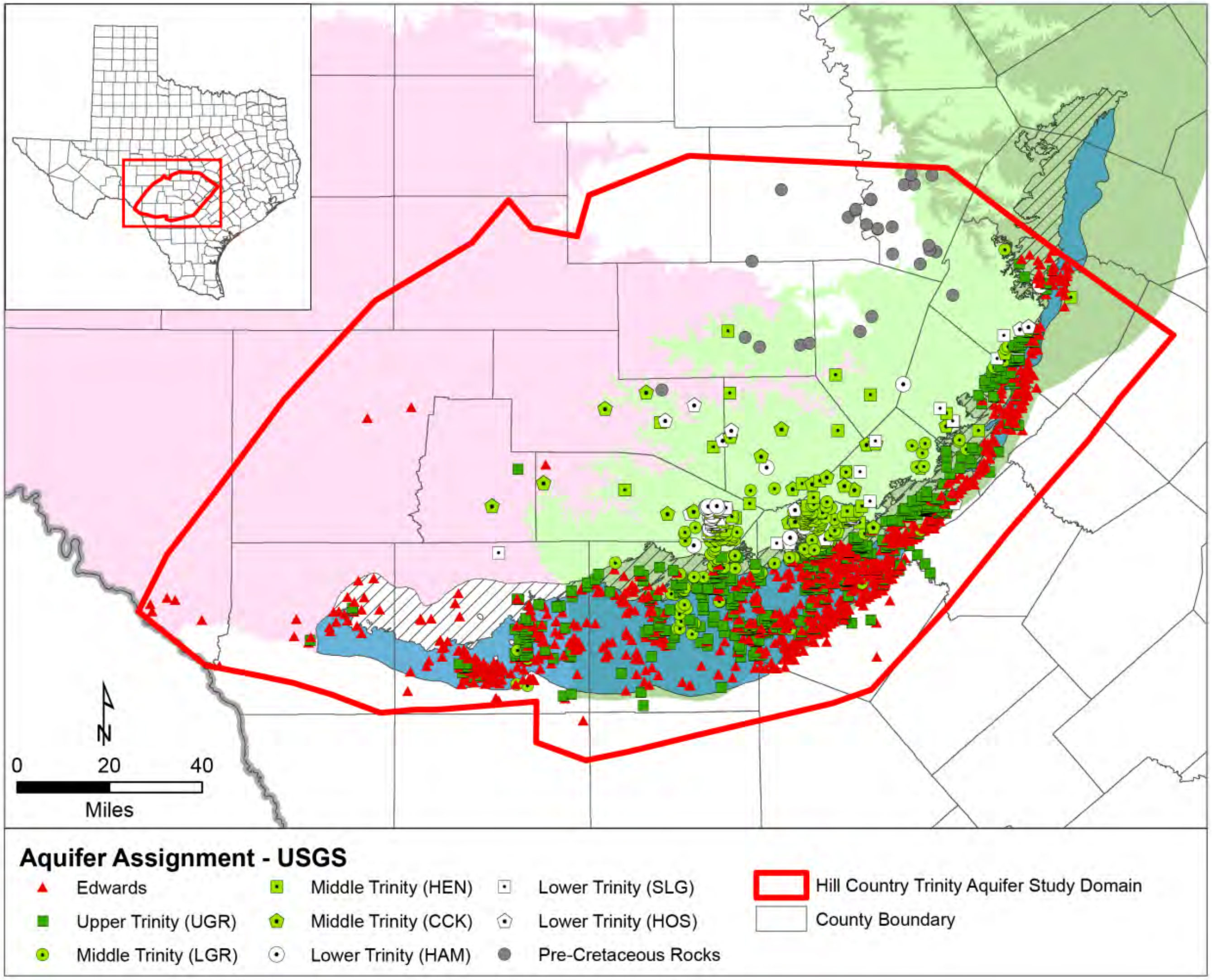

Figure 5.3.6 **Water well locations designated by well formation from the U.S. Geological Survey.**

5.4 Recharge

Recharge to the HCT Aquifer occurs as a combination of diffuse and local recharge. The percentage of precipitation that ultimately infiltrates and recharges aquifers varies from as low as 1-2 percent in the western portion of the HCT Aquifer to as much as 30 percent in the eastern portion of the aquifer (Green et al., 2012; Hauwert and Sharp, 2014). These percentages vary seasonally and temporally in response to precipitation frequency and intensity, antecedent moisture, vegetation, soil and rock type, temperature, humidity, and other factors. As a consequence of these factors, the percentage of precipitation that recharges the HCT Aquifer is typically smaller in the west and greater in the east. The two most dominant factors that control the recharge fraction in central Texas are the higher rates of evapotranspiration in the west and the higher rates of precipitation in the east. Actual recharge rates have a high degree of uncertainty.

The HCT Aquifer is bounded above by the Edwards Aquifer and below by Pre-Cretaceous rocks. Groundwater flow in the overlying Edwards Aquifer generally coincides with the flow in the HCT Aquifer (Figure 5.3.1) (Fratesi et al., 2015). Groundwater flow in the formations above the Edwards Aquifer is only of concern in the Gulf Coast province in that it provides opportunities for discharge from the HCT Aquifer. In addition to recharging the HCT Aquifer, losing streams also recharge the Edwards Group of the HCT Aquifer where the Edwards rocks cap the underlying Trinity Formation. This occurs at locations throughout the HCT Aquifer domain, but particularly in the northern and western portions of the HCT Aquifer where the aquifer domain extends into the eastern Edwards Plateau. The Edwards Plateau portion of the aquifer domain is important in that it contains the headwaters of several major river watersheds. Most of the recharge in the Edwards Group in the Plateau area discharges along the edge of the Plateau through springs, seeps, lower reaches of streams, and evapotranspiration. A small amount of the flow from the Edwards Group in the Plateau moves downward into the Upper and Middle Trinity aquifers.

5.5 Conduit/Diffuse Flow

Groundwater flow in the unconfined carbonate aquifers in the Edwards Plateau and the contributing zone of the San Antonio segment of the Edwards Aquifer has been shown to consist of a combination of diffuse and conduit flow (Woodruff and Abbott, 1979; Green et al., 2011; Fratesi et al., 2015; Toll et al., 2017). Toll et al. (2017) demonstrated that conduits or preferential flow, similar to what is expected in the upland portion of the HCT Aquifer, could be effectively accommodated by incorporating grid cells with high permeability embedded in a matrix of relatively low permeability. It is important that the extent of the preferential flow network be sufficiently pervasive to allow expedient draining of the aquifer. Successful replication of the ensemble of spring hydrographs (i.e., cumulative stream baseflow discharge) validated this approach (Toll et al., 2017).

5.6 Water Budget

There has been continued refinement in estimates and calculations of how much recharge to the Edwards Aquifer is sourced from the Trinity Aquifer. This refinement is due, in part, to improved conceptualization of the Trinity Aquifer-Edwards Aquifer interface based on a variety of perspectives including multi-well testing (Smith and Hunt, 2009, 2010, 2011), tracer testing (Johnson et al., 2010, 2012; Schindel and Johnson, 2011), gain-loss studies (Slade et al., 2002; Green et al., 2011), enhanced characterization of the geologic structure and hydrogeology (Ferrill et al., 2003, 2004, 2005, 2008), and refinements in groundwater models that include the Trinity Aquifer-Edwards Aquifer interface (Klemt et a., 1979; Maclay and Land, 1988; Lindgren et al., 2004). These refinements support the conceptualization that the Upper Glen Rose exhibits hydraulic properties that are more like the Edwards Aquifer than the rest of the Trinity Aquifer. Early estimates of Trinity-Edwards Aquifer interformational flow of 53,800 acre-ft/yr (Lowry, 1955) and 107,000 acre-ft/yr (Bader et al. 1993) included only the Cibolo Creek watershed. Interformational flow from the Trinity Aquifer to the Edwards Aquifer was not included in the model by Klemt et al. (1979). Subsequent models by Maclay and Land (1988), and Lindgren et al. (2004) did include inflow from the Trinity Aquifer as a source of groundwater. The domain of the model by Kuniansky and Holligan (1994) and Kuniansky and Ardis (2004) incorporated the Edwards-Trinity, Trinity, and Edwards aquifers, thus interflow was inherently included in the model. Maclay (1995) identified two areas of groundwater inflow along the updip limit of the San Antonio segment of the unconfined Edwards Aquifer, one area is northeastern Medina County and the other is in Comal County (Maclay and Land, 1988). The Maclay and Land (1988) model did not indicate significant inflow from the Trinity Aquifer to the Edwards Aquifer in either Kinney or Uvalde counties.

Steady-state simulation using the 2004 Edwards Aquifer groundwater availability model (Lindgren et al., 2004) calculated that inflow through the northern and northwestern model boundaries contributes 6.5 percent of total recharge to the Edwards Aquifer. Of this, 87.9 percent of the flow into the model area occurs through the northern boundary (Lindgren et al., 2004). For an annual recharge of 699,400 acre-ft/yr for the years 1939–2013 (Tremallo et al., 2014), this equates to approximately 40,000 acre-ft/yr of inflow from the Trinity Aquifer to the Edwards Aquifer.

Kuniansky and Holligan (1994) estimated that 53 percent of average annual recharge to the entire Edwards Aquifer, which equates to 360,000 acre-ft/yr, is from the Upper Glen Rose Formation of the Trinity Aquifer. Mace et al. (2000) contended that the Kuniansky and Holligan (1994) estimate of contributions to the Edwards Aquifer from the Trinity Aquifer is excessive. Mace et al. (2000) used the HCT Aquifer groundwater availability model to estimate that 59,000 acre-ft recharged the Edwards Aquifer from the Trinity Aquifer as interformational flow based on conditions representative of 1975. The Hill Country portion of the Trinity Aquifer only extends to the Dry Frio/Frio River watersheds to the west, excluding the West Nueces/Nueces River watersheds. The HCT Aquifer model refined by Jones et al. (2011) calculated that total groundwater flow through the Trinity Aquifer is approximately 321,000 acre-ft/yr. Of this flow, about 60 percent discharges to streams, springs, and reservoirs, and 35 percent or 111,000 acre-ft/yr, discharges through cross-formational flow to the Edwards (Balcones Fault Zone) Aquifer. The model by Jones et al. (2011) parsed out the cross-interformational flow rates as 660 acre-ft/yr in the west, 2,400 acre-ft/yr in the central area, and 350 acre-ft/yr in the east of the model domain (Figure 5.6.1).

The U.S. Geological Survey estimated that annual recharge of the Edwards Aquifer for the period of record (1934–2013) ranged from 43,700 acre-ft in 1956 to 2,486,000 acre-ft in 1992.

The median annual recharge for 1934–2013 is 556,950 acre-ft. These estimates do not include the Guadalupe River watershed because the historical method of estimating recharge is based on the interpretation that the Guadalupe River Basin watershed does not recharge the Edwards Aquifer (Tremallo et al., 2014).

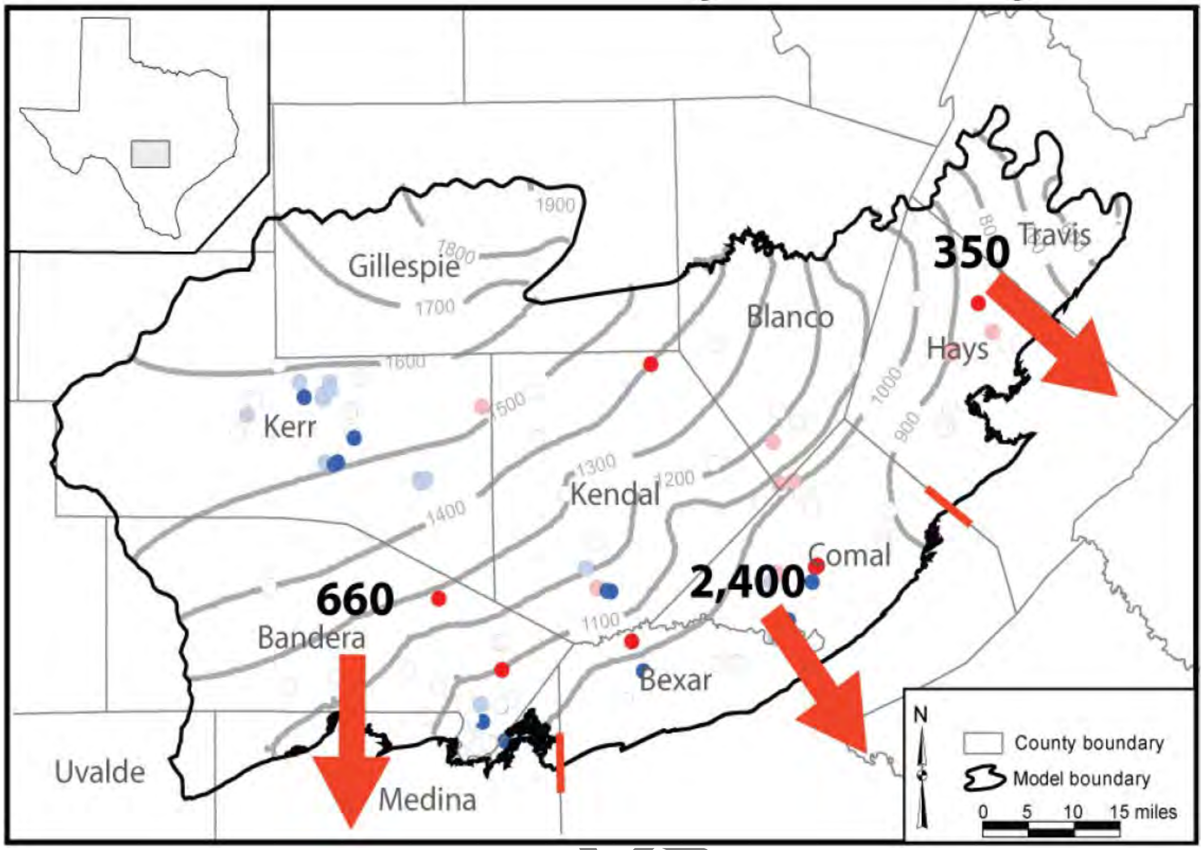

Figure 5.6.1 Cross-formational flow from the Trinity Aquifer to the Edwards Aquifer (acre-ft/yr) (From Jones et al., 2011).

6.0 References

Alexander, W.H., Jr., and Patman, J. H., 1969, Ground-Water Resources of Kimble County, Texas: Texas Water Development Board Report 95, May 1969.

Amsbury, D. L., 1974, Stratigraphic petrology of lower and middle Trinity rocks on the San Marcos platform, South-Central Texas: in B. F. Perkins, ed., Geoscience and Man, v. VIII: Louisiana State University Press, Baton Rouge, p. 1-35.

Amsbury, D. L., 1988, The middle Comanchean section of Central Texas, in O. T. Hayward, ed., Geological Society of America Centennial Field Guide, South-Central Section, p. 373-376.

Amsbury, D. L., 1996, Pearsall (Aptian Cretaceous) subsurface to outcrop sequence stratigraphy, Central Texas: Gulf Coast Association of Geological Societies Transactions, v. 46, p. 1-7.

Amsbury, D. L., and Jones, J. O., 1996, A field book for the early Cretaceous rocks of South-Central Texas: South Texas Geological Society, prepared for the 46th Annual Meeting of the Gulf Coast Association of Geological Societies and the 45th Annual Meeting of the Gulf Coast Section SEPM, 99 p.

Anaya, R. and Jones, I., 2009, Groundwater Availability Model for the Edwards-Trinity (Plateau) and Pecos Valley Aquifers of Texas. Texas Water Development Board Report 373. April 2009.

Anderson, M.P., and Woessner, W.W., 1992, Applied groundwater modeling, simulation of flow and advective transport: Academic Press, New York, NY.

Arnold, J.G., Allen, P.M., Muttiah, R., and Bernhardt, G., 1995, Automated base flow separation and recession analysis techniques. Ground Water 33(6): 1010-1018.

Arnold, J.G., and Allen, P.M., 1999, Automated methods for estimating baseflow and ground water recharge from streamflow records. Journal of the American Water Resources Association 35(2): 411-424.

Arnold, J. G., Allen, P. M., Muttiah, R., and Bernhardt, G., 1995, Automated Base Flow Separation and Recession Analysis Techniques. Groundwater, 33: 1010-1018. doi:10.1111/j.1745-6584.1995.tb00046.x

Ashworth, J.B., 1983, Ground-water availability of the lower Cretaceous formations in the Hill Country of south-central Texas. Report 273. Texas Department of Water Resources. 39 p.

Ashworth, J.B., Stein, W.G., Donnelly, A.C.A., Persky, K., and Jones, J.P. 2001, The lower Trinity aquifer of Bandera and Kerr counties, Texas, prepared for Plateau Regional Water Planning Group and Texas Water Development Board, 128 p.

Baker, B., Duffin, G., and Lynch, T., 1990a. Evaluation of water resources in part of Central Texas, Texas Water Development Board, Report 319, 43 p.

Baker, B., Duffin, G., Flores, R., and Lynch T., 1990b, Evaluation of water resources in part of north-central Texas, Texas Water Development Board, Report 318, 67 p.

Barker, R.A., and Ardis, A.F., 1996, Hydrogeologic framework of the Edwards-Trinity aquifer system, West-Central Texas: U.S. Geological Survey Professional Paper 1421-B. 61 p. with plates.

Barker, R.A., Bush, P.W., and Baker, Jr., E.T., 1994. Geologic history and hydrogeologic setting of the Edwards-Trinity Aquifer system, west-central Texas, U.S. Geological Survey Water-Resources Investigations Report 94-4093. 55 p

Barnes, V.E. 1983. Geologic atlas of Texas, San Antonio sheet: Austin, University of Texas, Bureau of Economic Geology, 8 p., scale 1:250,000, 1 sheet.

Barnes, V.E., 1979, Geologic atlas of Texas, Seguin Sheet: The University of Texas at Austin, Bureau of Economic Geology, 8 p., scale 1:250,000, 1 sheet.

Barnes, V.E., 1981a, Geologic atlas of Texas, Llano Sheet: The University of Texas at Austin, Bureau of Economic Geology, 8 p., scale 1:250,000, 1 sheet.

Barnes, V.E., 1981b, Geologic atlas of Texas, Austin Sheet: The University of Texas at Austin, Bureau of Economic Geology, 8 p., scale 1:250,000, 1 sheet.

Barnes, V.E., 1977, Geologic atlas of Texas, Del Rio Sheet: The University of Texas at Austin, Bureau of Economic Geology, 8 p., scale 1:250,000, 1 sheet.

Barnes, V.E., 1980, Geologic atlas of Texas, Sonora Sheet: The University of Texas at Austin, Bureau of Economic Geology, 8 p., scale 1:250,000, 1 sheet.

Bateman, R.M. and Konen, C.E., 1977, Wellsite log analysis and the programmable pocket calculator: Society Professional Well Log Analysts. B1–B35, Transactions, v. 18, p

Bebout, D.G., 1977, Sligo and Hosston depositional patterns, subsurface of South Texas. In: Cretaceous Carbonates of Texas and Mexico: Applications to Subsurface Exploration (Eds D.G. Bebout and R.G. Loucks), Bur. Econ. Geol. Univ. Tex. Austin Rep. Inv., 89, 79–96.

Bebout, D.G., Budd, D.A., and Schatzinger, R.A., 1981, Depositional and Diagenetic History of the Sligo and Hosston Formations (Lower Cretaceous) in South Texas, by 69 p., 55 figs., 4 tables.

Bebout, D. G., and Loucks, R.G., 1974, Stuart City Trend, Lower Cretaceous, South Texas—A carbonate shelf-margin model for hydrocarbon exploration: Texas Bureau of Economic Geology Report of Investigations 78, Austin, 80 p.

Bluntzer, R.L., 1992, Evaluation of ground-water resources of the Paleozoic and Cretaceous aquifers in the Hill Country of Central Texas: Texas Water Development Board Report 339, 161 p.

Broadhurst, W.L., Sundstrom, R.W., and Rowley, J.H., 1950, Public Water Supplies in Southern Texas, Geological Survey Water-Supply Paper 1070: Prepared by Water Resources Division, in cooperation with the Texas State Board of Water Engineers.

Broadhurst, W. L., Sundstrom, R.W., and Weaver, D.E., 1951, Public Water Supplies in Western Texas, Geological Survey Water-Supply Paper 1106: Prepared by Water Resources Division in cooperation with the Texas State Board of Water Engineers.

Broun, A. S., Wierman, D.A., Backus, A.H., and Hunt, B.B., 2007, Geological analysis of the Trinity Group aquifers in western Hays County, Texas with focus on implications to groundwater availability: in B.B. Hunt, C. M. Woodruff, Jr., and E.W. Collins, eds., Reimers Ranch and Westcave Preserve: Landscapes, water, and Lower Cretaceous stratigraphy of the

Pedernales watershed, western Travis County, Texas, Austin Geological Society, Guidebook 28, October 20, 2007, p. 64-81.

Broun, A. S., Wierman, D.A., Backus, A.H., and Llano, L., 2008a, Cypress Creek/Jacob's Well Hydrogeologic Report, Hays Trinity Groundwater Conservation District, December 2008, 43 p.

Broun, A. S., L. Llano, D. A. Wierman, and A. H. Backus, 2008b, The Geology of the Cypress Creek Watershed, Wimberley Area, Texas: Austin Geological Society, Austin, Texas, AGS Bulletin, Vol. 4, 2007-2008, p. 23-34.

Brown, D.S.,1999, Geologic framework and hydrogeologic properties of the Seco Creek Watershed, Texas, U.S. Geological Survey fact sheet.

Brune, G., and Duffin, G.L., 1983, Occurrence, availability, and quality of ground water in Travis County, Texas: Texas Department of Water Resources Report 276, 103 p.

BSEACD, 2017, Central Texas Water Resources.

Bush, PW, Ardis, A.F., and Wynn, K.H., 1993, Historical potentiometric surface of the Edwards-Trinity aquifer system and contiguous hydraulically connected units, west-central Texas: U.S. Geological Survey Water-Resources Investigations Report 92-4055, 3 sheets.

Christian, B., and Wuerch, D., 2012, Compilation of Results of Aquifer Tests in Texas. Texas Water Development Board Report 381. April 2012.

Chowdhury, A.H., 2009, A comparison of the old and new groundwater availability models for the Hill Country portion of the Edwards and Trinity Aquifers: Texas Water Development Board, Analysis Paper 09-20, 32 p.

Clark, A.K., Golab, J.A., and Morris, R.R., 2016, Geologic framework and hydrostratigraphy of the Edwards and Trinity aquifers within northern Bexar and Comal Counties, Texas: U.S. Geological Survey Scientific Investigations Map 3366, 1 sheet, scale 1:24,000, pamphlet, https://doi.org/10.3133/sim3366.

Clark, A.K., and Journey, C., 2006, Flow paths in the Edwards aquifer, northern Medina and northeastern Uvalde Counties, Texas, based on hydrologic identification and geochemical characterization and simulation (No. 2006-5200). US Geological Survey. Accessed July 11, 2017.

Collins, E. W., 2000, Geologic map of the New Braunfels, Texas, 30 × 60 minute quadrangle: Geologic framework of an urban-growth corridor along the Edwards aquifer, south-central Texas: University of Texas at Austin Bureau of Economic Geology Miscellaneous Map No. 39, 28 p., scale 1:100,000, 1 sheet.

Collins, E. W., and Hovorka, S. D., 1997, Structure map of the San Antonio segment of the Edwards Aquifer and Balcones Fault Zone, south-central Texas: structural framework of a major limestone aquifer: Kinney, Uvalde, Medina, Bexar, Comal and Hays Counties: The University of Texas at Austin, Bureau of Economic Geology, Miscellaneous Map No. 38, scale 1:250,000, text, 14 p.

Cope, E. D., 1880, On the zoological position of Texas: Washington, DC, U.S. Natural History Museum Bulletin, v. 17, 51 p.

Daniel B. Stephens & Associates, Inc., 2006, Aquifer Tests from County Availability Studies. Prepared for Texas Water Development Board under TWDB Contract # 2005-483-554. May 4, 2006.

Darling, B.K., 2016, Geochemical evaluation of hydrogeologic interaction between the Edwards and Trinity Aquifers – Travis, Hays and Comal counties, Texas. Presentation March 2016 access from Researchgate, May 15, 2018.

DeCook, K.J., 1963, Geology and ground-water resources of Hays County, Texas, U.S. Geological Survey Water-Supply Paper 1612. 80 p.

Duffin, G., and Musick, S.P., 1991, Evaluation of water resources in Bell, Burnet, Travis, Williamson, and parts of adjacent counties, Texas: Texas Department of Water Resources Report 326, 105 p.

Doctor, D.H., Jr., Alexander, E.C., Jr., Petrič, M., Kogovšek, J., Urbanc, J., Lojen, S., Stichler, W., 2006, Quantification of karst aquifer discharge components during storm events through end-member mixing analysis using natural chemistry and stable isotopes as tracers: Hydrogeol. J., 14 (1) (2006), 10.1007/s10040-006-0031-6.

Ewing, T. E., 1991, The tectonic framework of Texas: text to accompany "The Tectonic Map of Texas": Texas Bureau of Economic Geology, Austin, 36 p.

Fahlquist, L., and Ardis, A.F., 2004, Quality of water in the Trinity and Edwards aquifers, south-central Texas, 1996–98: U.S. Geological Survey Scientific Investigations Report 2004–5201.

Farlow, J.O., and eight others, 2006, Texas Giants, Dinosaurs of the Heritage Museum of the Texas Hill Country: The Heritage Museum of the Texas Hill Country, 150 p.

Ferrill, D. A., A. P. Morris, and R. N. McGinnis, 2009, Crossing conjugate normal faults in field exposures and seismic data: AAPG Bulletin, v. 93, p. 1471–1488

Ferrill, D. A., A. P. Morris, D. W. Sims, R. Green, N. Franklin, and D. J. Waiting, 2008, Geologic controls on interaction between the Edwards and Trinity aquifers, Balcones fault system, Texas: South Texas Geological Society Bulletin, v. 41, p. 21–45.

Ferrill, D.A., Morris, A.P. McGinnis, R.N., Smart, K.J., and Ward, W.C., 2011, Fault zone deformation and displacement partitioning in mechanically layered carbonates: The Hidden Valley fault, central Texas. AAPG Bull. 95, 1383–1397.

Ferrill, D.A., and Morris, A.P., 2008, Fault zone deformation controlled by carbonate mechanical stratigraphy, Balcones fault system, Texas. AAPG Bull. 92, 359–380.

Ferrill, D.A., Sims, D.W., Morris, A.P., Waiting, D.J., and Franklin, N., 2003, Structural Controls on the Edwards Aquifer/Trinity Aquifer Interface in the Camp Bullis Quadrangle, Texas Final report prepared for the Edwards Aquifer Authority and the US Army Corps of Engineers.

Ferrill, D.A., Sims, D.W., Franklin, N., Morris, A.P., and Waiting, D.J., 2005, Structural Controls on the Edward Aquifer/Trinity Aquifer Interface in the Helotes Quadrangle, Texas. Final report prepared for the Edwards Aquifer Authority and the US Army Corps of Engineers. 167.

Ferrill, D.A., Sims, D.W, Morris, A.P., Waiting, D.J., Franklin, N., and Schultz, A.L., 2004, Structural Framework of the Edwards Aquifer recharge zone in southcentral Texas: Geological Society of America Bulletin, v. 116, no. 3, p. 407–418, doi:10.1130/B25174.1.

Ferrill, D. A., R. N. McGinnis, A. P. Morris, and K. J. Smart, 2012, Hybrid failure: Field evidence and influence on fault refraction: Journal of Structural Geology, v. 42, p. 140–150, doi:10.1016/j.jsg.2012.05.012.

Fisher, W. L. and Rodda, P.U., 1967, Lower Cretaceous sands of Texas; stratigraphy and resources.

Flawn, P.T., A. Goldstein, Jr., P. B. King and C. E. Weaver, 1961, The Ouachita System: University of Texas, Austin, Bureau of Economic Geology Publication 6120, 401 p.

Foley, L.L., 1926, Mechanics of the Balcones and Mexia faulting: Bulletin of the American Association of Petroleum Geologists, v. 10, no. 12, p. 1261–1269.

Follett, C.R., 1966, Ground-water resources of Caldwell County, Texas, Texas Water Development Board, Report 174, 133 p.

Follett, C.R., 1973, Ground-water resources of Blanco County, Texas, Texas Water Development Board, Report 12, 135 p.

Fratesi, B.S., Green, R.T., Bertetti, P.F., McGinnis, R.N., Toll, N., Başağaoğlu, H., Gergen, L., and Winterle, J.R., 2015, Development of a Finite-Element Method Groundwater Flow model for the Edwards Aquifer: Prepared for the Edwards Aquifer Authority, 180p.

Fyre et al., 1984, The Vegetation Types of Texas: Texas Parks and Wildlife Department, 1p.

Gary, Marcus, 2018, Personal communication regarding EAA Interformational Flow Study.

George, P.G., Mace, R.E., and Petrossian, R., 2011, Aquifers of Texas: Texas Water Development Board Report 380, 172 p.

George, W.O., 1947, Geology and Ground-Water Resources of Comal County, Texas: Texas Board of Water Engineers Report, February 1947.

George, W.O., Breeding, S.D., and Hastings, W.W., 1952, Geology and ground-water resources of Comal County, Texas, U.S. Geological Survey Water-Supply Paper 1138, 140 p.

George, W.O., Cumley, J.C., and Follett, C.R., 1941, Records of wells and springs, drillers logs, water analyses, and map showing locations of wells and springs in Travis County Texas: Texas Board of Water Engineers duplicated report.

Green, R.T., Bertetti, F.P., and Candelario, M.O., 2011, Edwards Aquifer–Upper Glen Rose aquifer hydraulic interaction. In Interconnection of the Trinity (Glen Rose) and Edwards Aquifers along the Balcones Fault Zone and Related Topics, Proceedings from Karst Conservation Initiative Meeting, February 17, pp. 30–35.

Green, R., Bertetti, F.P., and Hernandez, M., 2012, Recharge Variability In Semi-Arid climates. Nature Education Knowledge 3(10):34. http://www.nature.com/scitable/knowledge/ library/recharge-variability-in-semi-arid-climates-26169682

Green, R.T., Bertetti, F.P., McGinnis, R.N., and Prikryl, J., 2012, Measuring Floodplain Hydraulics of Seco Creek and Medina River Where They Overlie The Edwards Aquifer: Southwest Research Institute, 69 p.

Green, R.T., Bertetti, F.P., and Miller, M.S., 2014, Focused Groundwater Flow in a Carbonate Aquifer in a Semi-Arid Environment. Journal of Hydrology. 517:284–297. doi: 10.1016/j.jhydrol.2014.05.015

Griffith, G., Bryce, S., Omernik, J., and Rogers, A., 2007, Ecoregions of Texas. Project report to Texas Commission on Environmental Quality, 134 p.

Guyton, W.F. and Rose, N.A, 1945, Quantitative studies of some artesian aquifers in Texas: Economic Geology, v. 40, No.3, p. 193-226.

Halbouty, M. T., 1966, Stratigraphic-trap possibilities in upper Jurassic rocks, San Marcos Arch, Texas: AAPG Bulletin, v. 50, no. 1, p. 3–24.

Hamlin, S., and Anaya, R., 2006, Texas Water Development Board GAM technical memo 06-01.

Hammond, W. W., 1984, Hydrogeology of the Lower Glen Rose Aquifer, South-Central Texas: Ph.D.dissertation, The University of Texas at Austin. 243 p.

Hauwert, N., 2009, Groundwater flow and recharge within the Barton Springs Segment of the Edwards Aquifer, southern Travis County and northern Hays Counties, Texas: Dissertation, University of Texas at Austin, Texas. Available at https://repositories.lib.utexas.edu/handle/2152/14107. Accessed November 3, 2016.

Hauwert, N.M., 2011, Water Budget of Stream Recharge Sources to the Barton Springs Segment of the Edwards Aquifer: City of Austin Watershed Protection Department Report. 25 p.

Hauwert, N.M., and Sharp, J.M., Jr., 2014, Measuring Autogenic Recharge over a Karst Aquifer Utilizing Eddy Covariance Evapotranspiration. Journal of Water Resource and Protection. 6. 869-879. http://dx.doi.org/10.4236/jwarp.2014.69081

Heitmuller, F.T., and Reece, B.D., 2003, Database of Historically Documented Springs and Spring Flow Measurements in Texas: U.S. Geological Survey Open-File Report 03-315. 4 p.

Hill, R. T., 1889, A brief description of the Cretaceous rocks of Texas and their economic value, in E. T. Dumble, ed., First annual report of the Geological Survey of Texas: Texas Department of Agriculture, Insurance, Statistics, and History, Austin, Texas, p. 105–141.

Hill, R.T., 1890, A Brief Description of the Cretaceous Rocks of Texas and Their Economic Value, First Annual Report of the Geological Survey of Texas, 1889, p. 105–141.

Homer, C., Dewitz, J., Fry, J., Coan, M., Hossain, N., Larson, C., Herold, N., McKerrow, A., VanDriel, J.N., and Wickham, J, 2007, Completion of the 2001 National Land Cover Database for the Conterminous United States. *Photogrammetric Engineering and Remote Sensing*, Vol. 73, No. 4, pp 337-341.

Homer, C.G., Dewitz, J.A., Yang, L., Jin, S., Danielson, P., Xian, G., Coulston, J., Herold, N.D., Wickham, J.D., and Megown, K., 2015, Completion of the 2011 National Land Cover Database for the conterminous United States-Representing a decade of land cover change information. *Photogrammetric Engineering and Remote Sensing*, v. 81, no. 5, p. 345-354.

Houston, N.A., Garcia, C.A., and Strom, E.W., 2003a, Selected hydrogeologic datasets for the Glen Rose aquifer, Texas. U.S. Geological Survey (USGS) Open-File Report 03-162 (CD-Rom).

Houston, N.A., Garcia, C.A., and Strom, E.W., 2003b, Selected hydrogeologic datasets for the Paluxy aquifer, Texas. U.S. Geological Survey (USGS) Open-File Report 03-163 (CD-Rom).

Houston, N.A., Garcia, C.A., and Strom, E.W., 2003c, Selected hydrogeologic datasets for the Twin Mountain-Travis Peak aquifer, Texas. U.S. Geological Survey (USGS) Open-File Report 03-164 (CD-Rom).

Hovorka, S.D., Mace, R.E., and Collins, E.W., 1998, Permeability structure of the Edwards Aquifer, South Texas—Implications for aquifer management: The University of Texas at Austin, Bureau of Economic Geology Report of Investigations, v. 250, 55 p.

Hunt, B.B., Andrews, A.,G., and Smith, B.A., 2016, Hydraulic Conductivity Testing in the Edwards and Trinity Aquifers using multiport monitor well systems, Hays County, Central Texas, Barton Springs/Edwards Aquifer Conservation District Data Series Report 2016-0831. 43 p.

Hunt, B.B. and Smith, B.A., 2010, Spring 2009 Potentiometric Map of the Middle Trinity Aquifer in Groundwater Management Area 9, Central Texas. BSEACD Report of Investigations 2010-0501, 2010.

Hunt, B.B., Smith, B.A., Gary, M.O., Broun, A.S., Wierman, D.A., Watson, J., and Johns, D., 2015, Surface-water and Groundwater Interactions in the Blanco River and Onion Creek Watersheds: Implications for the Trinity and Edwards Aquifers of Central Texas, South Texas Geological Society, 22 p.

Hunt, B.B., Smith, B.A., Kromann, J., Wierman, D.A., and Mikels, J.K., 2010, Compilation of pumping tests in Travis and Hays counties, central Texas. Barton Springs/Edwards Aquifer Conservation District Data Series Report 2010-0701. 86 p.

Imlay, R. L., 1945, Subsurface Lower Cretaceous formations of south Texas: American Association of Petroleum Geologists Bulletin, v. 29, no. 10, pp. 1416-1469.

Inden, R. F. and Moore, C. H. Jr., 1983, Beach environment, in P. A. Scholle, D. G. Bebout, and C. H. Moore Jr., eds., Carbonate depositional environments: American Association of Petroleum Geologists Memoir 33, p. 211-265.

Johnson, S., Schindel, G.M., and Veni, G., 2010, Dye tracer tests in the Edwards Aquifer, Balcones Fault Zone, San Antonio Segment, Bexar County, Panther Springs Creek. Edwards Aquifer Authority. Report 10-01. 112 pp.

Johnson, S., Schindel, G.M., and Veni, G., 2010, Tracing groundwater flowpaths in the Edwards Aquifer Recharge Zone, Panther Springs Creek Basin, northern Bexar County, Texas. Report No. 10-01, 39.

Johnson, S., Schindel, G., Veni, G., Hauwert, N., Hunt, B., Smith, B., and Gary, M., 2012, Tracing groundwater flowpaths in the vicinity of San Marcos Springs, Texas. Edwards Aquifer Authority. Report No. 12-01. 99 pp + attachments.

Jones, I.C., Anaya, R., and Wade, S.C., 2011, Groundwater Availability Model: Hill Country Portion of the Trinity Aquifer of Texas: Texas Water Development Board Report 377, 165 p.

Kelley, V.A., Ewing, J., Jones, T.L., Young, S.C., Deeds, N., and Hamlin, S., 2014, Updated Groundwater Availability Model of the Northern Trinity and Woodbine Aquifers: Prepared for the Texas Water Development Board, 942 p.

Klemt, W.B., Perkins, R.D., and Alvarez, H.J., 1975, Ground-water resources of part of Central Texas with emphasis on the Antlers and Travis Peak formations: Texas Water Development Board Report 195, v. 1, 63 p.

Klemt, W.B., Knowles, T.R., Edler, G.R., and Sieh, T.W., 1979, Ground-water resources and model applications for the Edwards (Balcones fault zone) aquifer in the San Antonio region: Texas Water Development Board Report 239, 88 p.

Kromann, J., 2015, Surface Water Recharge in Karst: Edwards-Trinity Aquifers – Nueces River System: Master of Science Thesis at The University of Texas at Austin. 209 p.

Kuniansky, E.L., 1989, Precipitation, streamflow, and base flow in west-central Texas, December 1974 through March 1977. Water-Resources Investigations Report 88-4218. 2 plates.

Kuniansky, E.L. and K.Q. Holligan. 1994. Simulations of flow in the Edwards-Trinity Aquifer system and contiguous hydraulically connected units, west-central Texas. U.S. Geological Survey. Water-Resources Investigations Report 93-4039. 40 p.

Kuniansky, E. L., and Ardis, A. F., 2004, Hydrogeology and ground-water flow in the Edwards-Trinity aquifer system, west-central Texas: Regional aquifer-system analysis—Edwards-Trinity: U.S. Geological Survey Professional Paper 1421-C.

Land, L.F., Boning, C.W., Harmsen, L., and Reeves, R.D., 1983, Streamflow losses along the Balcones Fault Zone, Nueces River Basin, Texas: U.S. Geological Survey Water-Resources Investigations Report 83-4372. 68 p.

Lang, L.W., 1953, Ground water in the Trinity Group in the San Antonio area, Texas: U.S. Geological Survey openfile rept., 4 p.

Langley, L., 1999, Updated evaluation of water resources in part of north-central Texas: Texas Water Development Board Report 349, 69 p.

Larkin, T. J., and Bomar, G. W., 1983, Climatic Atlas of Texas: Texas Department of Water Resources, 151 p Laubach, S.E., and Jackson, M.L. 1990, Origin of arches in the northwestern Gulf of Mexico basin: Geology, v. 18, no. 7, p. 595–598, doi:10.1130/0091-7613(1990)018<0595: OOAITN>2.3.CO;2.

LBG-Guyton Associates and NRS Consulting Engineers, 1995, Edwards/Glen Rose hydrologic communication: Prepared for the Edwards underground Water District, 121p.

LBG-Guyton Associates and NRS Consulting Engineers, 2003, Brackish Groundwater Manual for Texas Regional Water Planning Groups: Prepared for the Texas Water Development Board, 188p.

LBG-Guyton Associates, 2008, Groundwater Model for the Lower Trinity Aquifer in Bandera County, Texas and Surrounding Areas. Report prepared for Bandera County River Authority and Groundwater Conservation District. May 2008.

Lindgren, R.J., Dutton, A.R., Hovorka, S.D., Worthington, S.R.H., and Painter, S., 2004, Conceptualization and simulation of the Edwards Aquifer, San Antonio region, Texas. Scientific Investigation Report 2004-5277. U.S. Geological Survey.143 p.

Lindgren, R.J., Taylor, C.J., and Houston, N.A., 2009, Description and evaluation of numerical groundwater flow models for the Edwards aquifer, south-central Texas: U.S. Geological Survey Scientific Investigations Report 2009–5183. 25 p.

Livingston, P., 1947, Ground-Water Resources of Bexar County, Texas. Texas Board of Water Engineers Report.

Long, A.T., 1958, Ground-water geology of Real County, Texas: Texas Board Water Engineers Bulletin 5803. 46 p.

Long, A.T., 1963, Ground-water geology of Edwards County, Texas: U.S. Geological Survey Water-Supply Paper 1619-J. 29 p.

Long, A.T., 1962, Ground-water geology of Edwards County, Texas: Texas Water Commission. Bulletin 6208. 113 p.

Loucks, R.G., 1977, Porosity development and distribution in shoal-water carbonate complexes—subsurface Pearsall Formation (Lower Cretaceous) South Texas, in Bebout, D.G., and Loucks, R.G., eds., Cretaceous Carbonates of Texas and Mexico: University of Texas at Austin, Bureau of Economic Geology, Report of Investigations no. 89, p. 97–126

Lowry, R.L., 1959, A Study of Droughts in Texas. Texas Board of Water Engineers Bulletin 5914. December, 1959.

Lozo, F. E., and Smith, C.I., 1964, Revision of Comanche Cretaceous stratigraphic nomenclature, southern Edwards Plateau, Southwest Texas: Gulf Coast Association of Geological Societies Transactions, v. 14, p. 285–306.

Mace, R.E., Chowdhury, A.H., Anaya, R., and Way, S.-C., 2000a, A numerical groundwater flow model of the upper and middle Trinity Aquifer, Hill Country area: Texas Water Development Board Open File Report 00-02, 62 p.

Mace, R.E., Chowdhury, A.H., Anaya, R., and Way, S.-C., 2000b, Groundwater availability of the Trinity Aquifer, Hill County area, Texas—Numerical simulations through 2050: Texas Water Development Board Report 353, 117 p.

Mace, R.E., 2001, Estimating Transmissivity Using Specific-Capacity Data. Bureau of Economic Geology Geological Circular 01-2. 2001.

Maclay, R.W., and Land, L.F., 1988, Simulation of flow in the Edwards Aquifer, San Antonio Region, Texas, and refinement of storage flow concepts. U.S. Geological Survey Water-Supply Paper2336, 48 pp.

Manford, D., Dixon, R.M., and Dent, O.F., 1960, Channel Gain and Loss Investigations: Texas Streams, 1918 – 1958: Texas Board of Water Engineers, 284 p.

Manson, S., Schroeder, J., Van Riper, D., and Ruggles, S., 2017, *IPUMS National Historical Geographic Information System: Version 12.0* [Database]. Minneapolis: University of Minnesota. 2017. http://doi.org/10.18128/D050.V12.0, accessed March 2018.

McGinnis, R. N., D. A. Ferrill, K. J. Smart, A. P. Morris, C. Higuera-Diaz, and D. Prawica, 2015, Pitfalls of using entrenched fracture relationships: Fractures in bedded carbonates of the Hidden Valley Fault Zone, Canyon Lake Gorge, Comal County, Texas: American Association of Petroleum Geologists Bulletin, v. 99, p. 2221–2245.

Morris, A. P., D. A. Ferrill, and R. N. McGinnis, 2009a, Fault frequency and strain: Lithosphere, v. 1, no. 2, p. 105–109, doi:10.1130/L23.1.

Morris, A. P., D. A. Ferrill, and R. N. McGinnis, 2009b, Mechanical stratigraphy and faulting in Cretaceous carbonates: AAPG Bulletin, v. 93, no. 11, p. 1459–1470, doi:10.1306/04080909011.

Muller, D.A. and McCoy, W., 1987, Ground-water conditions of the Trinity Group aquifer in western Hays County: Texas Water Development Board LP-205, 62 p.

Muller, D.A., 1990, Ground-water evaluation in and adjacent to Dripping Springs, Texas, Texas Water Development Board, Report 322, 59 p.

Murray, G.E., 1961, Geology of the Atlantic and Gulf Coastal Province of North America: New York, Harper and Brothers, 692 pp.

Musgrove, M., Fahlquist, L., Houston, N.A., Lindgren, R.J. and Ging, P.B., 2010, Geochemical evolution processes and water-quality observations based on results of the National Water-Quality Assessment Program in the San Antonio segment of the Edwards aquifer, 1996-2006. U. S. Geological Survey. Accessed July 11, 2017, 93 p.

Myers B.N., 1969, Compilation of results of Aquifer Tests in Texas, Texas Water Development Board Report 98, p. 532.

National Water Quality Monitoring Council, 2017, National Water Quality Monitoring Council Database: Accessed 2017.

Nordstrom, P.L., 1982, Occurrence, availability, and chemical quality of ground water in the Cretaceous aquifers of north-central Texas: Texas Department of Water Resources Report 269, v. 1, 109 p., and v. 2, 387 p. obtained in electronic form: http://www.twdb.texas.gov/

Nordstrom, P.L., 1987, Ground-water resources of the Antlers and Travis Peak formations in the outcrop area of north-central Texas: Texas Department of Water Resources Report 298, 297 p. obtained in electronic form: http://www.twdb.texas.gov/publications/reports /numbered_reports/doc/R298/report298.asp.

Phelps, R. M., Kerans, C., Loucks, R.G., Scott, R.W., Da Gama, B.P., Jeremiah, J., and Hull, D., 2014, Oceanographic and eustatic control of carbonate platform evolution and sequence stratigraphy on the Cretaceous (Valanginian-Campanian) passive margin, northern Gulf of Mexico: Sedimentology, v. 61, p. 461–496.

Phelps, R.M. (2011) Middle-Hauterivian to Lower Campanian sequence stratigraphy and stable isotope geochemistry of the Comanche Platform, south Texas. PhD Dissertation, University of Texas, Austin, TX. 227 pp.

PRISM Climate Group, 2016, Prism Temperature Data Raster Map: Oregon State University, http://prism.oregonstate.edu.

Puente, C., 1978. Method of estimating natural recharge to the Edwards Aquifer in the San Antonio area, Texas. U.S. Geological Survey Water Resources Investigations 78-10. 34 p.

Reeves, R. D. and Small, T.A., 1973, Ground-Water Resources of Val Verde County, Texas, Texas Water Development Board, Report 172. June 1973

Reeves, R.D., 1967, Ground-water resources of Kendall County, Texas Water Development Board. Report 60, 64 p.

Reeves, R.D., 1969, Ground-water resources of Kerr County, Texas Water Development Board. Report 102, 59 p.

Ridgeway, C., and Petrini, H., 1999, Changes in groundwater conditions in the Edwards and Trinity aquifers, 1987–1997, for portions of Bastrop, Bell, Burnet, Lee, Milam, Travis and Williamson counties, Texas: Texas Water Development Board Report 350, 38 p. http://www.twdb.texas.gov/publications/reports/numbered_reports/doc/R350/Report350.asp.

Rose, P., 1972, Edwards Group, Surface and Subsurface, Central Texas: The University of Texas at Austin, Bureau of Economic Geology Report of Investigations No. 74, 198 p. 35 figs, 19 plates.

Rose, P. R., 1986a, Pipeline oil spills and the Edwards aquifers, Central Texas, in P. L. Abbott and C. M. Woodruff, Jr., eds., The Balcones Escarpment: Geology, hydrology, ecology and social development in Central Texas: Geological Society of America, Boulder, Colorado, p. 163–183.

Rose, P. R., 1986b, Oil and gas occurrence in Lower Cretaceous rocks, Maverick Basin area, Southwest Texas, in W. L. Stapp, ed., Contributions to the geology of South Texas: South Texas Geological Society, San Antonio, p. 408–421.

Rose, P.R., 2016a, Late Cretaceous and Tertiary burial history, central Texas: GCAGS Journal, v. 5, p. 141–179.

Rose, P.R., 2016b, Regional Stratigraphy of the Edwards Group and Associated Formations of Texas (Lower Cretaceous, Comanchean): In Defense of the Classical View: GCAGS Journal, v. 6, p. 111–134.

Sandidge, J. R., 1959, A review of Edwards Limestone production with special reference to south-central Texas, in F. E. Lozo, H. F. Nelson, K. Young, O. B. Shelburne, and J. R. Sandidge, eds., Symposium on Edwards Limestone in central Texas: The University of Texas Publication 5905, p. 131–151.

Schindel, G., and Johnson, S., 2011, Using tracer testing data for resource management planning. In Interconnection of the Trinity (Glen Rose) and Edwards Aquifers along the Balcones Fault Zone and Related Topics, Proceedings from Karst Conservation Initiative Meeting, February 17, 38. http://www.speleogenesis.info/directory/karstbase/pdf/seka _pdf9869.pdf.

Scott, R. W. (ed.), 2007, Cretaceous Rudistids and Carbonate Platforms: Environmental Feedback, SEPM Special Publication No. 87. Tulsa, Oklahoma.

Scott, R. W. and Filkorn, H. F. 2007. Barremian–Albian rudist zones, U.S. Gulf Coast. in R. W. Scott, ed., Cretaceous Rudists and Carbonate Platforms: Environmental Feedback. SEPM Special Publication, 87, 167–180.

Slade, R.M., Bentley, J.T., and Michaud, D., 2002, Results of streamflow gain-loss studies in Texas, with emphasis on gains from and losses to major and minor aquifers. U.S. Geological Survey Open-File Report 02–068. 136 p.

Slade, R.M., Veenhuis, J.E., Dorsey, M.E., Gardiner, H., and Smith, A.E., 1982, Hydrologic Data for Urban Studies in The Austin, Texas, Metropolitan Area, 1981: U.S. Geological Survey Open-File Report 83-44. 299 p.

Small, T., 1986, Hydrologic sections of the Edwards Aquifer and its confining unites in the San Antonio area, Texas, U.S. Geological Survey Water-Resources Investigations Report 85-4259. 46 p.

Smith, B.A. and Hunt, B.B., 2009, Potential hydraulic connections between the Edwards and Trinity aquifers in the Balcones Fault Zone of central Texas: Bulletin of the South Texas Geological Society, Volume L, Issue No. 2, October 2009, p. 15-34.

Smith, B.A., and Hunt, B.B., 2010, Flow potential between stacked Karst Aquifers in Central Texas, USA. In Advances in Research in Karst Media Environmental Earth Sciences, eds. B. Andreo, F. Carrasco, J.J. Duran, and J.W. LaMoreaux. p. 43–48.

Smith, B.A., and Hunt, B.B, 2011, Potential for vertical flow between the Edwards and Trinity Aquifer, Barton Springs Segment of the Edwards Aquifer. In *Interconnection of the Trinity (Glen Rose) and Edwards Aquifers along the Balcones Fault Zone and Related Topics, Proceedings from Karst Conservation Initiative Meeting*. p.11–14.

Smith, C. I., Brown, J. B., and Lozo, F. E., 2000, Regional stratigraphic cross sections, Comanche Cretaceous (Fredericksburg-Washita division), Edwards and Stockton Plateaus, West Texas: The University of Texas at Austin, Bureau of Economic Geology, 39 p., 6 plates.

Soil Survey Staff, Natural Resources Conservation Service, United States Department of Agriculture. U.S. General Soil Map (STATSGO2). Available online at https://websoilsurvey.nrcs.usda.gov/. Accessed 4/2/2018.

Stepchinski, L., R.T. Green, F.P. Bertetti, R.M. McGinnis, N.J. Toll, R.R. Nunu, N.E. Deeds, D. Lupton, S.B. Fratesi, K.D.H. Gulliver, M.E. Flores, J. Harding, M.O. Gary, S. Johnson, B.B. Hunt, B. Smith, 2017, Final Report for the Study of Brackish Aquifers in Texas – Project No. 4 – Trinity Aquifer. Prepared for the Texas Water Development Board, 348 p.

Stricklin, F. L., Jr., and Amsbury, D.L., 1974, Depositional environments on a low-relief carbonate shelf, middle Glen Rose Limestone, central Texas, in B. F. Perkins, ed., Geoscience and Man, v. VIII: Louisiana State University Press, Baton Rouge, p. 53-66.

Stricklin, F. L., Jr., Smith, C. I., and Lozo, F. E., 1971, Stratigraphy of Lower Cretaceous Trinity deposits of Central Texas: The University of Texas at Austin, Bureau of Economic Geology Report of Investigations No. 71, 63 p.

Stricklin, F.L. and Smith, C.I., 1973, Environmental Reconstruction of a Carbonate Beach Complex: Cow Creek (Lower Cretaceous) Formation of Central Texas: Geological Society of America Bulletin, v. 84.Rose, P. R., 1972, Edwards Group, Surface and Subsurface, Central Texas: The University of Texas at Austin, Bureau of Economic Geology Report of Investigations No. 74, 198 p.

Sundstrom, R.W., Broadhurst, W.L., and Dwyer, B.C., 1949, Public Water Supplies in Central and North-Central Texas, Geological Survey Water-Supply Paper 1069: Prepared in cooperation with the Texas Board of Water Engineers.

Texas Bureau of Economic Geology, Interpretation of sedimentary facies, depositional cycles, and tectonics: Austin, 39 p., 6 cross-sections.

Texas Commission on Environmental Quality, 2015, TCEQ Public Water Supply well data: personal communication from Sean Ables (TCEQ) to Steve Young (INTERA Incorporated) via email March 2015.

Texas Water Development Board, 2017, Groundwater Database (GWDB) Reports. http://www.twdb.texas.gov/groundwater/data/gwdbrpt.asp (Accessed 2017).

Theis, C.V., Brown, R.H., and Myers, R.R., 1963, Estimating the transmissibility of aquifers from the specific capacity of wells: methods of determining permeability, transmissivity, and drawdown, in U.S. Geological Survey Water-Supply Paper, 1536-1, p. 331-341.

Toll, N., Fratesi, S.B., Green, R.T., Bertetti, F.P., and Nunu, R.R., 2017, Water-Resource Management of the Devils River Watershed Final Report. Contract Report for the Devils River Conservancy.

Tucker, D. R., 1962a, Central Texas lower Cretaceous stratigraphy (abstract): Trans. Gulf Coast Assoc. Geol. Socs. v. 12, p. 839-896.

Tucker, D.R., 1962b, Subsurface lower Cretaceous stratigraphy, central Texas. PhD Dissertation, University of Texas. 167 p.

TWDB, 2001, Surveys of irrigation in Texas 1958, 1964, 1969, 1974, 1979, 1984, 1989, 1994 and 2000: Report 347.

TWDB, 2017a, Brackish Resources Aquifer Characterization System (BRACS) Database: website http://www.twdb.texas.gov/innovativewater/bracs/database.asp, accessed September 2017.

TWDB, 2017b, Groundwater database download: website http://www.twdb.texas.gov/groundwater/data/gwdbrpt.asp, accessed September 2017.

TWDB, 2017c, Historical agricultural irrigation water use estimates: Irrigation water use estimates website https://www.twdb.texas.gov/conservation/agriculture/irrigation/, accessed October 2017.

TWDB, 2017d, Submitted drillers' reports database download: website http://www.twdb.texas.gov/groundwater/data/drillersdb.asp, accessed September 2017.

TWDB, 2017e, Water use survey data: personal communication from Bill Billingsley (TWDB) to Jevon Harding (INTERA Incorporated) via email dated October 4, 2017.

TWDB, 2018a, Historical Groundwater Pumpage: website http://www.twdb.texas.gov/waterplanning/waterusesurvey/historical-pumpage.asp accessed February 2018.

TWDB, 2018b, Historical Surveyed Municipal and Industrial Water Intake: website http://www.twdb.texas.gov/waterplanning/waterusesurvey/estimates/index.asp, accessed February 2018.

U.S. Environmental Protection Agency (USEPA) and U.S. Geological Survey (USGS), 2012. National Hydrography Dataset Plus – NHDPlus 2.10 geospatial data. Website: http://www.horizon-systems.com/NHDPlus/NHDPlusV2_home.php.

U.S. Geological Survey, 2017. National water information system database: website https://waterdata.usgs.gov/nwis, accessed September 2017.

U.S. Geological Survey, 2016, National Elevation Dataset, https://nationalmap.gov/elevation.html.

U.S. Geological Survey, 2002, Physiographic divisions of the conterminous U.S.: website http://water.usgs.gov/GIS/metadata/usgswrd/XML/physio.xml#stdorder, accessed 2017.

U.S. Geological Survey, 1965, Surface Water Records of Texas, 1964: U.S. Geological Survey Water Data Reports, 496 p.

Vogelmann, J.E., Howard, S.M., Yang, L., Larson, C.R., Wylie, B.K., and Van Driel, J.N., 2001, Completion of the 1990's National Land Cover Data Set for the conterminous United States, *Photogrammetric Engineering and Remote Sensing* 67:650-662.

Walker, L.E., 1979, Occurrence, Availability, and Chemical Quality of Ground Water in the Edwards Plateau Region of Texas, TWDB Report 235.

Ward, W. C., and Ward, W.B., 2007, Stratigraphy of the middle part of Glen Rose Formation (Lower Albian), Canyon Lake Gorge, central Texas, in R. W. Scott, ed., Cretaceous rudists and carbonate platforms: Environmental feedback: SEPM Special Publication 87, p. 193–210.

W.E. Simpson Company and William F. Guyton Associates, 1993, North Bexar County Water Resources Study for the Edwards Underground Water District, September 1993.

Weeks, A.W., 1945, Balcones, Luling, and Mexica fault zones in Texas: Bulletin of the American Association of Petroleum Geologists, v. 29, p. 1733–1737.

Welder, F.A., and Reeves, R.D., 1964, Geology and groundwater resources of Uvalde County, Texas: Water Supply Paper 1584, 49p.

Wermund, E. G., 1996, Physiography of Texas: The University of Texas at Austin, Bureau of Economic Geology, 2 p.

Wierman, D.A., Broun, A.S., and Hunt, B.B. 2010, Hydrogeologic Atlas of the Hill Country Trinity Aquifer Blanco, Hays, and Travis Counties, Central Texas.

Winter, J. A., 1961, Stratigraphy of the Lower Cretaceous (subsurface) of South Texas: Gulf Coast Association of Geological Societies Transactions, v. 11, p. 15–24.

Wong, C.I., Kromann, J.S., Hunt, B.B., Smith, B.A., and Banner, J.L., 2014, Investigating Groundwater Flow Between Edwards and Trinity Aquifers in Central Texas. Groundwater. Volume 52, Number 4, July-August 2014. Pp 624-639.

Woodruff, C.M., Jr., and Abbott, P.L., 1979, Drainage-basin evolution and aquifer development in a karstic limestone terrain, South-Central Texas, USA. Earth Surface Processes. 4. pp. 319-334.

Young, K., 1972, Mesozoic history, Llano region: in Barnes, V. E., Bell, W. C., Clabaugh, S. E., and Cloud, P. E., eds., Geology of the Llano region and Austin area, field excursion, The University of Texas at Austin, Bureau of Economic Geology Guidebook 13, 77 p.

Young, S.C., Budge, T., and Snyder, G., 2005. Development and Application of a Groundwater Model for North Medina County. Report prepared for: Medina County Groundwater Conservation District, April 2005.

Young, S.C., Doherty, J., Budge, T., and Deeds, N., 2010, Application of PEST to Re-Calibrate the Groundwater Availability Model for the Edwards-Trinity (Plateau) and Pecos Valley Aquifers. Report prepared for the Texas Water Development Board, April 2010.

Zahm, C., Zahm, L., and Bellian, J.A., 2010, Integrated fracture prediction using sequence stratigraphy within a carbonatefault damage zone, Texas, USA: Journal of Structural Geology, v. 32, no. 9, p. 1363–1374, doi:10.1016/j.jsg .2009.05.012.